"THE LAXFORDIAN STRUCTURE OF THE KENMORE INLIER, LOCH TORRIDON, ROSS SHIRE".

Mohammad Niamatullah

A thesis submitted for the degree of
Doctor of Philosophy, University of Keele.

1983

BRITISH LIBRARY

IMAGING SERVICES NORTH

Boston Spa, Wetherby
West Yorkshire, LS23 7BQ
www.bl.uk

VOLUME CONTAINS CLEAR OVERLAYS

OVERLAYS HAVE BEEN SCANNED SEPERATELY AND THEN AGAIN OVER THE RELEVANT PAGE

BRITISH LIBRARY

IMAGING SERVICES NORTH

Boston Spa, Wetherby
West Yorkshire, LS23 7BQ
www.bl.uk

CONTAINS PULLOUTS

ACKNOWLEDGEMENTS

The research for this thesis was carried out under the tenure of a Quaid-e-Azam scholarship, the sponsorship of the Pakistan Government is gratefully acknowledged.

I would like to thank my supervisor,Dr R.G.Park,for suggesting an interesting project and for his invaluable help both in the field and at Keele. I would also like to thank my fellow research students at Keele for their encouragement, particularly Drs. P.A.Shami; E. Kerey; G. Anastasakis and R.A.Strachan. In addition I am indebted to Mr J. Constable for his long critical discussions which were very useful to me in this research; and also to members of the technical staff in the Geology Department for their help.

My thanks are also due to Mr & Mrs Gillanders of Arrina who provided me with excellent accommodation and hospitality during my field work. Similarly I must express my appreciation to Mr & Mrs Maclean, Robert and Helen for their help and good company.

I am also grateful to my parents, family members, relatives and many friends, from afar, who have encouraged me greatly over the last three years.

Finally I would like to thank Mrs Hazel M. Tomkinson and Mrs Christine A. Owen for the care and attention they have shown in typing the thesis very quickly.

ABSTRACT

Detailed mapping has been carried out of an area 12sq.km in extent around Kenmore on the south side of Loch Torridon together with a reconnaissance traverse on the north side of Loch Torridon in Diabaig. The Kenmore area exhibits particularly strong Laxfordian deformation. Foliated grey and pink granodioritic gneisses form the main body of the complex giving a banded appearance. Scourie dykes are present in the form of amphibolitic bands which are mainly strongly foliated. Isolated layers and pods of early amphibolite and probably metasedimentary rocks are also present.

Pre-Inverian structures are rare but Inverian foliation is quite strong and has been variably transposed in Laxfordian deformations. The first Laxfordian deformation is the main fabric-producing event in the Scourie dykes and produced a strong LS fabric with subvertical NW-SE oriented foliation and subhorizontal lineation. The second Laxfordian deformation produced abundant minor folds with subhorizontal axial surfaces and NW-SE oriented hinges. The folds have a close to similar geometry and have a good axial-planar fabric. The third Laxfordian deformation produced upright NW-SE oriented folds with a near parallel style, generally without an associated fabric. All three deformations are generally co-axial. Later deformations which were localized and mild produced cross-folds and breccia zones.

Two lower amphibolite-facies metamorphic episodes M_1 and M_2 were syntectonic with the first and second Laxfordian deformations respectively. Localized recrystallisation of low grade minerals after M_2 was probably partly syntectonic with the third Laxfordian deformation.

Qualitative strain analysis using grain aggregates in Scourie dykes

and fold profile shape shows a highly variable bulk strain pattern due mainly to the heterogeneous and locally very large D_1 strains associated probably with a steep dextral shear zone. D_2 in contrast appears to be due to a low-angle shear zone with a northwards transport direction.

CONTENTS

5. STRAIN PROFILES ACROSS THE KENMORE INLIER

6. GEOLOGY OF THE TORRIDON AREA (after Cresswell,1972)

7. STRAIN PROFILE ACROSS THE DIABAIG INLIER

CHAPTER I

INTRODUCTION

A. LOCATION AND EXTENT OF AREA

The area of the present study lies at the southern extremity of the belt of Lewisian gneisses running along the western sea board of N.W. Scotland (Fig. I-1) in the county of Ross-shire. The area comprises two separate inliers at the southern end of the southern district of the mainland Lewisian (Peach et al., 1907). The Kenmore inlier, which has been mapped in detail, lies on the south shore of Loch Torridon while the Diabaig inlier lies on its northern shore. The Lewisian outcrop in the Kenmore inlier covers an area of about 12 sq.km. in extent, most of which is exposed.

B. PHYSIOGRAPHY

The Kenmore inlier consist of hills of gentle slope, rising from the sea shore to a height of about 300 metres. Although many small lochs are present and some areas are covered by peat and glacial drift, most of the area is well exposed and rock surfaces are clean and fresh due to glacial activity. NE-SW oriented vertical joints and faults are common in the area and since most of the structures are NW-SE oriented, these clean joint and fault surfaces provide excellent cross sections. Exposures are also excellent on the sea shore where the rocks are well washed. Good clean hill surfaces and NE-SW oriented scarps provide excellent three dimensional views for study.

Fig. I-1. Tripartite sub-division of Peach et al. (1907) of the Lewisian outcrop on the mainland of NW Scotland. The box shows the location of the area.

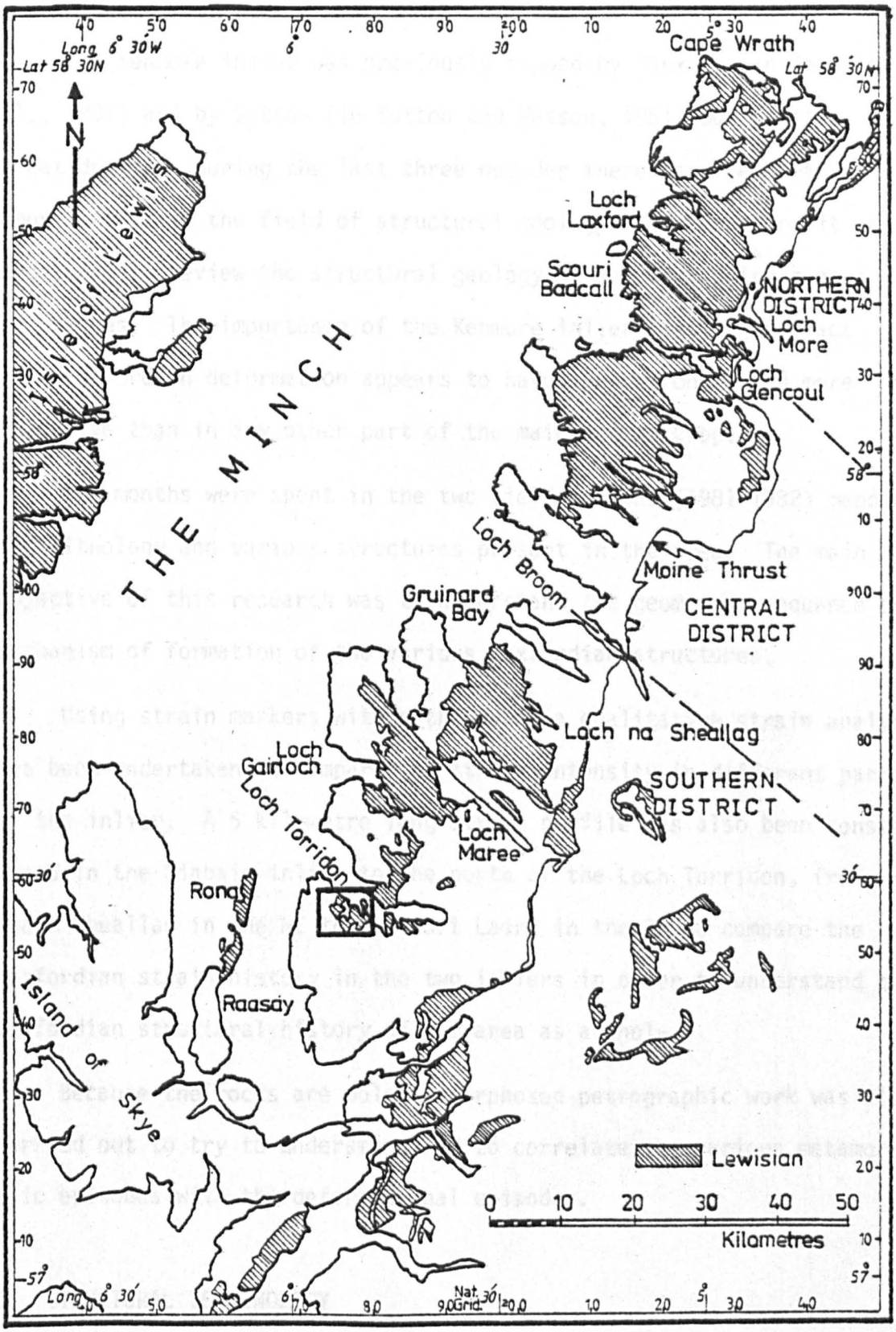
Long 6° 30W
Lat 58° 30N
N
Isle of Lewis
THE MINCH
Cape Wrath
Loch Laxford
Scouri
Badcall
NORTHERN DISTRICT
Loch More
Loch Glencoul
Loch Broom
Moine Thrust
CENTRAL DISTRICT
Gruinard Bay
Loch na Sheallag
SOUTHERN DISTRICT
Loch Gairloch
Loch Torridon
Loch Maree
Rona
Raasay
Island of Skye
Lewisian
0 10 20 30 40 50
Kilometres
Nat. Grid

C. THE AIMS OF THE PRESENT RESEARCH

The Kenmore inlier was previously mapped by Hinxman (in Peach et al., 1907) and by Sutton (in Sutton and Watson, 1951) but not in great detail. During the last three decades there have been many improvements in the field of structural geology, and therefore it was necessary to review the structural geology of the area using modern techniques. The importance of the Kenmore inlier lies in the fact that Laxfordian deformation appears to have been stronger and more extensive than in any other part of the mainland outcrop.

Ten months were spent in the two field seasons (1981-1982) mapping the lithology and various structures present in the area. The main objective of this research was to understand the geometry, sequence and mechanism of formation of the various Laxfordian structures.

Using strain markers within the dykes a qualitative strain analysis has been undertaken to compare the strain intensity in different parts of the inlier. A 5 kilometre long strain profile has also been constructed in the Diabaig inlier to the north of the Loch Torridon, from Ruadh Mheallan in the NE to Port Laire in the SW to compare the Laxfordian strain history in the two inliers in order to understand the Laxfordian structural history of the area as a whole.

Because the rocks are polymetamorphosed petrographic work was also carried out to try to understand and to correlate the various metamorphic episodes with the deformational episodes.

D. STRUCTURAL TERMINOLOGY

The structural terminology used in this thesis is given in Table I.1. It is the same as that used by Ramsay (1967) except for stresses.

Table 1 - 1

STRUCTURAL NOMENCLATURE

x, y, z	Cartesian co-ordinate axes.
e	Extension.
e_1 e_2 e_3	Principal extensions.
X Y Z	Measured ellipsoid axes from a deformed sphere of radius 1 $X = r(1 + e_1)$, etc.
λ	Quadratic extension.
$\lambda_1\lambda_2\lambda_3$	Principal quadratic extensions.
σ	Stress axis.
$\sigma_1\sigma_2\sigma_3$	Principal stresses.
a	Ratio of principal strains. $(1+e_1)/(1+e_2) = X/Y$.
b	Ratio of principal strains. $(1+e_2)/(1+e_3) = Y/Z$
r	Measure of amount of deformation, $r = a + b - 1$.

The amount of strain is given in the form of strain ratios $\sqrt{\lambda_2/\lambda_1}$ (or $1+ e_2/1+ e_1$). In order to correlate these strain ratios with percentages of shortening a curve drawn by Coward (1969) has been used (Fig. I-2).

E. METHODS OF RESEARCH

1. Field Techniques

Mapping of the area was carried out by using Ordnance Survey "Six-inch" (1:10,560) topographic maps. Both lithological and structural maps were prepared.

The orientation of a variety of penetrative and non-penetrative structures was measured using compass and clinometer. The most commonly measured penetrative planar structures include foliation surfaces and the axial planes of small scale folds. Penetrative linear structures recorded include shape-fabric lineation in the dykes, rodding in the gneisses and fold hinges of small-scale folds.

Lineations were usually measured on the foliation surfaces in terms of plunge angle where the foliation was steep and plunge directions where foliation was gently inclined. In the former case plunge direction was measured by plotting the exact plunge angle of the lineation and the foliation attitude on equal angle net. In the latter case the exact plunge angle was measured by plotting the foliation attitude and the plunge direction on an equal angle net. The axial surfaces of small scale folds were measured by inserting the notebook in a fold profile such that the axial trace of the fold and the hinge of the fold lie in the plane of the notebook, then the attitude of the notebook was measured as the axial surface of the fold. The plunge and bearing of the hinges of minor folds has been measured exactly in the same way as the attitude of lineations on a foliation surface, as has been described

Fig. I-2. Strain ratios $1+e_2/1+e_1$ are plotted against shortening percentage.

(after Coward, 1969).

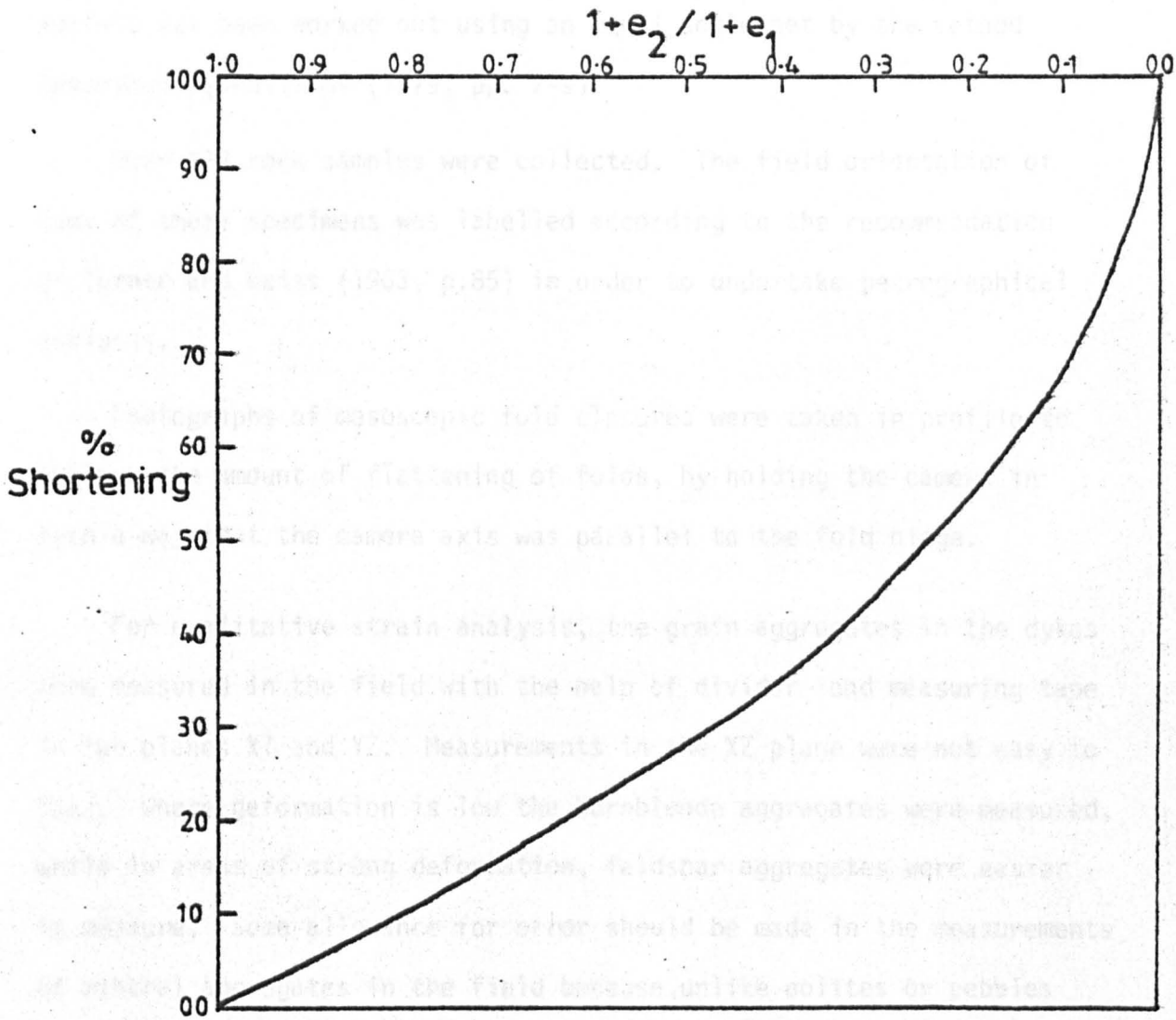
1+e2 / 1+e1
1·0
0·9
0·8
0·7
0·6
0·5
0·4
0·3
0·2
0·1
0·0
100
90
80
70
60
50
40
30
20
10
00
% Shortening

earlier. In unsuitable circumstances the attitude of the axial plane of minor folds was measured by recording the attitude of two lines of different orientation parallel to the axial surface of the fold in two differently oriented profile planes. Then the attitude of the axial surface has been worked out using an equal angle net by the method described by Phillips (1979, pp. 7-9).

Over 400 rock samples were collected. The field orientation of many of these specimens was labelled according to the recommendation of Turner and Weiss (1963, p.85) in order to undertake petrographical analysis.

Photographs of mesoscopic fold closures were taken in profile to analyse the amount of flattening of folds, by holding the camera in such a way that the camera axis was parallel to the fold hinge.

For qualitative strain analysis, the grain aggregates in the dykes were measured in the field with the help of divider and measuring tape in two planes XY and YZ. Measurements in the XZ plane were not easy to take. Where deformation is low the hornblende aggregates were measured, while in areas of strong deformation, feldspar aggregates were easier to measure. Some allowance for error should be made in the measurements of mineral aggregates in the field because,unlike oolites or pebbles they do not have well-marked boundaries.

2. Structural Analysis

From the data obtained from field mapping, the area has been subdivided into domains which are statistically homogeneous with respect to the gneissic foliation using equal area plots. The same subdivision has been used for other fabric elements for the sake of simplicity. This subdivision has been done as far as possible in such a way that the poles to the foliation are concentrated on a great circle indicating

cylindrical folding in that domain. However, in some domains poles to the foliation are concentrated on a small circle due to some conicity in the folding in those domains. In order to measure the conicity roughly (i.e. the cone angle in a plane containing the cone axis) and the orientation of the cone axis of the folds graphically, the equal area net has been rotated through a set of angles and the best fit line chosen to fit the actual distribution of the poles to the foliation.

In all the sub-domains, poles to the foliation of the gneisses and dykes, and other fabric elements wherever necessary, have been counted and contoured. When poles to the foliation were more than fifty in number, the Kalsbeek counting net (Kalsbeek, 1963) was used for counting them while for fewer poles the Mellis or circle method (Mellis,1942) was used.

Using the photographs of fold profiles taken in the field, folds have been classified on a geometrical basis by the isogonal classification of Ramsay (1967). Fold flattening has been measured according to Ramsay's (1962, 1967) and Hudleston's (1973a) methods by measuring change in the orthogonal thickness of layers with change of layer angle with the fold axial surface.

3. Petrographic Techniques

Thin sections were made from about 250 hand specimens. Most of the rocks were cut perpendicular to the foliation and lineations, but thin sections perpendicular to the foliation and parallel to the lineations were also prepared. Samples which contain small fold closures, were cut perpendicular to the fold axes.

Thin sections were examined by conventional methods to determine the minerals present, their approximate proportion, and to study rock texture.

Plagioclase composition was determined from albite twins using Michel-Levy's method (see Kerr, 1959, pp. 257-258).

E. PREVIOUS RESEARCH

For the first time the Lewisian rocks on the mainland in N.W. Scotland were systematically studied by Peach and his colleagues in 1907. The major petrographical division of the Lewisian rocks recognised by these early workers is:-

1. A "fundamental complex" composed mainly of gneisses having affinities with plutonic rocks but including a small area in which the rocks are probably of sedimentary origin.
2. A series of dykes and sills, including ultrabasic, basic and acid varieties, intrusive into the fundamental complex.

On a geological basis they subdivided the area into three districts (Fig. I-1). 1. The northern district extending from Cape Wrath to a line between Tarbert and Ben Dreavie, 2. The central district extending from this line to Loch Broom and 3. The southern district extending southward from a line between Gruinard Bay and Loch na Sheallag to the islands of Rona and Raasay. In the central district the fundamental complex is composed of grey pyroxene gneisses with pyroxenites, hornblendites, pyroxene granulites and garnet ampihibolites, with later basic intrusive rock relatively unmodified by the pre-Torridonian movements. The districts in the north and south of the central district were characterised by granular hornblende and biotite gneisses. Microcline augen gneisses were stated to be common in the southern district and rocks with presumed sedimentary origin were described in the neighbourhood of Gairloch and Loch Maree. Also granites

are less common in the north than in the south. "Terrestrial stresses" of pre-Torridonian age were said to have converted many of the later basic intrusive rocks into foliated amphibolites.

Sutton and Watson (1951) from studies in the Scourie and Loch Torridon areas proposed a metamorphic history for the mainland Lewisian based upon the structural relationships of the basic dykes to the fundamental complex and the progressive metamorphism of the dykes. They regarded the Lewisian as made up of two complexes. The older, or "Scourian" complex, which was formed before the intrusion of the dolerite dykes, was metamorphosed under granulite facies conditions in the central district and under amphibolite facies conditions to the south of Loch Broom and Gruinard Bay and in the small area near Loch Maree and Loch Torridon, with a dominant structural trend to the northeast.

The younger or "Laxfordian" complex involved metamorphic reconstitution of the fundamental complex in almandine-amphibolite facies with a northwest striking foliation. This was formed after the intrusion of the Scourie dykes.

During the great interval of time which separated the Scourian and Laxfordian metamorphic and tectonic events, the northwest trending dolerite dykes were intruded as an anorogenic swarm.

Evans (1965) established a structural and metamorphic episode, characterised by folding on NW-SE trending axes and by the production of a very well developed NW-SE foliation of variable dip, immediately preceding the dyke intrusion, and named it the "Inverian". Sutton and Watson (1969) regarded the Inverian as "Late Scourian" and the event which occurred before that as the "Early Scourian". Park (1970) proposed the name "Badcallian" for the early event.

Dearnley (1962) divided the Hebridean Lewisian similarly into two orogenic periods separated by the Scourie dykes. He correlated these older and younger orogenic periods with the Scourian and Laxfordian on the mainland of Scotland, as established by Sutton and Watson (1951). He also divided the Hebridean Lewisian into three structural districts, a central district showing Scourian deformation, and a northern and southern district intensely deformed in the Laxfordian orogeny.

The broad geological history established by these early authors has been partly confirmed by radiometric dates. From the recent geochronological work on the Lewisian by many workers the following approximate chronology has been suggested (cf. Park, 1980).

The Badcallian gneiss forming event in which granulite facies minerals and NE-SW oriented structures were produced, has been dated at c.2900 m.y. ago using lead isotopes (Moorbath et al., 1969). This episode probably terminated at c.2700 m.y. ago estimated using Rb-Sr whole rock ages and U-Pb ages on zircon (Pidgeon and Bowes, 1972; Moorbath et al., 1975).

The Inverian amphibolite facies metamorphism and deformation which affected the northern and southern districts produced NW-SE oriented subvertical foliation and local migmatisation followed by intrusion, and probably took place between c.2700 and c.2400 m.y. ago.

Intrusion of the Scourie dyke suite probably took place between c.2400 m.y. and ? 1900 m.y. ago from Rb-Sr and K-Ar dates (Evans and Tarney, 1964; Chapman, 1979).

After the emplacement of the Scourie dyke suite the Lewisian rocks in the northern and southern districts were metamorphosed and deformed in the Laxfordian orogeny which produced NW-SE oriented structures. The

rocks were metamorphosed under amphibolite facies conditions in the northern and the southern districts of the mainland. Although there are variations in the dates obtained from different areas by different workers, there is a general agreement on the age of c.1700 m.y. for the termination of the main Laxfordian amphibolite-facies metamorphism. According to Park (1980) there were two Laxfordian deformations in the period ending 1700 m.y. ago. .From the island of Rona a 1740±10 m.y.age was obtained by Lyon et al., (1973) from a pegmatite emplaced in the hinge zone of second-deformation Laxfordian folds (i.e. F_2 of the present work).

It has been suggested by Park (1980 and pers. comm.) that the third and fourth Laxfordian deformations took place during a period of greenschist-facies or lower retrogression and uplift which may have extended from c.1700 to c.1400 m.y.

There is much variation in the ages of especially late Laxfordian metamorphic and deformational episodes because of which Watson (1975) suggested that it was premature to make a formal subdivision of the Laxfordian events. However, it has been suggested by Watson (op.cit.) and Park (op.cit.) that the final cooling and uplift of the Laxfordian province was very slow, estimated by Sills (1983) as about $1C^{o}$ per one million years.

Detailed structural studies of small areas of the mainland and Outer Hebrides have been undertaken (e.g. Park, 1969, 1973; Cresswell, 1969, 1972; Dash, 1969; Coward, 1969; Crane 1978) but have failed to produce an overall agreement on the interpretation of the structural sequence. Yet some of the structures can probably be correlated for quite a long distance in the Lewisian. Highly asymmetric flat lying Laxfordian structures (F_2 in this thesis) can probably be correlated with the F_7 structures of the Diabaig inlier (Cresswell, op cit.) and

although at a long distance from the Outer Hebrides probably also with the flat-lying structures in South Uist (Coward, 1969, 1974) although different in their asymmetry and probably of different metamorphic grade. Simiarly NW-SE oriented upright late structures (F_3 in this thesis) are probably of the same age as the F_3 structures in South Uist (Coward, 1979, 1970), although again of different metamorphic grade. These upright structures are quite common in the Kenmore inlier but are absent in the Diabiag inlier.

In the last few years some work has been done to analyse the amount of strain semiquantitatively and qualitatively. Semiquantitative analysis has been undertaken by measuring the change in thickness of layers in the fold profile and from the fold shape (Coward, 1969) and by constructing the minimum strain ellipsoid using deformed quartz veins in host rock (Graham, 1980). Qualitative strain analysis in the Lewisian of the Outer Hebrides was done by measuring the discordant relationship of the dykes with the gneisses and by measuring the discordant relationship of the dykes with the gneisses and by using the shape fabric in the rocks (Coward, 1969,1976; Davies et al., 1975 and Lisle, 1977).

The Lewisian complex around Loch Torridon was initially described by Hinxman (in Peach et al., op. cit. pp.253-59) who subdivided the rocks in space and time into:

1. Those affected by a NE-SW foliation-producing event.
2. A basic dyke swarm.
3. Those affected by a NW-SE foliation producing event.

The area around Loch Torridon was subsequently studied by Sutton (in Sutton and Watson, 1951) who confirmed the tripartite division.

The first metamorphism of Sutton and Watson thought to be responsible for the transformation of a supracrustal series to a gneissic

complex foliated in a predominantly northeasterly direction.

The first metamorphism was followed by the intrusion of a series of dolerite dykes of north-west trend, indicating a period of crustal widening. According to them this event may be separated from the end of the first metamorphism by a period of denudation.

Their second metamorphism was responsible for the metamorphism of the dolerite dykes and of the complex produced in the first metamorphism with the production of a new complex foliated in a north-westerly direction. In the later stages of metamorphism, folding about north-west axes is succeeded by mylonitisation.

Most recently the area north of Loch Torridon was studied by Cresswell (1969, 1972). He recognised nine phases of deformation in that area, five of them being pre-dyke. He subdivided pre-dyke events into five deformations of which the first three culminated in the formation of north-easterly oriented structures (pre-Inverian deformation) and the latter two (Inverian deformation) were responsible for the formation of north-westerly oriented structures. He recognised four Laxfordian deformations, responsible for the formation of north-westerly oriented structures which affected both the dykes and the pre-Laxfordian complex. According to Cresswell dyke intrusion took place between the Inverian and Laxfordian deformations.

CHAPTER II

PETROGRAPHY

A. THE SCOURIE DYKES

It has been shown by many workers that the intrusion of the Scourie dykes took place over a prolonged period in which many suites of different composition have been injected but that the intrusions of the various compositions were not separated by any tectonic or metamorphic event (Teall, in Peach et al., 1907; Sutton and Watson, 1951 and Park, 1970). In parts of the Lewisian outcrop where dykes are undeformed, their intrusion sequence has been established by cross-cutting relationships or by multiple injection relationships. However, in the Kenmore inlier all the dykes have been deformed throughout the area and any original cross-cutting relationship has not been preserved after Laxfordian deformation.

In the inlier three petrographically distinct dyke groups are present:

a. The Main Amphibolite Suite.

b. Ultrabasic dykes.

c. "Soft Green" Dyke.

Of these three dyke groups the first one comprises most of the dykes and only a few dykes of the remaining two groups have been recorded. At a few places the first and second group dykes have been injected as multiple intrusions but in spite of a sharp contact between the two injections, the chronological relationship cannot be established due to later deformations. Only one dyke of the third group has been recorded but it is not in contact with any other dyke.

1. The Main Amphibolite Suite

Most of the dykes in the inlier belong to this category. Except at a place* 2 km south of Kenmore village, where a small part of one dyke is undeformed in the centre, all the dykes are deformed and have been converted into hornblende schist. In the field, the first foliation S_1 and the LS_1 fabric are quite clearly defined by alternating hornblende and feldspar-rich folia giving a good shape fabric foliation with the c-axis of the hornblende crystals lying parallel to it.

The dykes of this group comprise the "epidiorites" and "hornblende schists" of Teall (in Peach et al., 1907) of which the former is very localized. According to Teall (op. cit. p. 89) the epidiorites are plagioclase hornblende rocks with or without a mineral of the epidote group and the "hornblende schists" may be briefly described as foliated epidiorites. But since virtually all the dykes in the inlier are deformed and foliated, they fall into the category of hornblende schists. Mineralogically these are the same dykes which comprise the main dyke suite north of Loch Torridon and named "TD" basites by Cresswell (1969), and the "Second Period dykes" of Crane (1972) in the Kernsary area.

a. The undeformed dyke. Petrographic study has been done only from the undeformed central pod of the dyke present about 2 km south of the Kenmore village. This pod is about 5 m long and 2 m wide and is greenish black in colour and homogeneous looking in the field. It is present in the centre of the dyke, which has been deformed on its margins. Here the original igneous mineralogy and texture is still preserved with plagioclase laths making the main framework of the rock and interstitial pyroxene being rimmed by hornblende (see Pl. V - 1a). Also in places iron ore is present as a core rimmed by smaller hornblende grains.

* *Grid. Ref.* * *75605587*

Clinopyroxene forms about 22% of the rock. It is variable in shape, usually subhedral, and enclosed between interlocking plagioclase laths. Average grain size is about 0.3mm but crystals range between 0.05mm and 0.6mm in longest dimension. Pleochroism is very weak. Its colour scheme is X = colourless; Y = colourless; Z = very pale green. $C\Lambda Z = 40^{o}$. Normal 100 twinning is common.

All the grains are rimmed by a very thin layer of hornblende. Some of the pyroxene has been altered to uralite (fibrous amphibole), probably due to hydrothermal alteration.

Hornblende constitutes about 19% of the rock. It occurs in two forms. The first is as small subidioblastic and idioblastic grains of average diameter, about 0.05mm, occurring in the form of aggregates around a core of iron ore. In the second form it occurs as narrow crystallographically continuous rims around the core of pyroxene. It is strongly pleochroic with the colour scheme: X = pale yellow; Y = green and Z = green, with absorption $X<Y<Z$ $C\Lambda Z = -28^{o}$.

Plagioclase forms about 52% of the whole rock. It occurs as subhedral lath-shaped grains. When two plagioclase grains are in contact, the grain boundaries are either rational or irrational, but they are somewhat curved when plagioclase is in contact with some other mineral. The plagioclase laths are about 0.6mm in average length but range between 0.1 and 1mm.

The cores of the grains are slightly turbid due to very small inclusions while the rim is clear and free from them. The inclusions are very small and subrounded or needle shaped, mostly arranged in rows parallel to the cleavage. Albite, pericline and carlsbad-albite twins are common. Grains may or may not be zoned. When they are unzoned their composition is An 50% while in the zoned grains the

core has a composition of An 46% while the rims are An 33%.

Iron Ore occurs as subhedral to anhedral grains having a grain diameter of about 0.2 mm. In most places it is rimmed by aggregates of small hornblende grains. Sometimes it is also present in the cores of pyroxenes.

Quartz comprises about 2% of the rock. It occurs as xenoblastic grains with an average grain diameter of about 0.1 mm.

b. The dykes containing the first fabric. This is the most common fabric present in all the dykes and is penetrative throughout. Hornblende and plagioclase grains are separated into thin planar or flattened lens-shaped aggregates which are elongated in one direction or even rod-shaped giving respectively S, LS and L shape fabric foliation or lineation. Hornblende needles may be oriented either randomly or with a parallel alignment giving a mineral lineation parallel to the shape fabric lineation. However, in S or LS shape fabrics, hornblende needles may be aligned in the plane parallel to the shape fabric foliation with c - axes in variable directions.

In the central part of two dykes, layers of hornblendic material up to 10 cm thick are present which have been boudinaged into lenses.

Hornblende usually comprises between 43% and 55% of the rock but may be as much as 63% or as little as 27%. Its usual crystal length along the c - axis ranges between 0.6 mm and 2 mm with an average length of 1 mm, but it varies from 0.15 mm to 4 mm. Its width along the b - axis ranges from 0.12 mm to 2 mm, but in most cases it varies between 0.6 mm and 1.2 mm with an average of 0.8 mm. The majority of the slides have been cut perpendicular to the LS shape fabric in which most of the hornblende grains are oriented parallel to the shape fabric lineation, therefore, mainly basal or near-basal sections with two sets of cleavage intersecting at 124^{o} appear in the slide. This was also

observed by Teall (in Peach et al., 1907, p. 94) in the Ben Stack dyke.

Mostly the hornblende is subidioblastic in form. When hornblende grains are in contact with each other they usually have straight, rational or irrational grain boundaries, but when hornblende grains are in contact with other minerals, grain boundaries are mostly curved, generally convex towards the hornblende. Most grains are compact but some contain a few spherical quartz, or sometimes allanite, inclusions. The colour scheme is X = pale yellowish; Y = green, Z = bluish green.

Plagioclase usually comprises between 38% and 65% of the rock, but may make up as little as 25%. Grain diameters in the longest dimension vary between 0.1 mm and 2 mm with a mean of 0.7 mm. Grains are generally xenoblastic to subidioblastic. Grain boundaries are usually curved when plagioclase is in contact with any other phase but usually straight when two plagioclase grains are in contact and in such cases triple points are common.

Grains are twinned both on albite and pericline laws, both separately and together in the same grain. Although the composition varies from An 27% to An 44%, in most cases it is sodic andesine with composition ranging between An 30% and An 39%. Zoned grains are uncommon but both normal and reverse-zoned crystals have been observed with the core/rim composition difference not more than An 5%. In some cases oscillatory zoning has also been observed with as much as three zones.

Quartz is present in very variable amounts in the dykes. It comprises between 1% and 15% of the rock with an average of 6%. Its grain diameter varies between 0.05 mm and 1 mm with an average of 0.3 mm. Usually it occurs as xenoblastic grains with generally lobate grain boundaries when it is bigger in size, while small grains have

smoother boundaries.

Biotite has been observed in only 45% of the samples. When present it comprises up to 12% of the rock with an average amount of 3% in the rocks containing biotite (or 1.3% as an average of all the samples). Mostly it occurs as isolated flakes but when present in considerable amounts it occurs as interlocking flakes. Grain size in its longest dimension varies between 0.2 mm and 5 mm, with an average length of 1 mm. In many cases it is interlayered with chlorite.

Its colour scheme is mainly X = pale yellow; Y = Z = brown, but it also occurs with the colour scheme X = pale yellowish green, Y = Z = dark olive green.

Epidote may or may not be present in the rock. When present it never exceeds 1%. Its grain size ranges between .05 mm and 5 mm with a mean grain diameter of 0.2 mm. It usually occurs as subidioblastic grains. It is a colourless, non-pleochroic to slightly pleochroic variety. It usually occurs with chlorite, iron ore and some other minerals in isolated patches.

Sphene is the commonest accessory and has been recorded in virtually every slide. It constitutes between 1% and 2% of the rock. The grains are usually equal in size with grain diameter ranging between 0.05 mm and 0.3 mm with an average diameter of 0.1 mm along the long diameter of the lozenge. It usually occurs as subidioblastic to idioblastic crystals. The grains usually occur in the form of chain aggregates parallel to the foliation.

Apatite is also a common accessory, occurring as rounded to sub-idioblastic hexagonal grains dispersed through the slide with a mean grain diameter less than about 0.05 mm. It is mostly associated with plagioclase.

Allanite is a common accessory, usually occurring as minute yellowish grains with a mean grain diameter of 0.05 mm. Mostly it is associated with hornblende grains and forms the nucleus of a coloured, pleochroic halo in the host.

Chlorite may or may not be present in the rock. When present it never exceeds 2%. It occurs in three different forms:

The first type occurs as flakes interlayered with biotite or as completely separate flakes or is present along with hornblende. This variety is pleochroic from colourless to green.

The second occurs as needle-like crystals in the form of radiating aggregates like Japanese fans which may be isolated or in the form of aggregates. They have the same colour scheme as the flaky variety.

The third variety also occurs in the form of needles in radiating aggregates but in this case the aggregates are lens-shaped and occur along the 0001 cleavage of biotite.

c. The dykes containing the second fabric. It is difficult to differentiate S_2 from S_1 fabric in the field, except in relation to F_2 folds, and it is equally difficult to differentiate them under the microscope.

There is no change in the mineralogy of the S_2 fabric except that the plagioclase composition seems slightly more sodic (Fig. II - 1) with a composition range An 26% to An 31% (however, only a few thin sections with definite S_2 fabrics were examined).

The only textural difference is that there are more alternate plagioclase and hornblende-rich laminae per unit length than in S_1. Grain size seems somewhat smaller in this fabric in the field but there is actually no significant difference when studied under the microscope

Fig. II-1. Plagioclase composition in Scourie Dykes.

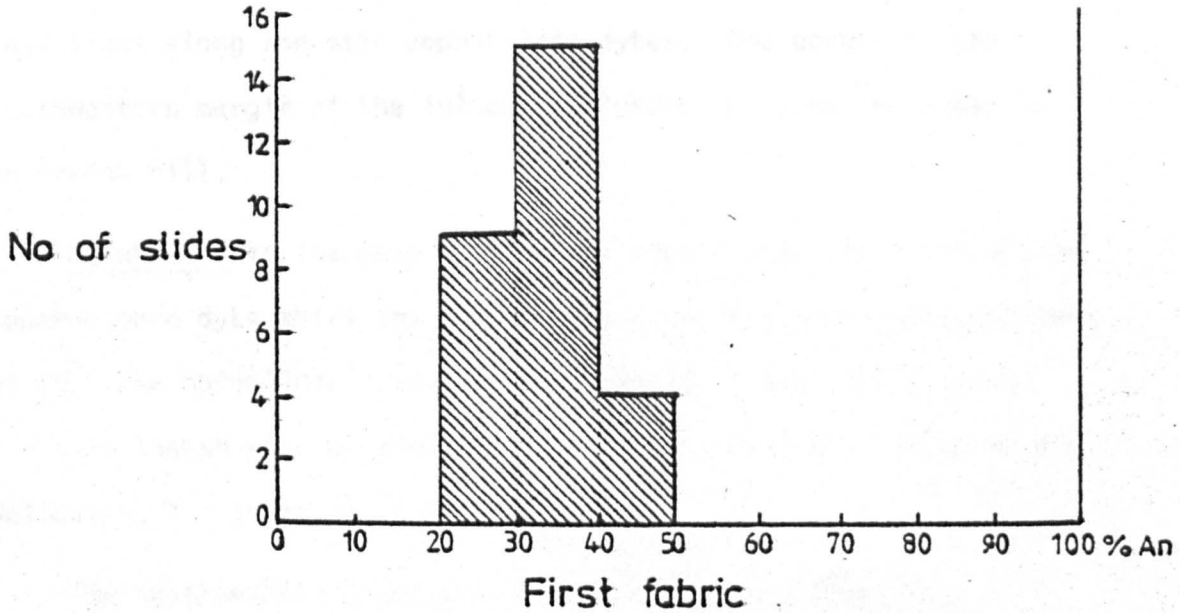
No of slides
16
14
12
10
8
6
4
2
0
0
10
20
30
40
50
60
70
80
90
100 % An
First fabric

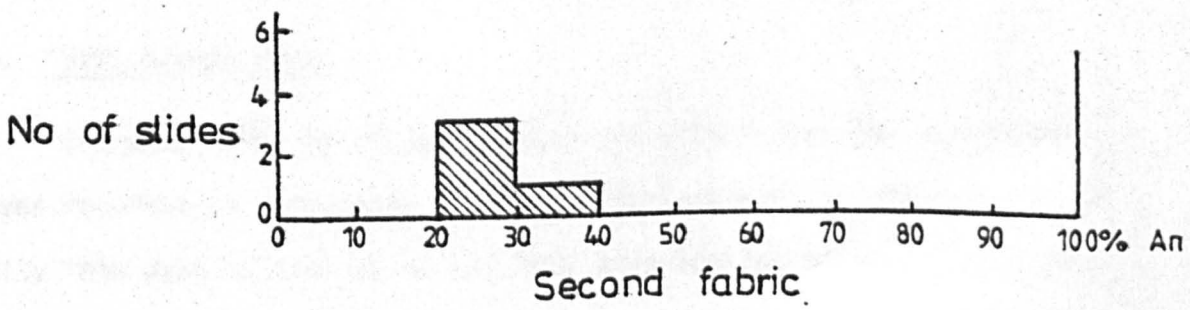
No of slides
6
4
2
0
0
10
20
30
40
50
60
70
80
90
100% An
Second fabric

2. Ultrabasic dykes

Only two thin dykes belonging to this group have been recorded in the inlier. Each is about one metre wide but cannot be traced for long distances. They have been intruded in the form of multiple injections along the main amphibolite dykes. One occurs at the southwestern margin of the inlier (Enclosure 1)and the other is on Arrina hill.

Hornblende is the main mineral and constitutes about 85% of the southwestern dyke while the Arrina dyke is nearly completely composed of it. The hornblende crystals range between 0.6 mm and 4 mm in c - axis length with an average of 1.4 mm. Its colour scheme is X = yellowish; Y = green and Z = bluish green.

The southwestern dyke contains up to 15% quartz while it is absent in the dykes of Arrina hill. The southwestern dyke contains only sphene as an accessory mineral while the dyke on Arrina hill contains sphene, apatite and iron ore as accessory minerals.

3. "Soft Green" Dyke

One dyke which is petrographically distinct from the others has been recorded on Ardheslaig peninsula (Enclosure 1). Petrographically this dyke is similar to the less acid-looking mica-rich dykes of the Gruinard area which Gunn (in Peach et al. 1907, p. 184) referred to as "Soft green dykes". The dyke in the Kenmore inlier is an isolated body which cannot be traced for a long distance and nothing can be said about its chronologic relationship with other dykes. However, in the Gruinard area these dykes are older than the main epidiorite dykes (equivalent to the main amphibolite suite in Kenmore).

Hornblende comprises about 57% of the rock. Its grain diameter (along the c - axis) ranges between 0.5 mm and 2 mm with an average

of 1.2 mm. Grains are inclusion free, idioblastic to subidioblastic in form with usually straight grain boundaries when two hornblendes in contact but somewhat curved when hornblende is in contact with plagioclase or quartz. Its colour scheme is X = yellowish; Y = green and Z = green with some bluish tint.

Plagioclase forms about 25% of the rock. It is usually of xenoblastic habit with grain size from 0.3mm to 1.5 mm with an average diameter of 0.6 mm. It is of glassy appearance and mostly untwinned.

Biotite forms about 15% of the rock. It is of subidioblastic habit with flake length between 0.3 mm and 5 mm with an average length of 1.2 mm. Its colour scheme is X = straw; Y = Z = deep brown with strong pleochroism and absorption X<Y = Z.

Quartz forms about 3% of the rock. Its grain size ranges between 0.1 mm and 1 mm with an average diameter of 0.3 mm. It is of xenoblastic habit with curved grain boundaries.

B. THE ACID GNEISSES

Although petrographically there are many different types of gneisses present throughout the area, it is neither possible nor necessary to discuss each type separately. Moreover they are so intermixed with each other that it is not possible to map them as separate rock units. The intermixing of the various rock types gives a strongly banded appearance to the gneissic terrain.

In this thesis the acid gneisses have been classified petrographically as follows:

1. Grey Gneisses.
2. Pink Gneisses.
3. Leucocratic Granite Sheets.

1. Grey Gneisses

Gneisses of this group are of granodioritic composition. They constitute the main part of the complex. They nearly always contain biotite and sometimes hornblende in addition. They may be completely devoid of microcline or contain it in small amounts. The gneisses of this group belong to Group IV 1 of Peach et al. (1907).

Plagioclase comprises between 30% and 80% of the rock but more usually between 60% and 70%. Its grain diameter ranges from 0.2 mm to 2 mm but typically from 0.6 mm to 1.2 mm. It is variable in shape, often of xenoblastic form with curved grain boundaries (except against the 0001 cleavage of biotite or sometimes when two plagioclase grains are in contact).

Most of the plagioclase is twinned on albite and pericline laws of which albite twinning is more common. Crystals are zoned both normally and reversed; oscillatory zoning is also present. Although its composition varies from An 19% to An 31%,the usual range is between 23% and 27% An.

Microcline may be completely absent but when present may constitute up to 15% of the rock. It always occurs as xenoblastic grains with curved grain boundaries and typically has embayed grain boundaries when situated between plagioclase grains. Its grain size varies between 0.2 mm to 2 mm with a typical grain diameter range between 0.3 mm and 0.6 mm.

Mostly the whole grain is twinned on the microcline law but sometimes only part of the grain is twinned.

Quartz may constitute 10% to 50% of the gneiss but usually occurs between 15% and 17%. Grain size ranges between 0.05 and 4 mm but typically between 0.4 mm and 0.9 mm. It is usually of xenoblastic

shape and generally occurs in the interstitial spaces of the feldspar grains. Grain boundaries are usually curved and lobate. Undulose extinction is universal.

Biotite is the main mafic mineral of the grey gneisses with only a few exceptions. Very rarely it is absent. Usually it occurs between 2% and 6% of the rock but sometimes constitutes up to 13%. Grains are subidioblastic in shape, ranging in the longest dimension between 0.2 mm and 4 mm but more often between 0.3 mm and 2 mm. Its usual colour scheme is X = pale green; Y = Z = dark olive green or X = pale tan, Y = Z = brown.

Hornblende may be absent or may form up to 8% of the rock. Grain shape is usually subidioblastic with some curved and ragged grain boundaries. In its maximum dimension the grain size ranges from 0.15 mm to 3 mm but is typically between 0.4 mm and 0.8 mm. Its colour scheme is X = pale yellow; Y = green and Z = bluish green.

Chlorite may or may not be present. It may form up to 5% of the rock, usually associated with biotite or hornblende but also as independent flakes. Its grain size is very variable with a maximum diameter of 1.5 mm.

Epidote is a common accessory, never exceeding 2%. It occurs as idioblastic to subidioblastic grains with curved or straight grain boundaries. It is a granular mineral with maximum grain size up to 0.5 mm in its longest dimension. It occurs in both colourless and greenish-yellow pleochroic varieties. Isolated grains may be present within plagioclase grains, or within biotite flakes. More often, it occurs along a biotite-plagioclase contact, with ragged biotite edges other than 0001, where it is usually oriented parallel to the gneissic foliation.

Apatite is a common accessory mineral, sometimes comprising as much as 1% in amount. It is variable in shape from idioblastic to xenoblastic. Grain diameter ranges between 0.1 mm and 0.2 mm usually and rarely up to 0.5 mm.

Sphene is uncommon, but is present in some rocks and never exceeds 5% in amount. It is usually subidioblastic or idioblastic in form. Its grain diameter never exceeds 0.1 mm.

2. Pink Gneisses

In the field, it is usually difficult to differentiate granite from granodiorite or any other acidic rock if it is of a pink colour. Whenever granodioritic rock is attacked by hematitic solutions its plagioclase turns into a pink colour which is very similar to K - feldspar in the field but in such a case the pink feldspar is inhomogeneously distributed through the rock. However, in this group only those rocks which look completely homogeneous in their pink colour in the field have been included and these are mainly granitic. The pink gneisses are present in the form of bands of varying thickness, ranging from a few centimetres to a few metres within the grey gneisses. In addition to granite, rocks of adamellitic and monzonitic varieties are also present. These rocks are generally foliated but non-foliated massive gneisses are also present.

Microcline comprises 40% to 62% of the rock. Its grain diameter varies between 0.5 mm and 2 mm but is typically between 0.8 mm and 1.3 mm. Grains are mostly of xenoblastic habit with usually curved boundaries, although sometimes relatively straight with occasional triple points. Microcline-microcline grain boundaries are relatively straight and there is generally a very thin layer of very fine-grained non-identified material between. Grain surfaces are commonly fresh.

Plagioclase usually forms between 4% and 34% of the rock but sometimes as much as 44%. The grain size ranges between 0.2 mm and 2 mm but typically between 0.5 mm and 1 mm. It is usually xenoblastic with curved and irregular grain boundaries. Sometimes it is dusty in appearance due to different minute inclusions of unidentified matter.

Grains are commonly twinned on the albite law but pericline twinning is also present. The composition is in the calcic oligoclase range (An 19% - An 27%), but occasionally sodic andesine (up to An 35%) is also present. Rarely some granites also contain plagioclase of albitic (An 5% - An 10%) composition.

Quartz usually constitutes between 15% and 45% of the rock, but in one sample (monzonitic) it is as low as 5%. Its grain size is very variable, and even in the same slides, it may vary from 0.05 mm to 10 mm. In mortar texture it is not very variable and ranges from 0.05 to 0.2 mm, but there are considerable variations in bigger grains which are usually ribbon-shaped and oriented parallel to the foliation. Grains are of xenoblastic shape and grain boundaries vary from straight to curved and lobate.

Chlorite may or may not be present. When present, it is variable in amount up to 4%. Flake length is variable and may be as long as 2 mm. It is always of a positive variety with colour scheme X = Y = pale green; Z = pale yellowish green or X = Y = green and Z = very pale yellowish, and with distinct pleochroism. Its flakes are always isolated and are oriented parallel to the foliation.

Biotite is absent in most rocks, but when present it forms up to 2% of the rock. It also occurs as isolated flakes varying in length from 0.2 mm to 1 mm. Its colour scheme is X = tan; Y = Z = dark brown or X = pale greenish yellow; Y = Z = greenish brown with strong

pleochroism and absorption X<Y=Z.

Muscovite is usually absent, but when present normally occurs up to 1% in amount though sometimes as much as 3%. Flake length is 0.1mm to 0.3mm. When it is present in quantity, the flakes are in the form of aggregates parallel to the foliation. It is usually associated with plagioclase, either within the plagioclase grains or wrapped around them.

Epidote is usually present. It occurs in the form of granular aggregates and comprises up to 1% of the rock. It may be colourless or very weakly pleochroic. The grain size usually ranges up to 0.2mm and rarely is as much as 0.7mm in its longest dimension.

3. Leucocratic Granite Sheets

These sheets are usually one-half to three metres thick penetrating into the gneisses parallel to the foliation throughout the inlier giving a banded appearance to the gneisses. They are highly acidic leucocratic rocks and appear as whitish to slightly pinkish foliated pegmatites in the field, because of which Horne (in Peach et al. 1907, pp.39-40) described them in the Loch Torridon area as follows:

".....A large portion of the gneisses is there composed of highly acidic rocks composed of quartz and feldspar, like a foliated pegmatite".

Hinxman (op.cit. p.255) states:

".....A large portion of it is highly acid, consisting chiefly of quartz and feldspar, and having the appearance of a foliated pegmatite. These pegmatitic bands which are now thoroughly incorporated and plicated with the gneisses may represent an early acid intrusion forming part of the rocks of the original complex".

The foliation in these bands is defined by alternating laminae of quartz and feldspar. More commonly they are of granitic composition, but some adamellitic and even granodioritic types have been found.

Microcline is usually the main constituent, forming between 18% and 69% of the rock but more typically between 45% and 60%. It usually occurs as xenoblastic grains with grain size ranging between 0.2 mm and 5 mm but more typically between 0.6 mm and 1.2 mm. Microcline-microcline grain boundaries, although straight, are not usually sharp . This is because of a change in the mineral composition, probably due to a solution effect, or to the presence of a very fine-grained mixture of minerals or sometimes to thin sleeves of muscovite. Most of the grains are twinned on the microcline law.

Plagioclase forms between 7% and 30% of the rock. It is of xenoblastic form. Grain size varies between 0.2 mm and 5 mm but more usually between 0.4 mm and 1.2 mm. Grains are twinned on the albite or pericline law but albite twinning is more common. Plagioclase composition ranges from An 22% to An 34% but compositions between An 22% to An 27% are more common.

Quartz comprises from 20% to 30% of the rock. The grain size is very variable; it ranges from as small as 0.01 mm to as large as 10 mm in its longest dimension. Most of the smaller grains have mean grain diameters between 0.1 mm and 0.2 mm while large grains show much variation in size. Smaller grains show uniform extinction while undulose extinction is normal in larger grains. Smaller grains usually, and larger grains sometimes, show diffuse grain boundaries which change their position on rotation of the microscope stage, but sometimes also show straight and sharp grain boundaries with good annealed texture. Larger grains are more usually elongated and ribbon-shaped.

Muscovite is an ubiquitous mineral in this rock type, but it never exceeds 2% of the rock and cannot be seen in the hand specimen. It usually occurs in the form of shredded aggregates of small thin flakes, but it also occurs in the form of isolated flakes. Its flake

length never exceeds 0.5 mm in the longest dimension.

Epidote may or may not be present. If present, it forms up to 1% of the rock. Grain size is very variable, ranging between 0.01 mm and 0.2 mm, rarely occurring as long as 0.5 mm in its longest dimension. Larger grains usually occur in isolation, while smaller grains occur in aggregates.

Biotite is rarely present and never exceeds 0.5%. Its flake length is usually small, never exceeding 0.7 mm. Its colour scheme is X = pale yellow, Y = Z = brownish with strong pleochroism and absorption X<Y=Z.

C. POSSIBLE METASEDIMENTARY ROCKS

In the inlier there are some scattered thin isolated bands which, due to their mineralogy, look like metasediments. Sutton (in Sutton and Watson, 1951) has also recorded several types of metasedimentary units around Loch Torridon. Two types of such band have been recognised in the Kenmore inlier:

1. Quartzites.
2. Strongly foliated dark coloured tonalitic gneiss interbanded with quartz-epidote bands.

1. Quartzites

In the field these are massive-looking to foliated white coloured or light grey bands of glassy appearance, but in thin section they are strongly foliated. They are 1 m to 3 m thick and cannot be traced more than 10 m along the strike. Two such bands have been recorded in the area, one on the western slopes of A'Bhainlir hill and the other on Ardheslaig peninsula, about half a kilometre NNW of Ardheslaig village (Enclosure 1).

Quartz consitutes between 80% and 96% of this rock. It is in

small grains with usual grain size ranging between 0.02 mm and 0.1 mm, but sometimes up to 4 mm in its longest dimension with a mean grain diameter of 0.07 mm. Longer grains are ribbon-shaped, usually with numerous subgrains, and show strong undulose extinction. Smaller grains show uniform extinction but still with irregular and diffuse grain boundaries which change their position on the rotation of the stage.

Plagioclase forms between 2% and 18% of these bands. Its grain size ranges between 0.2 mm and 1.5 mm with a mean grain diameter of about 0.4 mm. The grains are xenoblastic with curved grain boundaries, or are lens-shaped, which is probably due to mechanical breakdown of the boundaries. It is of calcic oligoclase composition.

Biotite forms up to 2% of the rock. Its flakes are isolated from each other and are parallel to the foliation. These flakes have a lens shaped outline and are between 0.1 mm and 0.5 mm in length with an average grain diameter of 0.3 mm. The colour scheme is either X = pale greenish yellow; Y = Z = green or X = pale yellow, Y = Z = brownish with pleochroism and absorption X<Y=Z.

Chlorite forms up to 1% of the rock. Its flakes may be associated with biotite flakes, parallel to the biotite cleavage or may be present in isolation. It is pleochroic from colourless to light green.

Epidote and muscovite occur in very small quantities.

2. Strongly foliated dark coloured tonalitic gneiss interbanded with quartz-epidote bands

These are small, isolated bodies never exceeding 4 m in thickness and cannot be traced more than 30 m along the strike. They are of very restricted occurrence. The best outcrop is about 300 m SW of Ardheslaig village (Enclosure 1). They are composed of alternating layers of a

tonalitic type of rock, interbanded with quartz-epidote layers. Due to the very limited occurrence, only two samples, from the outcrop near Ardheslaig village, have been examined.

a. Tonalitic gneiss. Plagioclase constitutes about 38% of the whole rock. Its grain size varies between 0.6 mm and 2 mm with a mean grain diameter of 1 mm. Grains are of xenoblastic habit, usually with curved grain boundaries except against biotite flakes, where grain boundaries are parallel to the 0001 biotite cleavage. Its composition is in the calcic oligoclase range (An 26%). It is strongly sericitized.

Quartz forms up to 27% of the rock. Its grain size is very variable, ranging between 0.2 mm and 6 mm with an average of 0.7 mm. It is of xenoblastic habit with curved grain boundaries.

Hornblende comprises about 25% of the rock. It is of subidioblastic habit. Grain size ranges between 0.1 mm and 4 mm but more usually between 0.6 and 1.2 mm. Its colour scheme is X = yellow; Y = green and Z = bluish green. $C\Lambda Z = -17^{o}$.

Antigorite usually occurs as pseudomorphs after hornblende, such that the amphibolite cleavage is still well preserved. Its colour scheme is X = pale yellow, Y = Z = yellowish green. It constitutes up to 5% of the rock.

Biotite forms about 3% of the rock. Its flake length usually ranges between 0.5 mm and 1.5 mm with an average of 0.8 mm. Its colour scheme is X = pale yellow, Y = Z = olive green.

Iron ore, apatite and allanite are accessory minerals.

b. Quartz-Epidote bands. This rock occurs as 4 cm to 12 cm thick flaggy layers of glassy appearance and of a whitish or greenish-white colour in the field. In thin section, quartz and epidote and feldspar are concentrated in separate folia such that there are more than

10 folia per centimetre.

Quartz is the main mineral, forming about 70% of the bands. Its usual grain size ranges between 0.2 mm and 3 mm. Grain boundaries are irregular and curved and grains are of xenoblastic habit.

Epidote forms about 12% of these bands. It is of two different varieties and compositions. One is a colourless non-pleochroic variety of idioblastic and subidioblastic habit with usually straight grain boundaries. The second variety is of xenoblastic habit with curved grain boundaries and is slightly pleochroic from colourless to greenish yellow. The colourless variety is more abundant, with its grain ranging between 0.2 mm and 0.5 mm.

Plagioclase forms about 10% of the rock. It is so strongly sericitized that it is difficult to measure its composition. Grains are of xenoblastic habit with curved grain boundaries.

Hornblende constitutes about 7% of the rock. It usually occurs as subidioblastic grains with straight grain boundaries. Its grain diameter ranges between 0.1 mm and 0.8 mm in its longest dimension with an average of 0.3 mm. Its colour scheme is X = pale greenish yellow; Y = green and Z = bluish green.

Chlorite is of a colourless to light green pleochroic variety. It occurs as xenoblastic grains and comprises about 1% of the rock.

D. SHEETS OF INTERMEDIATE COMPOSITION

At quite a few places, dark coloured mica-rich rocks are present. These are sheet-like bodies very much similar to the Scourie dykes but slightly lighter in colour in the field and they are somewhat migmatized. They are pre-dyke and form an integral part of the gneissic terrain.

Plagioclase forms 34% to 69% of the rock. Its grain size ranges

between 0.2 mm and 1.5 mm but typically between 0.5 mm and 0.8 mm. It is usually variably clouded due to the presence of abundant minute inclusions of unidentified matter. It is usually of xenoblastic habit with straight to curved grain boundaries. Grains are frequently twinned on the albite law. It is of calcic oligoclase (An 21% to An 28%) composition.

Microcline is not always present, and never exceeds 3%. Its grain size ranges between 0.15 mm and 1.5 mm. Grains are usually of xenoblastic habit with usually curved grain boundaries. Grains are commonly twinned in cross-hatched style.

Hornblende constitutes 20% to 32% of the rock. Its grain size ranges between 0.2 mm and 2 mm along its longest dimension with an average of 0.6 mm. It is of subidioblastic nature with straight to curved grain boundaries. Its colour scheme is X = yellowish; Y = green and Z = bluish green.

Biotite forms between 5% and 23% of the rocks. Its flake length ranges between 0.3 mm and 2 mm with a mean grain length about 0.8 mm. It is of subidioblastic habit. Its colour scheme is X = pale greenish yellow, Y = Z = olive green.

Quartz comprises between 5% and 12% of the whole rock. It is generally of xenoblastic habit. Its grain size ranges between 0.1 mm and 0.7 mm but typically between 0.2 mm and 0.4 mm.

Chlorite occurs in very small amount. It has been found only in a few slides in association with biotite flakes. It is an optically positive variety with colour scheme X = Y = green and Z = pale greenish yellow. It never exceeds 2%.

Iron ore may or may not be present and never exceeds 3%. Its grain diameter varies between 1 mm and 3 mm. It has usually a sub-

idioblastic form.

Apatite is very rare and never exceeds 1%. Its grain size usually ranges between 0.2 mm and 0.3 mm. It is usually of xenoblastic form with curved grain boundaries.

Sphene is also a common accessory. It occurs as small subidioblastic lozenge-shaped grains occurring in isolation. Grain diameter is usually 0.1 mm. It never exceeds 1% of the whole rock.

E. LAYERS AND LENSES OF MIGMATIZED EARLY BASIC

These are present throughout the area associated with grey gneisses. The bodies range from a couple of metres to a few tens of metres in length. They are strongly migmatized and traversed by numerous acidic veins. Here only the petrography of the palaeosome is given, because the neosome generally consist only of quartzo-feldspathic material.

Hornblende comprises between 42% and 73% of the rock. It is usually of subidioblastic habit with straight to curved grain boundaries which are also sometimes ragged. Its colour scheme is X = yellow; Y = green and Z = bluish green. $C\Lambda Z = -24^{o}$.

Plagioclase is the ubiquitous and the dominant feldspar. It occurs between 18% and 52%. Grains are twinned on pericline and albite laws of which the latter is more common. Its composition is Oligoclase-Andesine (An 25% to An 45%). Grains are usually of granoblastic habit with curved grain boundaries but are sometimes straight with triple points.

Microcline is usually absent, but when present it never exceeds 12%. Grains are commonly xenoblastic with curved grain boundaries.

Quartz usually occurs between 1% and 3% but sometimes forms up to 15%. It is of xenoblastic habit with curved grain boundaries.

Clinopyroxene occurs in some layers and constitutes up to 3% of the rock. It is a colourless variety, of xenoblastic habit, always with ragged grain boundaries.

Epidite is a common accessory, usually occurring up to 1%, but exceptionally it forms as much as 3%. It is a colourless variety of granular habit.

Allanite and apatite are present in minor amount.

Garnet has been recognised only in one slide. It is of subidioblastic habit and is strongly cracked. Average grain diameter is 1 mm. It forms about 1% of the rock.

F. THE LAXFORDIAN GRANITE SHEETS

In the inlier some pink granite sheets of Laxfordian age have been recognised (Enclosure 1) by their cross-cutting relationship with Scourie dykes. In most of them a mylonitic foliation is present which appears in hand specimen as very fine, not more than 1 mm thick, quartz folia with very small feldspar porphyroblasts, less than 2 mm across in diameter.

The best exposure of a granite sheet occurs on the southern slopes of the hill between Kenmore and Arrina, just north of Loch na Caorach (Enclosure 1). This sheet is about 2-3 m thick, and can be traced about 1 km along its strike, NNW-SSE in a discontinuous way. Another sheet of similar type is present about 400 m east of Loch a Choire Bhuidhe. This is about 15 m thick. A third sheet about 2 m thick is present just east of Loch Gaineamhach. None of these sheets can be traced far due to bad exposure.

A 1 m thick sheet of adamellitic composition is present on the hill southeast of Loch a Choire Bhuidhe, northwesterly oriented and crossing a dyke.

Microcline forms 32% to 50% of the rock. Its grain size including porphyroblasts, ranges between 0.1 mm and 3 mm with a mean grain diameter of 0.6 mm. It is usually of xenoblastic habit with irregular, curved and corroded grain boundaries. Crosshatched twinning is very common.

Plagioclase usually constitutes between 8% and 15% of the granite sheets, but forms up to 36% of the adamellitic sheet. Grain size ranges between 0.1 and 4 mm with an average of 0.5 mm. It is of xenoblastic habit with irregular, rounded and corroded grain boundaries. Albite twinning is common in the grains. Its composition range is at the oligoclase-andesine boundary (An 25% - An 32%).

Quartz comprises between 30% and 55% of the rock. Its grain size is very variable, ranging between 0.01 mm and 4 mm. There is not much variation in the size of the smaller grains which range between 0.02 mm and 0.2 mm. Larger grains are inequidimensional and are usually ribbon-shaped, while smaller ones are of granular habit.

Muscovite forms up to 1% of the rock. It usually occurs in the form of shredded aggregates. Its flake length usually ranges between 0.2 and 0.3 mm but is sometimes as long as 0.6 mm.

Epidote also constitutes up to about 1% of the rock. It is of granular habit with usual grain diameter ranging between 0.02 mm and 0.25 mm in the granitic sheets and between 0.1 mm and 0.4 mm in the adamellite. It is a colourless variety.

Chlorite may either be absent or present as an accessory mineral. Its flake length never exceeds 0.3 mm. It is a pale green variety with slight pleochroism.

Biotite also may either be absent or present in very small amounts. Grain size is very small but flakes up to 1 mm long are also present.

Its colour scheme is X = greenish yellow, Y = Z = green.

Sphene occurs as an accessory mineral in very small amounts in the adamellite, but is completely absent in the granites.

G. THE LAXFORDIAN PEGMATITES

Pegmatite veins and sheets of whitish or pinkish colour are present throughout the area. Their thickness ranges from a few centimetres to as much as 10 metres. They are sometimes concordant but mostly they are discordant to all the structures. They are variable in composition; some are microcline-rich while others are plagioclase-rich, and quartz is always present in small quantity. Other minerals which may or may not be present in individual sheets are biotite, muscovite and epidote in accessory amounts. Rock composition in some cases is uniform across the sheet while other sheets are zoned and have a quartz rich core. Usually the sheets are deformed and lineated or foliated in places, although completely undeformed sheets are also present.

Table II-1. Minerals present in different rock units. The mineral species are given in according to their proportion in the rocks.

Q = Quartz	Py = Pyroxene
K = K-feldspar	E = Epidote
P = Plagioclase	Sp = Sphene
H = Hornblende	Ap = Apatite
B = Biotite	Al = Allanite
M = Muscovite	Pr = Prehnite
Cl = Chlorite	Pm = Pumpellyite
I = Iron ore	

Table II 1

Lithological Group	Lithological unit	
Scourie dykes	Main Amphibolite Suite — Undeformed	P Py H Q I
	Main Amphibolite Suite — Deformed	H P Q B Sp ± E ± Ap ± Al ± Cl ± I ± Pr ± Pm
	Ultrabasic dykes	H ± Q ± Sp ± Ap ± I
	"Soft Green" Dyke	H P B Q
Acid Gneisses	Grey Gneisses	P Q B ± H ± M ± Sp ± E ± Cl ± Ap ± I
	Pink Gneisses	K Q P ± B ± M ± E
	Leucocratic Gneisses	K Q P M ± B ± E
Possible Metasedimentary rocks	Quartzites	Q P B Cl ± E ± M
	Tonalite gneiss	P Q H Anti B
	Quartz-Epidote bands	Q E P H
Sheets of Intermediate composition		P H B Q ± K Cl ± I ± Sp ± Ap
Layers and lenses of migmatized early basic		H P Q K Cl P ± E ± Ap ± Al ± G ± Pr ± Pm
Laxfordian Granite		Q K P M E ± Cl ± B ± Sp

Table II-2. Percentages of important minerals in various rock units. Figures in brackets are arithmetic mean values. tr. indicates phases present in small amounts.

Table II 2

Lithological Group	Lithological unit		Quartz	Plagioclase	K-feldspar	Hornblende	Pyroxene	Biotite	Muscovite	Chlorite	Epidote	Sphene
Scourie Dykes	Main Amphibolite Suite	Undeformed	2	52	-	19	22	-	-	-	-	-
		Deformed	1-15 (6)	25-65 (43)	-	27-63 (46)	-	0-12 (1.3)	-	0-2 (tr.)	0-1 (tr.)	1-2 (1.4)
	Ultrabasic dykes		0-15 7.5	-	-	85-100 (92)	-	-	-	-	-	0-tr
	"Soft Green" Dyke		3	25	-	57	-	15	-	-	-	-
Acid Gneisses	Grey Gneisses		10-50 (23)	30-80 (63)	0-15 (4.5)	0-8 (2)	-	2-13 (4)	-	0-5 (1.3)	tr.-2 (tr.)	0-5 (tr.)
	Pink Gneisses		5-45 (25)	4-44 (25)	40-62 (50)	-	-	0-2 (tr.)	0-3 (tr.)	0-4 tr.	0-1 (tr.)	-
	Leucocratic Granite Sheets		20-30 (26)	7-30 (25)	18-69 (45)	-	-	tr.	tr.-2 (0.7)	-	0-1 (0.7)	-
Possible Metasedimentary rocks	Quartzites		80-69 (88)	2-18 (10)	-	-	-	tr.2 (1)	tr.	tr.	tr.	-
	Tonalitic gneiss		27	38	-	25	-	3	-	5	-	-
	Quartz-Epidote bands		70	10	-	7	-	-	-	1	12	-
Sheets of intermediate composition			5-12 (9)	34-69 (48)	0-3 (1)	20-32 (26)	-	5-23 (13)	-	tr.-2 (tr.)	tr.	tr.-1 tr.
Layers and lenses of migmatized Early basic			1-15 (4.2)	18-52 (34.6)	0-12 (2.4)	42-73 (55)	tr.-3 (1)	-	-	tr.	tr.-3 (0.8)	-
Laxfordian Granite			30-55 (42)	8-36 (17)	32-50 (39)	-	-	tr.	tr.-1 (0.7)	tr.	tr.-1 (0.7)	-

Table II-3. Grain diameters in millimetres of important minerals in various rock units. Figures in brackets are arithmetic mean values. Grains have been measured along their longest dimension.

Table II 3

Lithological Group	Lithological unit		Quartz	Plagioclase	K-feldspar	Hornblende	Biotite	Pyroxene
Scourie Dykes	Main Amphibolite Suite	Undeformed	0.05-0.4 (0.1)	0.1-1 (0.6)	-	0.02-0-1 (0.05)	-	0.05-0.6 (0.3)
		Deformed	0.05-1 (0.3)	0.1-2 (0.7)	-	0.15-4 (1)	0.2-5 (1)	-
	Ultrabasic Dykes		0.05-0.5 (0.15)	-	-	0.6-4 (1.4)	-	-
	"Soft Green" Dyke		0.1-1 (0.3)	0.3-1.5 (0.6)	-	0.5-2 (1.2)	0.3-5 (1.2)	-
Acid Gneisses	Grey Gneisses		0.05-4 (0.6)	0.2-2 (1)	0.2-2 (0.4)	0.15-3 (0.7)	0.2-4 (0.7)	-
	Pink Gneisses		0.05-10 (0.6)	0.2-2 (0.7)	0.5-2 (1.1)	-	0.2-1 (0.4)	-
	Leucocratic Granite Sheets		0.01-10	0.2-5 (0.7)	0.2-5 (1)	-	0.1-0.8 (0.3)	-
Possible Metasedimentary rocks	Quartzites		0.02-4 (0.07)	2-1.5 (0.4)	-	-	0.1-0.5 (0.3)	-
	Tonalitic gneiss		0.2-6 (0.7)	0.6-2 (1)	-	0.1-4 (0.6)	0.5-1.5 (0.8)	-
	Quartz-Epidote bands		0.2-3 (0.8)	0.1-2 (0.4)	-	0.1-0.8 (0.3)	-	-
Sheets of intermediate composition			0.1-0.7 (0.3)	0.2-1.5 (0.6)	0.15-1.5 (0.25)	0.2-2 (0.6)	0.3-2 (0.8)	-
Laxfordian Granite			0.01-4	0.1-4 (0.5)	0.1-3 (0.6)	-	0.2-1 (0.4)	-

CHAPTER III

STRUCTURAL SEQUENCE AND GEOMETRY

A. INTRODUCTION

The aims of this chapter are to describe and interpret the geometry of the various small and large scale structures including folds and tectonic fabric (i.e. the foliation and the lineation), to try to correlate them, and to establish the sequence of structures in the inlier.

It will be shown that the area was affected by polyphase deformation and that, with the exception of a small pod near Ardheslaig, the whole area was deformed during the Laxfordian, of which three phases are important and widespread in the area.

The structural chronology has been established at certain places by the refolding relationship of the various structures with each other. Then some important features of these folds, and associated with these folds, were studied at those places where the refolding relationship was observed, in order to correlate structures of a specific age with the structures present in the other parts of the inlier. Those important features associated with the folds, which could be in any combination are given below:

(1) Their geometry in profile - e.g. concentric or similar style.

(2) Their orientation in space - i.e. attitude of their axial surfaces and their hinges.

(3) Whether any fabric is associated with them.

(4) Their association and symmetry with large scale structures and

(5) Whether they are folding the Scourie dykes or are cut off by the dykes.

Detailed structural analysis of the rocks of this inlier reveals that the area was affected by at least six phases of deformation as briefly outlined below:-

(1) First Pre-Inverian deformation (DP1). Formation of PS1 foliation.

(2) Second Pre-Inverian deformation (DP2). PS1 has been tightly folded and transposed into PS2.

(3) Inverian deformation (DI). Strong IS foliation and IF folds. The foliation is axial planar to the folds but is so strong all over the area that it has destroyed the early foliation at most places.

(4) First Laxfordian deformation (DL1). Strong LS_1 fabric and occasional F_1 folds.

(5) Second Laxfordian deformation (DL2). F_2 folds and LS_2 axial planar fabric.

(6) Third Laxfordian deformation (DL3). F_3 folds and S_3 axial planar foliation.

(7) Late Laxfordian deformation. Late cross folds, cataclasis and brecciation.

Out of these deformations only 3 to 6 are important in the present context and only 5 and 6 involve significant regional folding. Since the thesis is concerned primarily with the Laxfordian deformation, D_2 and D_3 will be used for convenience in this thesis for the second and third Laxfordian deformations (DL2 and DL3) and F_2 and F_3 will be used respectively for the folds associated with these deformations.

The Scourie dykes were intruded between the 3rd and 4th deformations.

1. The Structural Sequence

The Pre-Inverian (Badcallian) structures are the earliest structures to have been observed in the areas around Loch Torridon and in other parts of the Lewisian. They are northeast-southwest oriented structures. These Pre-Inverian structures were later cut off by strong northwest-southeast oriented Inverian structures in the northern and southern districts of the Lewisian outcrop (see Chapter I). The Inverian deformation was followed by the intrusion of the Scourie dykes which along with the host gneisses were affected by strong Laxfordian deformation which produced northwesterly oriented structures. The Laxfordian deformation was also mainly restricted to the northern and the southern districts of the seaboard, only very thin zones of the Laxfordian deformation affecting the central district.

Although the Scourie dykes have probably been introduced over a long time span, which lasted up to hundreds of million years (see section F, Chapter I), there is no evidence that they are separated by any deformation. The dykes have therefore been used as stratigraphical markers to differentiate the pre- and post dyke structures. Those structures which are cut off by dykes have been classified as pre-dyke structures while the structures which deform the dykes have been classified as post-dyke structures.

a. Pre-dyke structures. Among the pre-dyke structures, the most important is the northwesterly striking planar IS fabric in the gneisses which is much reoriented and modified in the Laxfordian deformation. In most of the area dykes are concordant with this gneissic foliation (Pl. III-1a) but in some places discordant relationships are also present (Pl. III-1b). Original concordant relationship have also been observed

Plate III-1a. Completely concordant dyke. Dyke is strongly deformed and its foliation is parallel to the gneissic foliation (77905673).

Plate III-1b. Dyke is discordant to the host gneisses, although weakly deformed. (78635555).

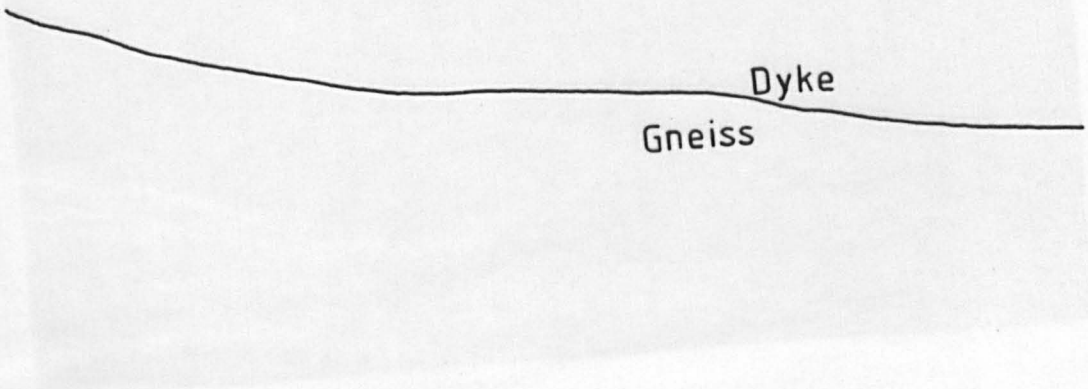
Dyke
Gneiss

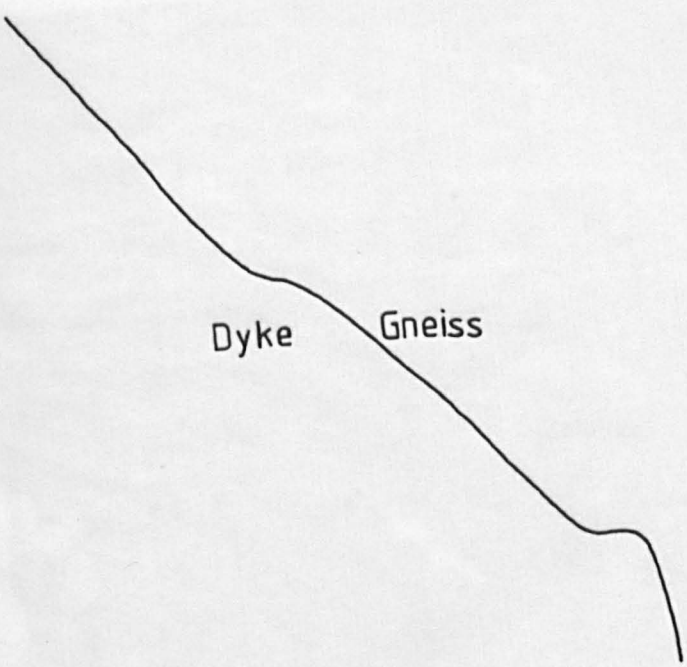
Dyke
Gneiss

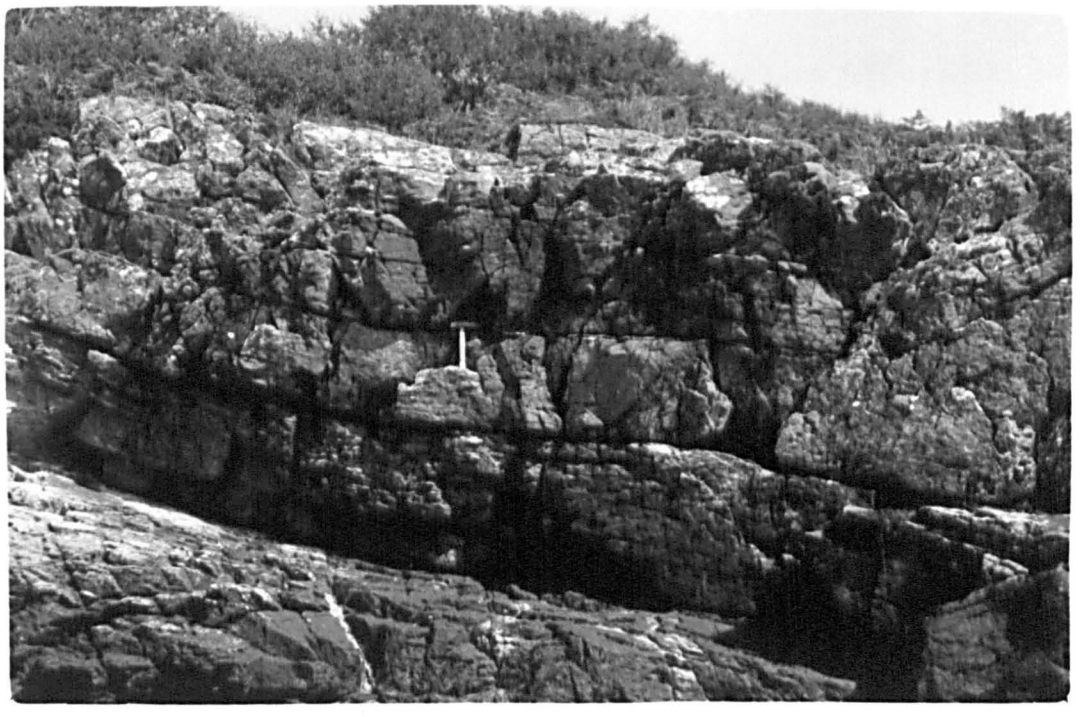

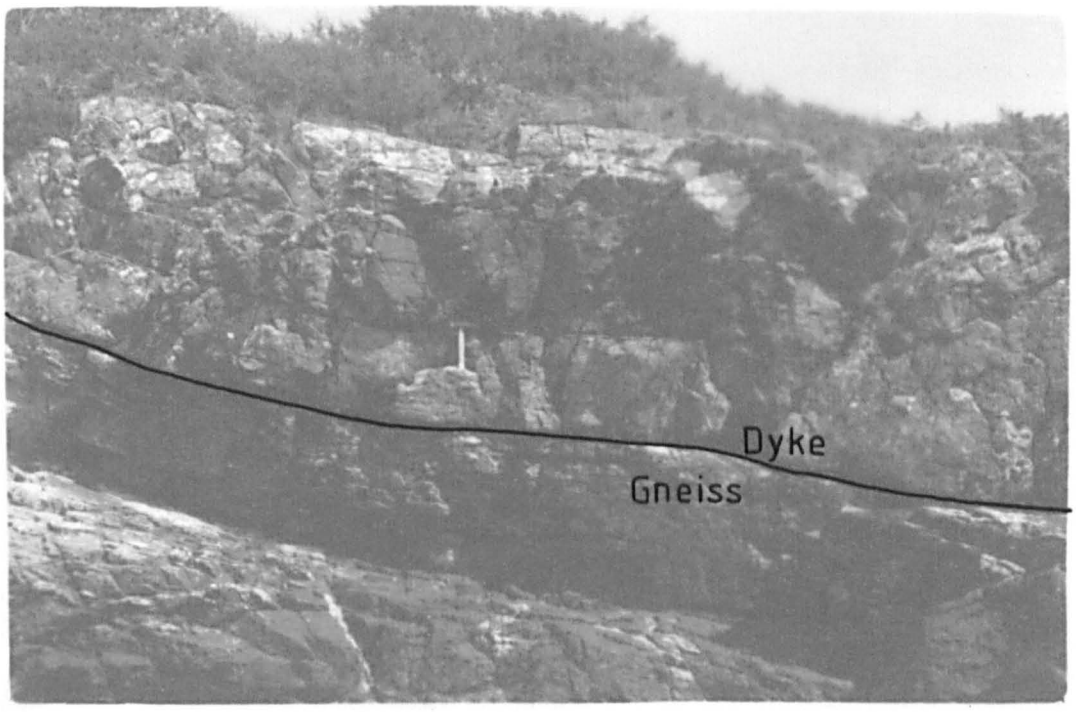
Dyke
Gneiss

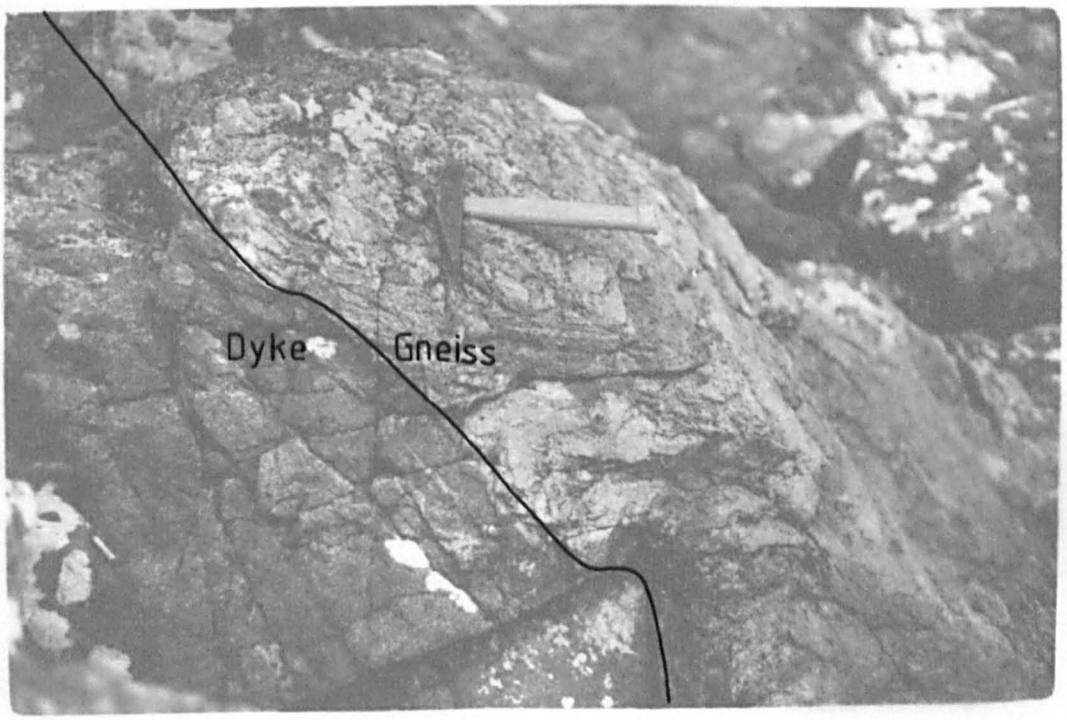
Dyke
Gneiss

in some areas leading Park and Cresswell (1972, 1973) to use the term sheets for such sill-like intrusions. In some places where dykes are discordant and their contacts are undeformed, small dyke apophyses have been intruded into the gneisses along their foliation planes (pl. III-2a). On the other hand concordance has been observed in areas of strong deformation where dyke discordance has been reduced or even obliterated due to Laxfordian deformation, while in the areas of low Laxfordian deformation discordant relationships are still preserved. Therefore it has been suggested that the concordant nature of the dykes is due to a combination of both factors.

The gneissic banding and all types of foliation are strongly oriented in a NW-SE direction. All types of metamorphically produced s-surface are defined as foliation here. They may be:

(1) Alternating laminae of mafic and felsic minerals or of feldspar and quartz in which mineral grains are either randomly or preferentially oriented.

(2) Preferential orientation of mineral grains especially of platy habit but without lamination of different minerals, or

(3) The combination of (1) and (2).

All are penetrative in hand specimen. A large scale banding within the gneisses is by sheets of more leucocratic granitic and more biotite rich granitic gneiss.

The Inverian foliation IS is itself a transposed earlier foliation but the transposition is so strong that, except at a few places, it has almost destroyed all previous structures. One of the localities where this transposition can be demonstrated is shown in plate III-2b. At

Plate III-2a. A small discordant dyke branch from which small apophyses penetrate concordantly into the gneiss (77425598).

Plate III-2b. Strongly transposed Inverian foliation in the gneiss. The Pre-Inverian banding is still preserved and is subvertical to the right (75155768).

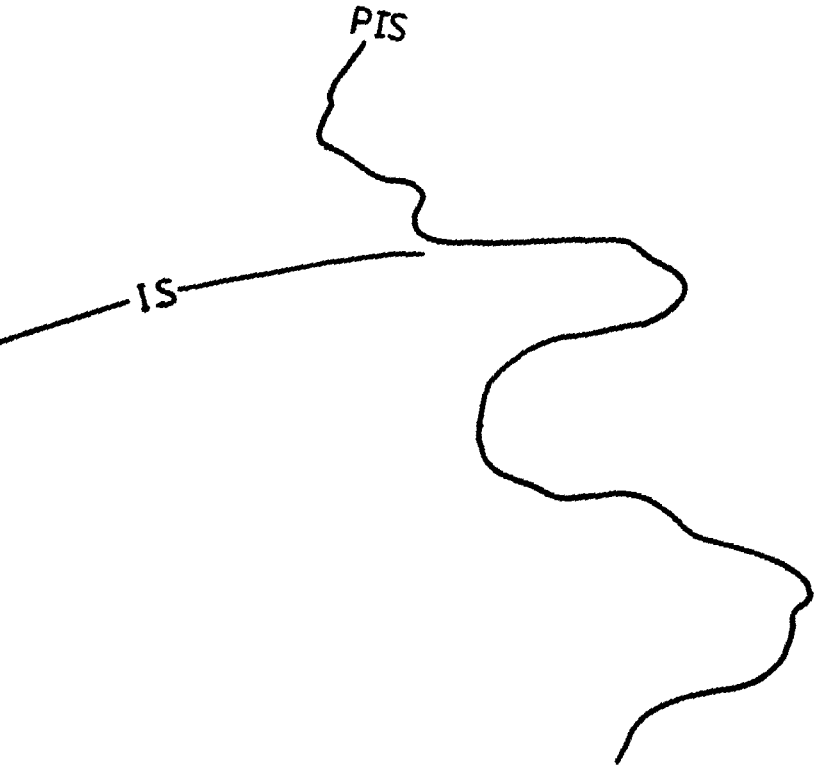
PIS
IS

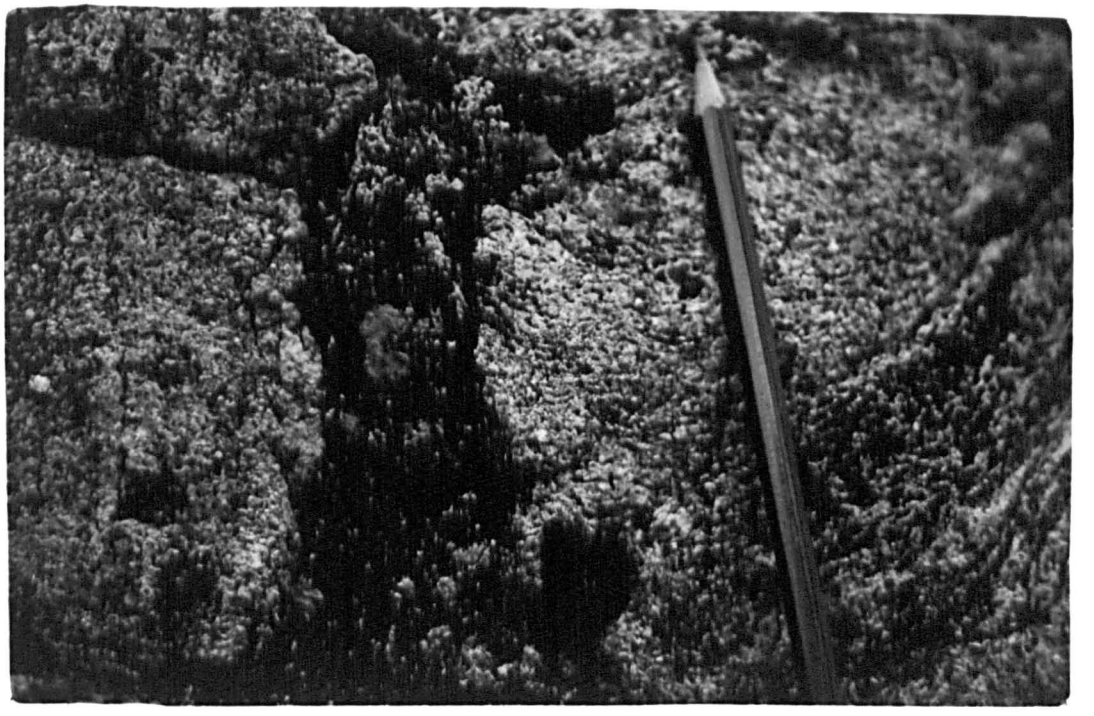

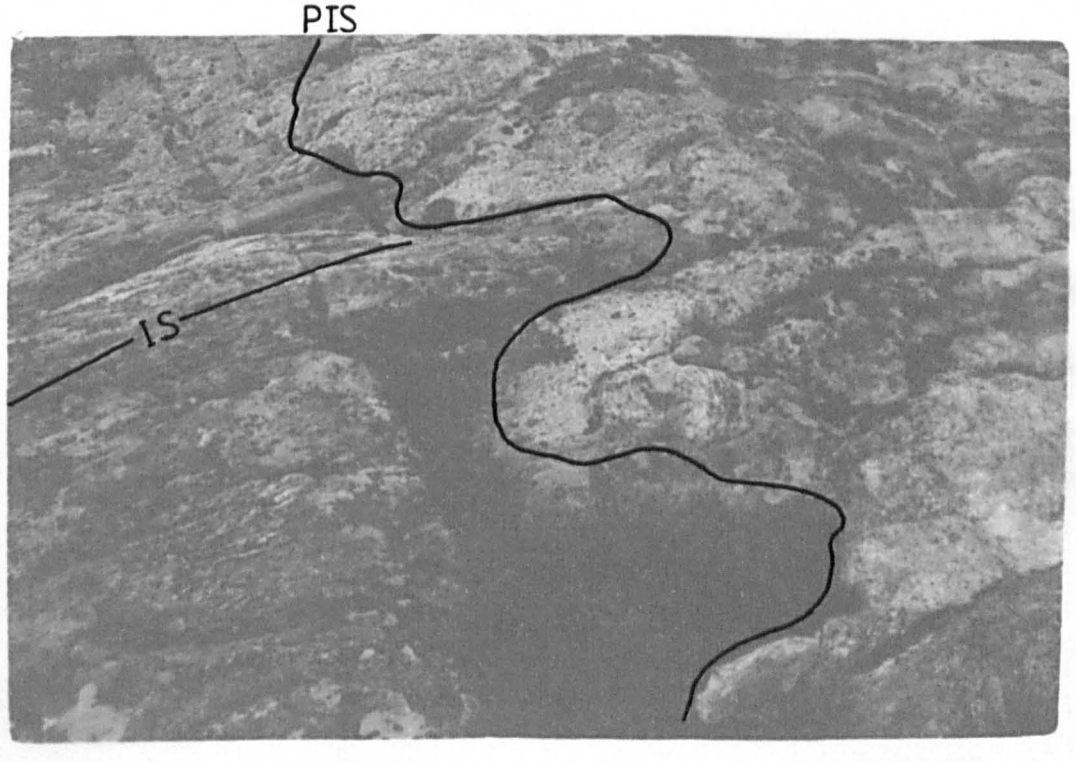
PIS
IS

Plate III-3a. Intrafolial fold closure in transposed Inverian foliation (77905388).

Plate III-3b. Gneissic Inverian foliation is cut off by a nearly undeformed dyke (75015767).

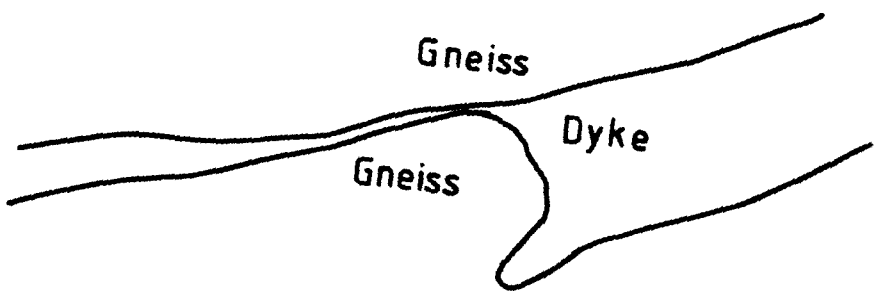
Gneiss
Dyke
Gneiss

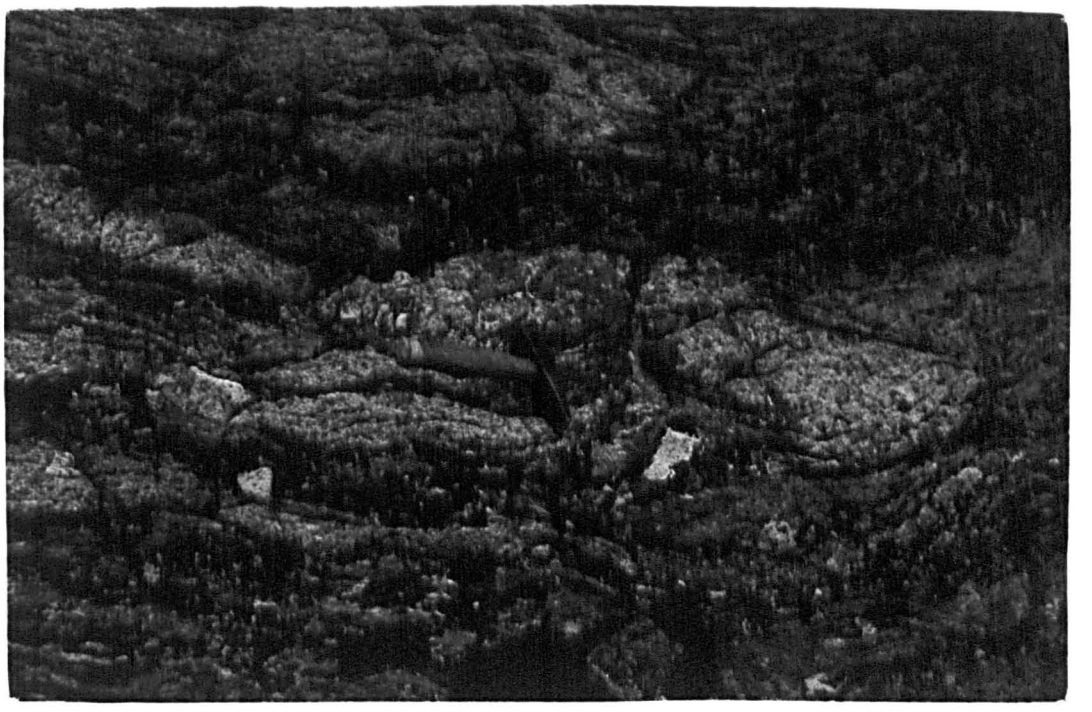

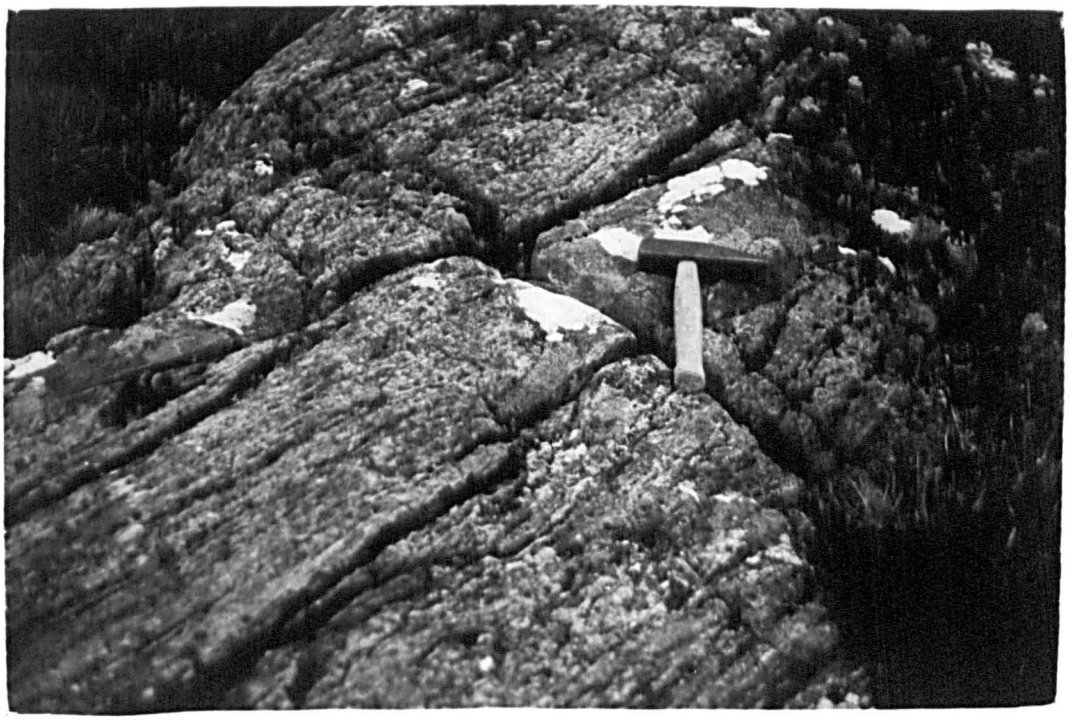

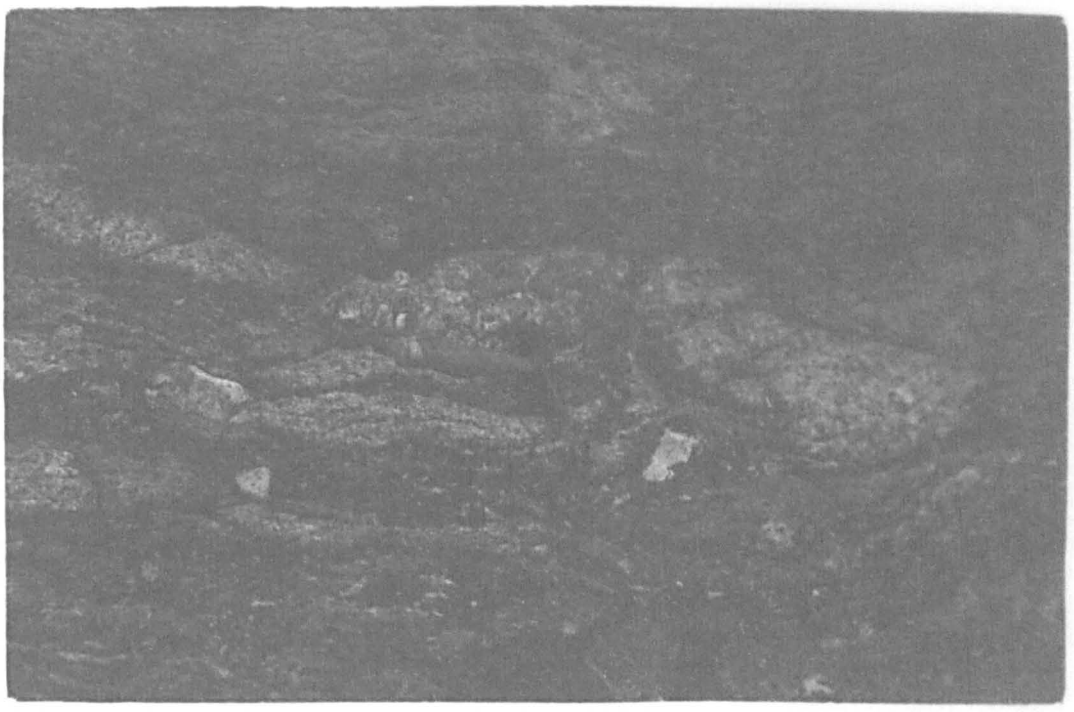

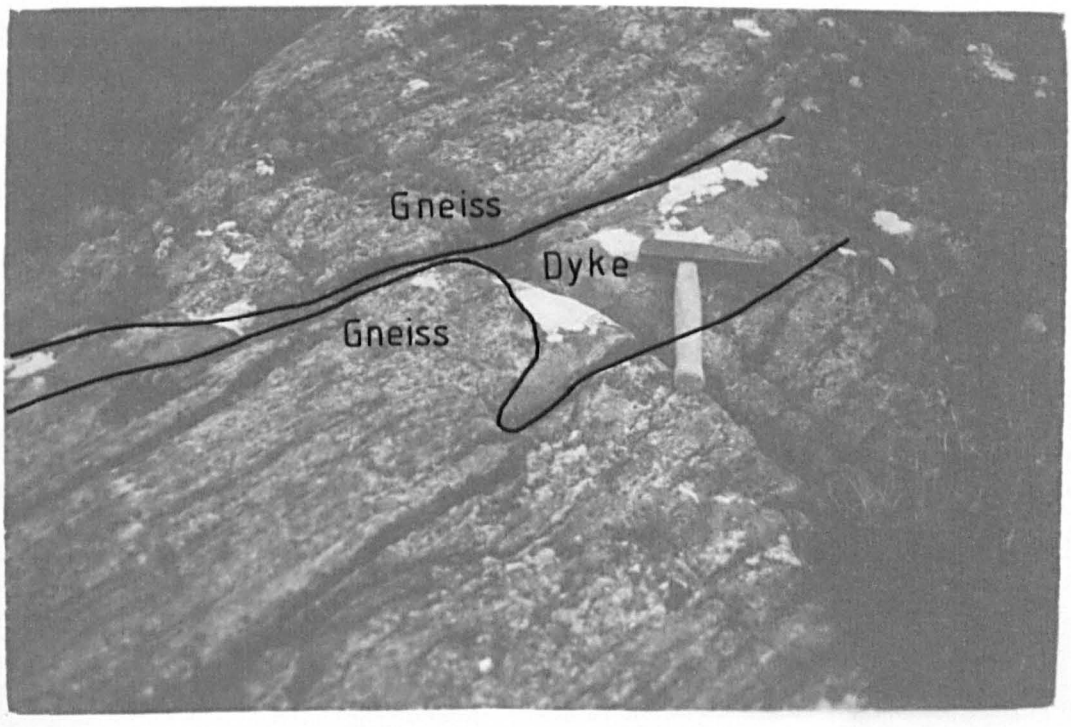
Gneiss
Dyke
Gneiss

Plate III-4a. The Pre-Inverian foliation (PS_2) is disrupted by narrow shear zones of Inverian age in the gneisses in the Ardheslaig pod. Tight intrafolial fold closures in the pre-Inverian foliation indicate the presence of an earlier foliation (PS_1) (78485586).

Plate III-4b. Acid veins in the dyke have been folded into F_1 folds (with subvertical axial trace) which have been refolded by subhorizontal F_2 folds (axial trace is parallel to the pencil) within the dyke (76205766).

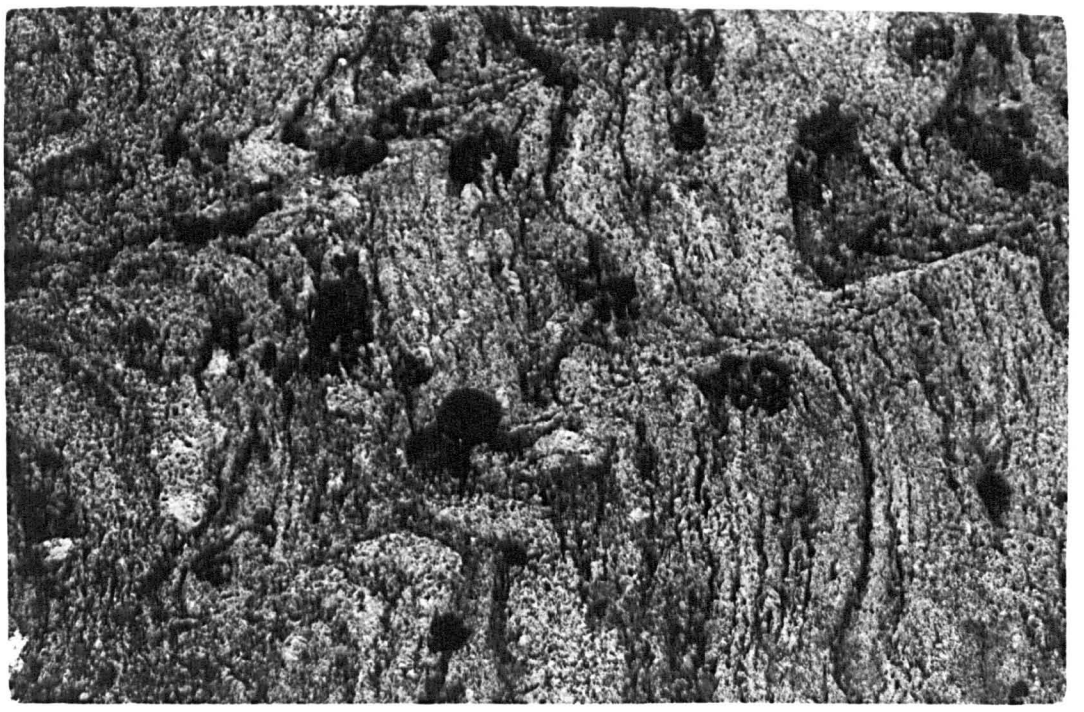

some places intrafolial fold closures can be seen (Pl. III-3a). The IS foliation is shown cut by a nearly undeformed dyke in plate III-3b.

In one small pod* about 50 x 70 m in extent, Pre-Inverian structures are preserved in a nebulitic type of hornblende-granite gneiss with north to northeasterly-oriented PSI foliation. This PSI foliation has been folded by Inverian folds (Pl. III-4a) consisting of narrow zones of strong deformation alternating with undeformed zones. The recognition of these folds is only possible by correlating them with those in the Scourian blocks north of Loch Torridon. The presence of some fold closures (see Pl. III-4a) in this pod indicate the presence of an early foliation which has been tightly folded in the Inverian deformation. Close to this pod, where northwesterly oriented Inverian IS foliation is present, the dykes are somewhat discordant to it (see Pl. III-1b).

b. Post-dyke structures. The rocks were strongly deformed in the Laxfordian and post-dyke structures are abundant throughout the area.

The First Laxfordian deformation produces a strong shear fabric in the area which is an LS shape-fabric as defined by Flinn (1965). Folds of this generation are rarely observed except at some places where veins cross the dykes or gneissic screens are present in the dykes which have been folded (Pl. III-4b). Probably this deformation was the strongest and most important in obliterating the discordant relationship of the dykes with the gneisses.

The Second Laxfordian deformation produces folds with an axial planar fabric. This deformation also produces the same type of shape fabric in the dykes which was produced in the first Laxfordian deformation, and therefore it is difficult to differentiate the two fabrics in the

* *785558*

field unless LS_1 has been folded into F_2 folds or S_2 is axial planar to the F_2 folds at the dyke contacts. This deformation does not produce large scale structures except about one kilometre west-northwest of Kenmore and on the top most part of 'A Bhainlir' hill. In places, dykes have been folded into F_2 folds on outcrop scale (Pl. III-5a), but F_2 folds are mainly on a small scale and are quite widespread in the gneisses, within the dykes where LS_1 fabric has been folded, and at the dyke contacts. Generally they are asymmetric with S-type asymmetry looking northwest which verge towards southwest (Roberts, 1974 & Bell, 1981), but M-type folds are also present which are parasitic on the hinges of the large scale folds. They are quite tight structures, therefore usually their axial surface is parallel to the gneissic and dyke foliation. Mostly they are co-axial with the first-deformation structures so that the shape fabric lineation L_1 is usually parallel to their fold axes (Pl. III-5b), but sometimes they are non-coaxial with D_1 structures and L_1 crosses the F_2 fold axis at a low angle and is folded (Pl. III-6a). At many places the Inverian foliation also has been modified and transposed into the Laxfordian foliation (Pl. III-6b) and it is therefore difficult to differentiate the two.

The rocks were strongly sheared during (and especially in the later stages of) the D_2 deformation and this shearing continued after the D_2 deformation. Strong shearing was confined to narrow zones (Pl. III-7a,b).

The Third Laxfordian deformation is also important. It folds all the previous structures and the dykes into NW-SE oriented upright folds on both a large and a small scale. The folding is variable in intensity in different areas. Refolding relationships between these folds and the F_2 folds are widespread, and the refolding is co-axial in most places

Plate III-5a. Dykes folded subhorizontally into F_2 folds of similar style. Cliff is about 6 metres high on the left edge (78125788).

Plate III-5b. LS_1 fabric in dyke co-axially folded into F_2 fold. Camera axis is above a small antiform in the axial plane of the fold oblique to the fold hinge (75305775).

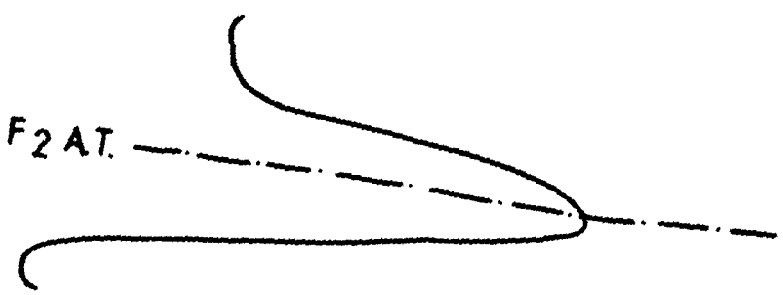
F2 A.T.

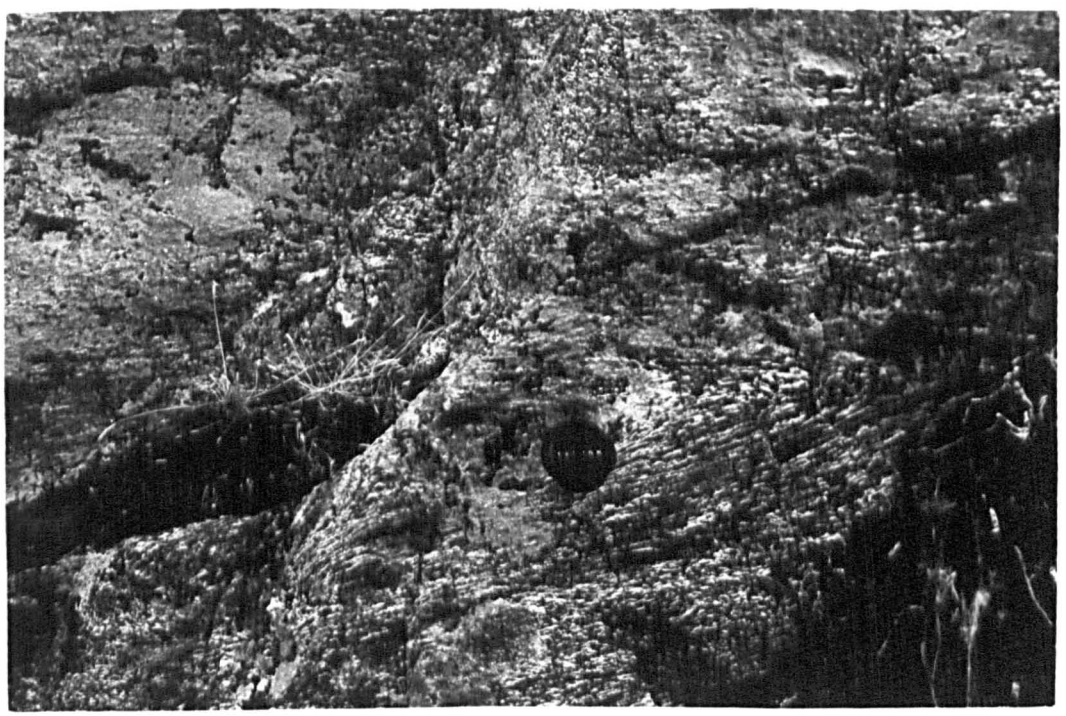

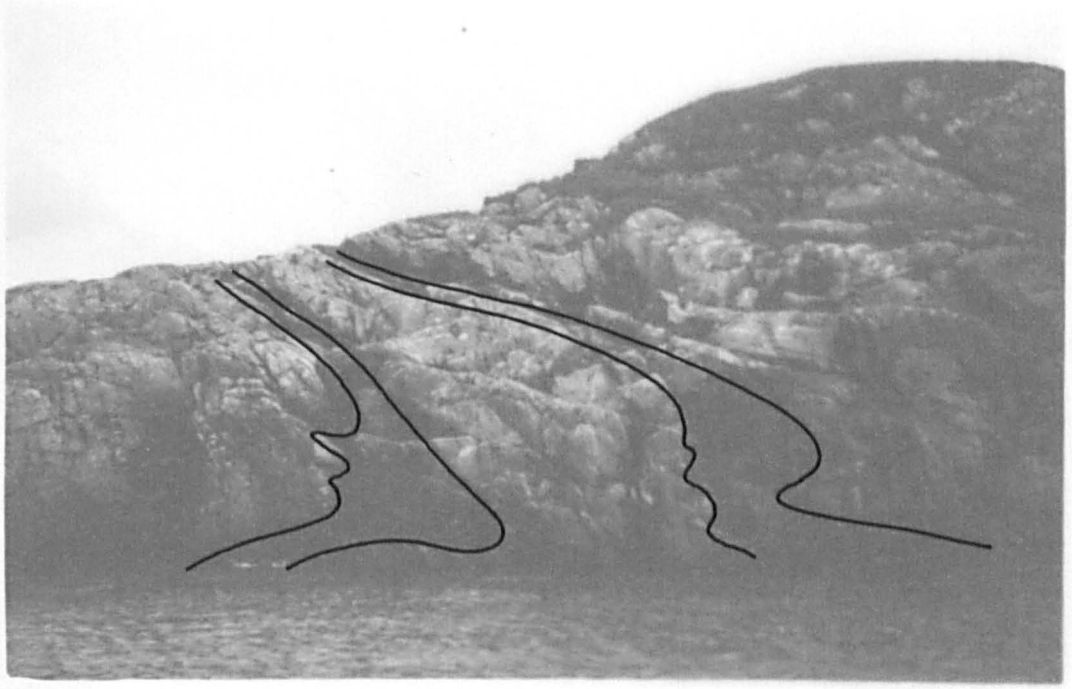

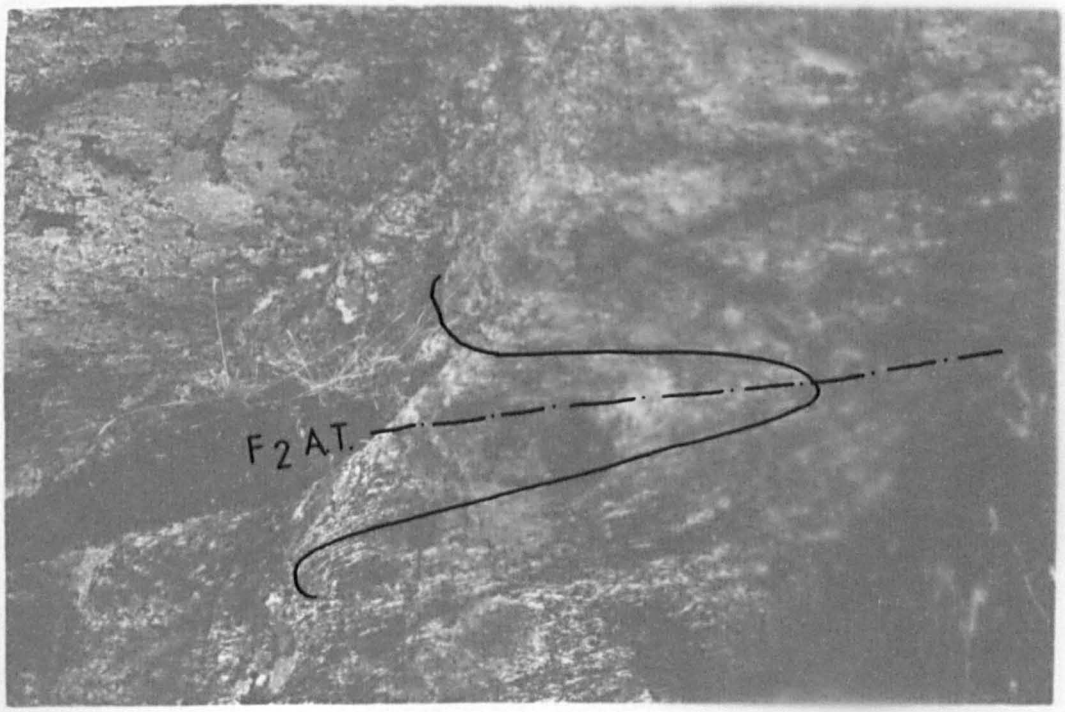
F2 A.T.

Plate III-6a. LS_1 dyke fabric folded non-coaxially into subhorizontal F_2 fold. The fold is strongly asymmetric so that one limb covering most of the picture contains the lineation running oblique to the photograph edge while the lineation is parallel to the pencil on the short limb (77735746).

Plate III-6b. Gneissic fabric strongly transposed into Laxfordian S_2 foliation. Thick gneissic band has been folded into an F_2 fold (76655641).

IS
IS
(S1S2)

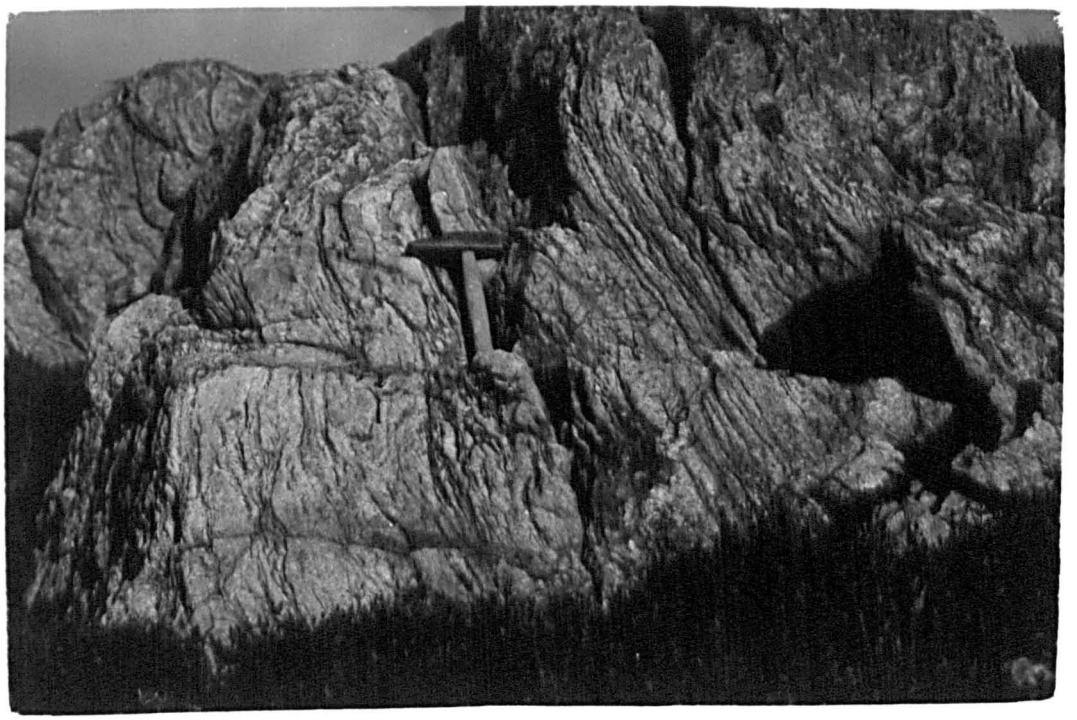

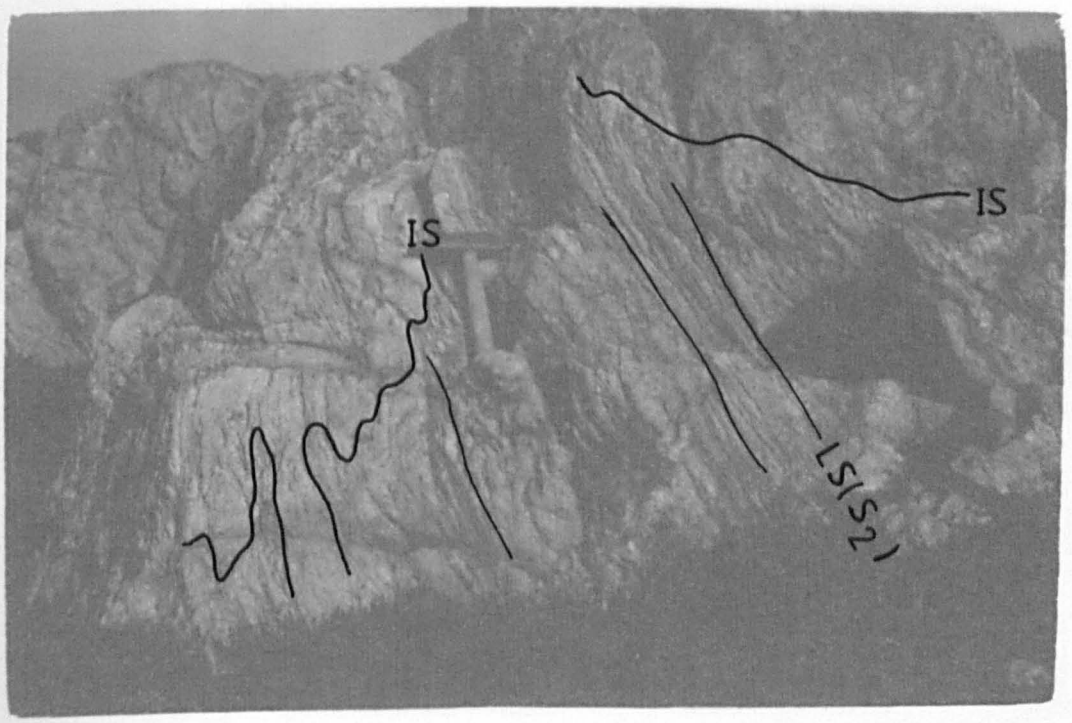
IS
IS
LS(S2)

Plate III-7a. The S_1 fabric (in the middle of the picture) in the dyke has been strongly sheared and transposed into S_2 foliation (gently inclined to the left in the top and bottom part of the picture). Vertical scarp facing NW (74085679).

Plate III-7b. In a dyke the LS_1 fabric has been strongly sheared and transposed into the S_2 fabric. Some narrow shear zones also cut the F_2 fold (75325614).

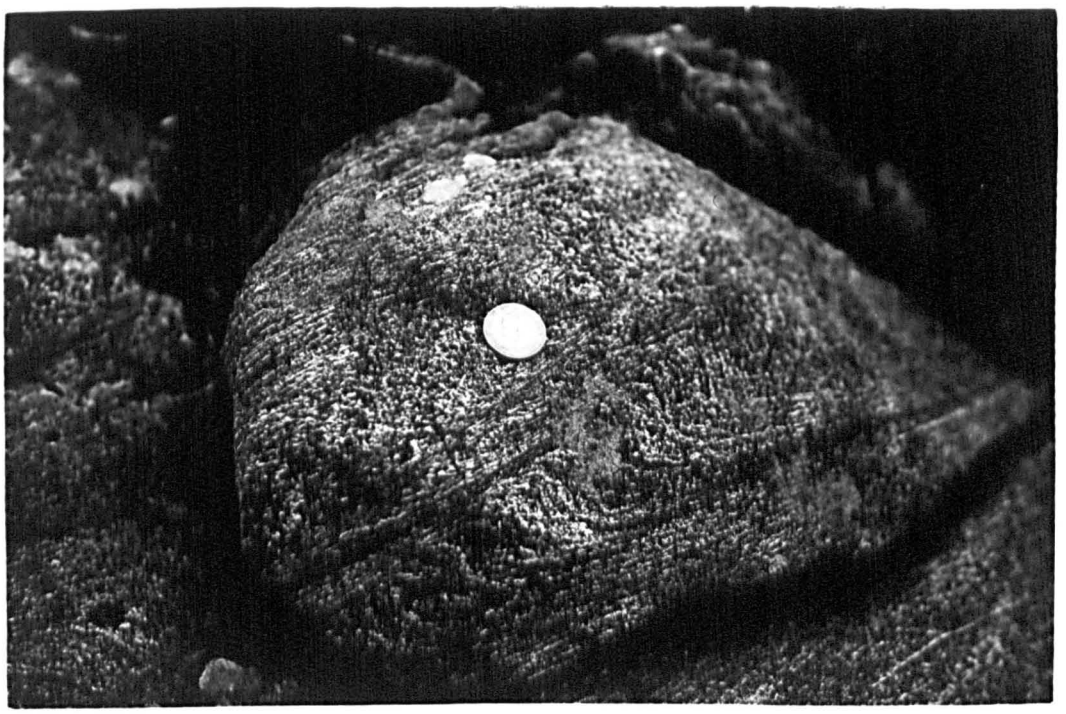

(Pl. III-8a), although at some localities refolding is non-coaxial and F_2 fold axes cross the F_3 fold axes at a low angle (Pl. III-8b). In most of the area there is no fabric associated with this deformation but within a kilometre wide belt running southwest of Ardheslaig in a NW-SE direction, an axial planar fabric is present within the gneisses only where quartz has been deformed and is lying parallel to the axial planes of the folds (Pl. III-9a). A fabric lineation is also associated with F_3 folds but because they are co-axial with the F_2 folds and with the early lineations over most of the area, it is generally impossible to differentiate this lineation from the earlier ones.

The Late Laxfordian or post D_3 deformation was very localized and was of low intensity. In this deformation the rocks have been folded into upright folds with northeast-southwest to east-west oriented axial planes. They are open and concentric (Pl. III-9b) and no fabric is associated with them.

Late deformation also produces cataclastic structures. Such structures are common in the southeastern part of the area to the south of Loch a Mhuilinn and in the northern parts of Ardheslaig. In these areas blocks of various size, ranging up to a couple of metres in diameter have been displaced from their original sites and are sometimes rotated. In some places cataclasis is confined to narrow zones surrounded by non-cataclastic rocks. These cataclastic zones are oriented northwest-southeast and usually dip at a high to moderate angle. The relationship of the NE-SW folds and the cataclasis is unknown but both appear to post-date F_3.

Plate III-8a. Subhorizontal F_2 fold (top left of the picture) in gneiss has been co-axially refolded by a subvertical F_3 fold. The hammer handle is parallel to the trace of the F_3 axial trace in vertical section (75355477).

Plate III-8b. An F_2 fold in gneiss has been folded non-coaxially by an upright F_3 fold (the pencil is parallel to the trace of the axial surface of the F_3 fold). The hinge of the F_2 fold crosses the hinge of the F_3 fold (77765496).

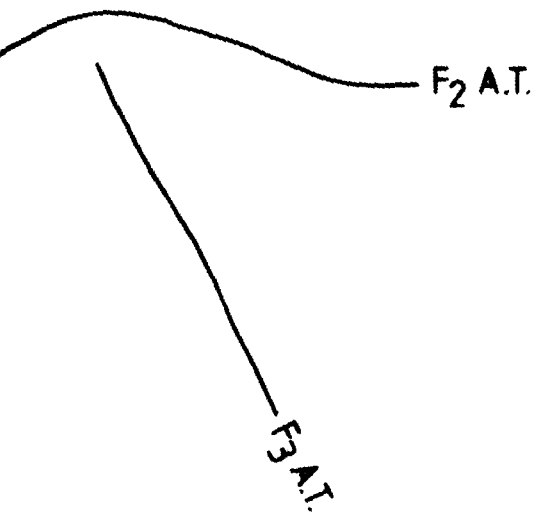
F_2 A.T.
F_3 A.T.

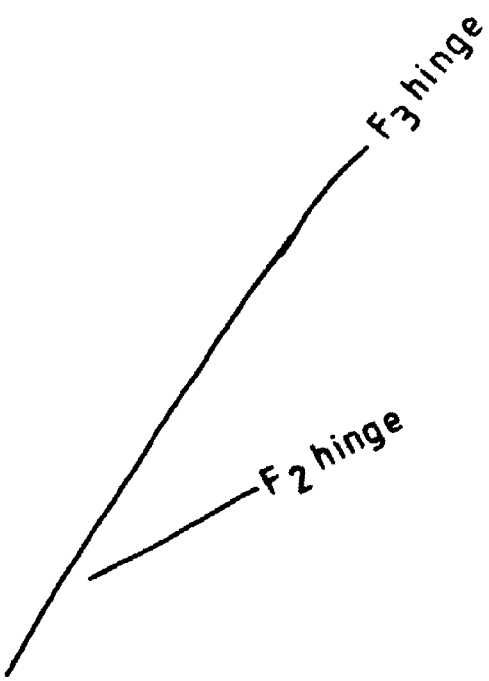
F_3 hinge
F_2 hinge

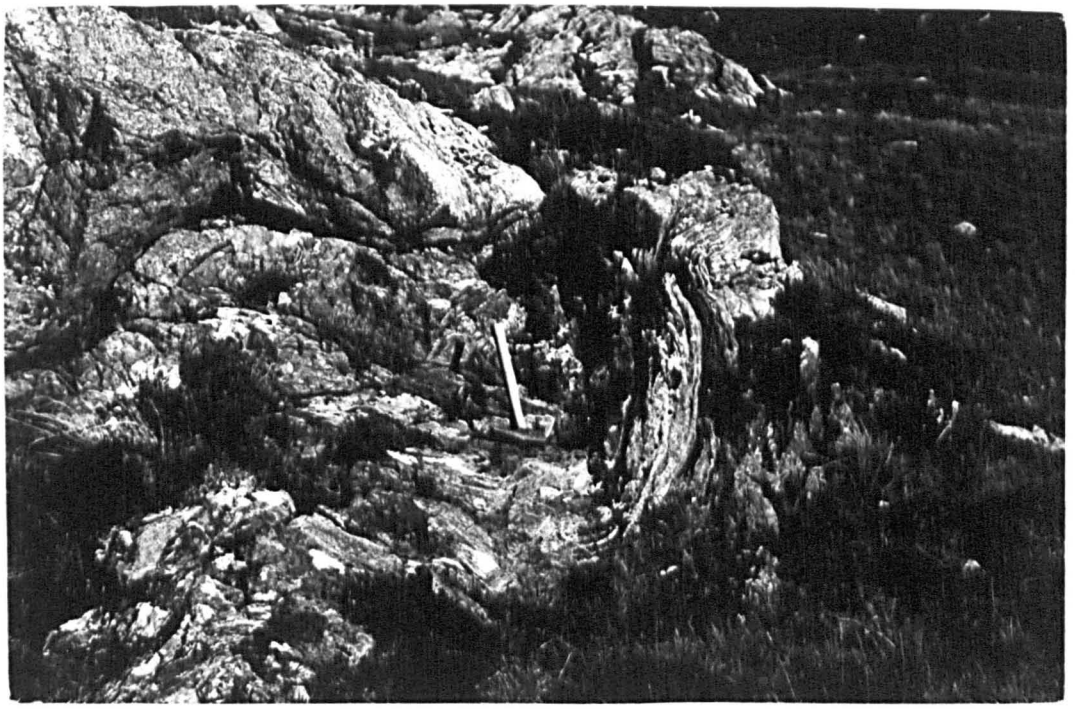

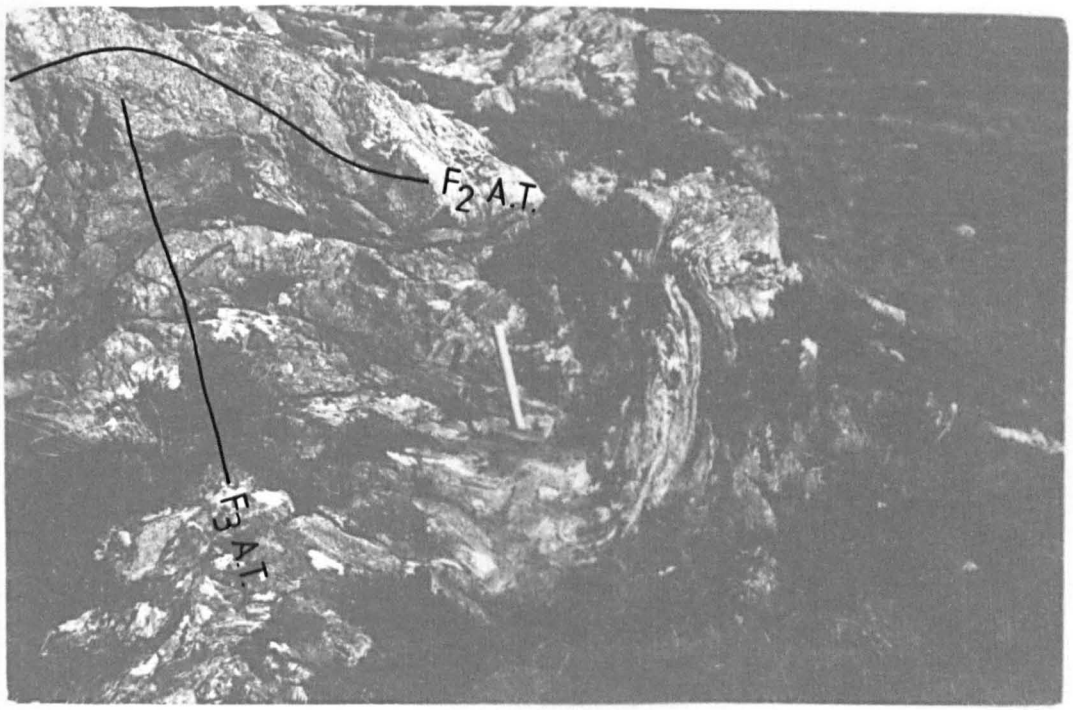
F_2 A.T.
F_3 A.T.

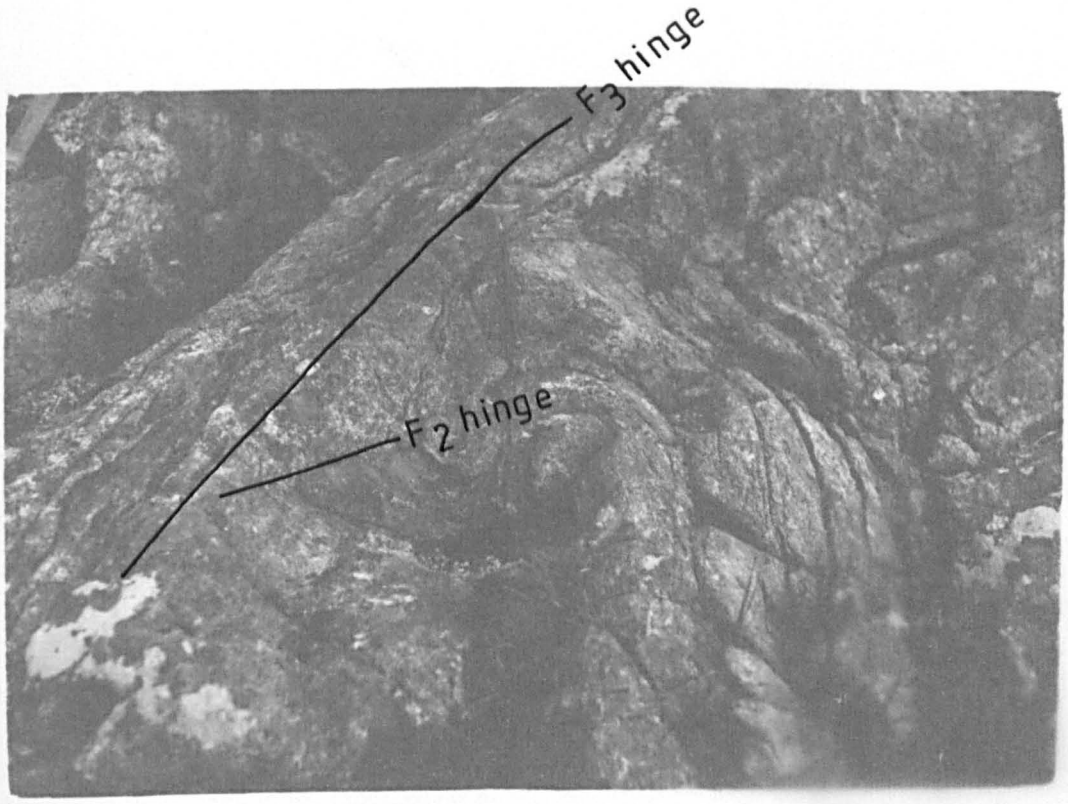
F_3 hinge
F_2 hinge

Plate III-9a. Upright F_3 fold in acid gneiss. The axial planar fabric is parallel to the pencil (77605498).

Plate III-9b. Upright open post-F_3 folds in acid gneisses (78555701).

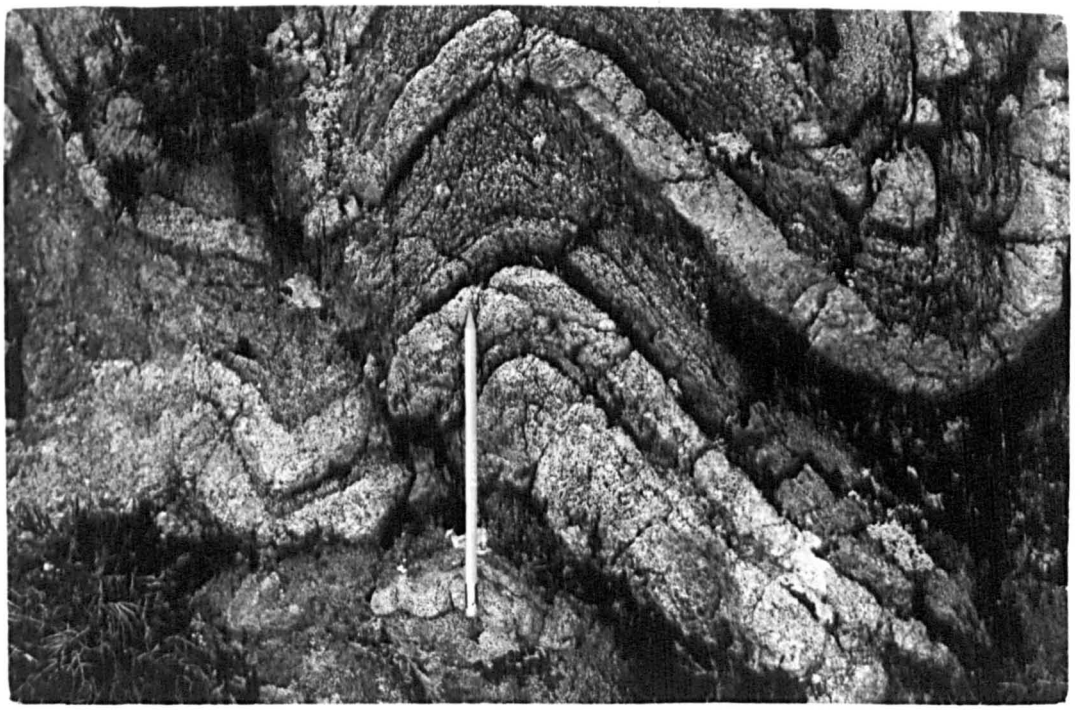

2. Map Pattern (Major Structures)

The general trend of the planar fabric of Inverian and Laxfordian age in the gneisses and dykes is northwest-southeast and mainly dips towards the southwest. With the exception of a locality near Arrina and on A'Bhainlir hill, where mappable F_2 folds are present (see page 41), the most important element defining the map pattern is macroscopic F_3 folding. The broad swing in the axial surfaces of these folds in the eastern part of the inlier is probably post D_3 (Enclosure 2). This is confirmed by the NE-SW to E-W oriented small scale post F_3 folds described above.

A belt about one kilometre wide of intense F_3 folding is present at the southwestern edge of the area, mainly south of Loch a Choire Bhuidhe, running northwest-southeast. A second belt of strong F_3 folding extends from the northeastern slope of A'Bhainlir to Ob na h-Acairseid. This is a belt slightly over a kilometre wide running northwest-southeast in its northern part and north-northwest south-southeast in its southern part. The rocks in the central part of the area are more uniformly dipping towards the southwest at a moderate to high angle in the northwestern part and at variable angles in the southeastern part and are gently undulating on the southwestern slope of A'Bhainlir and southwest of it. Some gentle undulations are also present on the northern part of Ardheslaig peninsula, where long limbs of F_3 folds dip towards the northeast. F_3 folds hinges are either subhorizontal or plunge at a low angle mainly towards the northwest.

The rocks around Ardheslaig lie at the lowest structural level while the rocks at the southwestern edge of the area, i.e. around Meall Dearg and to the west of Loch Choire Bhuidhe, are in the uppermost part

of the structural sequence (Enclosure 2).

The enveloping surface of these major folds dips to the southwest and the hinge-zone of a regional F_3 antiform, the Loch Torridon antiform passes through the south shore of Loch Torridon (Park, 1973) or more precisely through Ardheslaig. The gneisses and dykes to the north of the loch are dipping to the northeast (Cresswell, 1969, 1972; Park, 1973).

B. PATTERN AND DISTRIBUTION OF STRUCTURES

Using the equal area net, the map has been divided by trial and error into twelve domains of homogeneous structural pattern (Fig. III-1), of the gneissic foliation. This was done by plotting poles to the foliation for areas in which traces of axial surfaces are rectilinear, and modifying these areas until adjacent foliation poles define a single π-axis (Turner and Weiss, 1963; Ramsay, 1964, 1967). In each domain generally 70 to 150 measurements have been taken. The same divisions are used for other fabric elements as well for the sake of simplicity, and these domains have been subdivided into subdomains wherever necessary. The pattern and distribution of structures in these domains will be discussed in turn.

1. Domain 1

In the northern part of this domain, on the hill between Kenmore and Arrina, all the foliation dips at a moderate to high angle towards the southwest with a constant strike towards the northwest. However, in most of the southern part it has been folded into upright F_3 folds. Statistical analysis of the foliation reveals that the poles to the foliation are well concentrated and fall on a great circle (Fig. III-2a,b) showing cylindrical folding (Turner and Weiss, op. cit.; Ramsay, op. cit) in this domain, and the π-axis plunges at about 5^{o} towards $N44^{o}W$. The

Fig. III-1. The distribution of domains in the Kenmore inlier. Domain numbers are given inside each domain. Stippled area is the Lewisian outcrop.

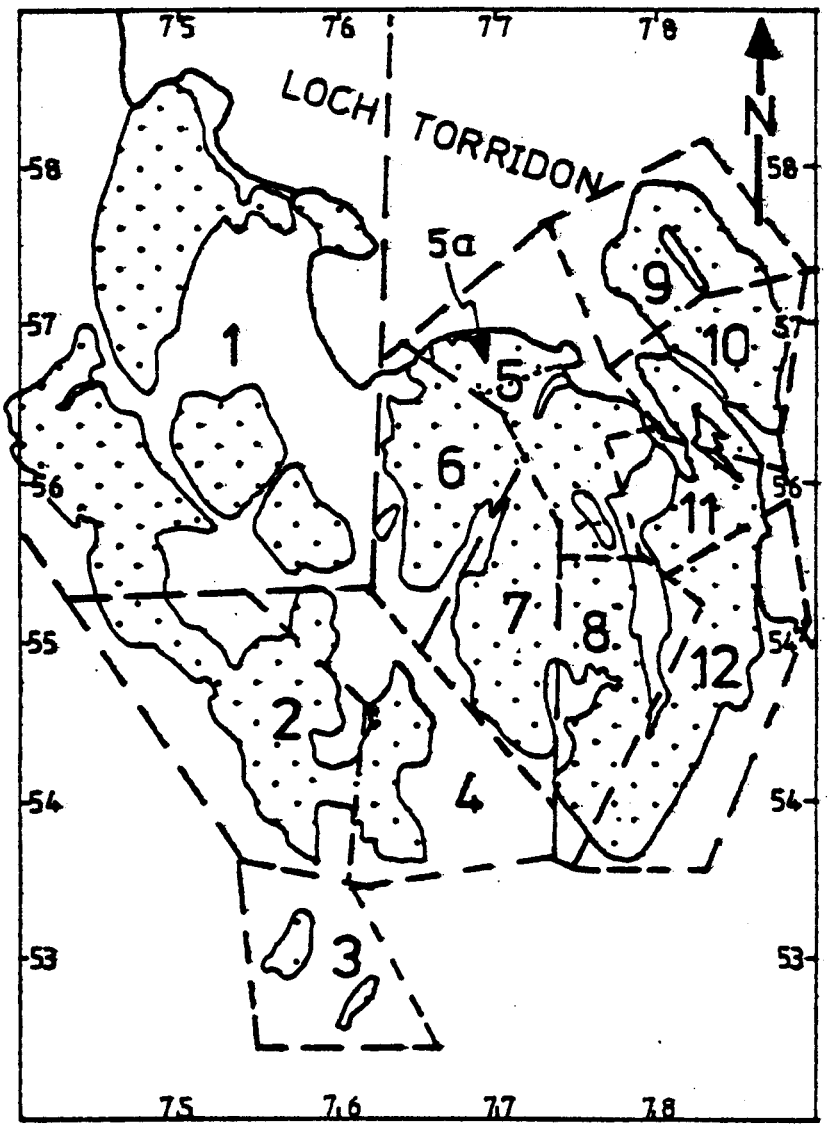
7·5
7·6
7·7
7·8
LOCH TORRIDON
N
58
57
56
55
54
53
5a
1
2
3
4
5
6
7
8
9
10
11
12

Fig. III-2a. Contoured plot of 477 poles to the gneissic foliation in domain 1, contours at 0.2%, 2%, 4%, 6% and 8% per 1% area. Crosses are the plot of the gneissic lineations. Circle with dot is the girdle axis.

Fig. III-2b. Contoured plot of 155 poles to the dyke foliation in domain 1, contours at 0.6%, 2%, 4%, 6% and 8% per 1% area. Solid circles are the dyke lineations. The best fit line and girdle axis are plotted from Fig. III-2a.

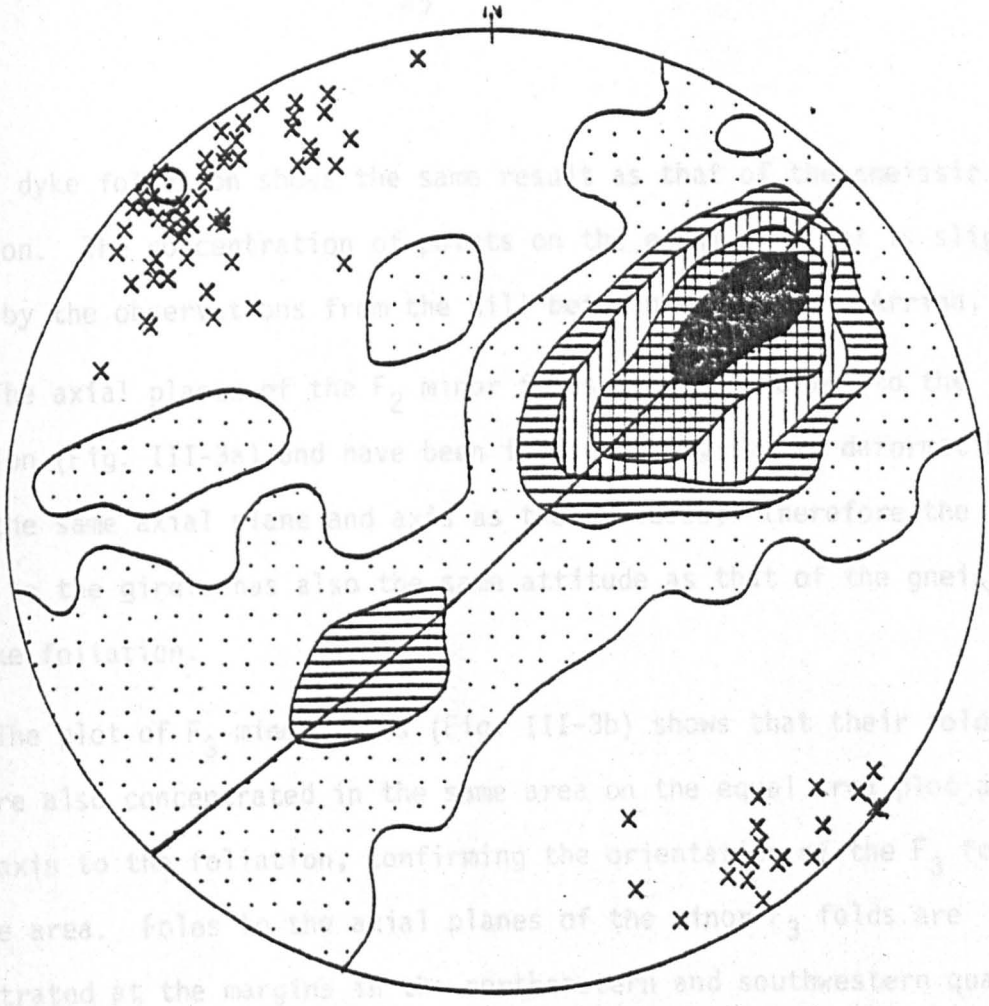

a

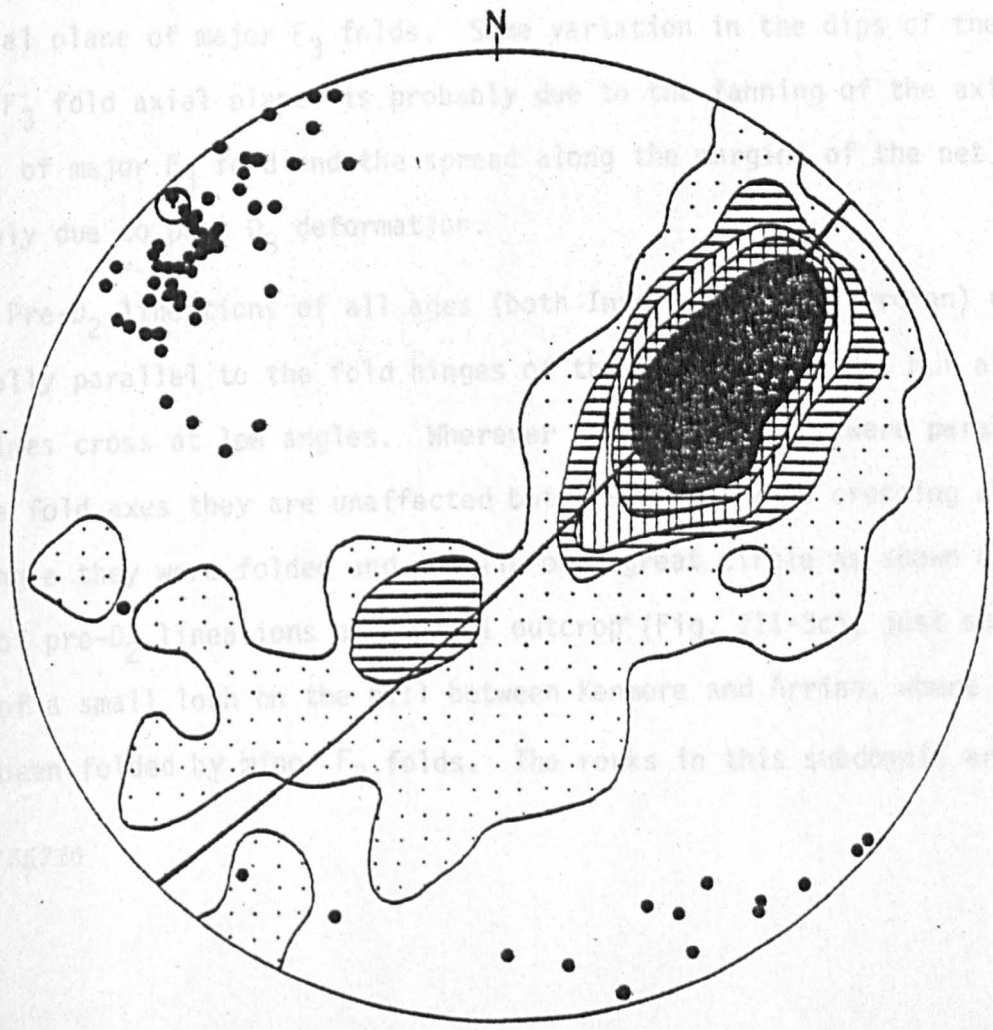

b

plot of dyke foliation shows the same result as that of the gneissic foliation. The concentration of points on the equal area net is slightly biased by the observations from the hill between Kenmore and Arrina.

The axial planes of the F_2 minor folds are subparallel to the foliation (Fig. III-3a) and have been folded during the D_3 deformation, along the same axial plane and axis as the gneisses; therefore the π-axis to the girdle has also the same attitude as that of the gneissic and dyke foliation.

The plot of F_3 minor folds (Fig. III-3b) shows that their fold axes are also concentrated in the same area on the equal area plot as the π-axis to the foliation, confirming the orientation of the F_3 fold for the area. Poles to the axial planes of the minor F_3 folds are concentrated at the margins in the northeastern and southwestern quadrants of the equal area net indicating the subvertical attitude of the F_3 axial plane of major F_3 folds. Some variation in the dips of the minor F_3 fold axial planes is probably due to the fanning of the axial planes of major F_3 fold and the spread along the margins of the net is probably due to post D_3 deformation.

Pre-D_2 lineations of all ages (both Inverian and Laxfordian) are generally parallel to the fold hinges of the F_2 and F_3 folds, but also sometimes cross at low angles. Wherever these lineations were parallel to the fold axes they are unaffected but where they were crossing at a low angle they were folded and now lie on a great circle as shown by the plot of pre-D_2 lineations on a small outcrop* (Fig. III-3c), just southeast of a small loch on the hill between Kenmore and Arrina, where they have been folded by minor F_2 folds. The rocks in this subdomain are not

* *74735716*

Fig. III-3a. Contoured plot of 109 poles to the axial planes of the F_2 minor folds in domain 1, contours at 0.9%, 2%, 4%, 6% and 8% per 1% area. Solid circles are the fold axes of the mesoscopic F_2 folds. The best fit line and girdle axis are plotted from Fig. III-2a.

Fig. III-3b. Contoured plot of 43 poles to the axial planes of mesoscopic F_3 folds in domain 1, contours at 2.3%, 4%, 8% and 12% per 1% area. Solid circles are the fold axes of the mesoscopic F_3 folds.

Fig. III-3c. Contoured plot of 42 pre-D_2 gneissic lineations on a small outcrop (74735716) on the hill between Kenmore and Arrina, contours at 2.4%, 4%, 8% and 16% per 1% area.

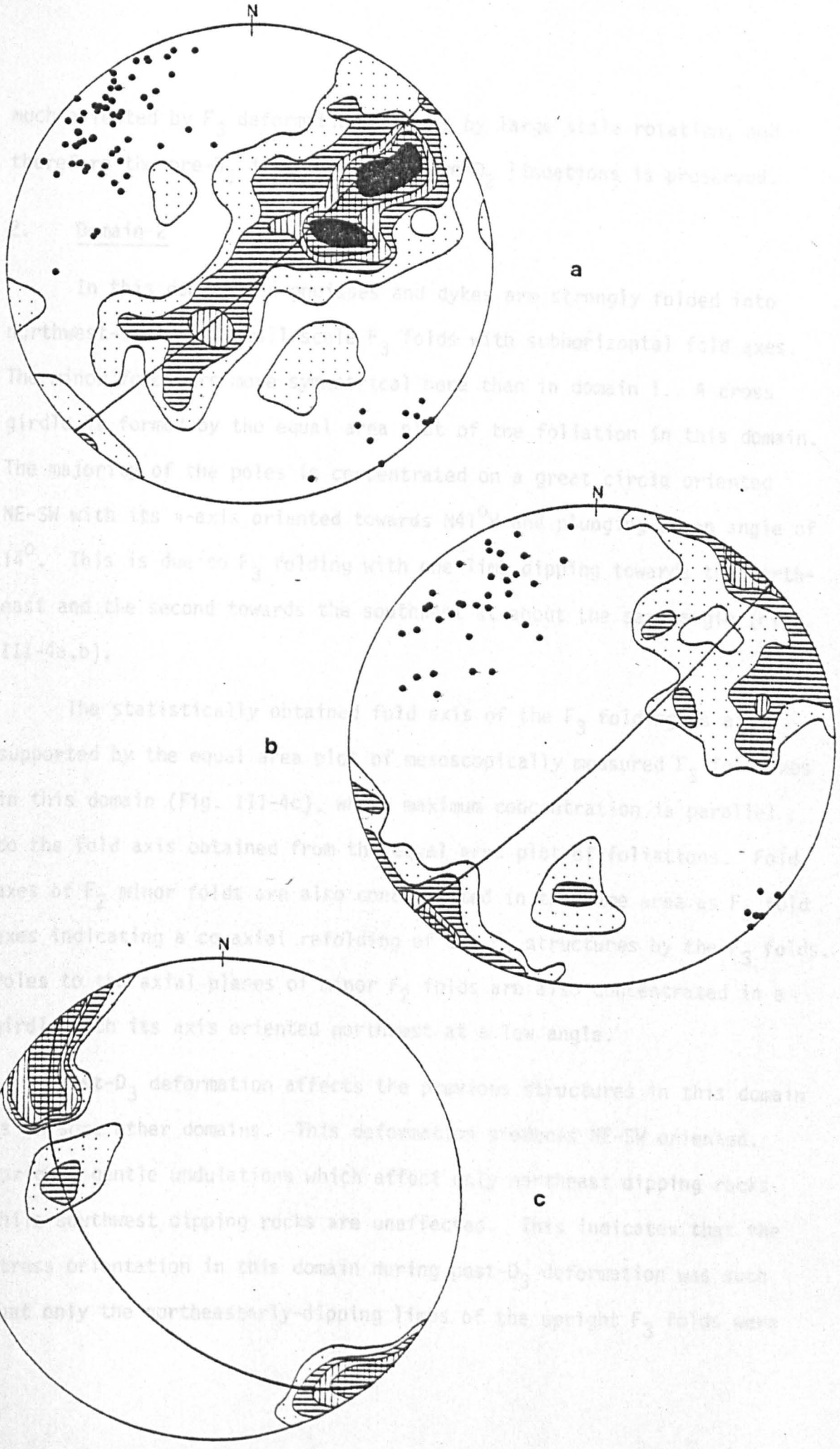
N
a
N
b
N
c

much affected by F_3 deformation, except by large scale rotation, and therefore the pre-D_3 distribution of pre-D_2 lineations is preserved.

2. Domain 2

In this domain the gneisses and dykes are strongly folded into northwest-southeast small scale F_3 folds with subhorizontal fold axes. The minor folds are more symmetrical here than in domain 1. A cross girdle is formed by the equal area plot of the foliation in this domain. The majority of the poles is concentrated on a great circle oriented NE-SW with its π-axis oriented towards N41^{o}W and plunging at an angle of 14^{o}. This is due to F_3 folding with one limb dipping towards the northeast and the second towards the southwest at about the same angle (Figs. III-4a,b).

The statistically obtained fold axis of the F_3 folding is also supported by the equal area plot of mesoscopically measured F_3 fold axes in this domain (Fig. III-4c), whose maximum concentration is parallel to the fold axis obtained from the equal area plot of foliations. Fold axes of F_2 minor folds are also concentrated in the same area as F_3 fold axes indicating a co-axial refolding of the F_2 structures by the F_3 folds. Poles to the axial planes of minor F_2 folds are also concentrated in a girdle with its axis oriented northwest at a low angle.

Post-D_3 deformation affects the previous structures in this domain as in some other domains. This deformation produces NE-SW oriented, upright, gentle undulations which affect only northeast dipping rocks while southwest dipping rocks are unaffected. This indicates that the stress orientation in this domain during post-D_3 deformation was such that only the northeasterly-dipping limbs of the upright F_3 folds were

Fig. III-4a. Contoured plot of 144 poles to the gneissic foliation in domain 2, contours at 0.7%, 2%, 4% and 6% per 1% area. Crosses are the plot of the gneissic lineations. Circle with dot is the girdle axis of F_3 fold and solid circle is the girdle axis of post F_3 fold.

Fig. III-4b. Contoured plot of 24 poles to the dyke foliation in domain 2, contrours at 3.7% and 7.4% per 1% area. Solid circles are the plot of the dyke lineations. The best fit lines and girdle axes are plotted from Fig. III-4a.

Fig. III-4c. Plot of the mesoscopic F_2 and F_3 folds in domain 2.

○ = poles to the axial planes of the F_2 folds,

● = poles to the axial planes of the F_3 folds,

▲ = plot of the F_2 fold axes,

■ = plot of the F_3 fold axes

The best fit lines and girdle axes are plotted from Fig. III-4a.

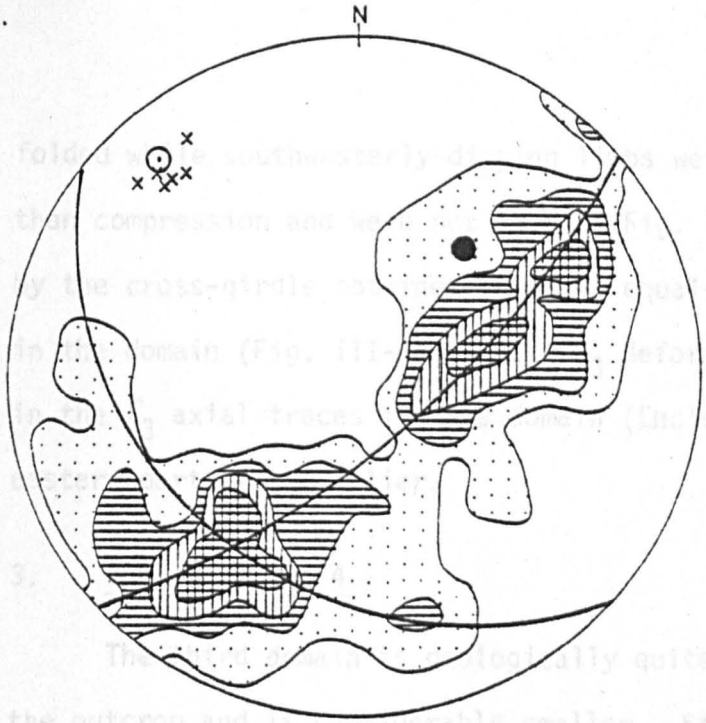

a

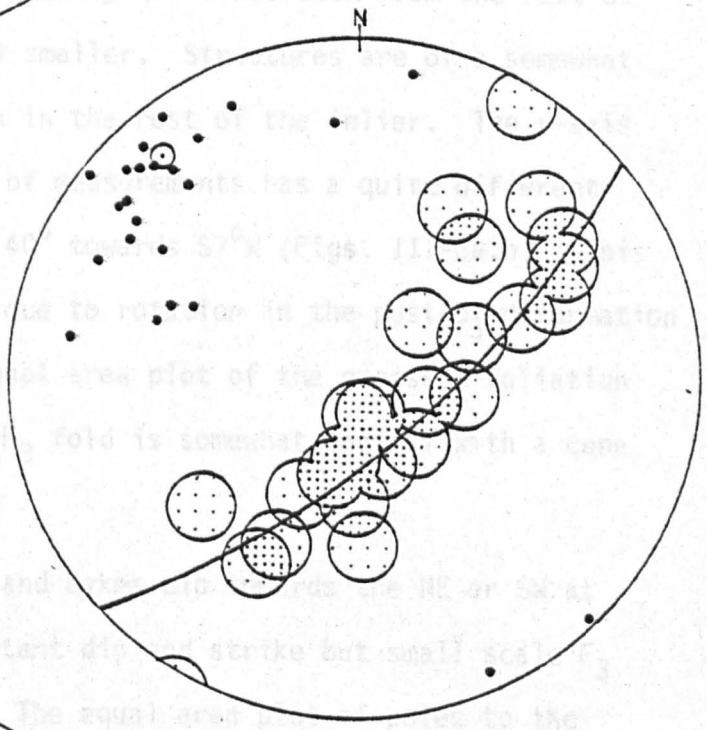

b

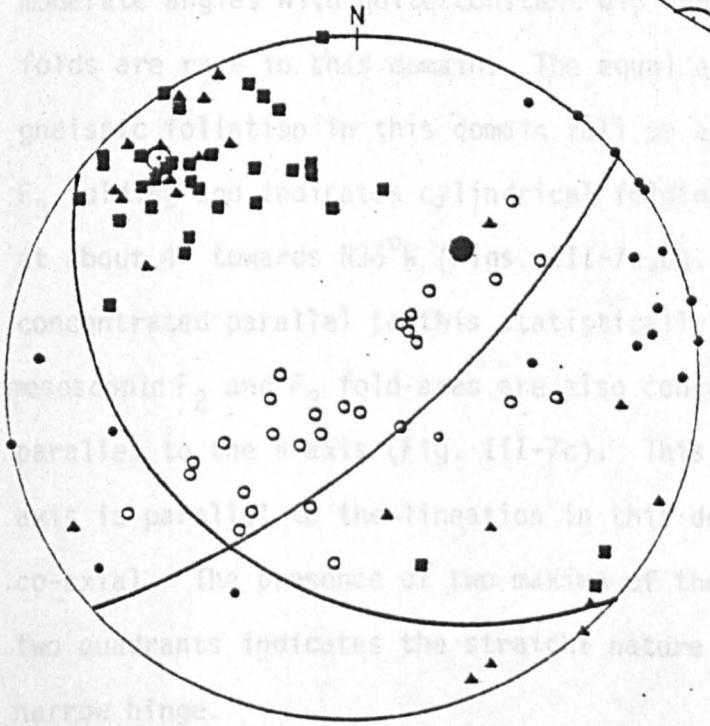

c

folded while southwesterly-dipping limbs were under more extension rather than compression and were not folded (Fig. III-5). This can also be seen by the cross-girdle obtained from the equal-area plot of the foliation in the domain (Fig. III-4a). Post D_3 deformation does not cause a spread in the F_3 axial traces in this domain (Enclosure 2) as it does in the eastern part of the inlier.

3. Domains 3 and 4

The third domain is geologically quite isolated from the rest of the outcrop and is considerably smaller. Structures are of a somewhat different orientation here than in the rest of the inlier. The π-axis obtained from a limited number of measurements has a quite different orientation, plunging at about 40^{o} towards $S7^{o}W$ (Figs. III-6a,b). This change in orientation might be due to rotation in the post-D_3 deformation affecting the whole domain. Equal area plot of the gneissic foliation indicates that the large-scale F_3 fold is somewhat conical with a cone angle of about 30^{o}.

In domain 4 the gneisses and dykes dip towards the NE or SW at moderate angles with quite constant dip and strike but small scale F_3 folds are rare in this domain. The equal area plot of poles to the gneissic foliation in this domain fall on a great circle which is due to F_3 folding and indicates cylindrical folding here. The π-axis plunges at about 4^{o} towards $N36^{o}W$ (Figs. III-7a,b). The lineations are also concentrated parallel to this statistically plotted fold axis. The mesoscopic F_2 and F_3 fold axes are also concentrated in the same area parallel to the π-axis (Fig. III-7c). This all reveals that the F_3 fold axis is parallel to the lineation in this domain and deformations were co-axial. The presence of two maxima of the poles to the foliation in two quadrants indicates the straight nature of the fold limbs with a narrow hinge.

Fig. III-5. Only the northeasterly dipping limb of the F_3 fold has been refolded by post F_3 folds while the southwesterly dipping limb of F_3 fold is unaffected.

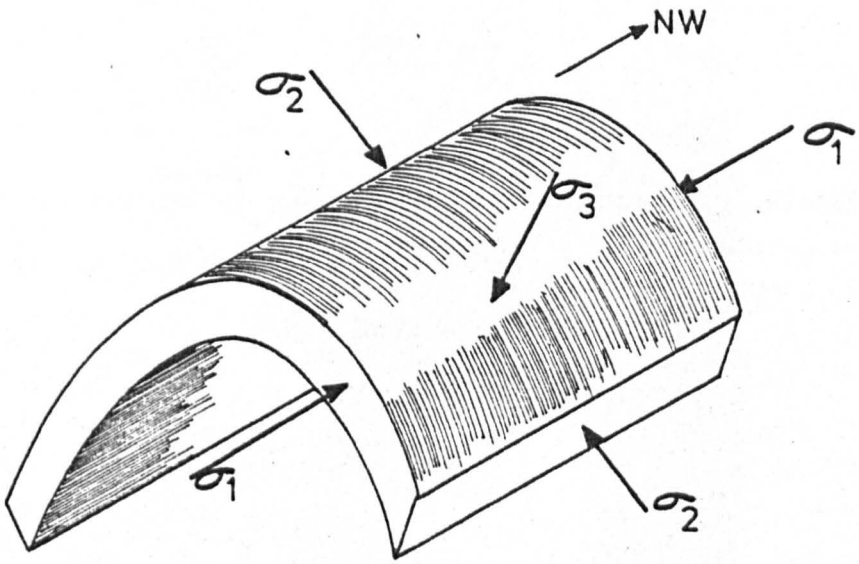
NW
σ_2
σ_1
σ_3
σ_1
σ_2

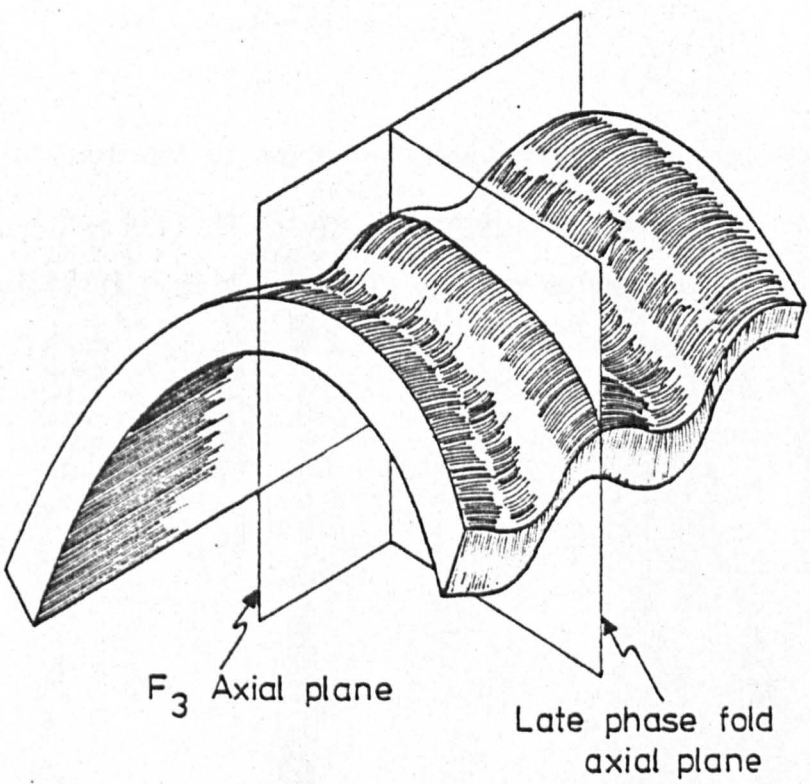
F_3 Axial plane
Late phase fold
axial plane

Fig. III-6a. Contoured plot of 24 poles to the gneissic foliation in domain 3, contours at 4.3% and 8.6% per 1% area. Circle with dot is the girdle axis.

Fig. III-6b. Contoured plot of 6 poles to the dyke foliation in domain 3, contours at 17% and 33% per 1% area. Solid circles are the plot of the dyke lineation.

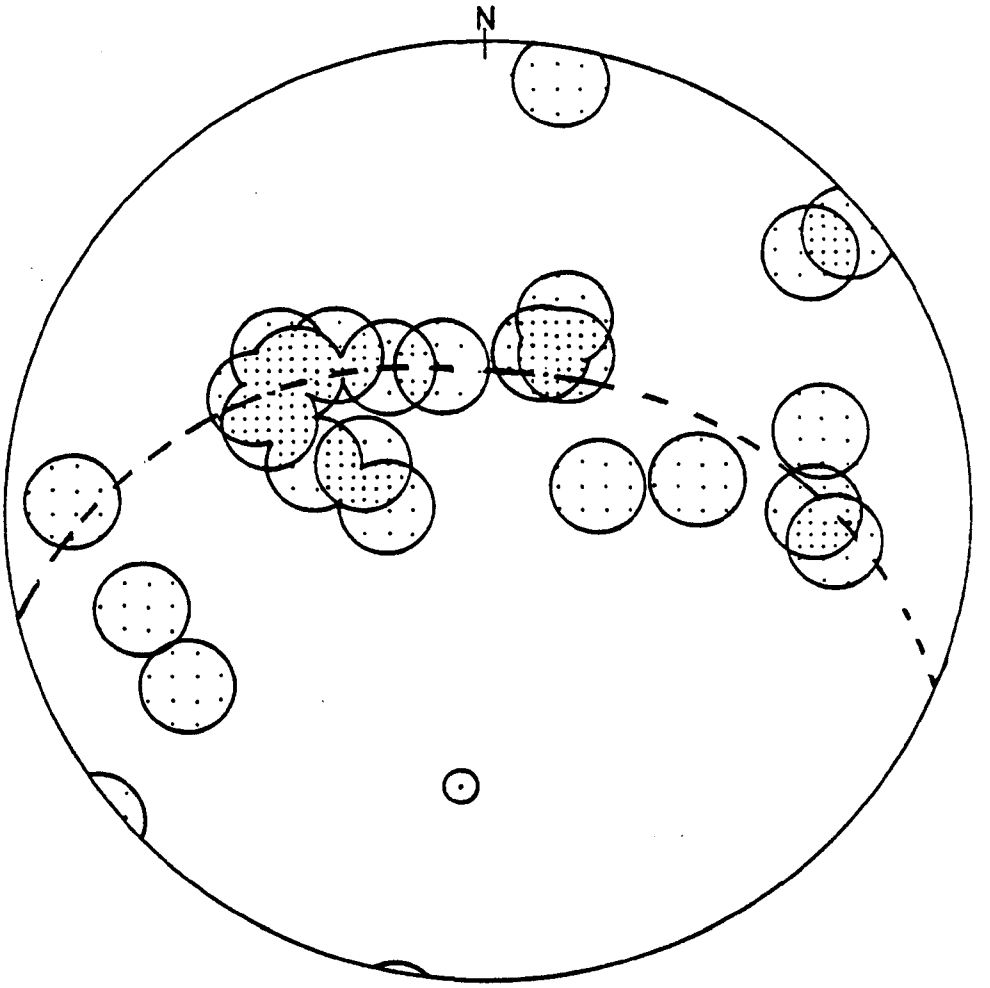

a

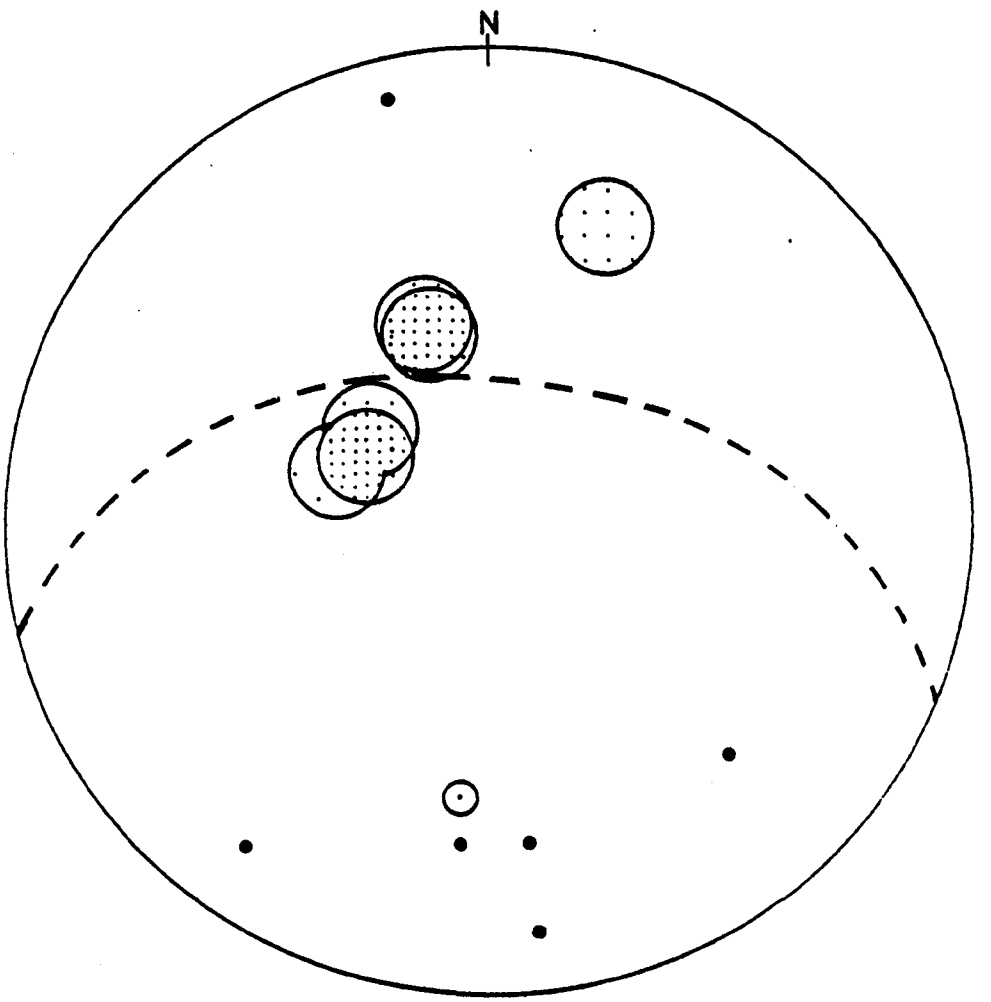

b

Fig. III-7a. Contoured plot of 78 poles to the gneissic foliation in domain 4 at 1.3%, 2%, 4%, 6% and 8% per 1% area. Crosses are the plot of the gneissic lineations. Circle with dot is the girdle axis.

Fig. III-7b. Contoured plot of 17 poles to the dyke foliation in domain 4, contours at 6% and 12% per 1% area. Solid circles are the plot of the dyke lineations. The best fit line and girdle axis are plotted from Fig. III-7a.

Fig. III-7c. Plot of the mesoscopic F_2 and F_3 folds in domain 4.

○ = poles to the axial planes of the F_2 folds,

● = poles to the axial planes of the F_3 folds,

▲ = plot of the F_2 fold axes,

■ = plot of the F_3 fold axes.

The best fit line and girdle axis are plotted from Fig. III-7a.

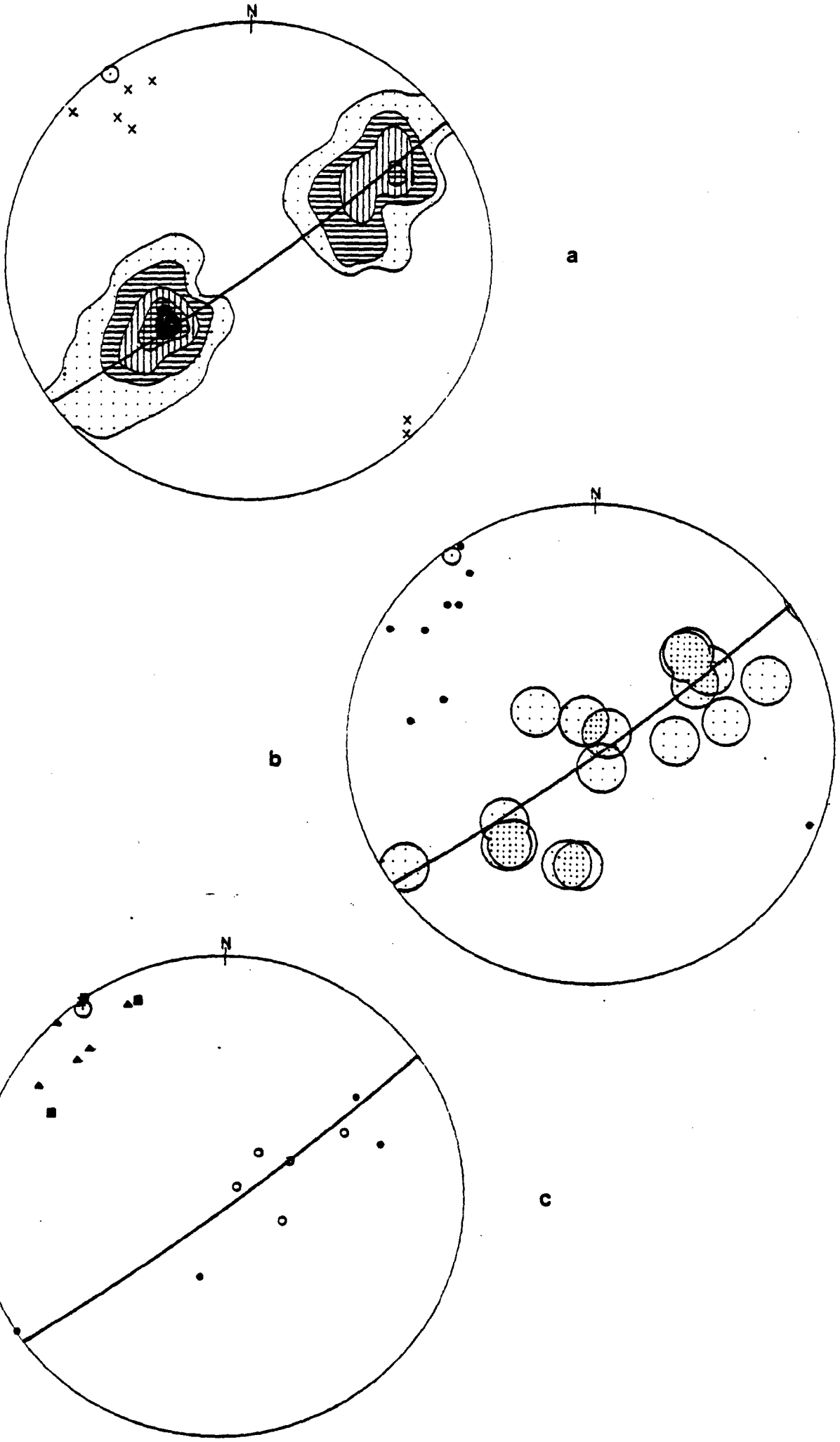
N
a
N
b
N
c

4. Domain 5

The gneisses and dykes are much contorted in this domain into upright NW-SE oriented mesoscopic F_3 folds. Minor folds are nearly symmetrical and are of M-type. The equal area plot of poles to the foliation shows maxima in the northeastern and southwestern quadrants with a nearly subhorizontal girdle axis (Fig. III-8a,b), which is a result of F_3 folding. The scatter of poles to the foliation and in the mesoscopic F_3 folds, which strike from north-south to nearly east-west, and the moderate plunges in the F_3 fold hinges, are probably due to post-D_3 deformation. The domain contains a swing from northwesterly oriented F_3 folds in the west of the domain to north-northwesterly oriented F_3 folds in the southeast. This swing in the axial traces of F_3 folds is probably post-D_3.

Pre-D_3 lineations, which make a low angle to the F_3 fold axis in the domain have been folded. This folding in the pre-D_3 lineation can best be demonstrated in a smaller subdomain in the northern part of the domain (Fig. III-1). Here F_3 folds have not been much affected by post-buckle flattening and in this smaller area axial traces of the F_3 folds are rectilinear and not much affected by the post-D_3 deformation. In this subdomain the plot of the poles to the foliation gives a somewhat better great circle and π-axis- which is also the F_3 fold axis as confirmed by the same orientation of the plot of hinges of minor F_3 folds in the subdomain (Figs. III-9a,b). Pre-D_3 lineations were slightly oblique to the F_3 fold axes, about 18° anticlockwise; i.e. the F_3 fold axis has a bearing of $S30^{\circ}E$ while the lineations had a mean orientation of $S48^{\circ}E$ (Fig. III-9c). These lineations were folded by F_3 folds and the plot of these lineations is concentrated approximately in a small circle.

Fig. III-8a. Contoured plot of 150 poles to the gneissic foliation in domain 5, contours at 0.3%, 2%, 4% and 6% per 1% area. Crosses are the plot of the gneissic lineations. Circle with dot is the girdle axis.

Fig. III-8b. Contoured plot of 85 poles to the dyke foliation in domain 5, contours at 1.2%, 2%, 4%, 6% and 8% per 1% area. Solid circles are the plot of the dyke lineations. The best fit line and girdle axis are plotted from Fig. III-8a.

Fig. III-8c. Plot of the mesoscopic F_2 and F_3 folds in domain 5.

○ = poles to the axial planes of the F_2 fold axes,

● = poles to the axial planes of the F_3 fold axes,

▲ = plot of the F_2 fold axes,

■ = plot of the F_3 fold axes.

The best fit line and girdle axis are plotted from Fig. III-8a.

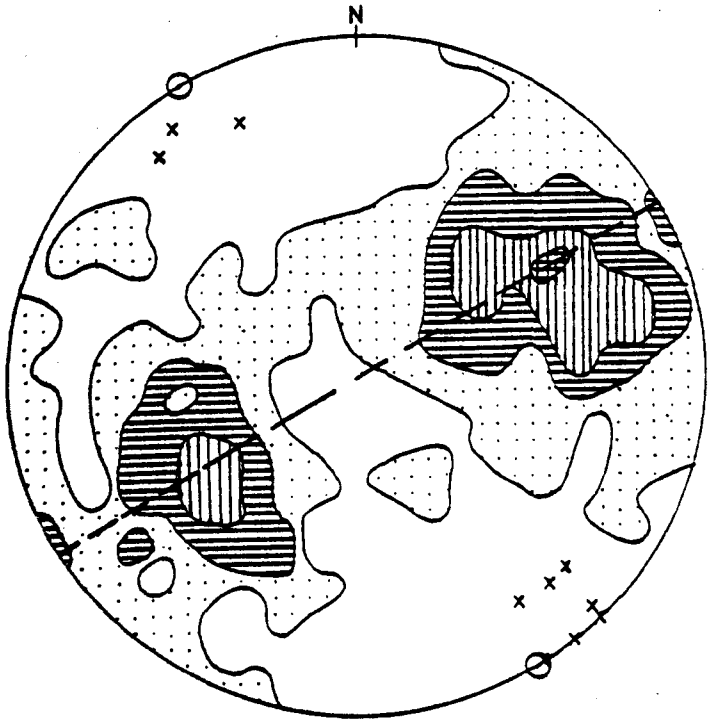

a

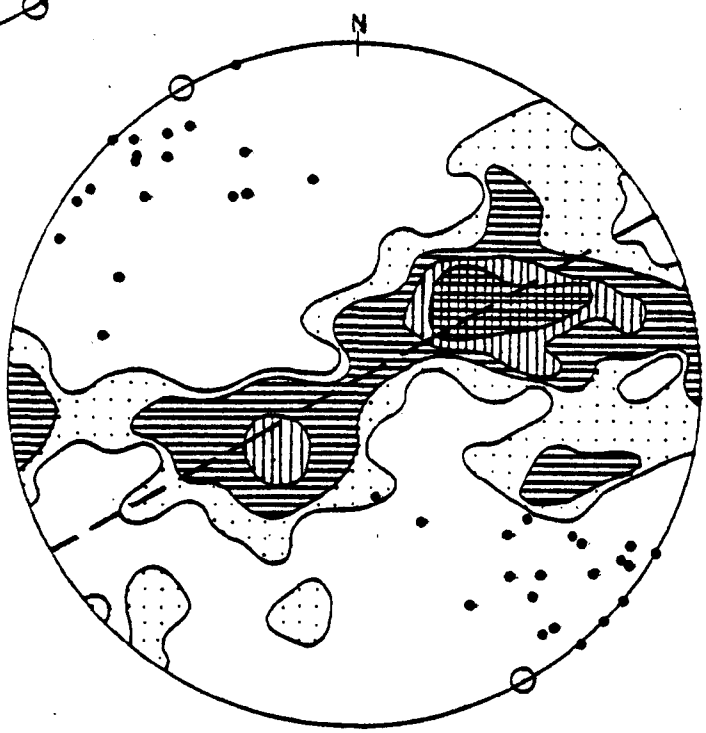

b

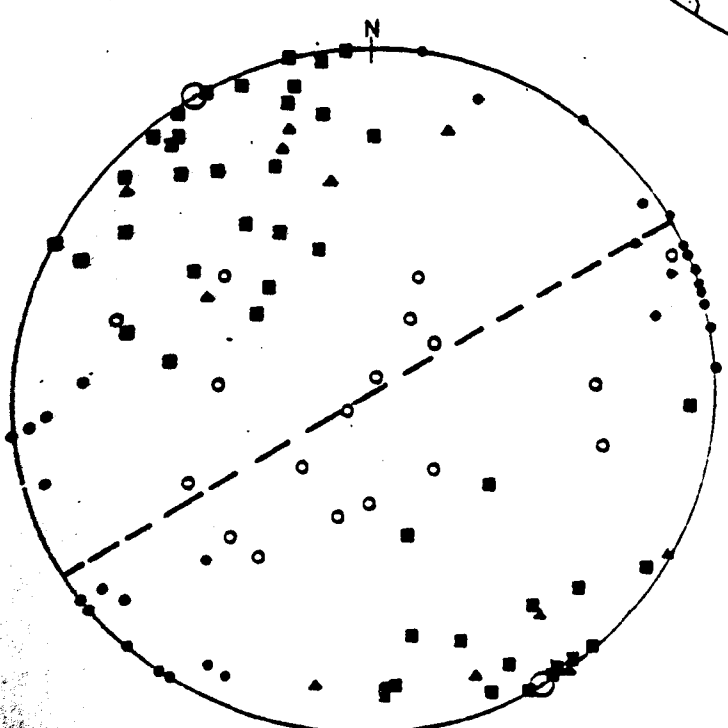

c

Fig. III-9a. Contoured plot of 70 poles to the gneissic foliation (striped) in a subdomain of domain 5, contours at 1.4%, 2%, 3% and 4% per 1% area, and contoured plot of 31 lineations (dotted), contours at 3.2%, 10% and 15% per 1% area. Circle with dot is the girdle axis.

Fig. III-9b. Contoured plot of 30 mesoscopic F_3 fold axes in a subdomain of domain 5, contours at 3.3%, 6%, 9% and 12% per 1% area. Open circles are the poles to the axial planes of the mesoscopic F_3 folds.

Fig. III-9c. Plot of high density contours of mesoscopic F_3 folds (crosses) in a subdomain of domain 5 and high density contours of pre L_3 lineations (spotted). The best fit line and girdle axis are plotted from the Fig. III-9a.

a

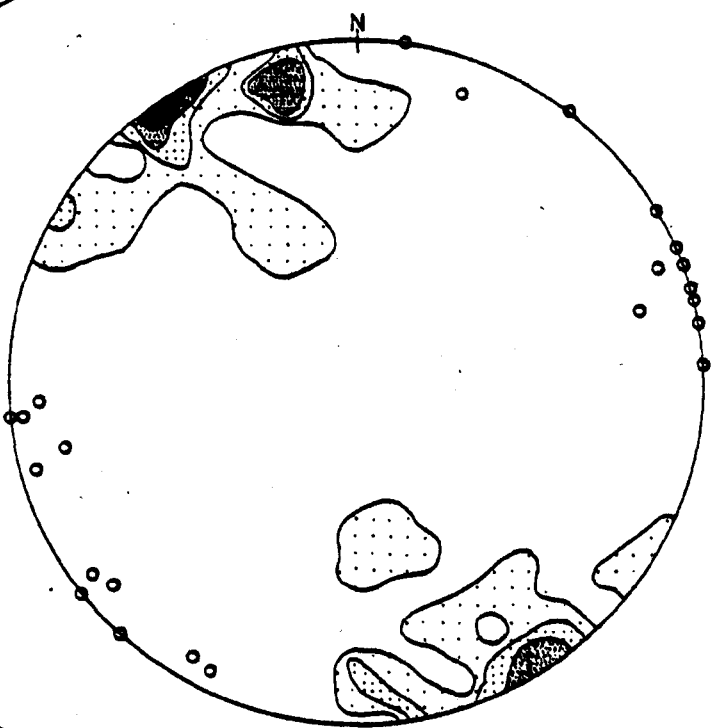

b

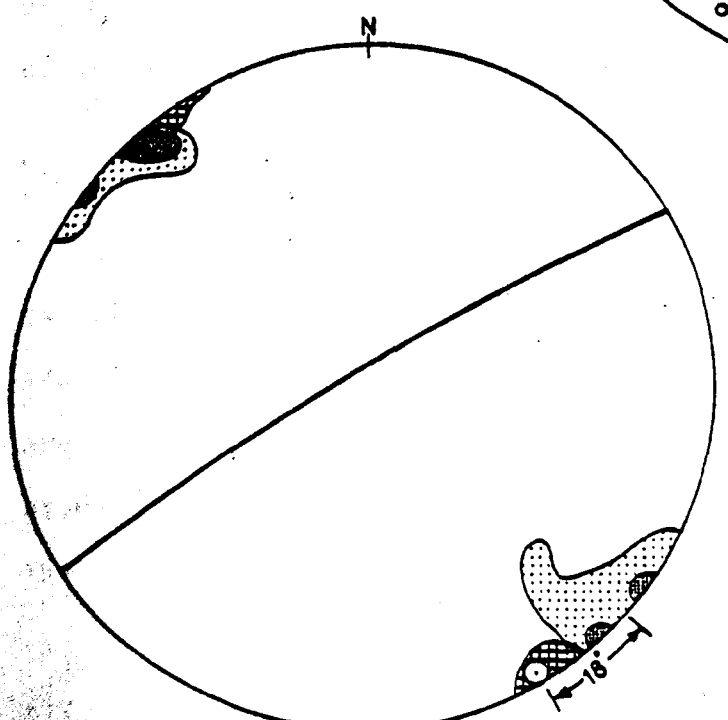

c

5. Domains 6 and 7

The structures in these domains are very simple and straightforward. The gneisses and dykes mainly dip towards the southwest. Sometimes they dip towards the northeast due to upright F_3 folding. All over the area, the mesoscopic fold axes and lineations are parallel suggesting the co-axial nature of the deformation. The equal area plot of the planar and linear elements in these domains is very simple. In domain 6, poles to the foliation are concentrated on a great circle suggesting cylindrical folding during D_3. In domain 7, the poles to the foliation are concentrated on a small circle indicating that the F_3 folds are somewhat conical with a cone angle about 10^{o}. In domain 6 the π-axis plunges at about 2^{o} towards S49^{o}E (Figs. III-10a,b) while in domain 7 it plunges at 15^{o} towards N26^{o}W (Figs. III-11a,b). In both domains the π-axes are also F_3 fold axes as confirmed by the plot of mesoscopic F_3 fold axes (Figs. III-10c and III-11c) respectively.

The F_2 and F_3 fold axes and the lineations of all ages are concentrated parallel to the π-axes revealing the co-axial nature of the folding of all pre-D_2 lineations in the D_2 deformation as well as in the D_3 deformation.

6. Domain 8

The distribution and orientation of the structures in this domain is somewhat different and strange. Apparently in the field the rocks are folded on a NNW-SSE nearly subhorizontal axis. Small scale F_3 folds are quite abundant. The equal area plot to the foliations in this domain gives a π-axis plunging at a low angle towards the SSE (Figs. III-12a,b). The lineation data is insufficient in this domain, but fold axes of minor

Fig. III-10a. Contoured plot of 129 poles to the gneissic foliation in domain 6, contours at 0.8%, 2%, 4%, 6% and 8% per 1% area. Crosses are the plot of the gneissic lineations. Circle with dot is the girdle axis.

Fig. III-10b. Contoured plot of 45 poles to the dyke foliation in domain 6, contours at 2.2% and 4.4% per 1% area. Solid circles are the plot of the dyke lineations. The best fit line and girdle axis are plotted from Fig. III-10a.

Fig. III-10c. Plot of the mesoscopic F_2 and F_3 folds in domain 6.

○ = poles to the axial planes of the F_2 folds,

● = poles to the axial planes of the F_3 folds,

▲ = plot of the F_2 fold axes,

■ = plot of the F_3 fold axes.

The best fit line and girdle axis are plotted from Fig. III-10a.

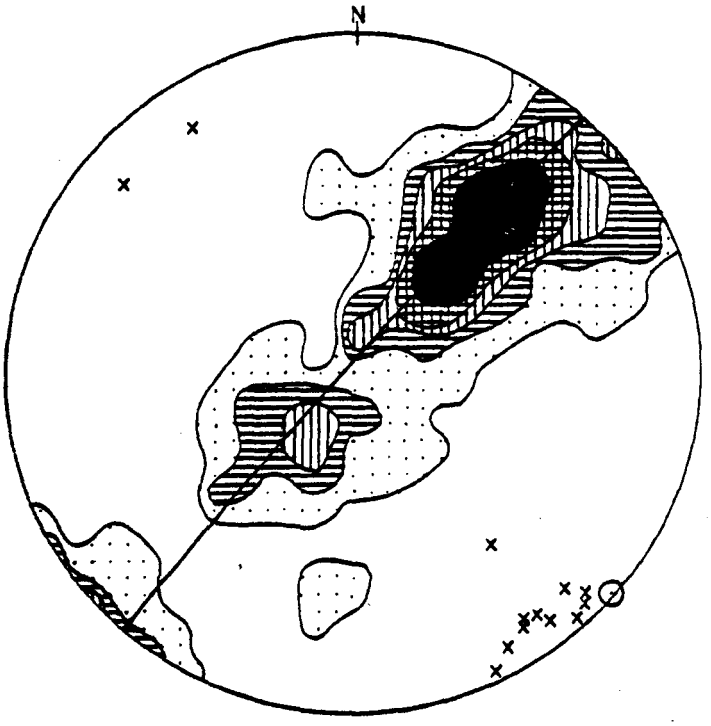

a

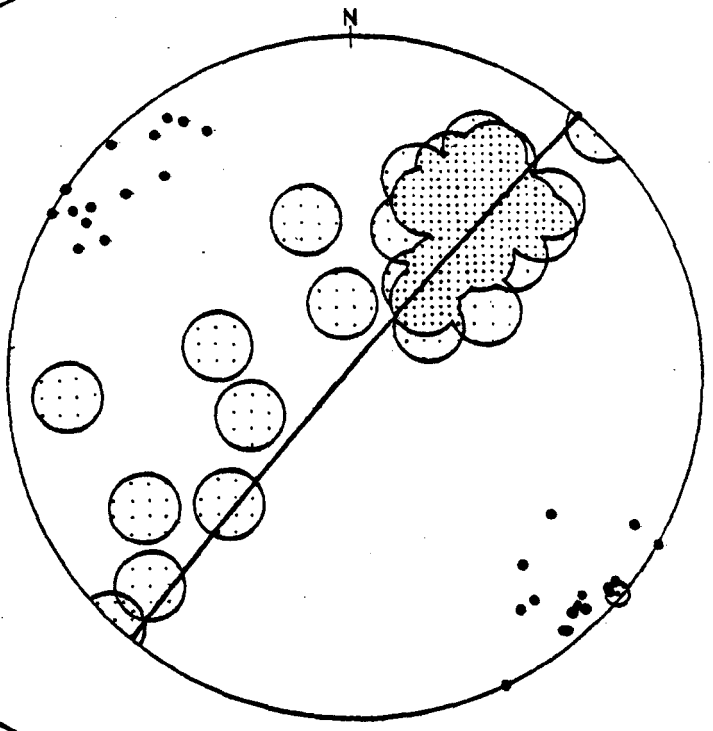

b

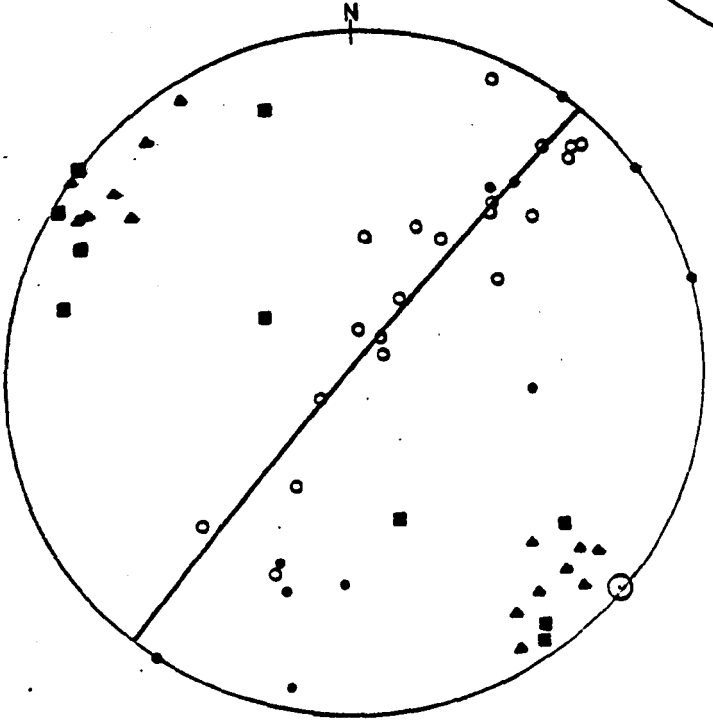

c

Fig. III-11a. Contoured plot of 126 poles to the gneissic foliation in domain 7 of 0.8%, 2%, 4%, 6% and 8% per 1% area. Crosses are the plot of the gneissic lineations. Circle with dot is the girdle axis.

Fig. III-11b. Contoured plot of 43 poles to the dyke foliation in domain 7, contours at 2.3% and 4.6% per 1% area. Solid circles are the plot of the dyke lineations. The best fit line and girdle axis are plotted from Fig. III-11a.

Fig. III-11c. Plot of mesoscopic F_2 and F_3 folds in domain 7.

○ = poles to the axial planes of the F_2 folds,

● = poles to the axial planes of the F_3 folds,

▲ = plot of the F_2 fold axes,

■ = plot of the F_3 fold axes.

The best fit line and girdle axis are plotted from Fig. III-11a.

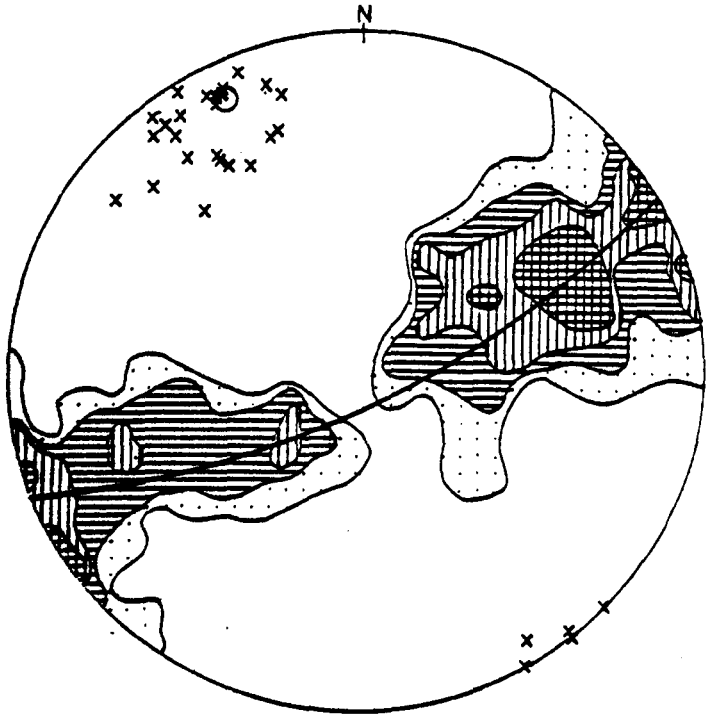

a

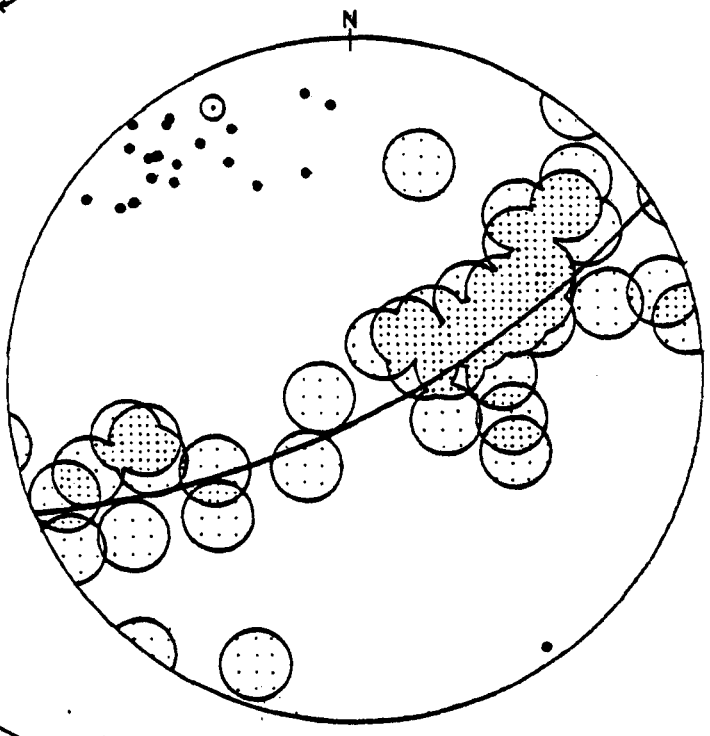

b

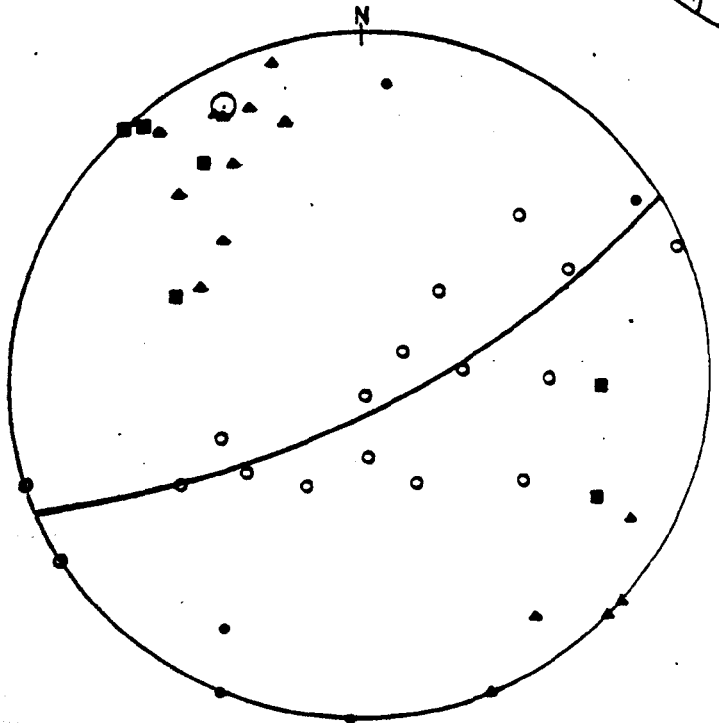

c

Fig. III-12a. Contoured plot of 96 poles to the gneissic foliation in domain 8, contouring at 1%, 2%, 4% and 6% per 1% area. Crosses are the plot of the gneissic lineations. Circle with dot is the girdle axis.

Fig. III-12b. Contoured plot of 75 poles to the dyke foliation in domain 8, contours at 1.3%, 4%, 6% and 8% per 1% area. Solid circles are the plot of the dyke lineations. The best fit line and girdle axis are plotted from Fig. III-12a.

Fig. III-12c. Plot of the mesoscopic F_2 and F_3 folds in domain 8.

○ = poles to the axial planes of the F_2 folds,

● = poles to the axial planes of the F_3 folds,

▲ = plot of the F_2 fold axes,

■ = plot of the F_3 fold axes.

The best fit line and girdle axis are plotted from Fig. III-12a.

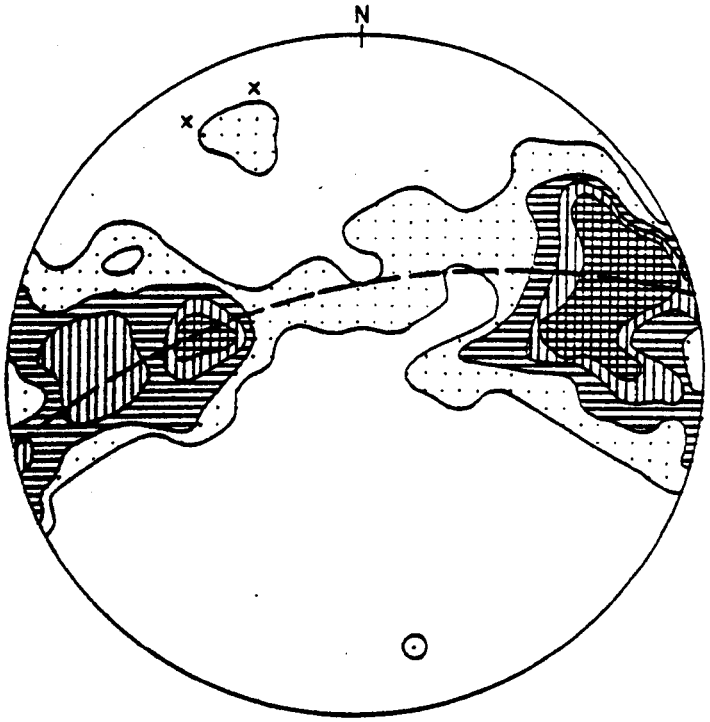

a

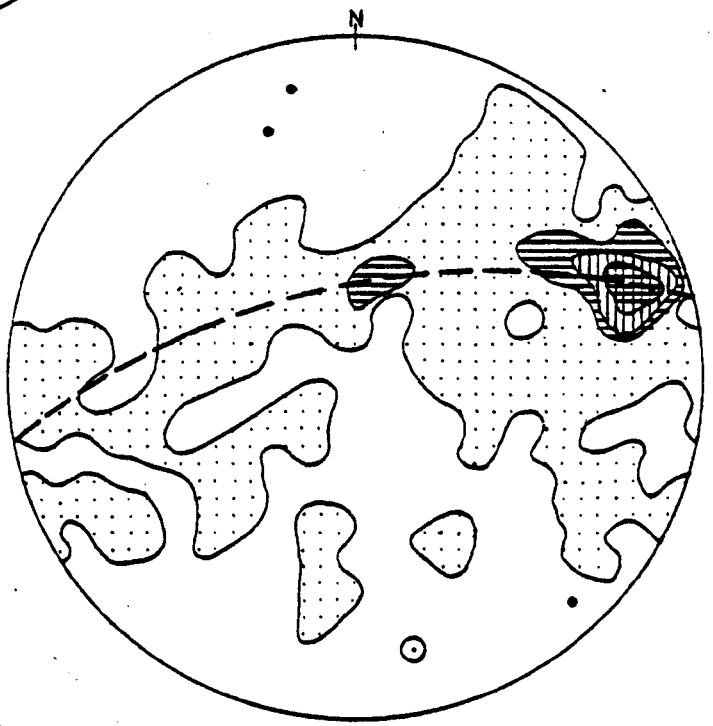

b

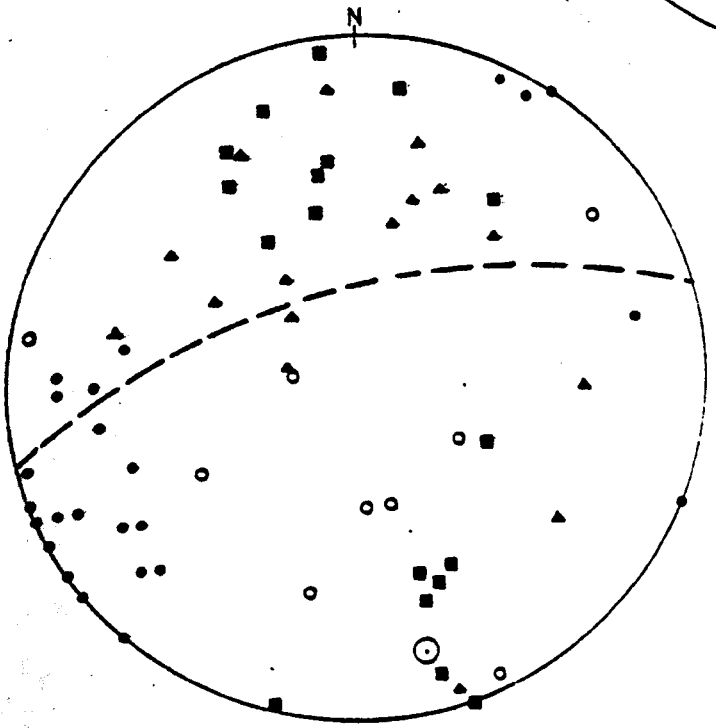

c

F_2 and F_3 folds instead of plunging in a direction parallel to the π-axis of the poles to the foliation as in case of co-axial folding or showing any other obvious distribution due to non-coaxial folding, apparently plot haphazardly (Fig. III-12c). Most of them plunge at various angles on azimuths in between NNE and NW. It is difficult to explain this pattern simply and it is worth noting that it is not easy to obtain the best fit line for the plot of poles to the foliation. Later (post D_3) brittle structures are very common in this domain and may affect the orientation of the minor F_2 and F_3 folds. However, they might also have been expected to have a more obvious effect on the plot of the foliations.

7. Domains 9 and 10

The gneisses and the dykes mainly dip towards the NE with a NW strike, but variations are present in their attitudes due to the upright F_3 folds, which plunge at low angles towards the SE. The statistical plot of the foliation also reveals that gneisses and dykes mainly dip towards the NE.

In domain 9, the poles to the foliation on the equal area net are concentrated in a great circle (Figs. III-13a,b) with a NE-SW-oriented girdle indicating the presence of cylindrical F_3 folds in this domain. The π-axis, which is the F_3 fold axis of major folds in the domain plunges at about 8^{o} towards S51^{o}E. This distribution is due in part to subhorizontal F_2 folds as well, which are both S- and Z-type.

In domain 10 on the other hand, poles to the foliation on the equal area net are concentrated in a small circle (Figs. III-14a,b) with ENE-WSW girdle revealing that the F_3 folds are slightly conical in the domain with an approximately 10^{o} cone axis. The cone axis plunges at about 25^{o} towards S27^{o}E. In this domain as well, some spread is due to subhorizontal F_2 folds.

Fig. III-13a. Contoured plot of 94 poles to the gneissic foliation in domain 9, contours at 1%, 2%, 6% and 8% per 1% area. Crosses are the plot of the gneissic lineations. Circle with dot is the girdle axis.

Fig. III-13b. Contoured plot of 38 poles to the dyke foliation in domain 9, contours at 2.3% and 4.6% per 1% area. Solid circles are the plot of the gneissic lineations. The best fit line and girdle axis are plotted from Fig. III-13c.

Fig. III-13c. Plot of mesoscopic F_2 and F_3 folds in domain 9.

○ = poles to the axial planes of the F_2 folds,

● = poles to the axial planes of the F_3 folds,

▲ = plot of the F_2 fold axes,

■ = plot of the F_3 fold axes.

The best fit line and girdle axis are plotted from Fig. III-13a.

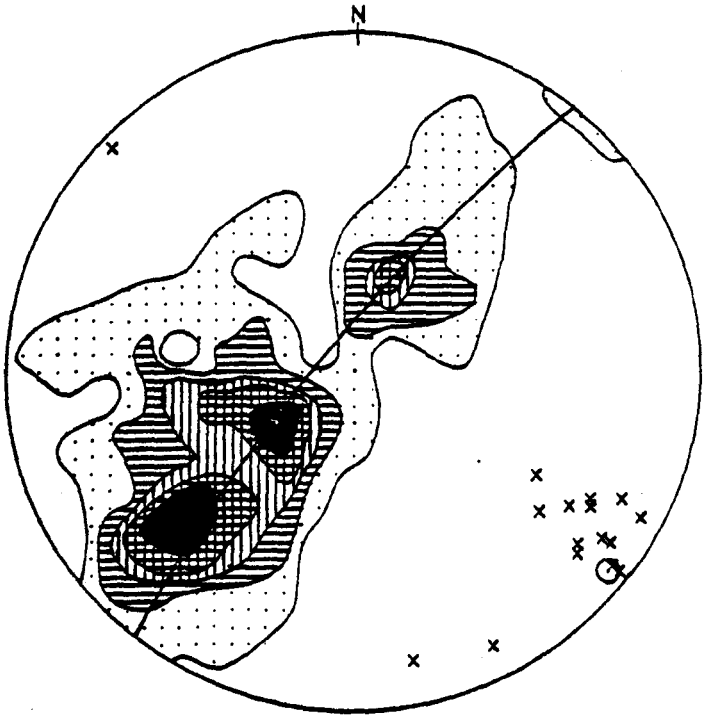

a

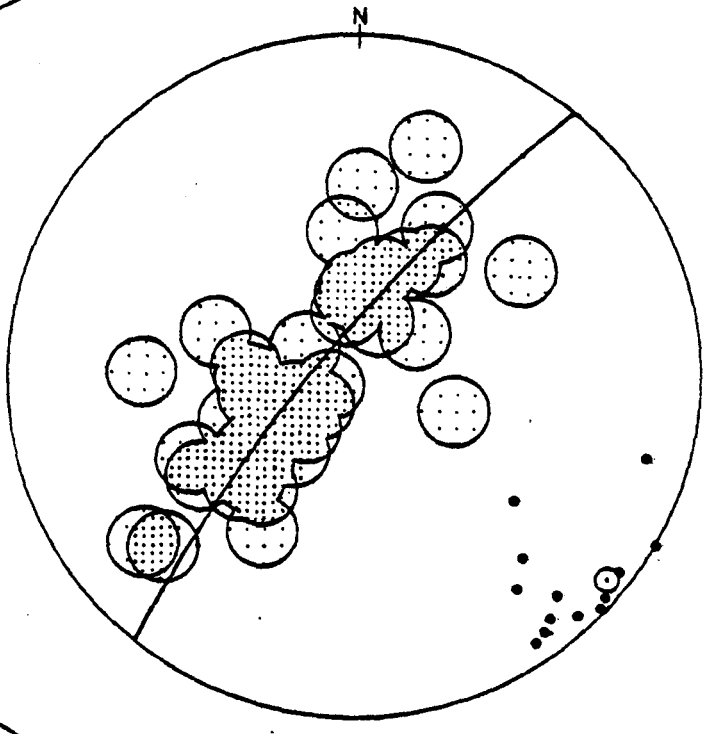

b

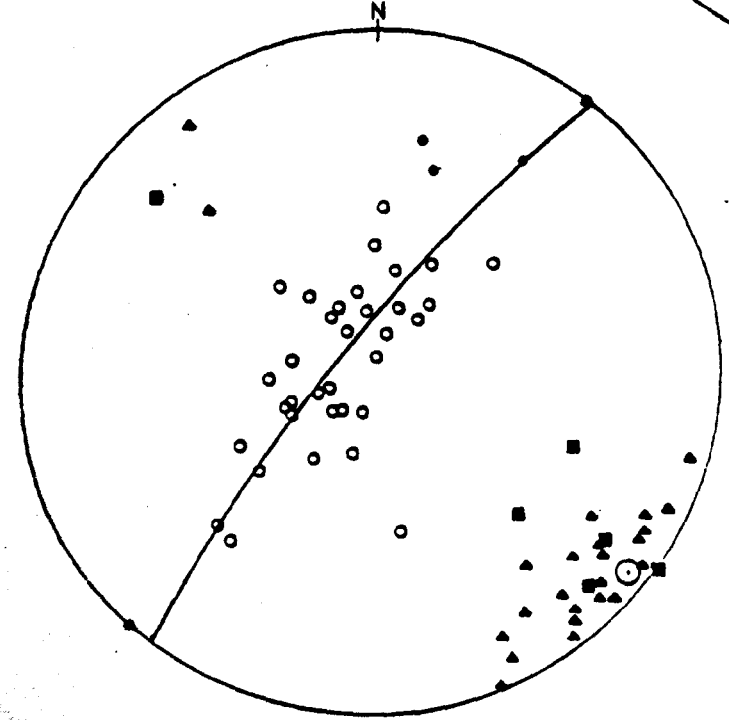

c

Fig. III-14a. Contoured plot of 133 poles to the gneissic foliation in domain 10, contours at 0.75%, 2% and 4% per 1% area. Crosses are the plot of the gneissic lineation. Circle with dot is the girdle axis.

Fig. III-14b. Contoured plot of 25 poles to the dyke foliation in domain 10, contours at 4% and 8% per 1% area. Solid circles are the dyke lineations. The best fit line and girdle axis are plotted from (Fig. III-14a).

Fig. III-14c. Plot of the mesoscopic F_2 and F_3 folds in domain 10.

○ = poles to the axial planes of the F_2 folds,

● = poles to the axial planes of the F_3 folds,

▲ = plot of the F_2 fold axes,

■ = plot of the F_3 fold axes.

The best fit line and girdle axis are plotted from Fig. III-14a.

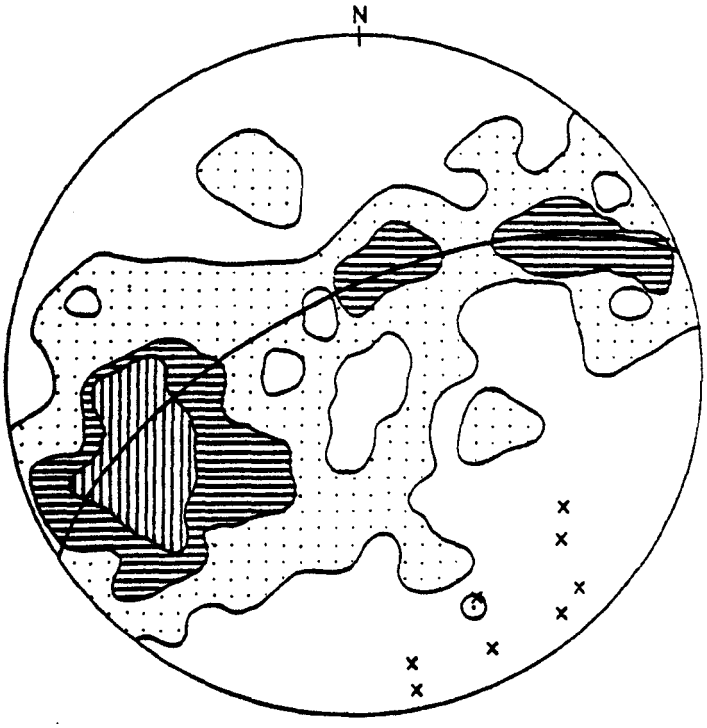

a

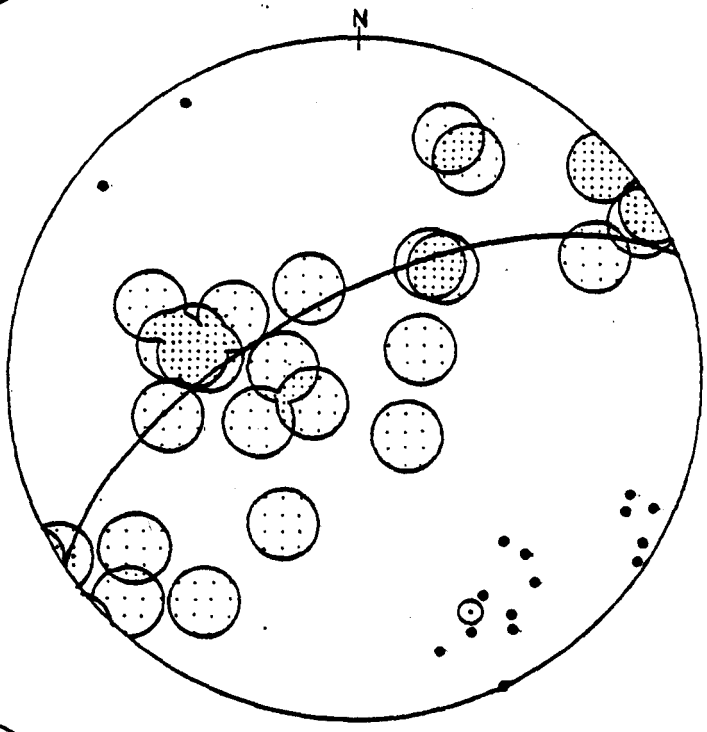

b

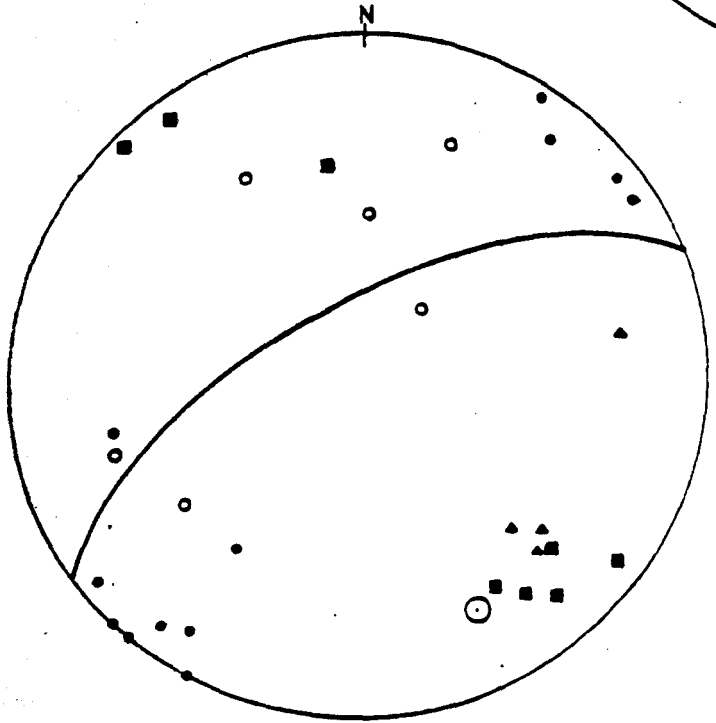

c

In domain 9, all the lineations and the axes of the minor F_2 and F_3 folds are parallel to the axis of the major F_3 folds (Figs. III-13a, b,c) revealing the co-axial nature of the folding. While in domain 10 the axis of the major F_3 fold is slightly asymmetric on the equal area plot to the lineations and to the axes of the F_2 and F_3 minor folds (Figs. III-14a-c) indicating slight non-co-axiality. The plot of minor F_3 folds on the equal area net is slightly asymmetric to the major F_3 fold, but unfortunately not much data is available from this domain. The same asymmetric relationship in the orientation plot of minor and major F_3 folds is also present in domain 11, where better data are available, and therefore the reasons for the asymmetric relationship in the equal area plot will be discussed for that domain.

8. Domain 11

The geometry of the structures in this domain is unique in the inlier. The gneisses and dykes are strongly folded into upright north-northwesterly plunging F_3 folds. The same orientation is obtained by plotting the poles to the gneissic and dyke foliation (Figs. III-15a,b). In this domain as well, the folds are slightly conical, which is revealed by the equal area plot of poles to the foliation. The cone angle is about 6^{o} and the axis plunges at about 40^{o} towards $N14^{o}W$.

The minor F_2 and F_3 folds are parallel to the lineation in the gneisses and dykes. The equal area plots show that the major F_3 fold (π-axis) is not oriented parallel to the minor F_3 folds and the lineations (Figs. III-15c,d), although the latter two have the same orientation. There might be several possible reasons for this offset, as discussed below:

Fig. III-15a. Contoured plot of 102 poles to the gneissic foliation in domain 11, contours at 1%, 2%, 4% and 6% per 1% area. Crosses are the plot of the gneissic lineations. Circle with dot is the girdle axis.

Fig. III-15b. Contoured plot of 31 poles to the dyke foliation in domain 11, contour intervals at 3.2% and 6.4% per 1% area. Solid circles are the dyke lineations. The best fit line and girdle axis are plotted from Fig. III-15a.

Fig. III-15c. Plot of the mesoscopic F_2 and F_3 folds in domain 11.

○ = poles to the axial planes of the F_2 folds.

● = poles to the axial planes of the F_3 folds,

▲ = plot of the F_2 fold axes,

■ = plot of the F_3 fold axes.

The best fit line and girdle axis are plotted from Fig. III-15a.

Fig. III-15d. Contoured plot of 25 F_3 fold axes in domain 11, contour interval at 4%, 8%, 12% and 16% per 1% area. Open circles are poles to the axial planes of the mesoscopic F_3 folds. The best fit line and girdle axis are plotted from Fig. III-15a.

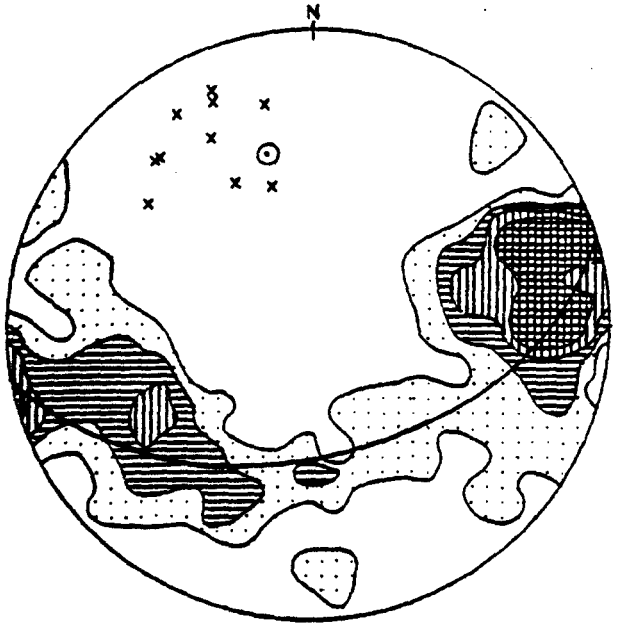

a

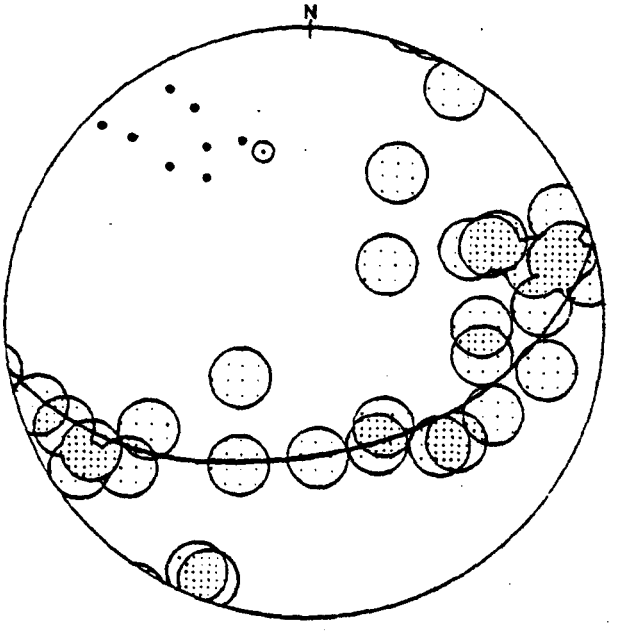

b

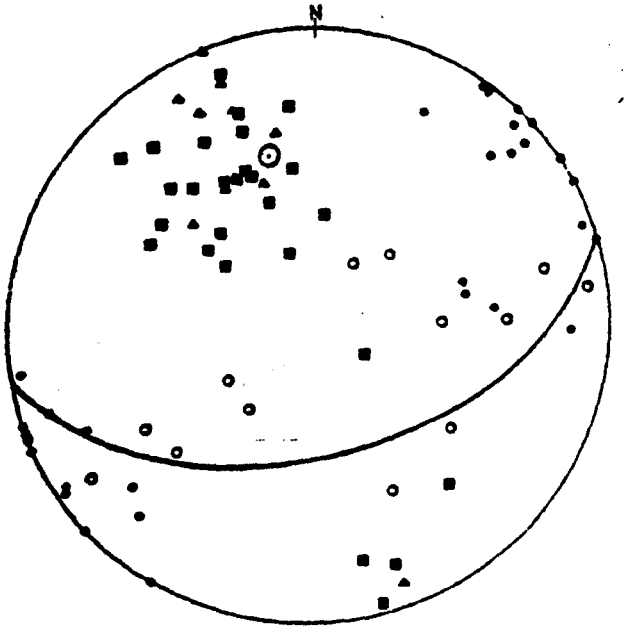

c

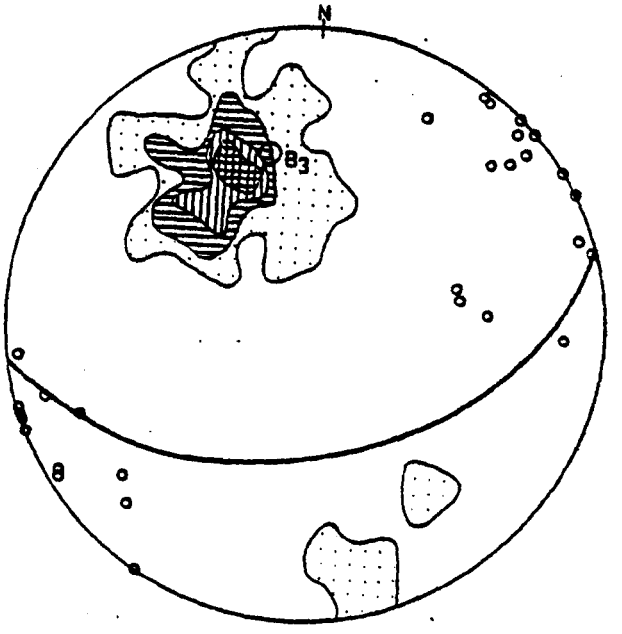

d

(1) The minor F_3 folds may have formed before the formation of the major F_3 fold, and there may have been a change in the local stress field between the time when the later minor folds formed and the time when the major folds formed. The first formed minor folds were presumably controlled by the linear anisotropy of the rocks and so have axes parallel to the lineations. All these structures were then refolded later during the formation of the major F_3 folds.

(2) The minor and major F_3 folds formed at the same time but the stress orientation was such that the major F_3 folds formed at an angle to the early lineations while the small scale folds were controlled by the linear anisotropy of the rocks and their axes were parallel to the shape fabric lineation in the rocks (Watkinson & Cobbold, 1981).

(3) The third possibility is that the girdle formed in the D_3-deformation is somewhat distorted by the post-D_3 deformation and therefore the π-axis may be incorrectly located.

The third explanation is considered unlikely since the post-D_3 deformation is insufficiently important in this domain. A similar type of problem is present in domain 10 (which supports reason 2) but unfortunately not much data is available in that domain. In a subdomain of domain 5, a contrasting case is present where the early lineation has been folded by major F_3 folds and minor F_3 folds are parallel with the major F_3 fold rather than with the early lineations. A comparison of this domain (11) with the subdomain of domain No. 5 suggests that for these two contrasting cases there is a critical angle between the major fold axis and the early lineations. If the angle between the major fold axis and the early lineations is greater than that critical angle then minor folds will form parallel to the major fold axis, as is the case

in the subdomain of domain 5 (Fig. III-9c). On the other hand if the angle between the major fold axis and the early lineations is less than that critical angle, the minor folds will form parallel to the linear anisotropy instead, which is probably the case in this domain and in domain 10.

9. Domain 12

Everywhere in this domain upright major F_3 folds are most probably affected by post-D_3 cross-folding. The equal area plot to the gneissic foliation shows that the poles are concentrated in the northeastern and the southwestern quadrants (Figs. III-16a,b), but their concentration is not good and it is difficult to draw a best-fit line. This spread in the poles to the foliation is partly due to F_3 folding and partly to post F_3 folding which is not strong enough to produce a good distribution on this plot, but is sufficiently effective to destroy the simple D_3 distribution.

Due to post-D_3 cross folding the early lineations and the axes of minor F_2 and F_3 folds have been rotated subvertically and now plunge at an angle to the NW and SE but with approximately the same bearing as the π-axis of the poles to the foliation.

10. Summary

In summarizing the above information, it can be said that the gneissic and dyke foliations are subparallel and have been folded along the same axial planes and fold axes. Throughout the inlier the attitude of the gneisses and the dykes have been controlled by the northwest-southeast to north-south oriented upright F_3 folds with subhorizontal to gently plunging fold hinges. The geometrical data related to the major structures are summarized in Fig. III-17. A major F_3 antiform and a major synform are present in the area. The synformal hinge-zone passes

Fig. III-16a. Contoured plot of 139 poles to the gneissic foliation in domain 12, contours at 0.7%, 2%, 4% and 8% per 1% area. Crosses are theplot of the gneissic lineation. Circle with dot is the girdle axis.

Fig. III-16b. Contoured plot of 49 poles to the dyke foliation in domain 12, contours at 2% and 4% per 1% area. Solid circles are the dyke lineations. The best fit line and girdle axis are plotted from Fig. III-16a.

Fig. III-16c. Plot of the mesoscopic F_2 and F_3 folds in domain 12.

○ = poles to the axial planes of the F_2 folds,

● = poles to the axial planes of the F_3 folds,

▲ = plot of the F_2 fold axes,

■ = plot of the F_3 fold axes.

The best fit line and girdle axis are plotted from Fig. III-4a.

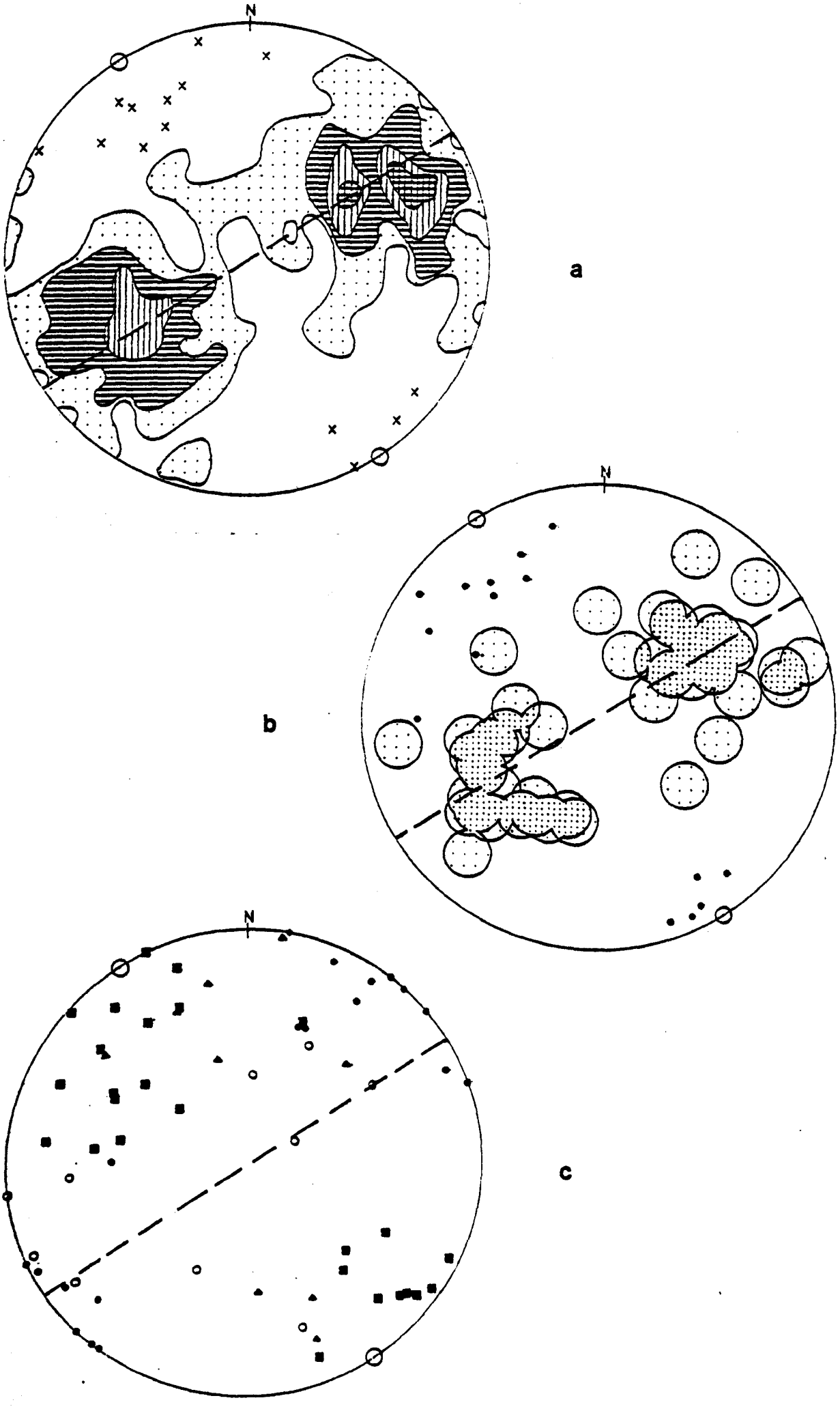
N
a
N
b
N
c

Fig. III-17. Summarised structural data from the various subareas. Solid lines in the stereograms are the certain best fit lines for the poles to the gneissic foliation in the domains, dashed lines are uncertain best fit lines. Small circles with dots within the stereograms are the F_3 fold axes for these domains. Where folds are somewhat conical their cone angle is also given. Numbers within circles on the map are domain numbers. Plunge direction and amount of F_3 fold axes are marked in each domain.

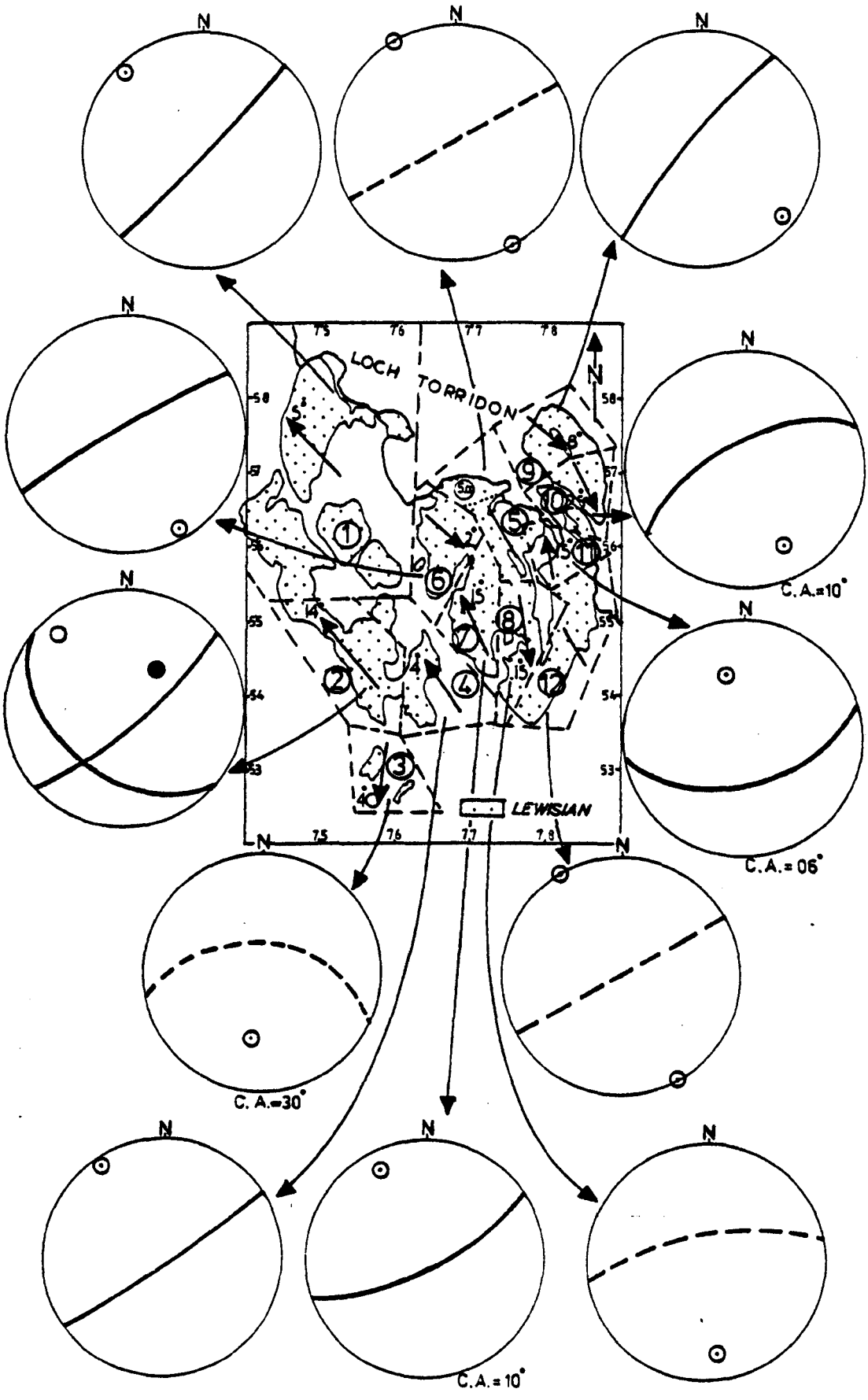
N
LOCH TORRIDON
LEWISIAN
75
76
77
78
58
57
56
55
54
53
C.A.=10°
C.A.=06°
C.A.=30°
C.A.=10°

through subareas 2,4 and the southern parts of subarea 1 (Figs. III-2,4, 7 and Enclosure 2), which is confirmed by the nearly equal density maxima in the northeastern and southwestern quadrants of the contoured stereograms. In fact observations in the domain 1 are biased by the uniformly SW dipping rocks on the hill between Kenmore and Arrina. The rocks on the southwestern edge of the area dip towards the southwest in these domains and totally in domain 3 (see Fig. III-6). In domains 6, 7 and the northern part of domain 1 the rocks dip more uniformly towards the southwest (Figs. III-1,10 and 11), since the synformal hinge zone is present southwest of it and antiformal hinge zone is to the NE of it. A major F_3 antiformal hinge zone passes through domain 5 and parts of domains 8 and 12 which is also obvious from the plot of the foliation in these subareas (Figs. III-8,12 and 16). Rocks in the northeastern part of the area i.e. on Ardheslaig peninsula mainly dip towards the NE which is also shown by the maxima of the poles to the foliations in the southwestern quadrants of these domains (Figs. III-13 and 14). While most of the rocks in domain 11 dip towards SW (Fig. III-15) indicating that another antiformal hinge zone is present between domain 11 to the SW and domain 9 and 10 to the NE (see sections B-7 and 8).

The axial surfaces of the F_2 folds are subparallel to the gneissic and dyke foliation (Figs. III-18a,b) and have been folded along the same axes and planes. The F_2 fold axes are generally concentrated in the same area of the equal area plot as the F_3 fold axes (Fig. III-18c), proving co-axial deformations. However in some localized places non-coaxial relationships are present between pre-D_2 lineations, F_2 fold axes and F_3 fold axes.

Fig. III-18a. Contoured plot of 1,693 poles to the gneissic foliation in the whole area, contoured at 0.05%, 1%, 2%, 4% and 6% per 1% area.

Fig. III-18b. Contoured plot of 265 poles to the axial planes of the mesoscopic F_2 folds in the whole area, contours at 0.4%, 1%, 2%, 3% and 4% per 1% area. Solid circles are the plot of 180 fold axes.

Fig. III-18c. Contoured plot of 190 poles to the axial planes of mesoscopic F_3 folds in the whole area, contours at 0.5%, 2%, 5% and 10% per 1% area. Solid circles are the plot of 212 fold axes.

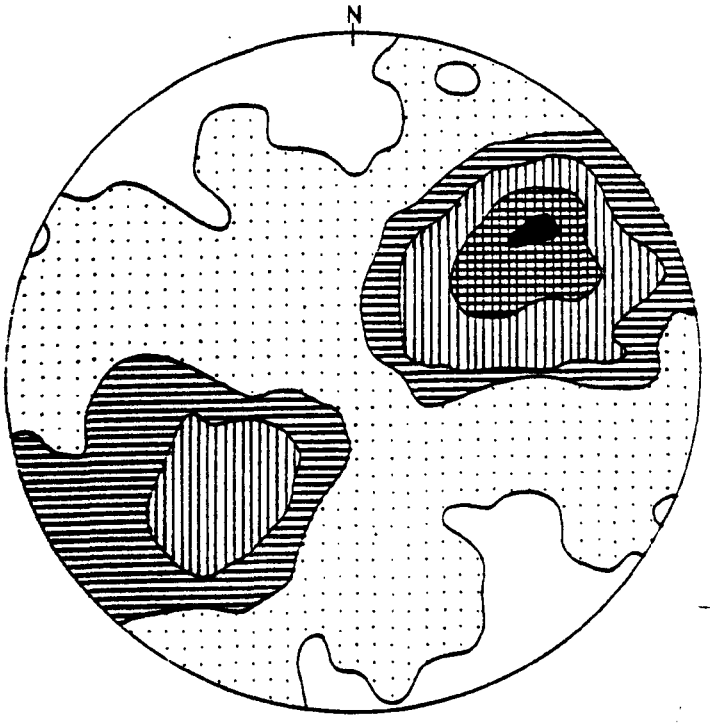

a

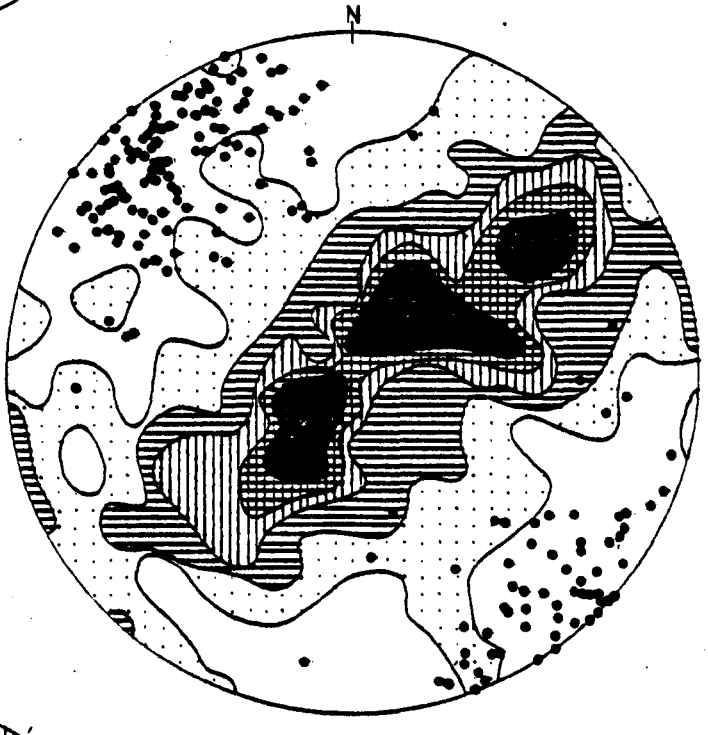

b

c

Most of the area was mildly affected by post-D_3 cross folding due to which there is some distortion in the maxima of the foliation plot, the lineations and the minor fold axes. Bending of the axial traces of major F_3 folds is also probably post-D_3. Minor post-D_3 folds are rare in the area, they are upright with axial planes oriented from nearly E-W to NE-SW (Fig. III-19). Their fold axes plunge according to their position on the F_3 folds in most of the area but in the southwestern part they plunge only towards the NE because only NE-dipping rocks are folded there.

C. DESCRIPTION OF POST DYKE STRUCTURES

1. D_1 Structures

Shape fabric is the main structure produced in the first deformation. Macroscopic folding is not recognized in the area and mesoscopic folding is rare.

a. D_1 Fabric. This can be recognized in the dykes and is quite common throughout the area, although difficult to differentiate from the D_2 fabric. The fabric is approximately parallel to the dyke margins. In the Scourie dykes a good schistosity is developed by the preferred orientation of hornblende and feldspar on preferred planes, and by mineral concentration and segregation along these planes. Usually these minerals are also concentrated in elongated domains, and in some cases exclusively in rod-shaped domains giving S, LS and L-shape fabrics respectively (Flinn, 1965). In general these fabrics tend to be LS-type but more linear than planar.

Fig. III-19. Equal area plot of the mesoscopic post D_3 folds from the whole area. Open circles are the poles to their axial planes and solid circles are the plot of fold axes.

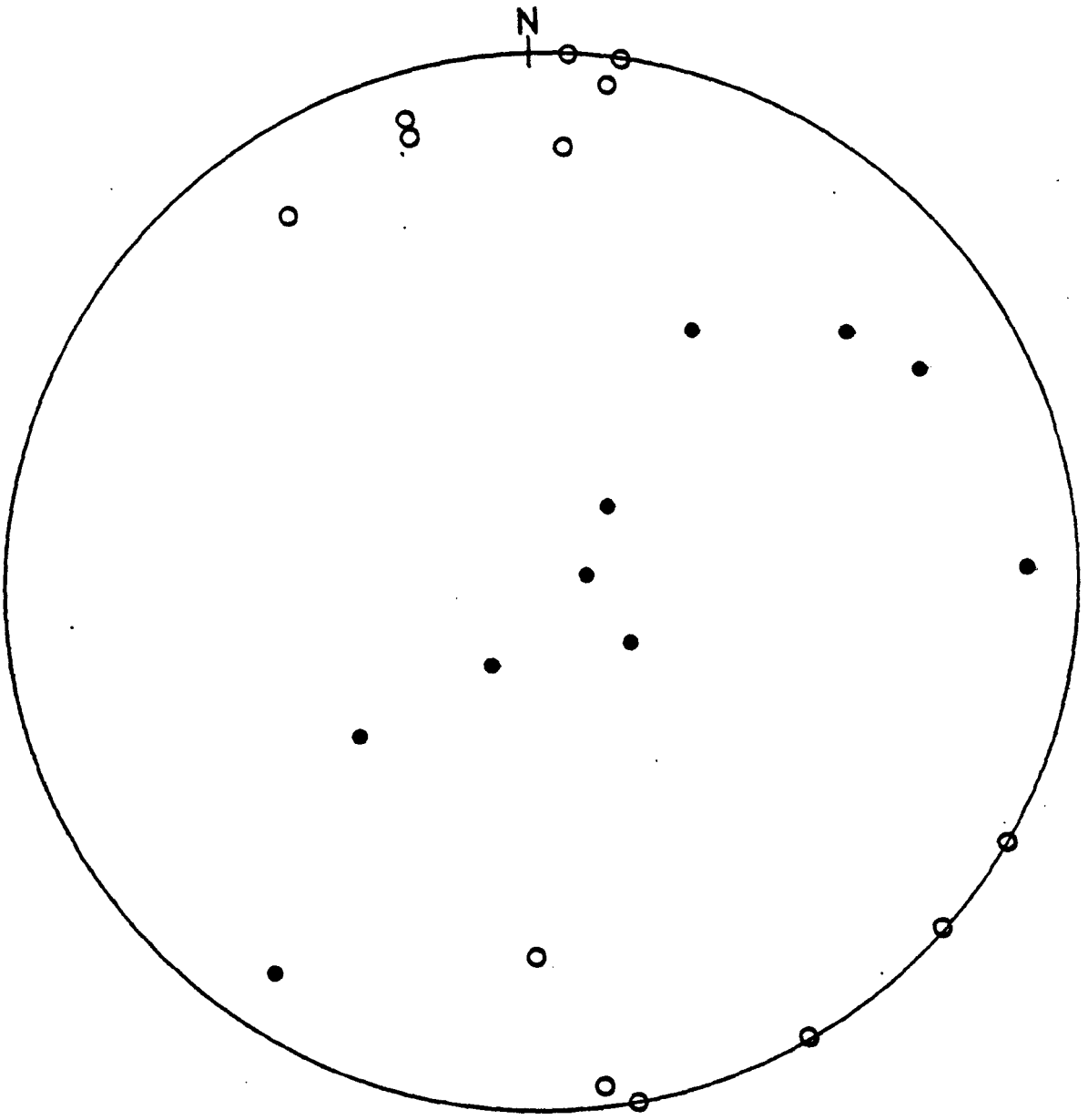
N

It is not possible to differentiate this fabric from the pre-dyke Inverian fabric in the gneisses, because the earlier gneissic planar fabric is subparallel to the S_1 fabric. Therefore it is difficult to say in individual cases whether the fabric originally had a subparallel relation with the dykes or whether it was brought into parallelism with the dykes due to deformation.

b. F_1 Folds. F_1 folds are very rare and can be recognised only with certainty in the dykes where a gneissic screen or vein was present and folded in this deformation (see Pl. III-4b). The S_1 fabric is axial planar to such folds. The F_1 folds are refolded by F_2 folds co-axially.

2. D_2 Structures

Folds are the widespread structures produced in the second deformation. They fold the gneisses and dykes, the LS_1-shape fabric of the dykes and the early lineation. A new axial planar foliation and a lineation are also important structures of the second Laxfordian deformation.

a. F_2 Folds. These generally have subhorizontal to gently-dipping axial surfaces, subparallel to the gneissic and dyke foliation (LS_1), with NW-SE oriented subhorizontal hinges. They are mostly mesoscopic structures with wavelengths generally less than one metre and amplitudes less than half a metre. Large-scale folds are very rare and do not exceed 50 metres in wavelength and 25 metres in amplitude. These large-scale folds are present on the hill near Kenmore and on A'Bhainlir hill. Microscopic folds are also present.

The folds are variable in style as seen in profile. Mostly they have a similar or near similar geometry (class 2, class 1c or 3 near to class 2, of Ramsay 1967), with variable orthogonal thickness on the hinge and limbs while the layer thickness measured parallel to the axial surface is nearly the same throughout the layer, and the dip isogons are always subparallel or at low angles to the axial surface (Fig. III-20). They are usually tight to close (Fleuty, 1964), although some open folds are also present.

Usually they are strongly asymmetrical, mostly of S-type looking NW i.e. which verge towards the SW (Roberts, 1974; Bell, 1981), although some M-type folds are also present. Z-type folds looking NW are rare.

Synforms and antiforms are of the same style when layers of the same composition and competence have been folded but folds are usually of cuspate type when they affect the contact of two different types of rock - e.g. dyke contacts with acid or intermediate gneisses (Pl. III-10). The cusps point from the dykes into the gneisses indicating that the dykes had a lower competency.

In profile their shape is variable, mostly having rounded hinges with curved limbs (Pl. III-11a) but folds with narrow hinge zones are straight limbs are also present (Pl. III-11b). On unfolding the later F_3 folds, it can be seen that the F_2 folds are flat-lying subhorizontal structures.

b. Relationship with D_1 Structures. Because F_1 folds are rare, very little can be said about the F_1-F_2 relationship. In most places F_2 axes are parallel to the early lineations indicating the co-axial nature of the deformation (Pl. III-5b). However, in some places due

Fig. III-20. Two examples of typical F_2 folds from the area. (a and b) fold profile with dip isogons, (c and d) t' versus α plot for various folded layers from profiles a and b respectively.

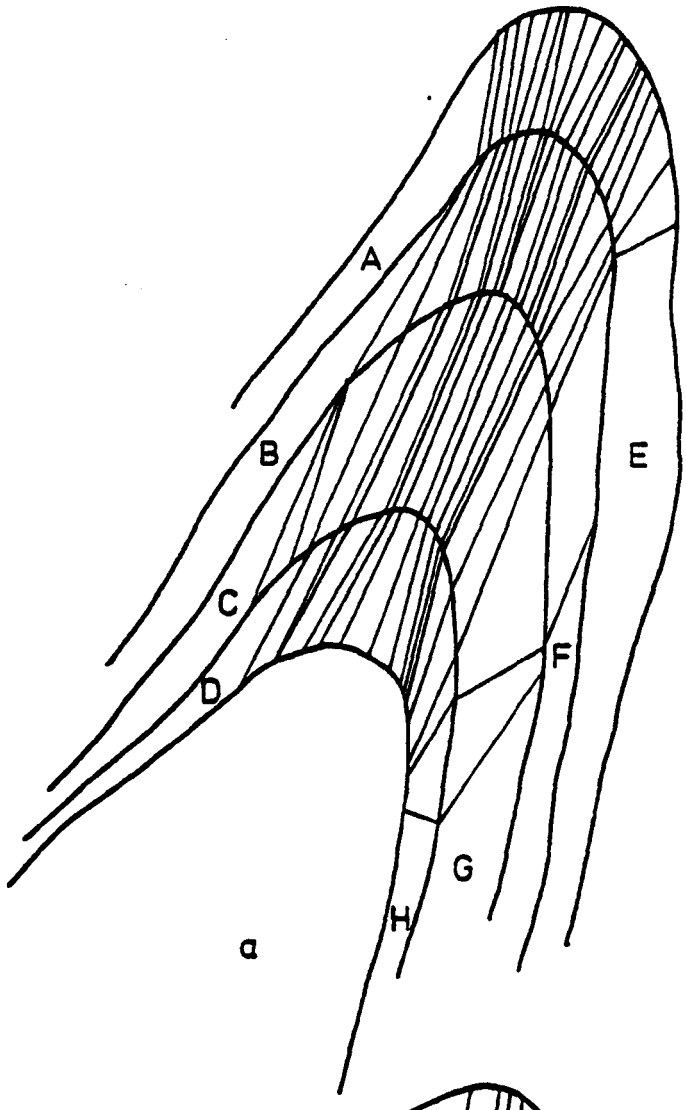
A
B
C
D
E
F
G
H

a

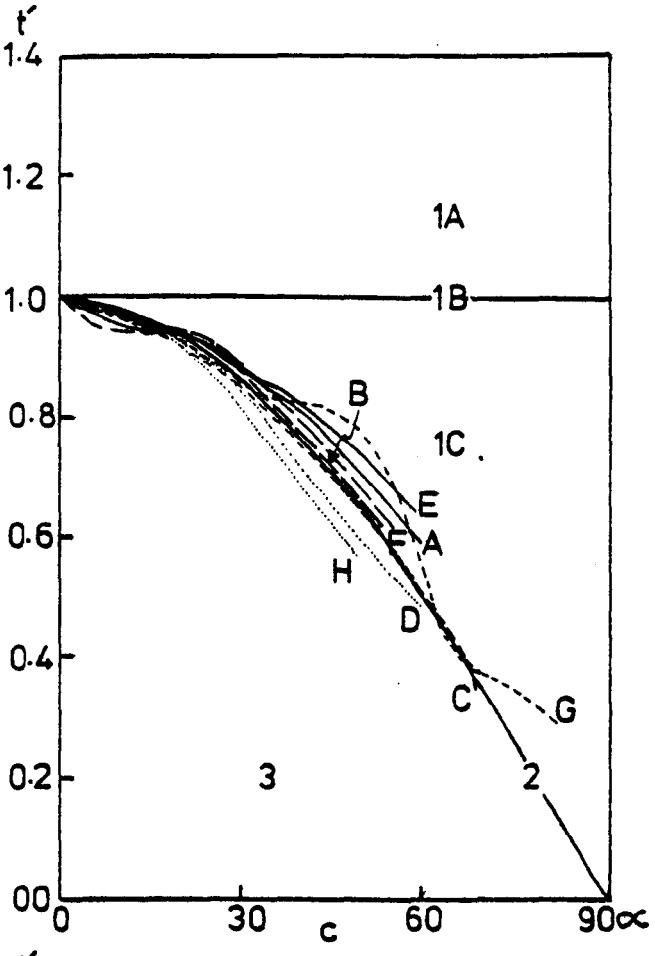
t'
1·4
1·2
1·0
0·8
0·6
0·4
0·2
00
1A
1B
1C
3
2
B
E
A
F
H
D
C
G
0
30
60
90∝

c

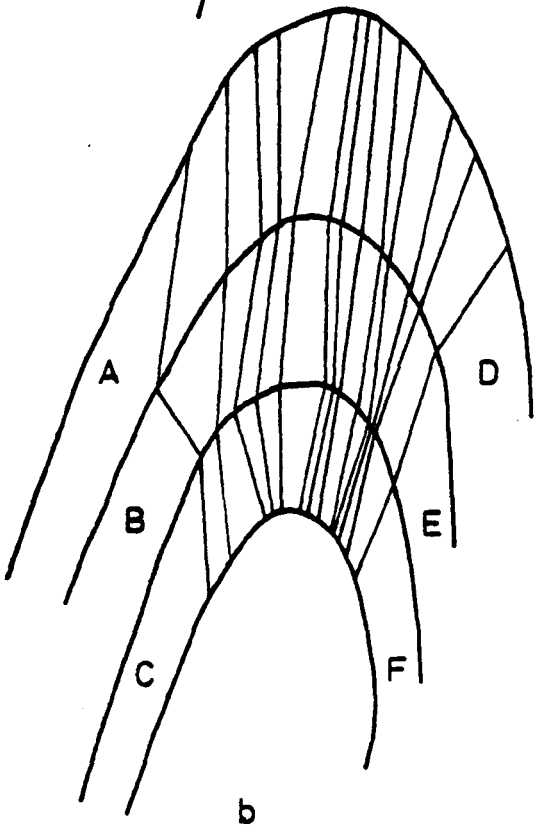
A
B
C
D
E
F

b

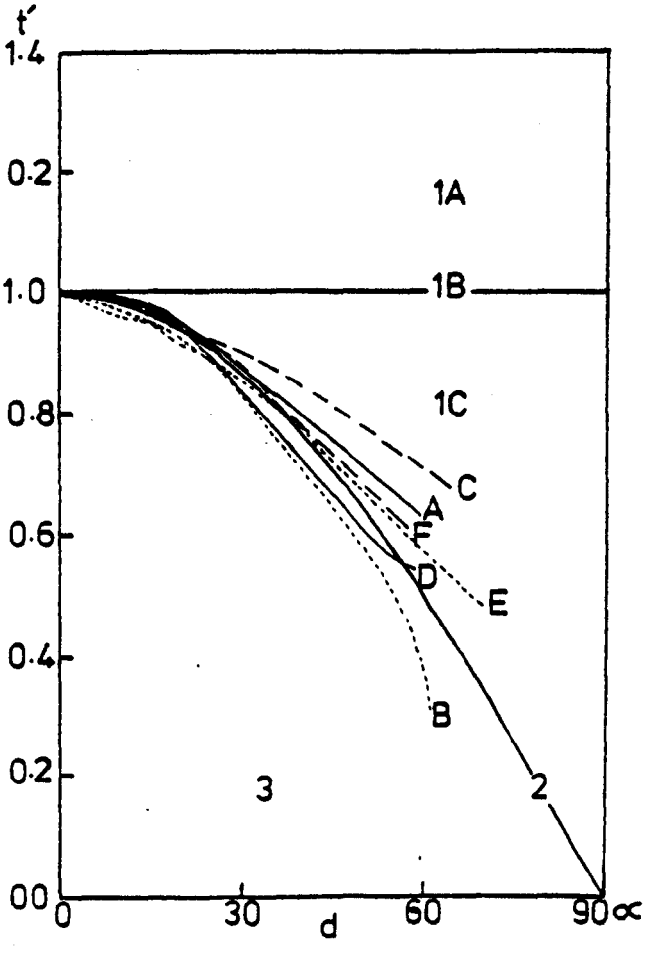
t'
1·4
0·2
1·0
0·8
0·6
0·4
0·2
00
1A
1B
1C
3
2
C
A
F
D
E
B
0
30
60
90∝

d

Plate III-10. F_2 folds of cuspate nature at a dyke contact with sub-horizontal axial surfaces. The cusps points towards the gneiss (77395496).

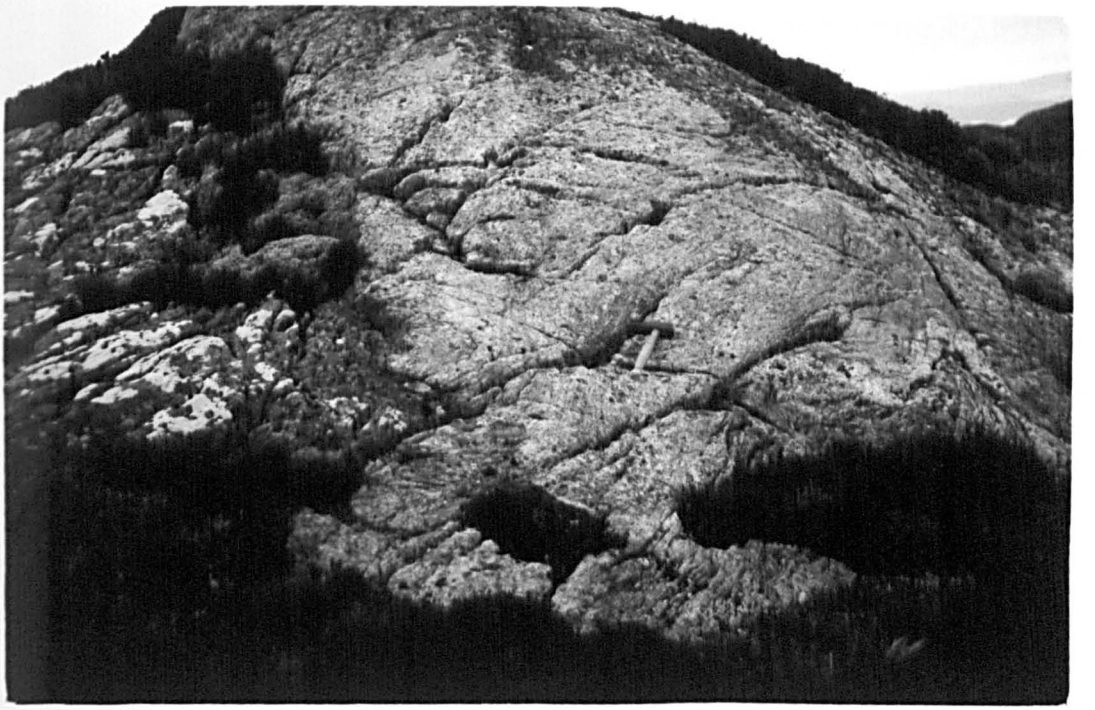

Plate III-11a. F_2 fold in gneiss with curved hinge zone (73915661)

Plate III-11b. F_2 fold in gneiss with sharp hinges and straight limbs (74965510).

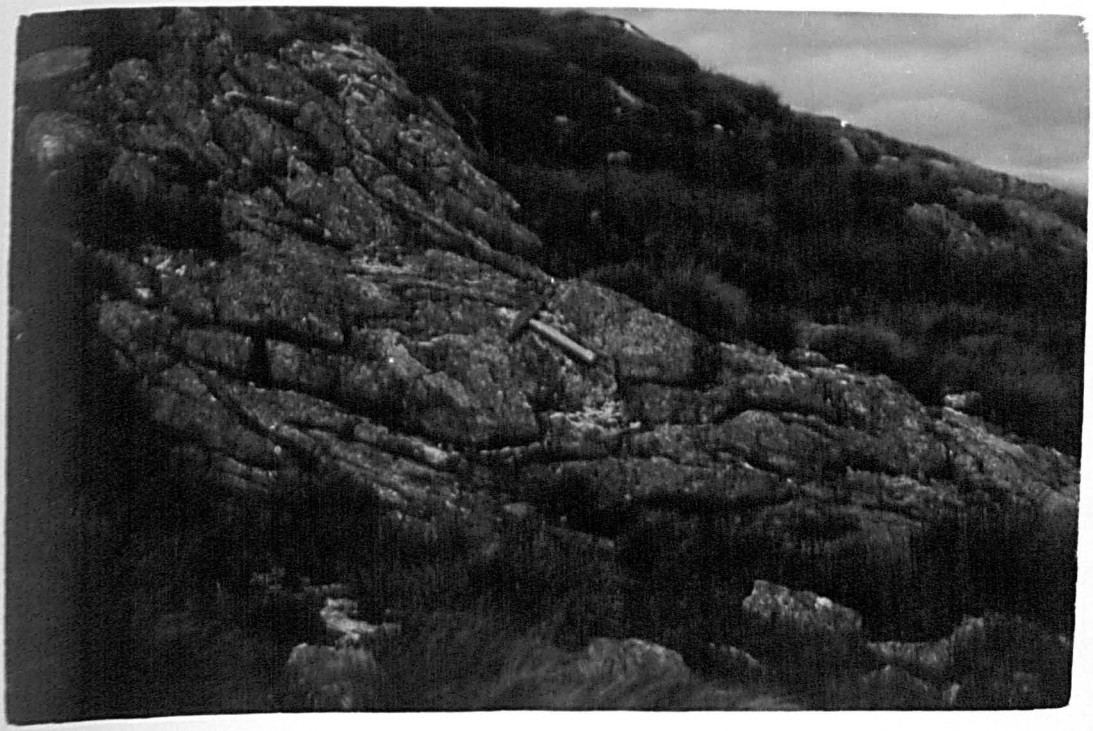

to slight non-coaxiallity, F_2 folds fold the pre-L_2 lineations (Pl. III-6a). In a small area, this folded lineation has been plotted on an equal area net, and is concentrated on a great circle (Fig III-3c).

c. D_2 Fabric. The S_2 foliation is axial-planar to the F_2 folds. In the symmetric F_2 folds it is parallel to the axial surface but in asymmetric folds it is sometimes parallel to the axial surface and sometimes more to the long limbs of the asymmetric folds. In the Scourie dykes the fabric is more or less parallel to the dyke margins, but where dyke contacts are folded it is axial planar. It is also defined by the hornblende and feldspar aggregates present in separate domains and is penetrative like LS_1. The longer axes of hornblende and biotite lie in the plane of the foliation. Because it is of the same nature as S_1, it is therefore difficult to differentiate it with certainty unless S_1 has been folded into F_2 folds or S_2 is axial planar to the F_2 folds. Only in a few places, particularly on Ardheslaig peninsula, is this difference clear. Here both the LS_1 fabric and the F_2 folding are well developed. The LS_1 fabric has been transposed into the new S_2 foliation. Although transposition of the LS_1 fabric is quite strong, some F_2 intrafolial folds can still be seen. In some places, where biotite is present in quantity, foliation has been strongly crenulated (Pl. III-12a).

In the acid gneisses, the S_2 foliation is mainly defined by the preferred orientation of mineral grains, especially those of tabular habit. Where F_2 folds are quite tight and deformation is strong, the early gneissic foliation has also been transposed into S_2 and the pre-S_2 foliation can be recognised only from the gneissic banding (Pl. III-6b).

Plate III-12a. S_1 fabric in the dyke has been crenulated into F_2 folds and a weak S_2 crenulation cleavage runs parallel to the short edge of the photograph (74615759).

Plate III-12b. Ultrabasic lenses in gneiss with their long axes in the thin section parallel to the axial plane of the F_2 folds (78295721).

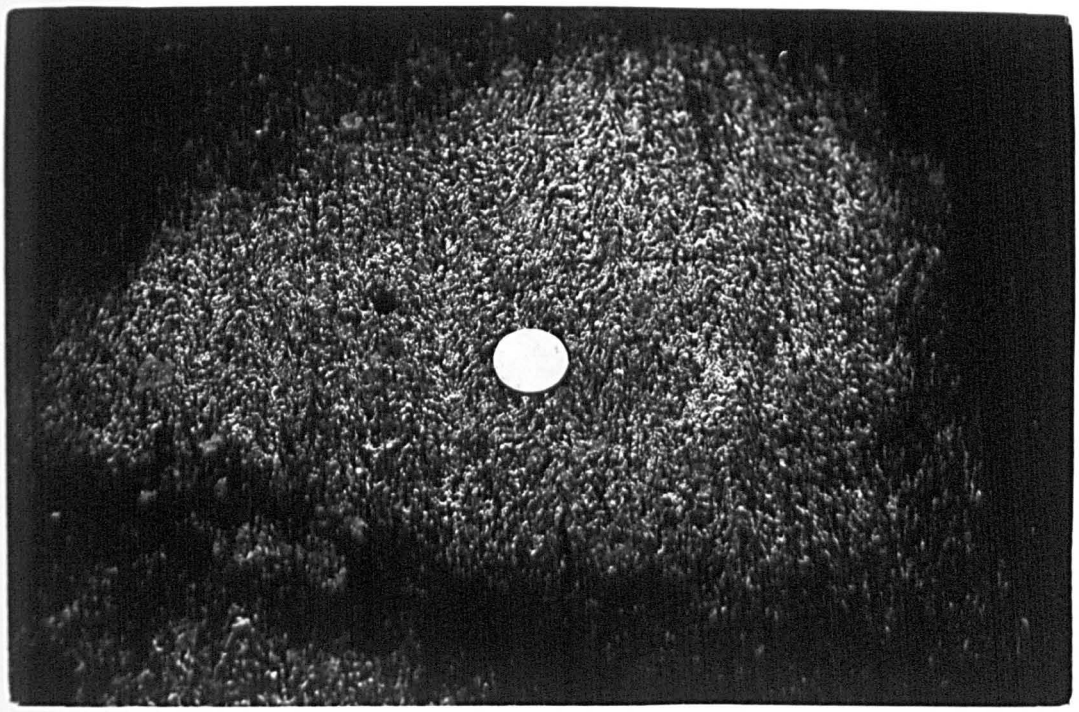

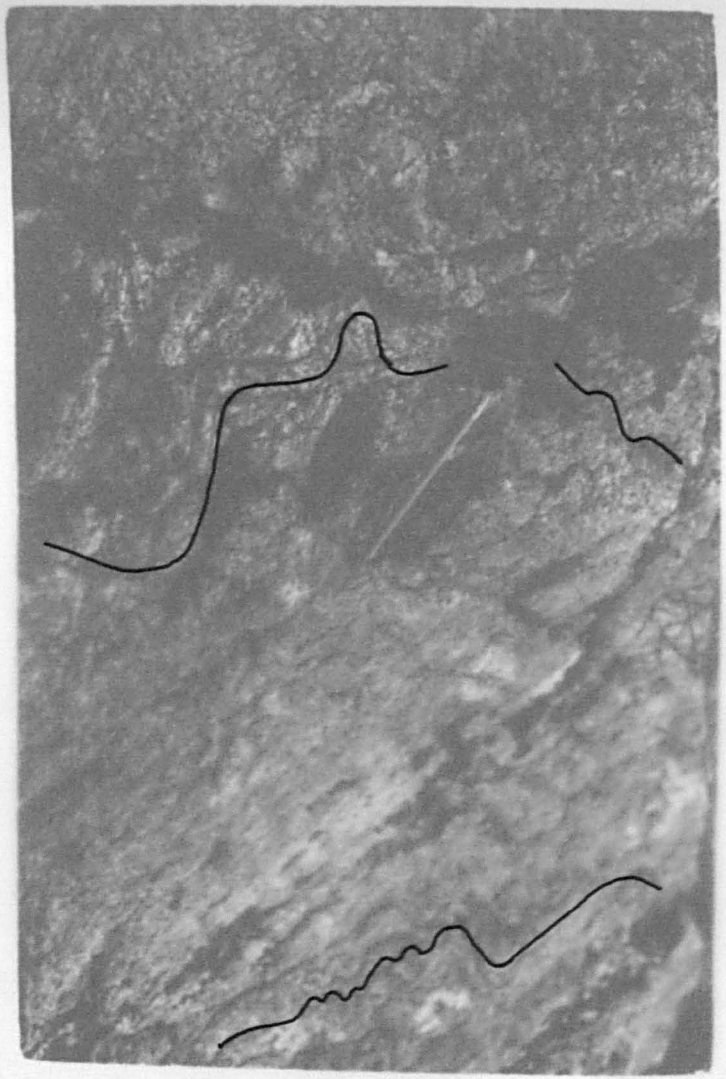

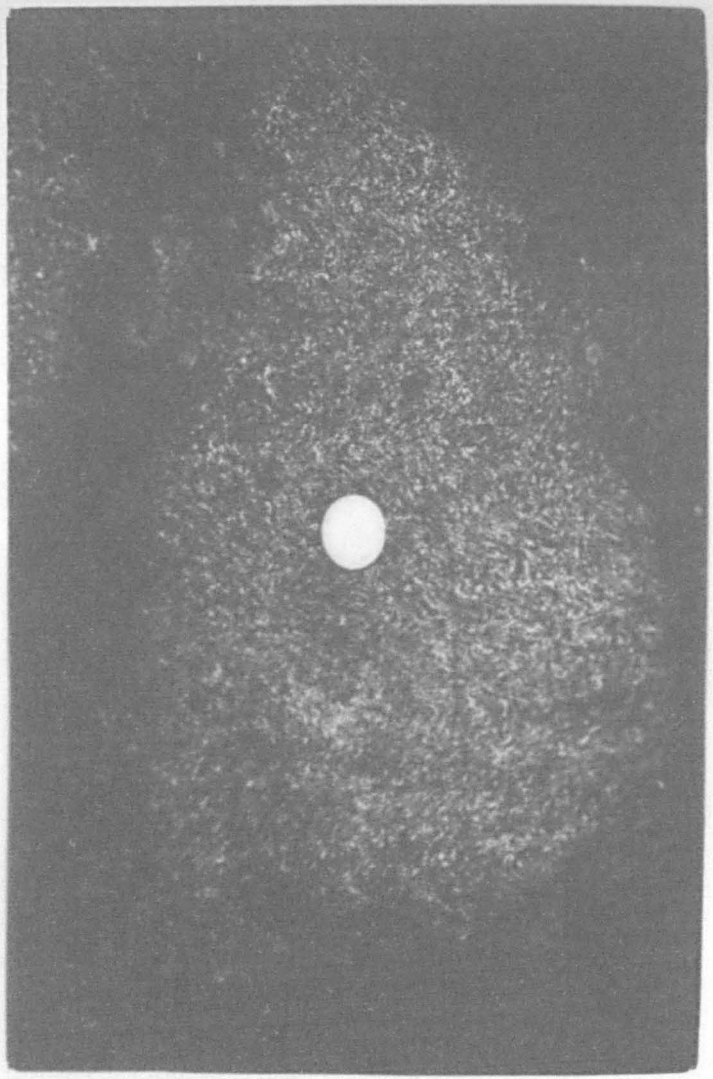

Fabric lineations in the dykes and gneisses are defined by the elongate domains of equant grains and lie in the plane of the shape fabric foliation giving an LS shape fabric. The lineation is everywhere parallel to the F_2 fold axes and so is co-axial.

Where a mineral lineation is present in the form of hornblende needles or biotite flakes it is arranged in such a way that the longest axes of the minerals are parallel to each other and to the F_2 fold axes. The association of this mineral lineation with the fold axes indicates a co-eval relationship.

All over the area, pre-dyke early basic and ultrabasic pods and lenses are present with their longest axes measuring about half a metre on average. These bodies are probably boudinaged structures formed by the extension of early basic and ultrabasic layers in pre-Laxfordian deformations. The plane containing the longest and intermediate axes is always parallel to the gneissic foliation wherever the gneiss has not been folded into F_2 folds, but wherever F_2 folds are present the XY plane of these lenses is always oriented parallel to the F_2 axial surface (Pl. III-12b) and their major axes always lie parallel to the F_2 fold axis.

3. D_3 Structures

The outcrop pattern of the dykes and gneisses is controlled by these structures. Upright folds with subhorizontal or gently plunging axes fold all previous structures. Locally a good axial planar fabric is present.

a. F_3 Folds. These are variable in size, ranging from macroscopic folds with wavelengths of kilometres and amplitudes of hundreds of metres to mesoscopic folds and even microscopic folds with wavelengths and amplitudes of millimetres.

These folds usually have broad and rounded hinge zones and are variable in tightness with interlimb angles ranging from gentle to tight (Fleuty, op. cit.).

In profile, F_3 folds are generally of concentric style (Pl. III-13a) with constant orthogonal thickness throughout the folded layer with converging dip isogons. However a large variation is present and their geometry ranges from class 1A to class 3 (Fig. III-21) for various layers, depending on the competency of the individual layer in a multilayer system. In the folded belt just SW of Ardheslaig they are highly flattened and their geometry is closer to similar folds (Fig. III-22). Except in rare cases where the curves on the t'/α diagram are irregular on the limbs of fold, the curves have a gentle slope showing uniform flattening on the hinge zone and on the limbs of minor folds.

In cross-profile along the axial surface, even on a mesoscopic scale they are typically disharmonic in nature (Pl. III-13b).

At the hinge zone of the major F_3 synform in the southwestern part of the area minor F_3 folds are somewhat symmetrical and generally of M-type. While in most of the central area and in most part of strongly folded belt south and southwest of Ardheslaig they are generally of Z-type asymmetry looking NW or they verge towards the NE (Roberts, 1974; Bell, 1981), but M-type folds are also present.

Plate III-13a. Dyke and gneisses folded into upright F_3 concentric fold (77915667).

Plate III-13b. Dyke and gneisses folded into upright F_3 disharmonic folds (77615526).

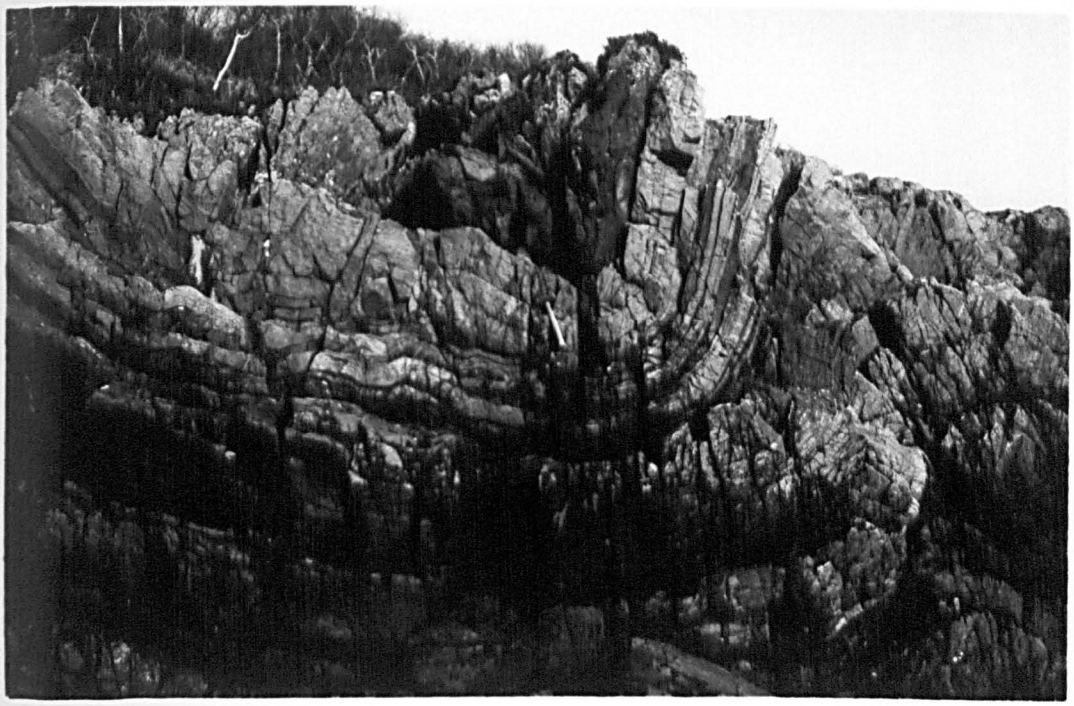

Fig. III-21. Two examples of typical F_3 folds from the area.
(a & b) fold profile with dip isogons,
(c & d) t' verses α plot for various folded layers from profiles a and b respectively.

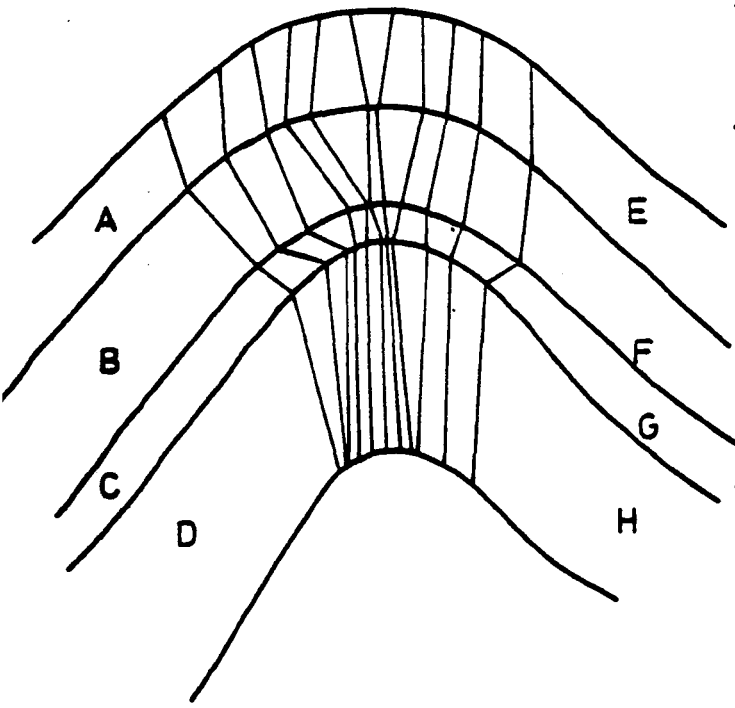
A
B
C
D
E
F
G
H

a

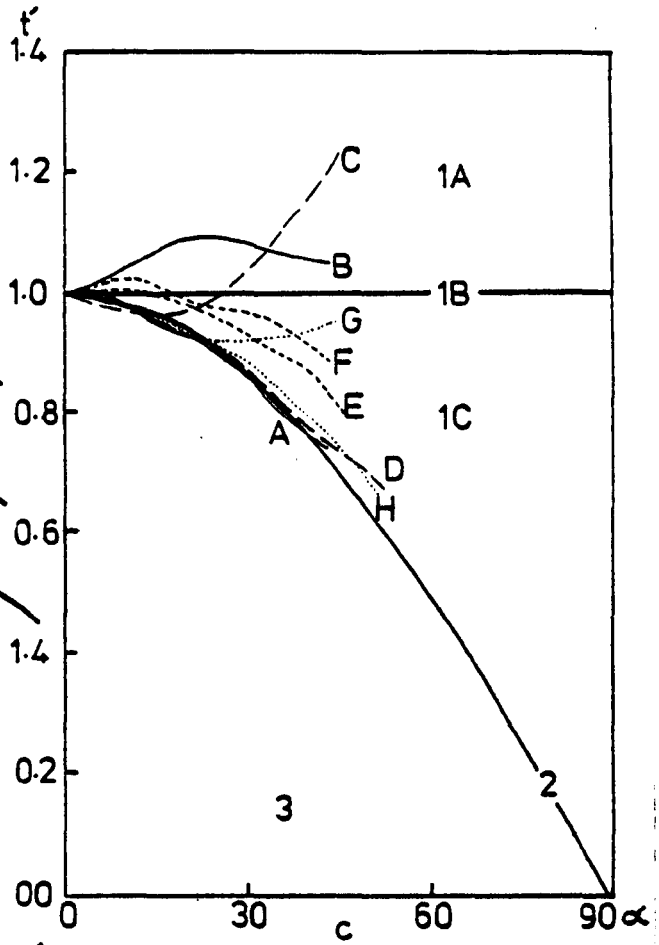
t'
1·4
1·2
1·0
0·8
0·6
1·4
0·2
00
0
30
60
90 α
C
B
G
F
E
A
D
H
1A
1B
1C
3
2

c

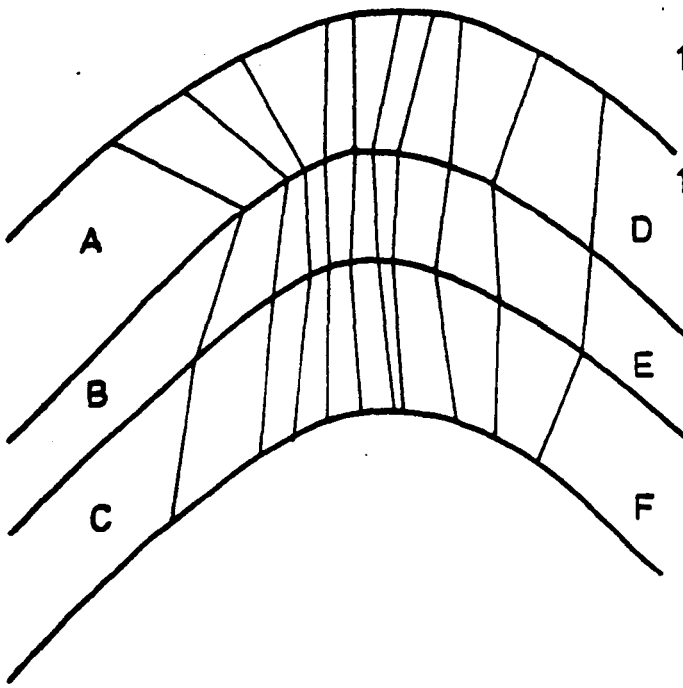
A
B
C
D
E
F

b

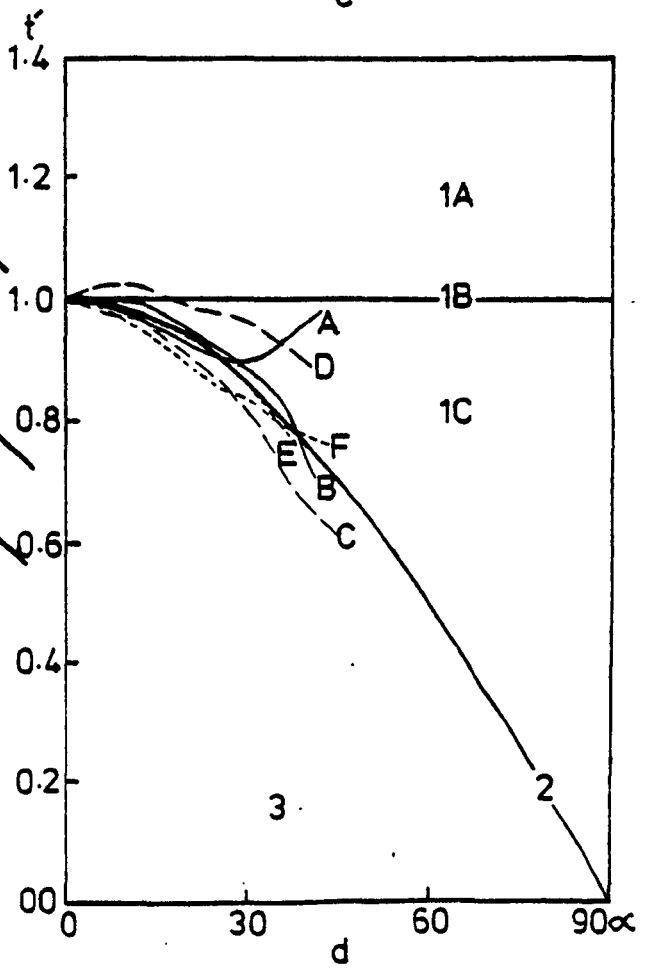
t'
1·4
1·2
1·0
0·8
0·6
0·4
0·2
00
0
30
60
90 α
1A
1B
1C
A
D
E
F
B
C
3
2

d

Fig. III - 22. An example of a highly flattened F_3 fold from the folded belt SW of Ardheslaig. (a) fold profile with dip isogons, (b, c, d and e) t' versus α plot for various folded layers from profile a.

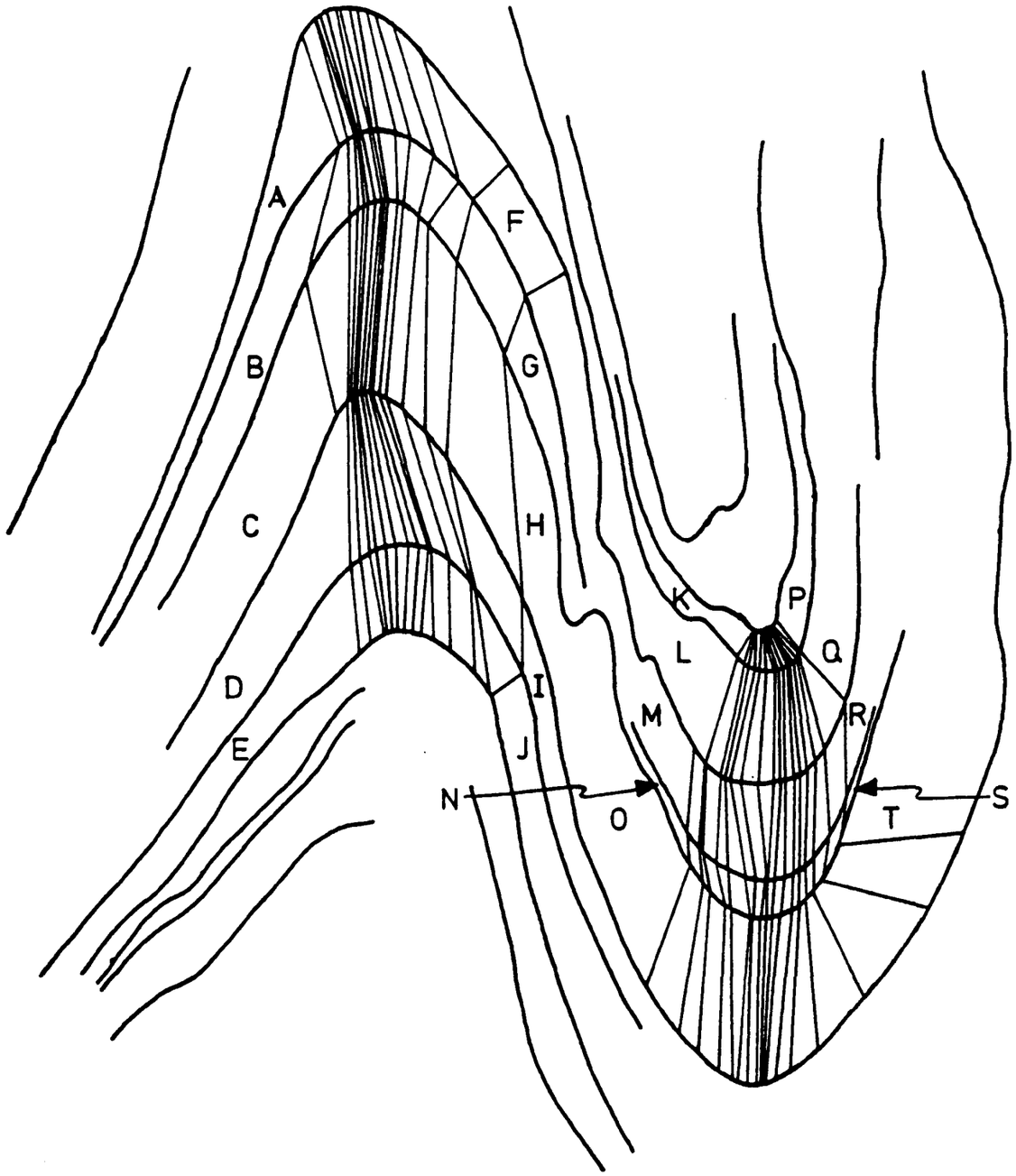
A
B
C
D
E
F
G
H
I
J
K
L
M
N
O
P
Q
R
S
T

a

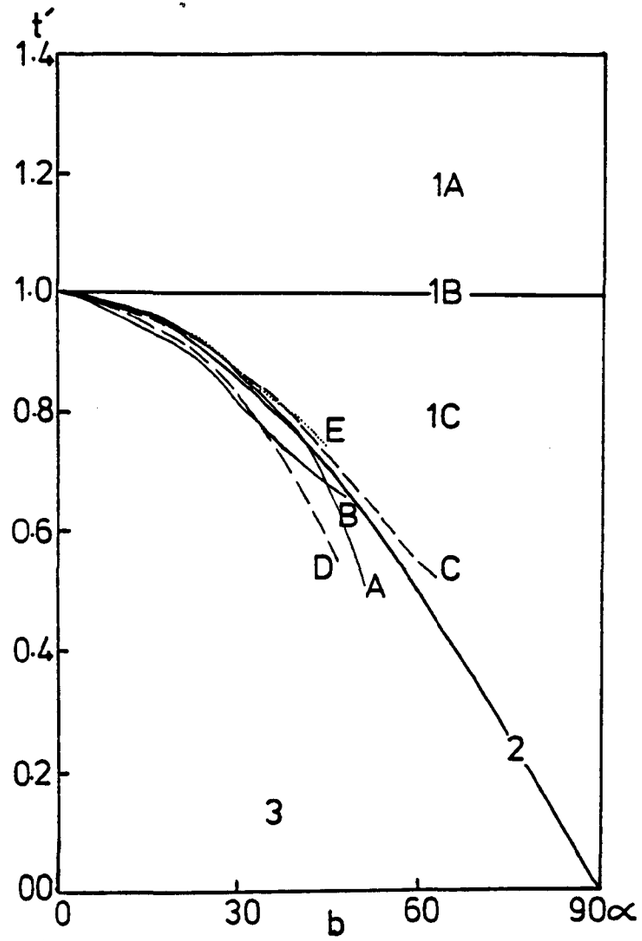
t′
1·4
1·2
1·0
0·8
0·6
0·4
0·2
00
1A
1B
1C
E
B
D
A
C
2
3
0
30
60
90∝
b

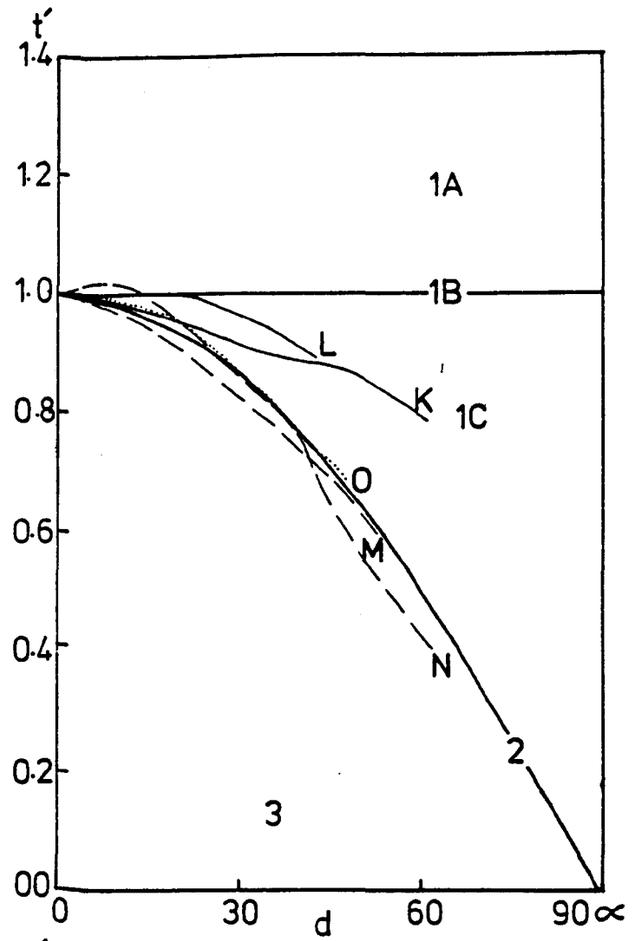
t′
1·4
1·2
1·0
0·8
0·6
0·4
0·2
00
1A
1B
1C
L
K
O
M
N
2
3
0
30
60
90∝
d

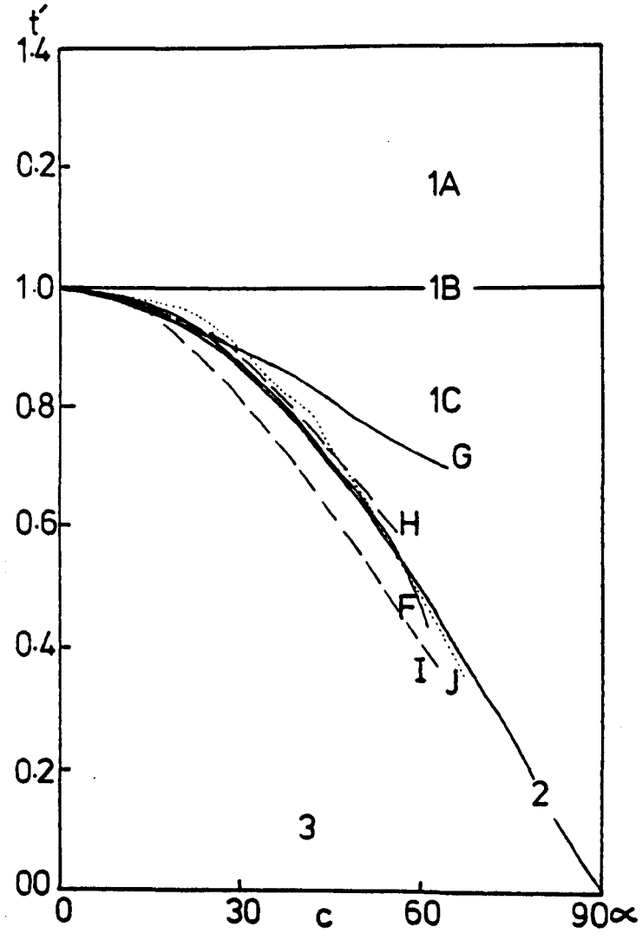
t′
1·4
0·2
1·0
0·8
0·6
0·4
0·2
00
1A
1B
1C
G
H
F
I
J
2
3
0
30
60
90∝
c

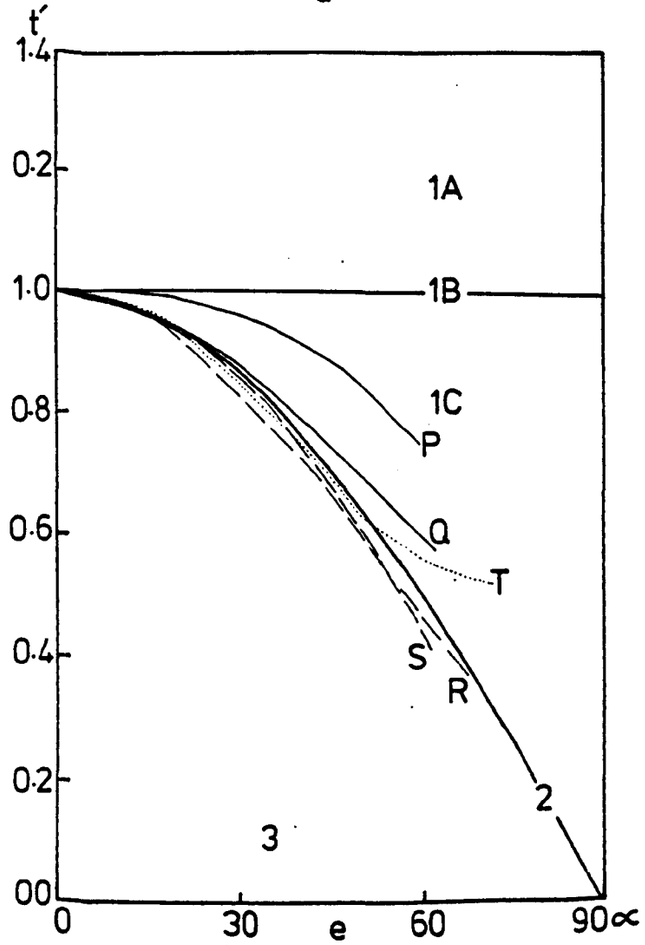
t′
1·4
0·2
1·0
0·8
0·6
0·4
0·2
00
1A
1B
1C
P
Q
T
S
R
2
3
0
30
60
90∝
e

b. Relationship with earlier structures. Of the previous folds, only the F_2 folds are widespread. In profile the F_2/F_3 interference pattern is of class 3 type of Ramsay (op. cit.). The refolding is co-axial in most places (e.g. Pl. III-8a), but slightly non-coaxial refolding is present locally (e.g. Pl. III-8b).

Because of the co-axial nature of the deformation with all the early deformations in the area, the early lineations are unaffected by F_3 folding except at some places (e.g. subarea of domain 5 and domain 11) where due to slight non-coaxial deformation the pre D_3-lineations have been folded and are distributed on a small circle (Fig. III-9a and 15d).

c. D_3 Fabric. The S_3-foliation is not a widespread structure and is present only in the central and southern part of the strongly folded belt south and southwest of Ardheslaig. The foliation is subparallel to the axial surface (Pl. III-9a). Its strongest development is in the central and southern part of the strongly folded belt just south of Ardheslaig. This foliation has been developed only in the gneisses while the dykes are unaffected. The foliation is defined by platy quartz deformation bands and by the parallel orientation of biotite and hornblende (Pl. III-14a,b). Biotite and hornblende have been mechanically rotated into parallelism and quartz has been deformed plastically but no obvious recrystallisation of any mineral has taken place.

The L_3 lineation occurs only in the same part of the strongly deformed belt just SW of Ardheslaig. Again it is present only in the gneisses and is difficult to differentiate from previous lineations in most places, unless there is some non-coaxiallity in the deformations.

Plate III-14a. Gneissic foliation folded into F_3 fold. A new axial planar fabric is developed by flow of quartz. Biotite flakes have been mechanically rotated parallel to S_3. Plagioclase is undeformed (plane polarised light x13).

Plate III-14b. Same as above (crossed nicols. x13).

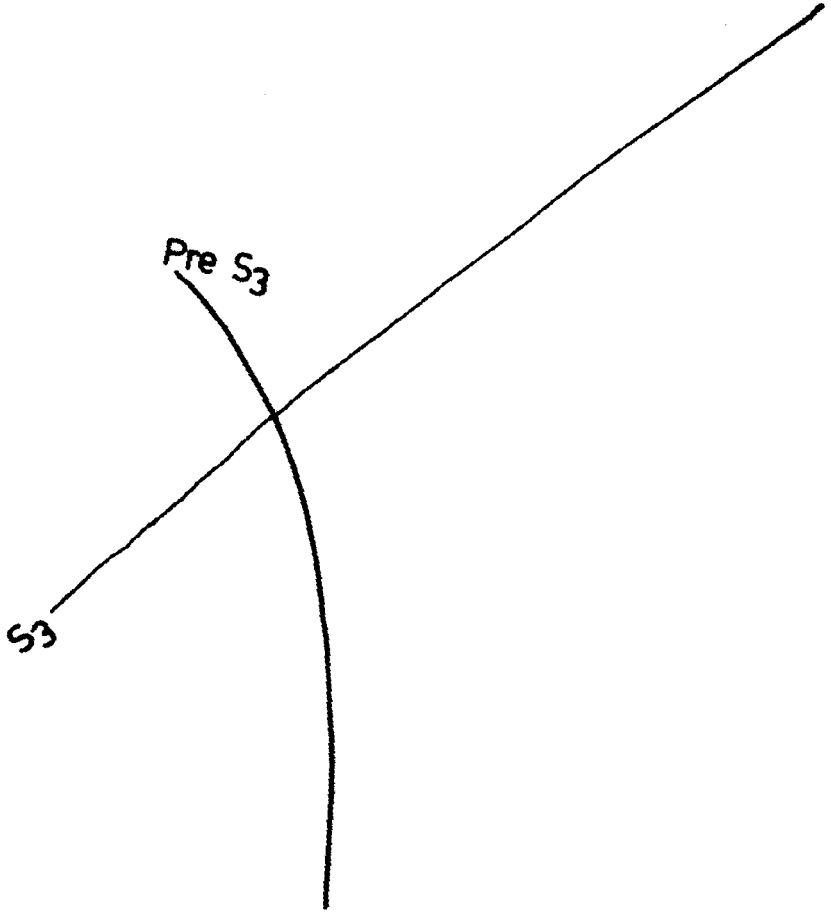
Pre S_3
S_3

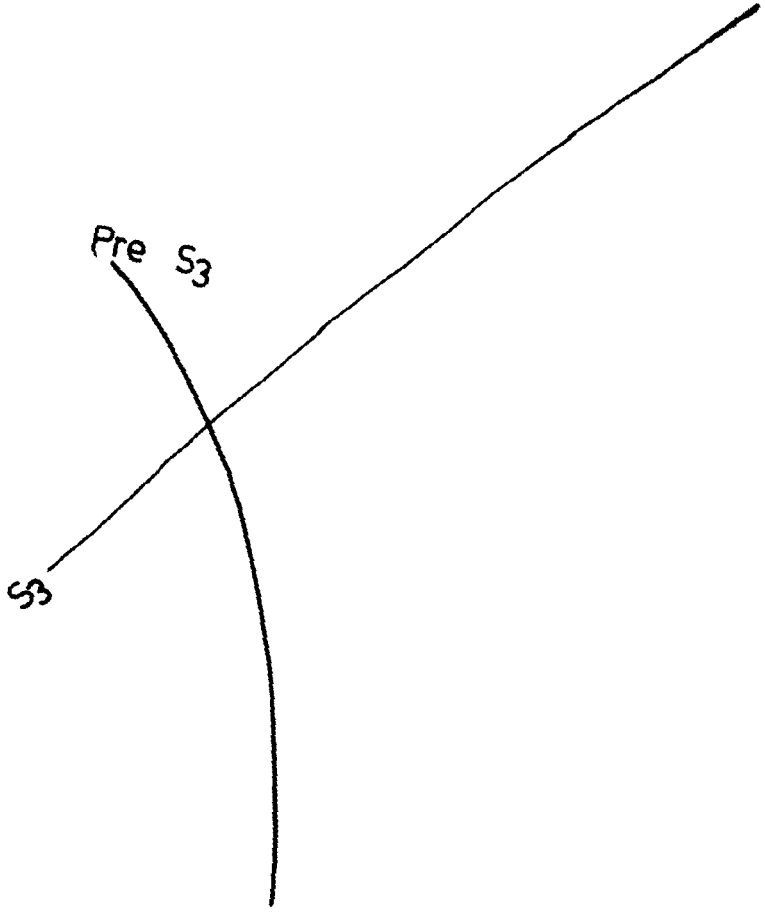
Pre S_3
S_3

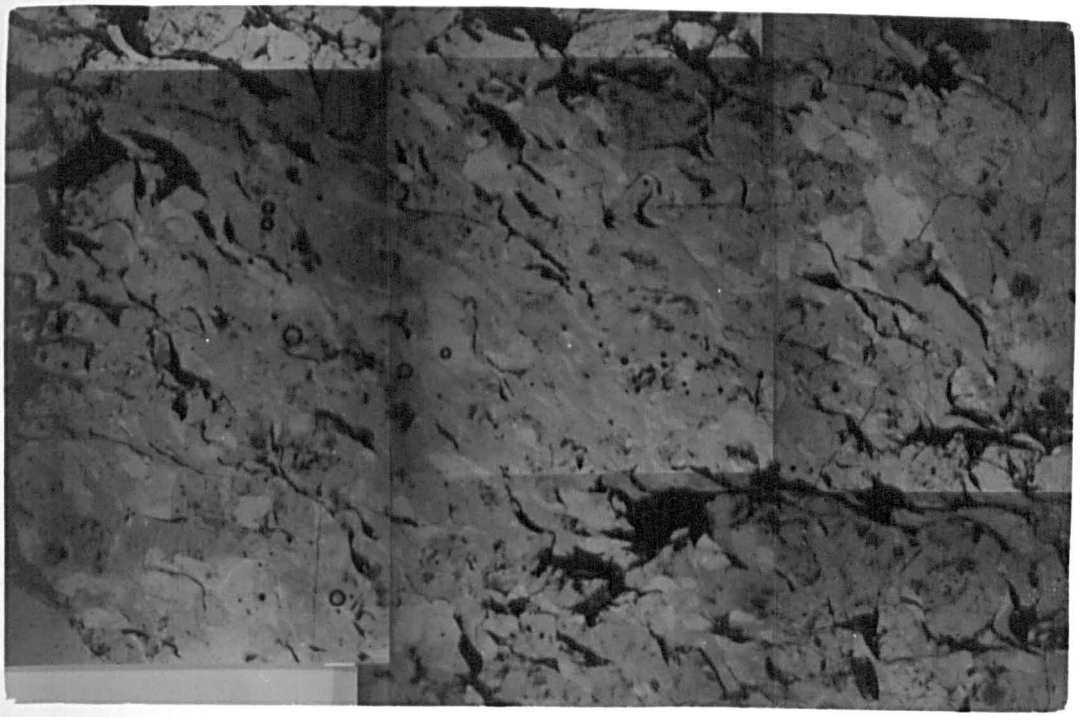

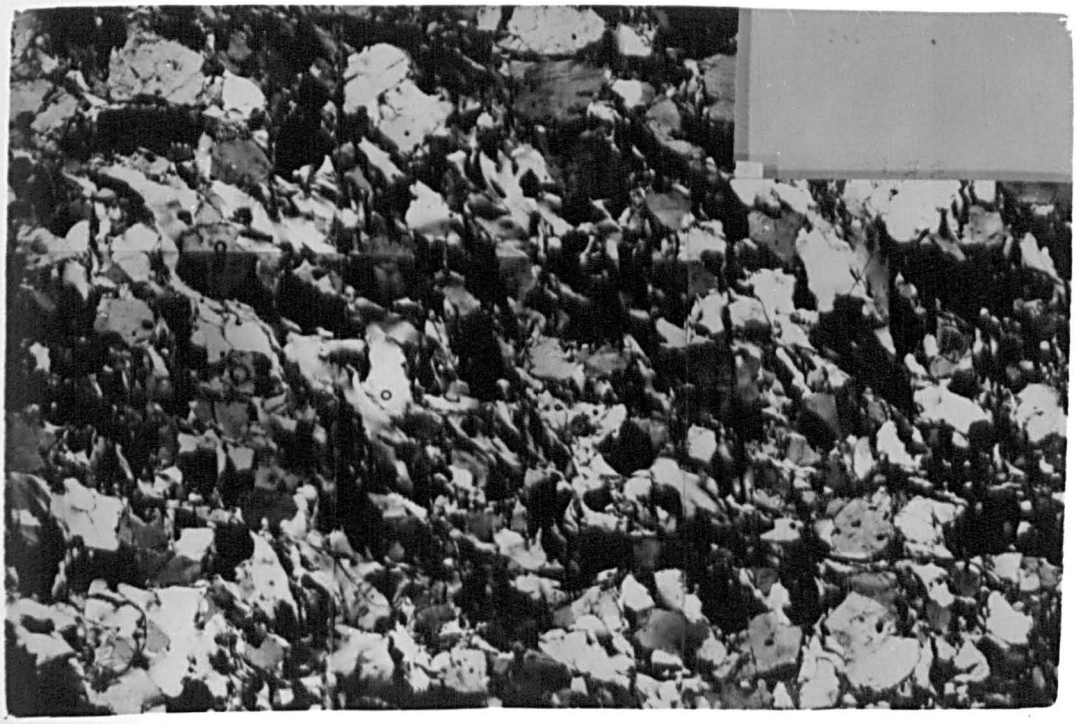

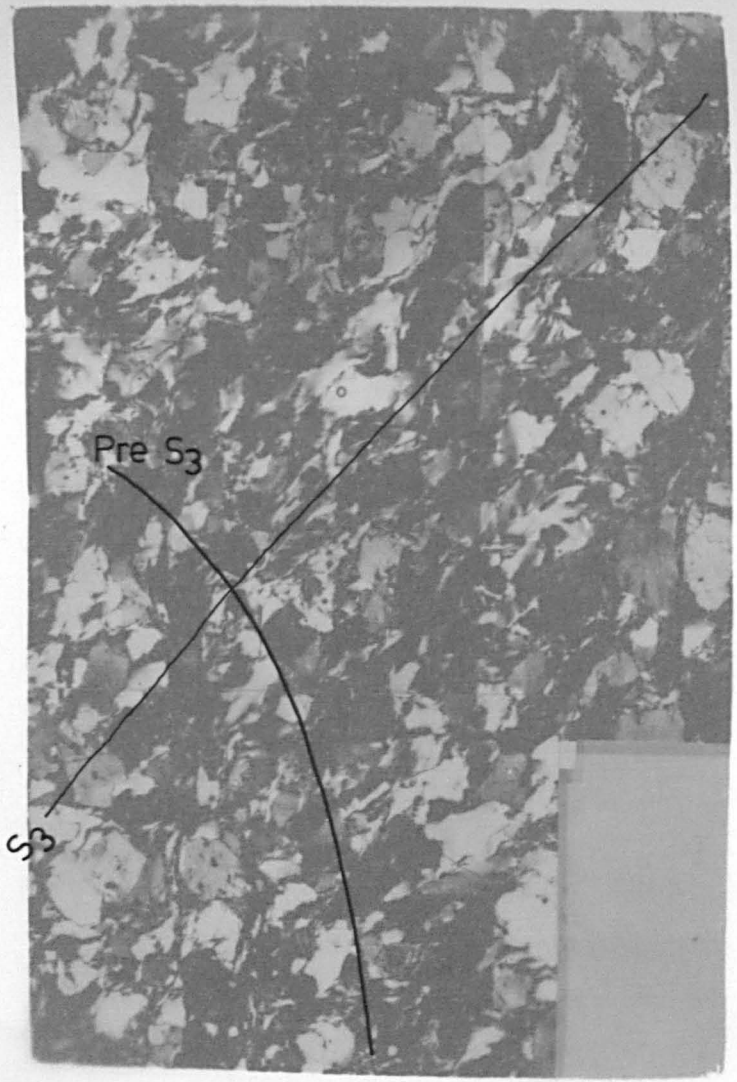
Pre S_3
S_3

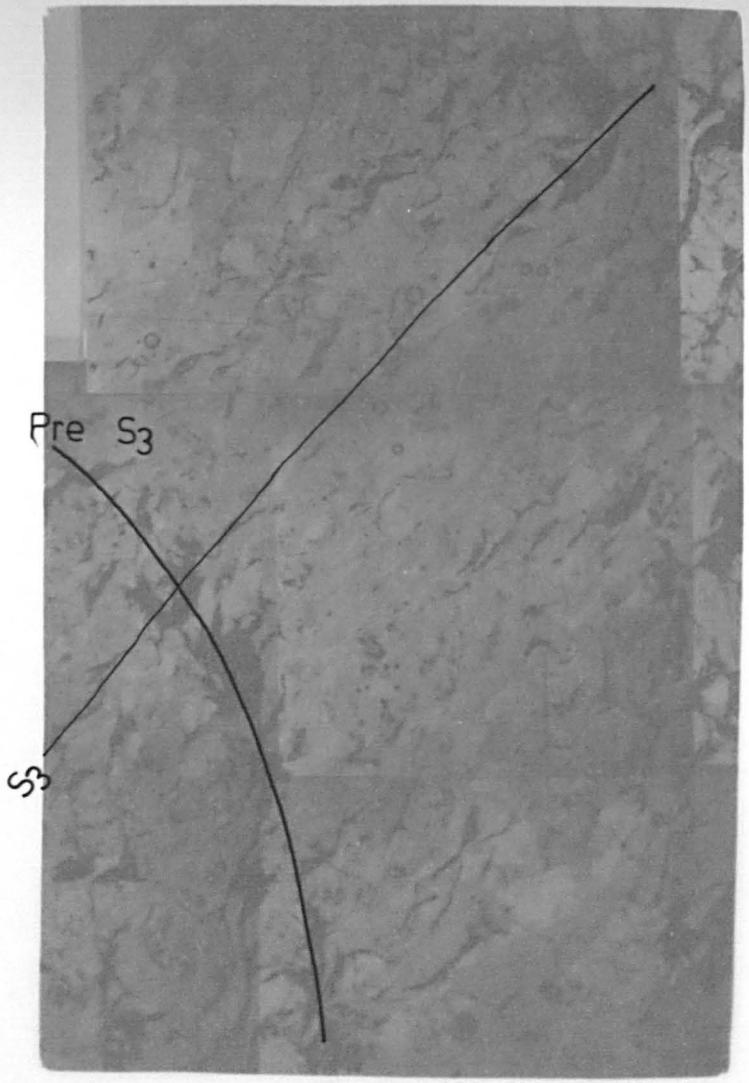
Pre S_3
S_3

The fabric lineation as defined by rod-shaped bodies in the gneissic foliation and the intersection lineation defined by the intersection of S_3 with gneissic foliation are parallel with each other and in most places, when observed together with F_3 folds, are parallel to their axes.

Sometimes rocks have been sheared in narrow zones parallel to their axial surface (Pl. III-15a). These shears are not very ductile.

4. Post D_3 Structures

The structures produced in the post-D_3 deformation are very mild and localized. Open to gentle folds and brittle structures are produced.

a. Post D_3 folds (Late folds). These are open, upright NE-SW to E-W oriented folds (Pl. III-9b) with a variable plunge angle generally towards the NE. Because they are post-F_3, their plunge angle and direction depends on their position on the F_3 folds. If they occur on steeply-dipping limbs of F_3 folds, they plunge at a high angle and if they occur on the crest or trough of F_3 folds they have a nearly sub-horizontal hinge.

When many layers are involved in folding, in cross profile their geometry is of class 1C type to class 1B type as an average of many layers with slightly convergent dip isogons as a whole (Fig. III-23). Individual layers have been folded variably from class 1A to class 3, depending upon their competency.

The stress orientation during the deformation was such that the NE-dipping limbs of F_3 folds are most affected while SW-dipping limbs were not much affected in the southwestern part of the inlier (see page 46 and Figs. III-4a,5). While in the northeastern part

Plate III-15a. F_3 fold in gneiss with some strongly sheared limbs (78175577).

Plate III-15b. A basin and dome type interference structure formed by refolding of an F_3 fold by a post-F_3 fold (77595526).

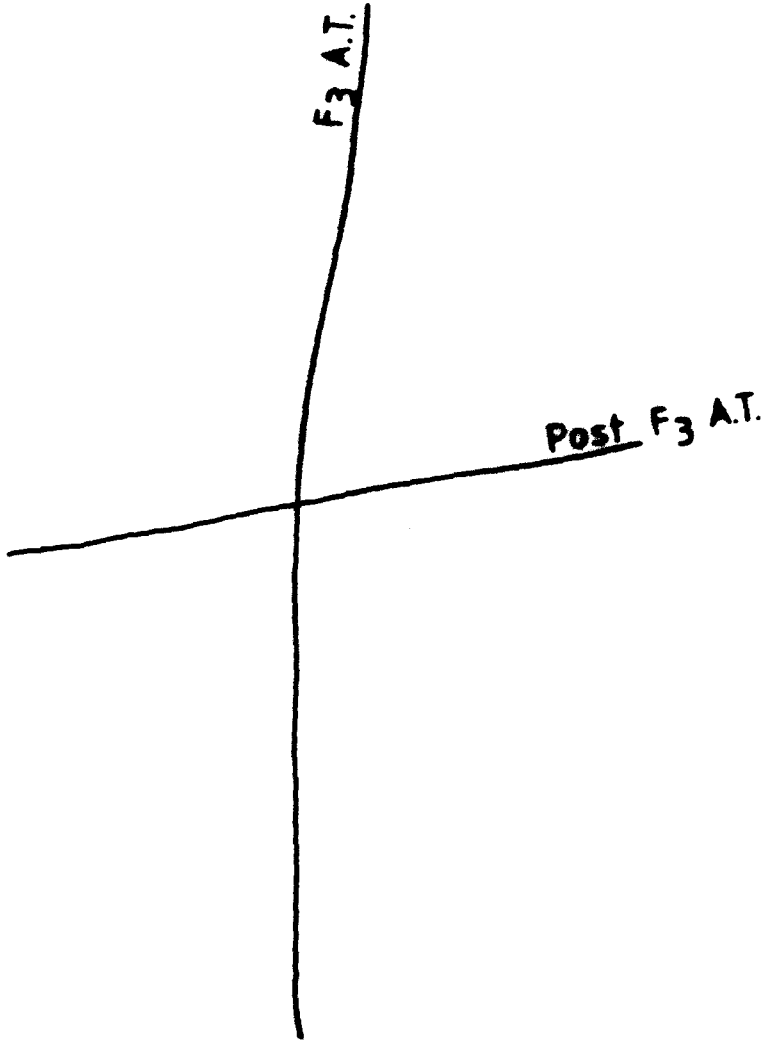
F3 A.T.
Post F3 A.T.

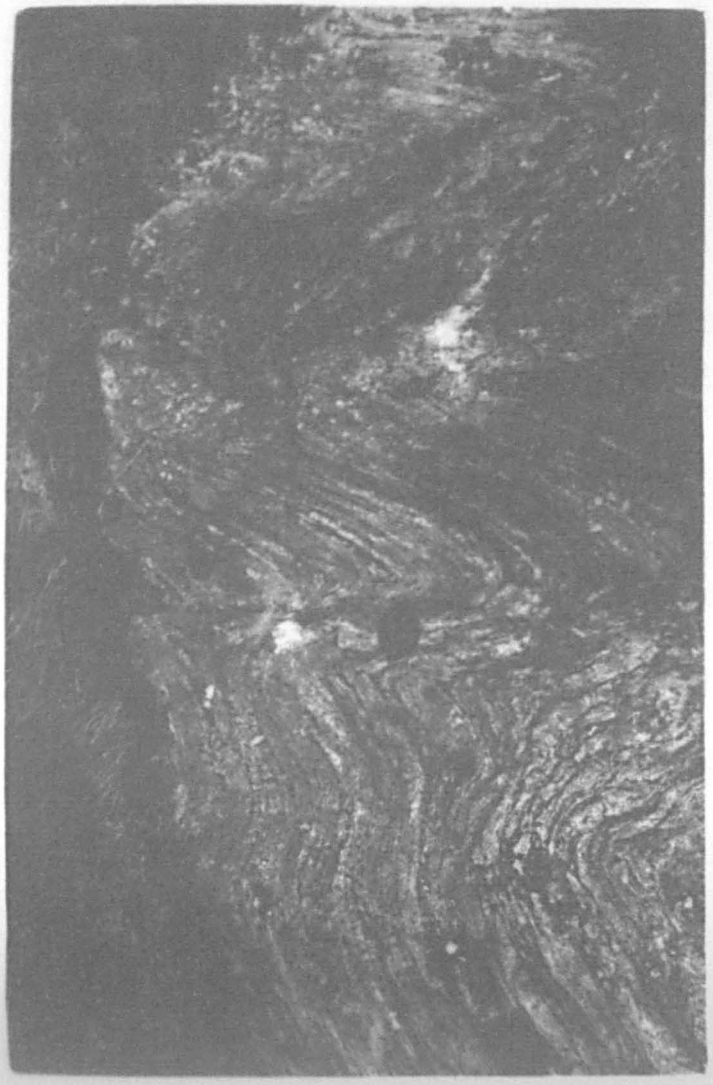

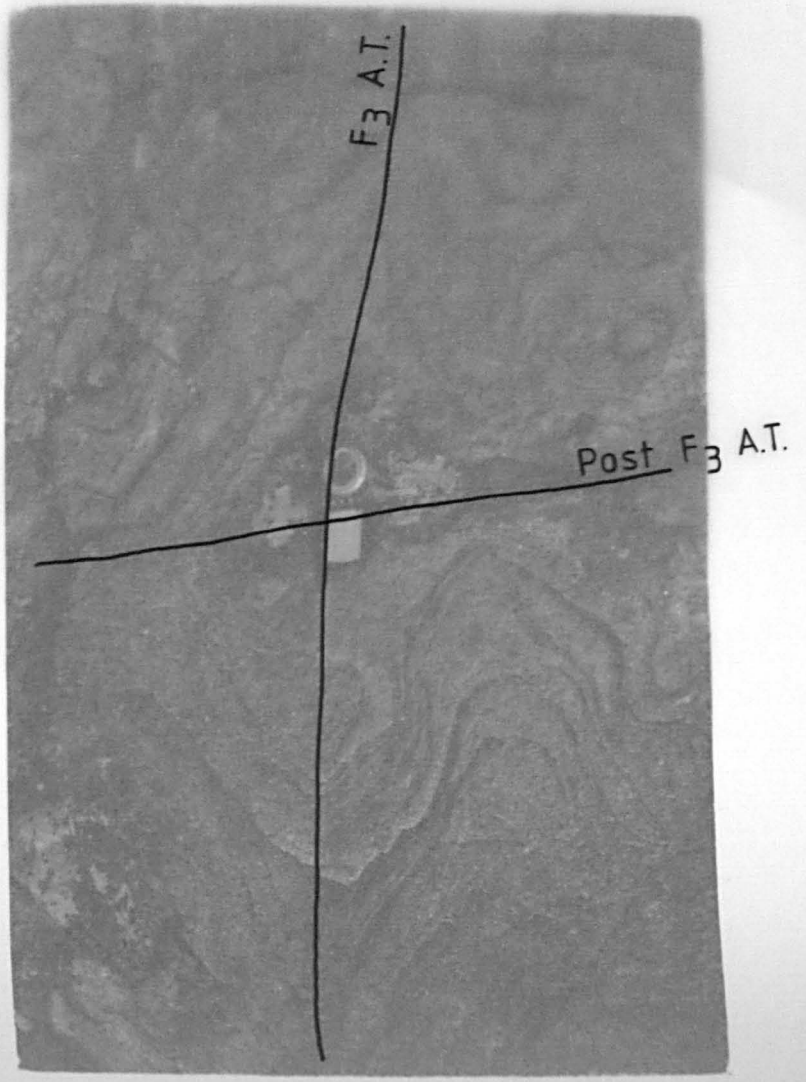
F3 A.T.
Post F3 A.T.

Fig. III-23. An example of post F_3 fold from the area.
(a) fold profile with dip isogons,
(b, c and d) t' versus α plot for various
folded layers from profile a.

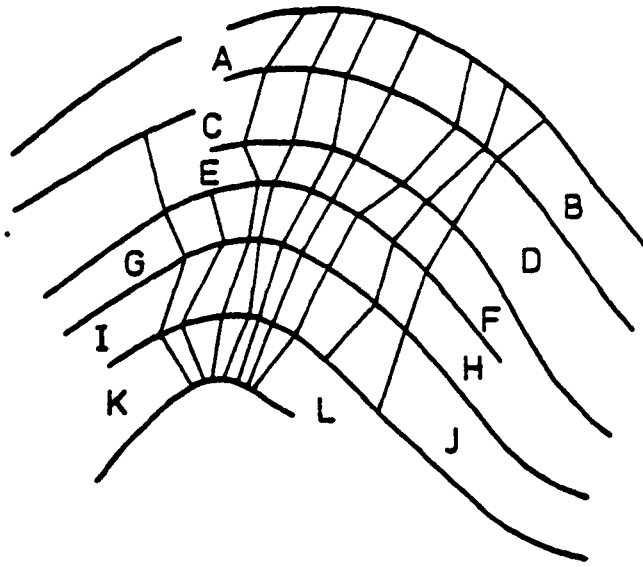
A
C
E
G
I
K
L
J
H
F
D
B

a

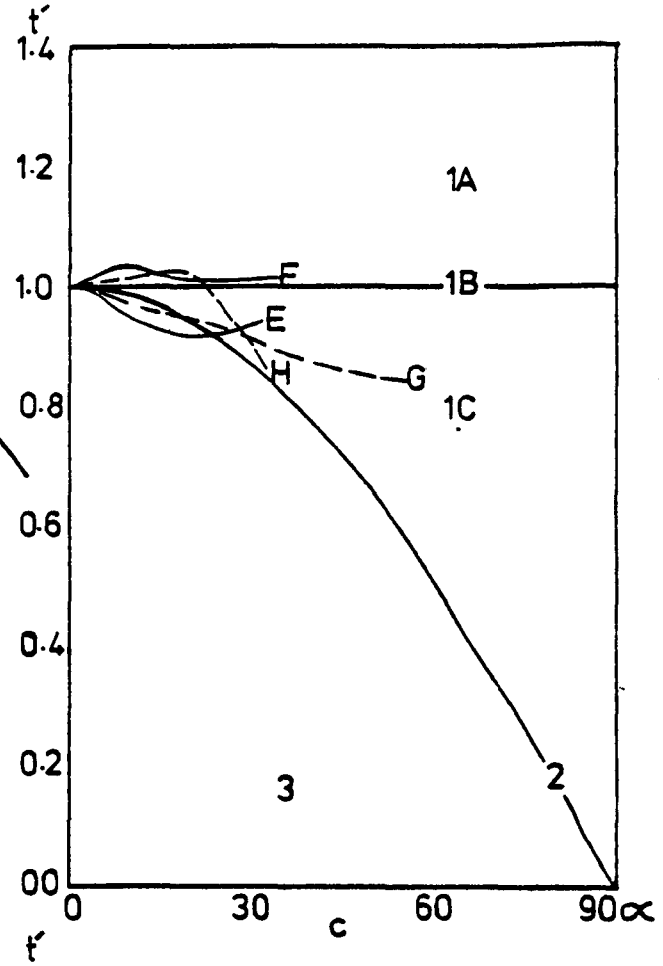
t'
1·4
1·2
1·0
0·8
0·6
0·4
0·2
00
1A
1B
1C
3
2
E
E
H
G
0
30
60
90∝

c

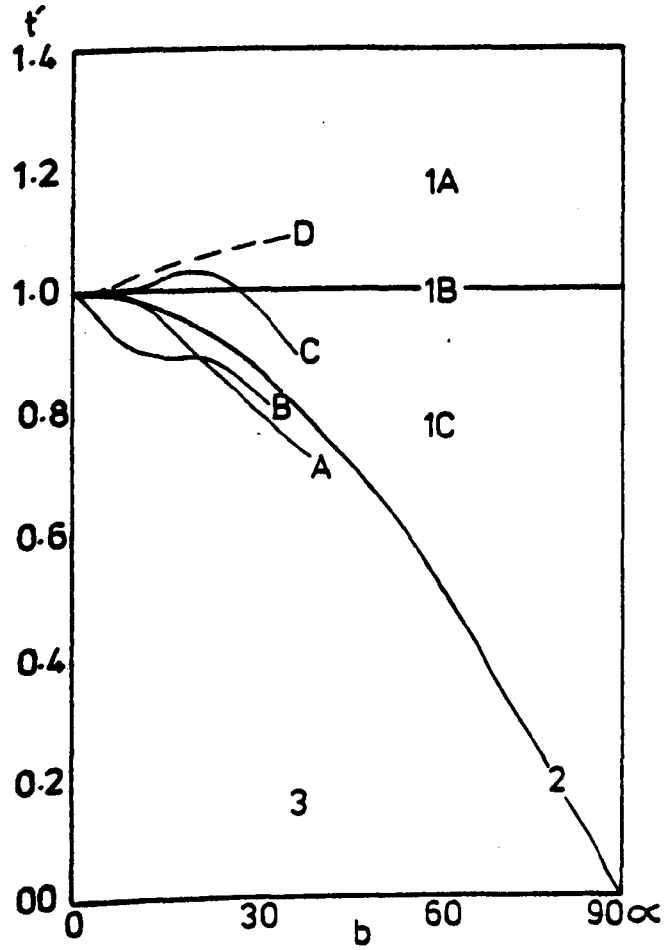
t'
1·4
1·2
1·0
0·8
0·6
0·4
0·2
00
1A
1B
1C
3
2
D
C
B
A
0
30
60
90∝

b

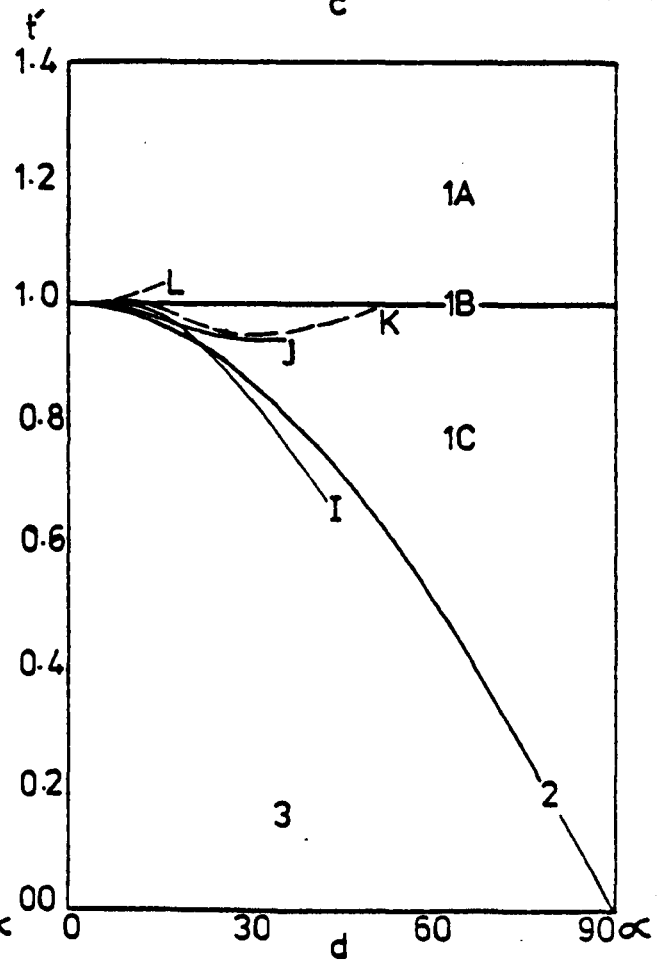
t'
1·4
1·2
1·0
0·8
0·6
0·4
0·2
00
1A
1B
1C
3
2
L
K
J
I
0
30
60
90∝

d

of the inlier both limbs of F_3 folds i.e. NE dipping and SW dipping have been equally affected and their axial surfaces have been folded on subvertical axes (Enclosure 2).

Because of their localized development, interference with earlier folds is rare. However, at one place a class 1 type "basin & dome" type interference figure is produced with F_3 folds (Pl. III-15b).

b. Brittle structures. In some places late brittle structures are also present. They occur particularly in two areas, one in the northern part of the Ardheslaig peninsula and the second in the south of Loch a Mhuilinn. In these areas blocks up to two metres in diameter across have been displaced and also rotated in some places.

At some places specially on Ardheslaig peninsula some breccia zones are also present which strike NW-SE and dip at a high to moderate angle towards the NE. In the southwestern part of the area breccia zones also dip towards the SW at a low angle. Rock fragments of various sizes up to 10 cm across are present.

CHAPTER IV

STRAIN ANALYSIS

INTRODUCTION

In the past geologists have used many kinds of objects and methods for quantitative analysis of the amount of strain in deformed rocks. The work of Cloos (1947) on deformed oolites is a well known early example and other geologists have since determined the strain using many different methods including the use of deformed fossils and pebbles from deformed conglomerates. Unfortunately, there are no suitable objects for precise quantitative strain analysis in many gneissic terrains such as the Lewisian which have the most complex and prolonged deformational history.

However, there are some methods which can be used to make a qualitative or quasi-quantitative analysis of the strain in such rocks. These are by using: (1) the shape fabric of the dykes, i.e. by measuring the grain aggregates of feldspar or hornblende in the dykes which result from the breakdown of the igneous texture; (2) the discordant relationship of the dykes with the gneisses; (3) the average thickness of the dykes in different areas; (4) the amount of post-buckle flattening of the folds in profile and (5) the surface of no finite longitudinal strain determined with the help of folded and stretched veins. All of the methods described above have been used in this study for a qualitative determination of strain in the area under study and methods (1) and (4) have been used in detailed qualitative and quasi-quantitative analyses respectively. The various aspects of this study are described and discussed as follows:

A. METHODS OF STRAIN MEASUREMENT.

B. STRAIN ANALYSIS OF THE KENMORE INLIER.

C. STRAIN PROFILE ACROSS THE DIABAIG INLIER.

D. COMPARISON OF STRAIN PATTERN AND INTENSITY IN THE KENMORE AND DIABAIG INLIERS.

A. METHODS OF STRAIN MEASUREMENT

The following methods have been used in measuring strain in this study:

1. The shape fabric in the dykes.
2. Measurement of flattening of buckle-folded layers.
3. Angular relationships between dykes and gneisses as a measure of strain.
4. The minimum strain ellipsoid using deformed quartz veins.

1. The shape fabric in the dykes

In the Scourie dykes the ophitic and subophitic igneous texture has been broken down into aggregates of smaller grains of variable shape and size. The grain aggregates can be used as strain markers giving the strain intensity in different areas as in a loose sense they correspond to strain ellipsoids. Grain aggregates of the mafic and felsic minerals in shear zones present in dykes were also used as strain ellipsoids in measuring strain intensity and type by Coward (1976) working in Botswana and Scotland.

Because the first three Laxfordian deformations in the area were of a co-axial nature, with nearly the same orientation of the principle axes of the bulk strain ellipsoid, the later deformations merely superimpose their strain upon the shape fabric produced in the first deformation. Therefore the shape fabric indicates the total Laxfordian deformation or finite strain in the rocks and cannot be used to study the

strain of each individual deformation or progressive deformation. During Laxfordian deformation the rocks were not affected by an intense metamorphism which could have destroyed the shape fabric in the dykes.

The use of mineral aggregates as strain markers in the Scourie dykes is open to criticism on the grounds that the difference in strength and viscosity of hornblende and feldspar could produce different amounts of strain in the two minerals. The amphibolite-facies metamorphism in the early Laxfordian history could produce some complexities in the shape fabric and to some extent could work in the opposite sense to the deformation, since under stress conditions minerals grow with greater ease in some directions than in others so that the aggregate shapes do not reflect genuine strain ellipsoids. Moreover, volume change within shear zones can affect the shape of the strain ellipsoid (Ramsay and Wood, 1973). For these reasons the measured shapes cannot be used in a genuinely quantitative analysis of the strain but only to give a qualitative analysis of the strain variations throughout the area.

Another problem is that in some places there is a small scale variation in the axial ratios of these mineral aggregates. This occurs where narrow shear zones are present or in mesoscopic folds where the strain markers are of a more linear habit in the hinges and more planar on the limbs. Probably the same is the case in bigger folds as well. This phenomenon was also recognised by Graham and Coward (1973) in the Outer Hebrides. Because of these variations in the shape fabric, a big spread is present when these shapes are plotted on the Flinn diagram, both in the oblate and the prolate fields, as will be seen later in this chapter. However, generally on a mesoscopic scale there is considerable homogeneity in the shape of these grain aggregates.

The most important limitation of this method for strain analysis, even in a qualitative sense, is that these grain aggregates are present (and hence have been measured) only in the Scourie dykes which shows the variations in the strain intensity in the dykes only and nothing can be said about the variations in the strain intensity in the gneisses using this method.

2. Measurement of flattening of buckle-folded layers

According to Ramsay (1967) the shape of the buckles is initially a sine wave of the form $y = A \sin 2\pi x/W$, where A is the amplitude and W is the wavelength of the fold. As the fold develops the initial sine function becomes modified so that the curvature of the layer becomes more uniform. As a result, the fold curves may closely approximate to circular arcs and the fold is termed a concentric fold.

In environments where the rock materials are ductile during deformation, it is common for the shape of the buckled layers to become modified by the superimposition of a fairly homogeneous strain. De Sitter (1958) has suggested that there is a value of maximum shortening of the competent layers by buckling alone. He also showed that with parallel concentric folds, which have their limbs parallel to the axial-surface, the layer is unlikely to contract more than $\pi/2$ of its original length, i.e. 36 percent. De Sitter suggested that the further compressive strain leads to the modification of the parallel shape of the buckled layers by a process of flattening, and folds formed in this way have been termed flattened parallel folds (Ramsay, 1962).

It has been shown by Ramsay that if we take a series of harmonically buckled multilayers and flattened them normal to the axial surface, in the case of extreme flattening the style of individual layers comes to

lie close to the similar fold. The curves of folds of class 1B, 1C and 3 will move towards class 2, but will never reach class 2 (Ramsay, 1967, Fig. 7-102).

Superimposed flattening can be worked out graphically in terms of $\sqrt{\lambda_2/\lambda_1}$. Ramsay (op.cit.) has computed a series of curves with various values of $\sqrt{\lambda_2/\lambda_1}$ in a graph of t' against α ((Fig. IV-1a), where t' is the ratio of the orthogonal thickness of a layer at a given slope to that at the hinge and α is the limb slope). In another graph he has computed various values of $\sqrt{\lambda_2/\lambda_1}$ curves on the graph of T' against α ((Fig. IV-1b) where T' is the ratio of the axial planar thickness of a layer at a given slope to the layer thickness at the hinge). From these diagrams the flattening strain of a fold at any given dip angle α can be calculated. Hudleston (1973a) provided a graph for measuring flattening by plotting various values of $\sqrt{\lambda_2/\lambda_1}$ by taking ϕ ((Fig. IV-2a) the angle between a dip isogon and the normal to the tangent to a layer) as ordinate against α (dip angle) as abscissa. He also produced a modification of his ϕ against α graph and Ramsay's t' /α graph to obtain results on straight lines. In the former modification he plotted $(\alpha-\phi)$ against α or Tan $(\alpha-\phi)$ against α (Fig. IV-2b). In the modified Ramsay graph he plotted t'^2 against $\text{Cos}^2\alpha$ on a log scale (Fig. IV-2c) to obtain values of $\sqrt{\lambda_2/\lambda_1}$ in straight lines. The usefulness of the straight line representation lies in the fact that plotted data from natural folds may be approximately represented by best-fit straight lines using the technique of linear regression by least squares.

The curves computed by Ramsay (op.cit.) and Hudleston (op.cit.) enable flattening strain for natural folds to be determined in two dimensions only within the profile plane, providing that the original fold axis was parallel to one of the principal directions of three-

Fig. IV-1a. Values of t' in flattened parallel folds with variations in $\sqrt{\lambda_2/\lambda_1}$

(After Ramsay, 1967)

Fig. IV-1b. Values of T' in flattened parallel folds with variations in $\sqrt{\lambda_2/\lambda_1}$

(After Ramsay, 1967)

a.

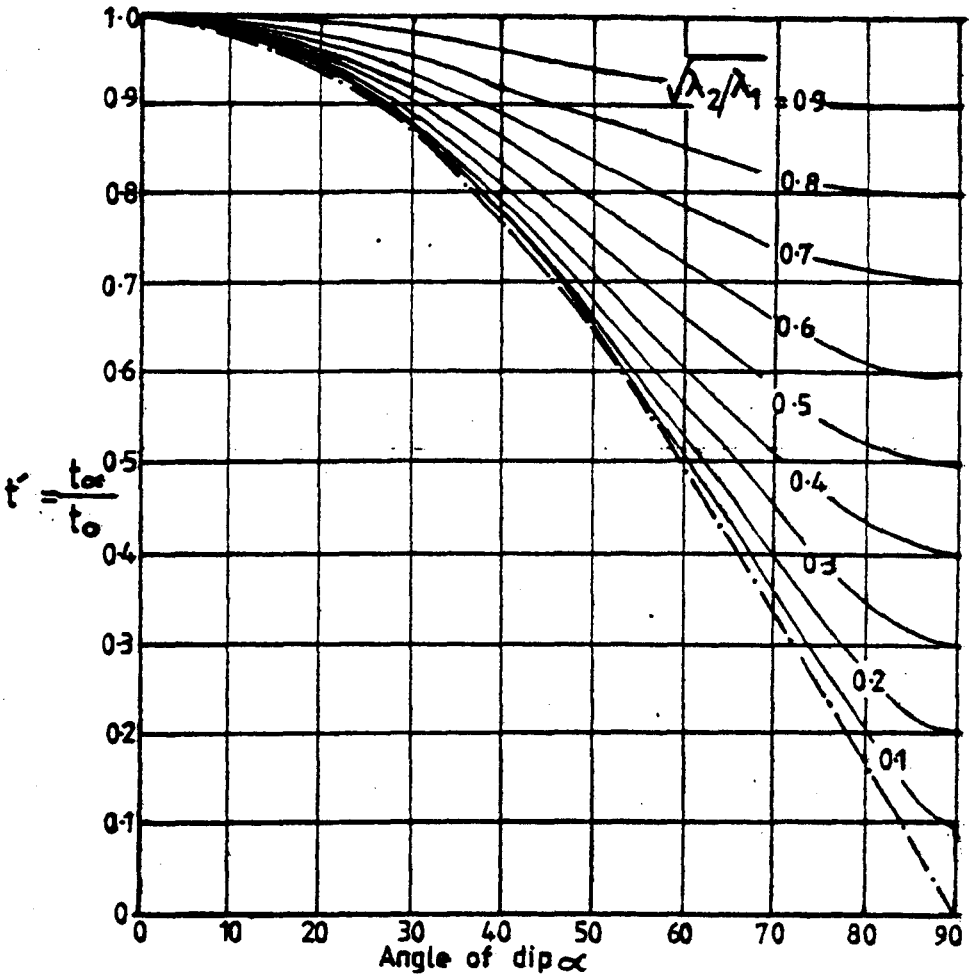
$t' = \frac{t_\alpha}{t_0}$
1·0
0·9
0·8
0·7
0·6
0·5
0·4
0·3
0·2
0·1
0
$\sqrt{\lambda_2/\lambda_1}$ = 0·9
0·8
0·7
0·6
0·5
0·4
0·3
0·2
01
0 10 20 30 40 50 60 70 80 90
Angle of dip α

b.

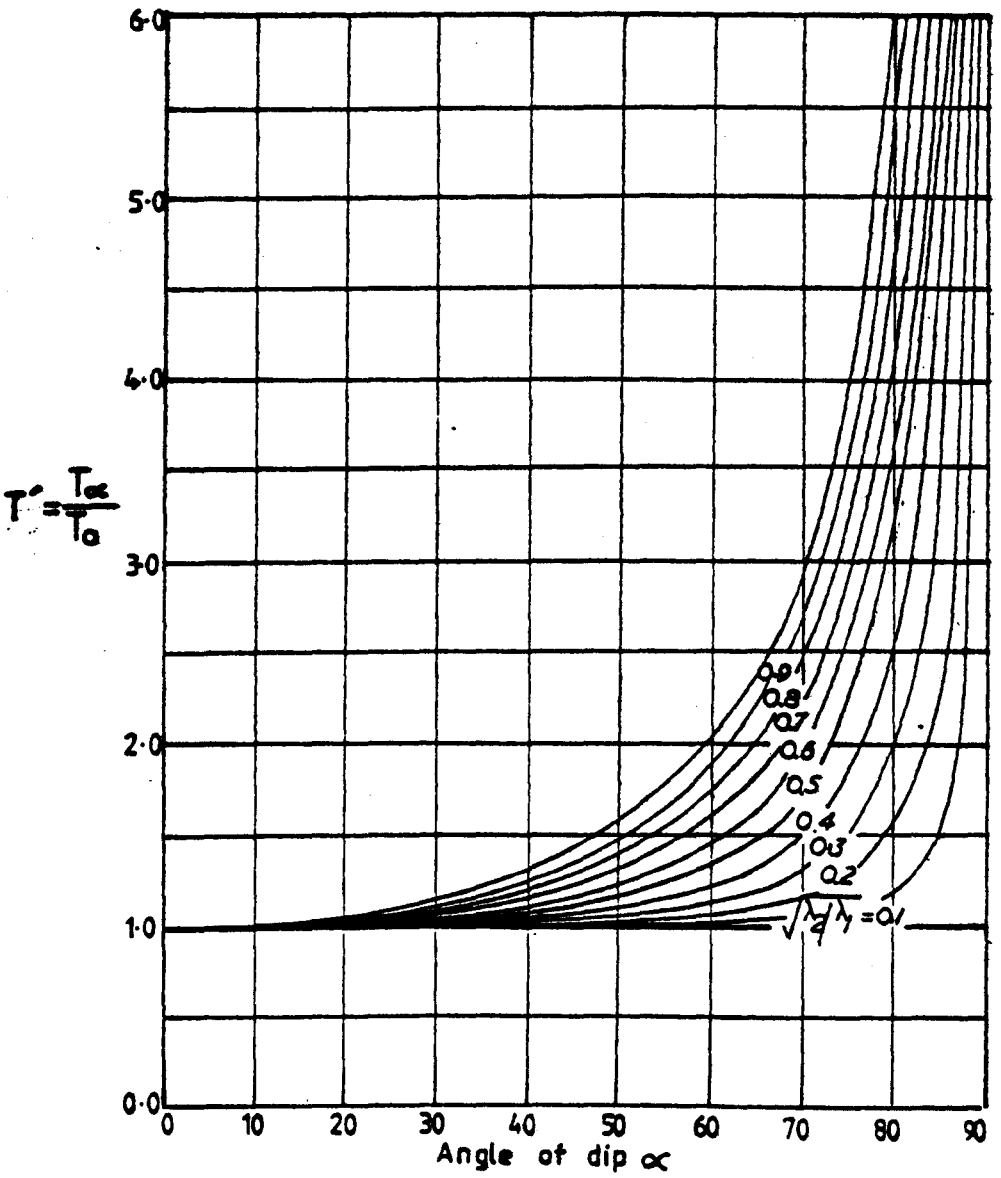
$T' = \frac{T_\alpha}{T_0}$
6·0
5·0
4·0
3·0
2·0
1·0
0·0
0·9
0·8
0·7
0·6
0·5
0·4
0·3
0·2
$\sqrt{\lambda_2/\lambda_1}$ = 0·1
0 10 20 30 40 50 60 70 80 90
Angle of dip α

Fig. IV-2a. Variation of ϕ with dip in flattened parallel folds for various values of $\sqrt{\lambda_2/\lambda_1}$

(After Hudleston, 1973a)

Fig. IV-2b. Straight line relationship in the variations of tan $(\alpha-\phi)$ with in flattened parallel folds for various amounts of flattening.

(After Hudleston, 1973a)

Fig. IV-2c. Linear relationship in the variation of $t\alpha^2$ with $\cos^2\alpha$ in flattened parallel folds for various amounts of flattening.

(After Hudleston, 1973a)

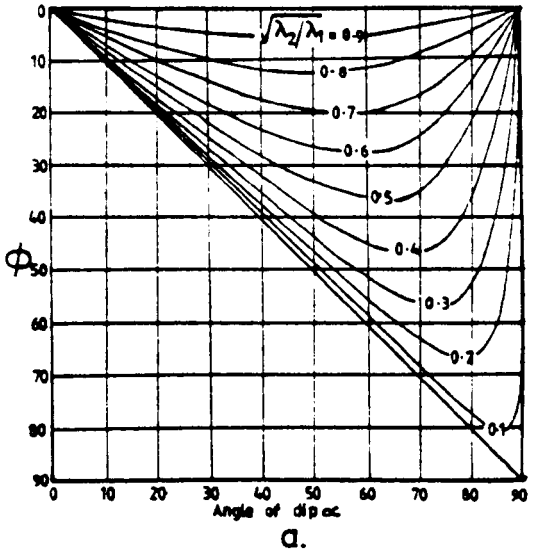
$\sqrt{\lambda_2/\lambda_1}$=0·9
0·8
0·7
0·6
0·5
0·4
0·3
0·2
0·1
Φ
Angle of dip α

a.

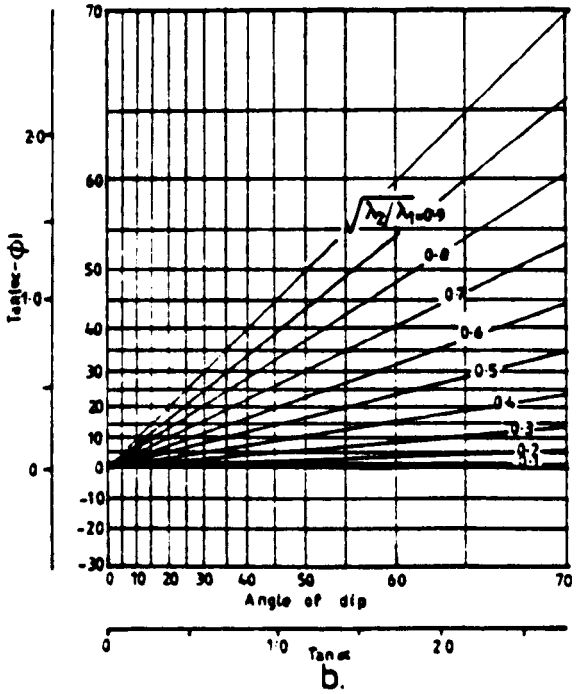
$\sqrt{\lambda_2/\lambda_1}$=0·9
0·8
0·7
0·6
0·5
0·4
0·3
0·2
0·1
Tan(α-Φ)
Angle of dip
Tanα

b.

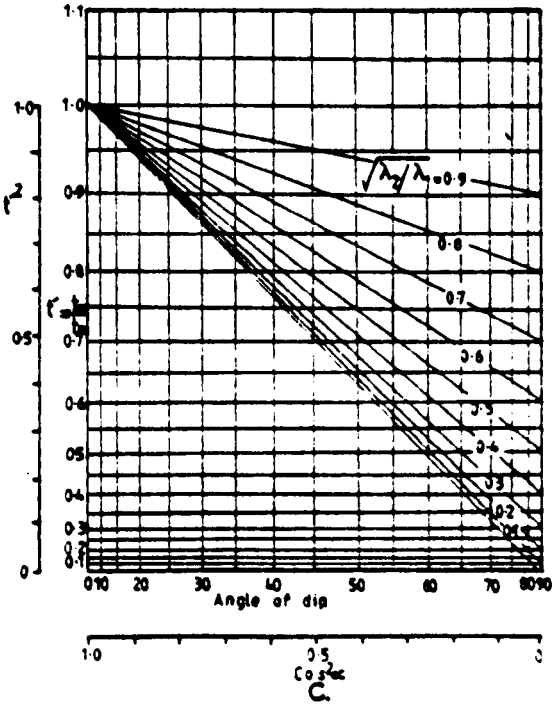
$\sqrt{\lambda_2/\lambda_1}$=0·9
0·8
0·7
0·6
0·5
0·4
0·3
0·2
0·1
Angle of dip
$Cos^2\alpha$

c.

dimensional strain, a condition which in most cases may not be met (Flinn, 1962). If the fold axis is not a principal direction of strain, the strain within the profile plane cannot be determined from the layer geometry (Mukopadhyay, 1965; Ramsay, 1967). It has been shown by Mukopadhyay (op. cit.) that complete determination of the strain is possible if flattening is measured in three planes of different orientations, provided that any one of the principal directions of strain lies in the axial plane and that the fold axis varies in orientation within the axial plane. Since flattening has been measured only in one profile plane of the folds, which is more or less in the same orientation throughout, the term "apparent flattening" rather than "flattening" should be applied to the present work in the Kenmore inlier.

It has been shown by Hudleston (1973a) and Hudleston and Stephanson (1973) that in the case of post-buckle flattening, or if the two processes (buckling and flattening) operate together, there is a slight but significant change in the two curves which can be measured only at higher dip values, usually more than 70^{o}. This is due to the fact that if flattening is post-buckle, the hinge zone will be more strained than the limbs, whereas if flattening and buckling operate together then the strain intensity on the limbs and hinge zone will be the same. In the Outer Hebrides it has been shown by Coward (1969) that in multilayer buckle folds, some layers give a straight line, while others show a slight upward bend at high angles in the plot of t' or ϕ against α which indicates that in the same fold some layers first deform and then the geometry changes due to superimposed homogeneous strain, while in others buckling and flattening operate together depending upon the layer thickness and viscosity differences etc. According to Hudleston (op. cit.), buckling and flattening processes go together, especially in the case of low viscosity contrast, in changing fold geometry from parallel folds. Naturally occurring folds might be

expected to show a range of behaviour between these two end members, depending on the properties of individual layers, and hence on the stage of development of a buckle fold at which flattening becomes important.

It has been shown by Biot (1961), Sherwin and Chappel (1968) and Hudleston (1973b) that the layers with a low viscosity contrast always suffer a shortening before buckle amplification. In the case of single layers embedded in another medium of comparatively low viscosity, Sherwin and Chappel (op. cit., Fig. 3) provide a graph, with the help of which it is possible to have a rough estimate of viscosity contrast between the folded layer and the embedded medium, and the ratio of the principal bulk strains within the profile plane of the fold. This method was later used in detail by Hudleston (1973b, c).

The problem with the rocks of the Kenmore inlier is that, except for a few folded pegmatitic veins in dykes, nowhere are single-layer folds present which could be used for estimating viscosity ratios or the total amount of strain in the layers. Although folded dykes are present, the gneisses in which those dykes are embedded cannot be treated as a homogeneous surrounding medium.

If a layer is embedded in a medium of lower viscosity and folded by buckling, it will attain a dominant wavelength depending on the thickness of the layer, the viscosity ratio of the layer and the surrounding medium and the ratio of principal quadratic elongation of strain in the fold profile (Hudleston, 1973b). In a multilayer sequence (usually the case in geological environments) the dominant wavelength is the result of interference of a number of layers of various viscosities and thicknesses. Therefore it is not possible to measure the viscosity ratio of the individual layers in multilayer

buckles.

The usefulness of the study of fold profile geometry in the Kenmore inlier is that it enables a rough comparison to be made between the F_2 and F_3 strain elements which make up the total finite strain observable in the Scourie dyke shape fabric.

3. Angular relationship between dykes and gneisses as a measure of strain

It has been shown by many workers (e.g. Flinn, 1962; Ramsay,1967; Lisle, 1976; Ramberg and Ghosh, 1977 and Skjernaa, 1980), that all planes rotate towards the XY plane of the bulk strain ellipsoid during progressive deformation.

Lisle used the concordance and discordance of dykes in the Lewisian rocks of the Outer Hebrides to compare the amount of deformation, initially discordant dykes become more and more concordant, but the angle between dykes and gneisses cannot be zero due to deformation. It could, however, be so small as to be difficult to observe.

It was shown by Coward (1969, 1973, 1974) and Coward et. al., (1970) as well that the Scourie dykes are more concordant in the areas where rocks have been strongly deformed while original discordant relationships are still preserved in the areas of low deformation in South Uist.

Over most of the Kenmore inlier the dykes are concordant to the gneisses and only in a few places is there some discordance. Another problem in using this method with precision in Kenmore is that in some of the dykes the concordant relationship may be primary, due to sill-like intrusions as already described in Chapter III (see also Cresswell, 1969). Therefore it was not possible to use the extent of discordance for determining the strain intensity in various parts. However, it

has been observed that the discordant dykes are present in the low deformation areas No. 6, 7 and part of 11 (see Fig. III-1), i.e. In the Loch na Craig pod and in the low deformation area just beside Ardheslaig.

4. The minimum strain ellipsoid using deformed quartz veins

This method was first introduced by Flinn (1962) and was later developed by Talbot (1970). This method determines the shape, orientation and ratio between the three axes of the strain ellipsoid in rocks by defining the surface of no finite longitudinal strain and is very effective where all the requirements are fulfilled.

One of the most important requirements however, is the presence of large numbers of veins injected in a wide variety of orientations prior to deformation, so that they would be able to define the boundary between the poles to the extended planes and the poles to the shortened planes, which will in turn define the shape of the cone formed by lines of no finite longitudinal strain. Slight inaccuracy in determining the two areas (i.e. the extension field and the shortening field) will cause enough change in the apical angle and the shape of the cone to affect the ratios of the principal axes of the strain ellipsoid.

It is not possible to use this method in the inlier for the determination of the strain ratio or the shape and orientation of the strain ellipsoid, because nowhere in the area were post-dyke veins in many orientations present before deformation. Some folded and stretched veins were found at one locality crossing the dykes, but the poles to the folded veins are concentrated only along a great circle, giving the extension and the shortening fields along that plane only, and it was not possible to determine the shape and orientation of the strain ellipsoid or the ratios between its three principal axes.

B. STRAIN ANALYSIS OF THE KENMORE INLIER

Strain has been measured in the Kenmore inlier using:

1. Shape fabric in the Scourie dykes.
2. Amount of apparent flattening of F_2 and F_3 folds in the Kenmore inlier.

1. Strain analysis using the shape fabric in the Scourie dykes

At 121 different places, measurements of the shape fabric were made in the dykes in such a way as to cover the whole of the inlier. When the shape fabric is associated with small scale structures, like mesoscopic folds or small shear zones, there is much variation, but to avoid this problem the measurements were taken in more or less homogeneously deformed areas on a mesoscopic scale.

The strain variations across the area may be illustrated by contouring the XZ ratios using firstly best-fit contours, ignoring any structural control or heterogeneity, see map 3 (Enclosure 3). Four different deformational classes are recognised, the boundaries between the classes being arbitrary and transitional. These are:-

Deformational Class 1. XZ ratio less than 20 : 1
2. XZ ratio 20 : 1 to 50 : 1
3. XZ ratio 50 : 1 to 100 : 1
4. XZ ratio more than 100 : 1

From the map it is obvious that most of the area is in class 2. The least deformed area (class 1) occurs mainly as isolated patches or lenses of which the largest is the central Loch na Craig pod. The low deformation area at Ardheslaig contains a small pod which is completely unaffected by Laxfordian deformations. The areas of strong deformation

Fig. IV-3. Five subareas of the Kenmore inlier, divided on the basis of deformation intensity.

(a) The Ardheslaig Peninsula

(b) The central belt

(c) The Loch na Craig pod

(d) The southwestern belt

(e) The Loch Gaineamhach outcrop

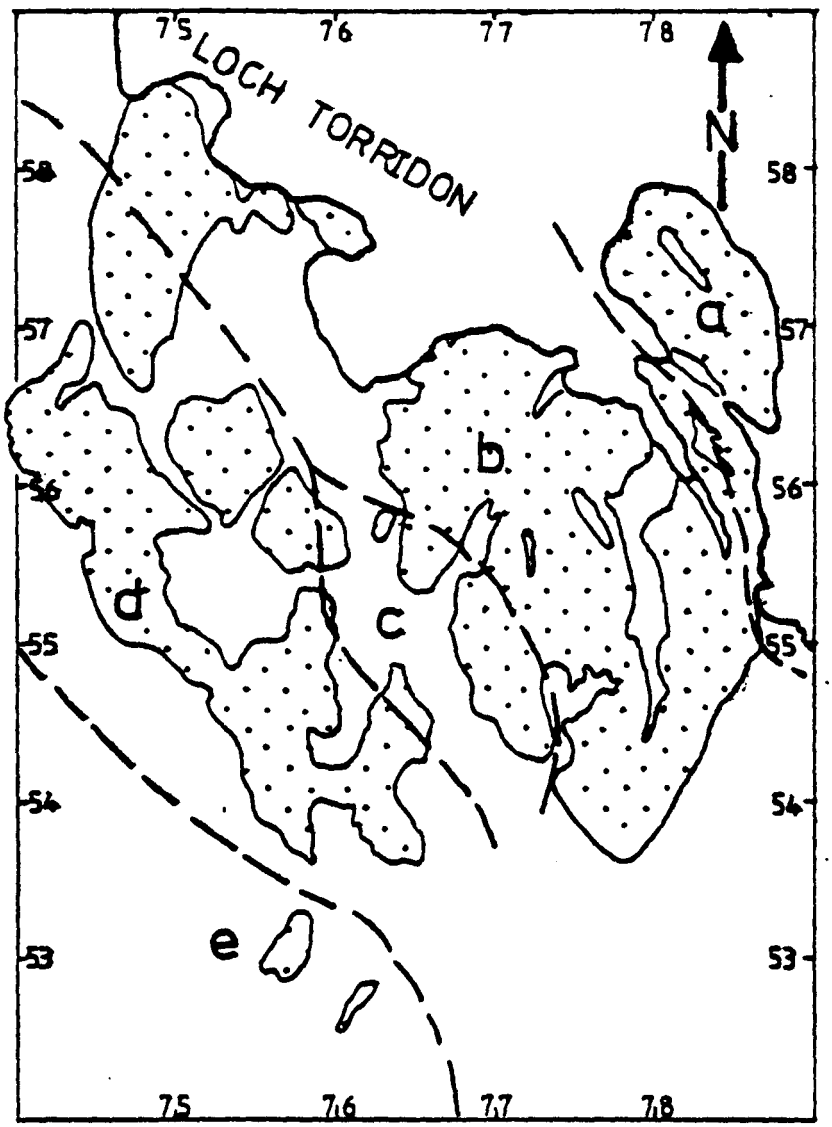
7'5
7'6
7'7
7'8
LOCH TORRIDON
N
58
57
56
55
54
53
a
b
c
d
e

(classes 3 and 4) are in the form of narrow belts, the strongest deformation being concentrated in the Ardheslaig peninsula and in the Loch Gaineamhach outcrop.

The contoured plot is however unrealistic since the zonal boundaries, especially those of very strong deformation cross the strike of the rocks and the dykes, but nowhere has any offset in the dykes or in the gneisses been observed. Another strain contour map (Enclosure 4) was therefore produced using the XZ ratios at each station, but contouring subjectively, taking into consideration the orientation of dykes and late structures. This is therefore the more realistic map. The four deformational classes used are the same as on the first strain map.

The areas of very low and very high deformations are in the same general area as on the first strain map (Enclosure 3). The biggest least deformed pod on this map (at Loch na Craig) is at the same place on this map and another low deformation pod beside Ardheslaig with the undeformed Scourie block is also at the same place here. The most strongly deformed rocks are in the northeastern corner of the inlier i.e. on Ardheslaig peninsula. In this map (Enclosure 4), the zonal boundaries and the belts of high strain are parallel to the gneissic layering and to the dykes, corresponding to the orientation of shear zones in the field.

For convenience, the Kenmore area has been subdivided into five zones based on intensity of deformation, the area boundaries being more or less parallel to the contours of map 4 (Fig. IV-3). These are:

(a) The Ardheslaig peninsula.

(b) The central belt.

(c) The Loch na Craig pod.

(d) The southwestern belt.

(e) The Loch Gaineamhach outcrop.

The XY, YZ and XZ ratios of the mineral aggregates for the five subareas have been plotted separately in graphical form (Figs. IV-4 to 8 for subareas a to e respectively) together with their arithmetic mean values. Flinn diagrams in which $1+e_1/1+e_2$ have been plotted as ordinate and $1+e_2/1+e_3$ as abscissa are also shown for each subarea and because of considerable spread on the diagrams, their arithmetic mean values are also given for comparison. A convenient measure of the magnitude of strain is the r value (Watterson, 1968) where $r = a + b - 1$.

$a = 1+e_1/1+e_2$ and $b = 1+e_2/1+e_3$

This has also been calculated for each subarea. The summary of all this information for the five subareas has been plotted on Fig. IV-9.

It can be seen that the XY and XZ ratios can be directly correlated with r values because values of r of course depend on these ratios. It is also obvious that the strain is lowest in the Loch na Craig pod where XY and XZ ratios are 7:1 and 14:1 respectively and the r value is 8 which is the lowest among the five subareas. In the highest strain areas, the XY and XZ ratios in the Loch Gaineamhach outcrop are 37:1 and 79:1 respectively and their r value is 38, while for the Ardheslaig peninsula, the XY and XZ values are 23:1 and 104:1 respectively and the r value is 27. The axial ratios and r values for the central and the southwestern belt, although very different from the other sub areas are rather similar to each other.

Two strain profiles have been constructed across the area, SSW-NNE oriented MN (Enclosure 5) through the western part of the area and SW-

Fig. IV-4. Measurements on grain aggregates in Scourie dykes from Ardheslaig peninsula.

(a) XY, YZ and XZ ratios on grain aggregates.

(b) Plot of XY ratios against YZ ratios on Flinn diagram.

A.M. is the arithmetic mean.

Each point is the mean of 3 measurements; the error is between 15 and 20%

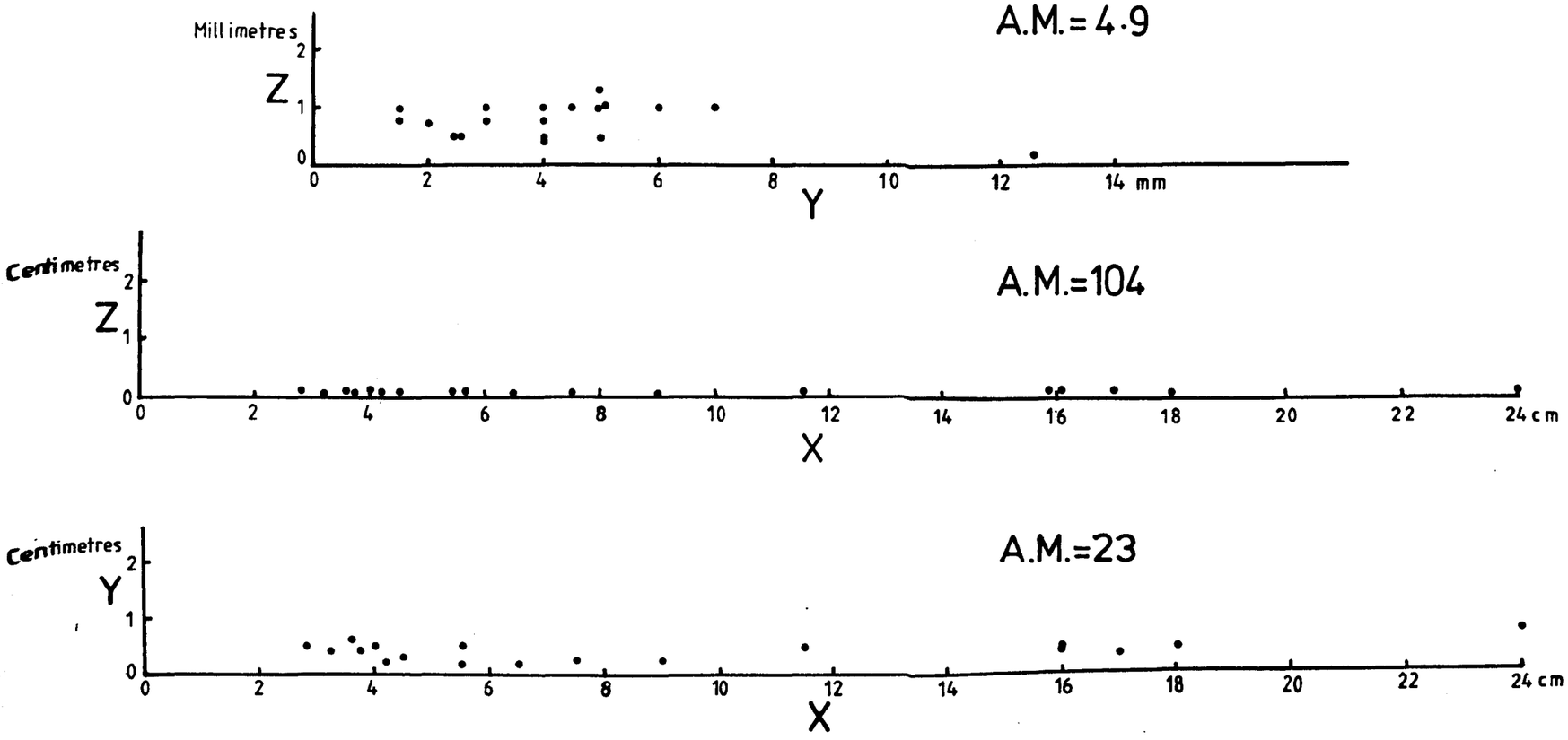
Millimetres
Z
A.M.=4.9
Y
14 mm
Centimetres
A.M.=104
X
24 cm
Centimetres
Y
A.M.=23
X
24 cm

a

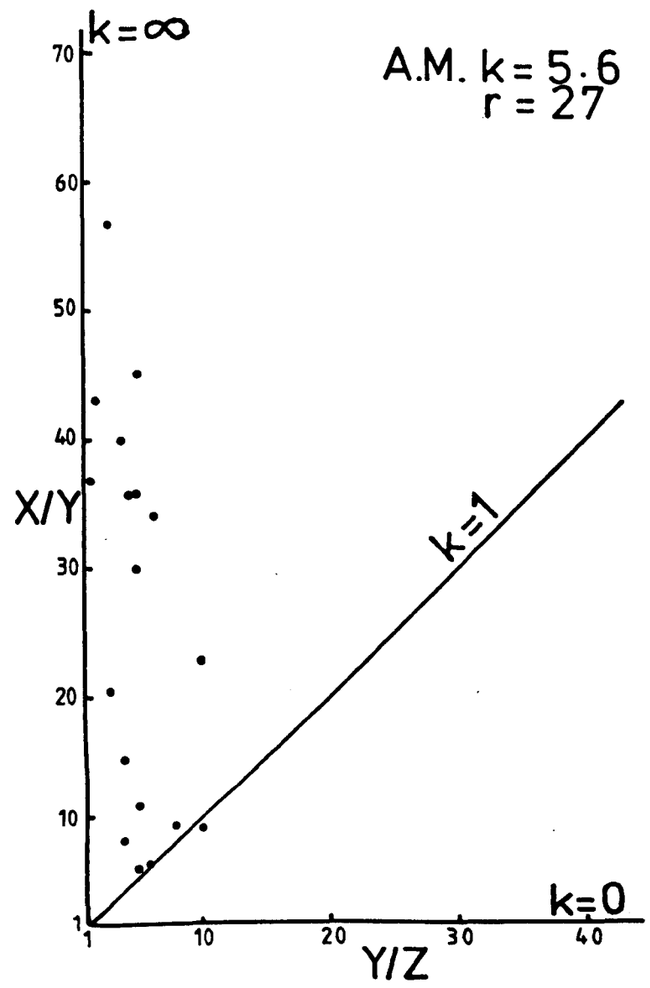
k=∞
A.M. k=5.6
r=27
X/Y
k=1
k=0
Y/Z

b

Fig. IV-5. Measurements on grain aggregates in Scourie dykes from the central belt.

(a) XY, YZ and XZ ratios on grain aggregates.

(b) Plot of XY ratios against YZ ratios on Flinn diagram.

A.M. is the arithmetic mean.

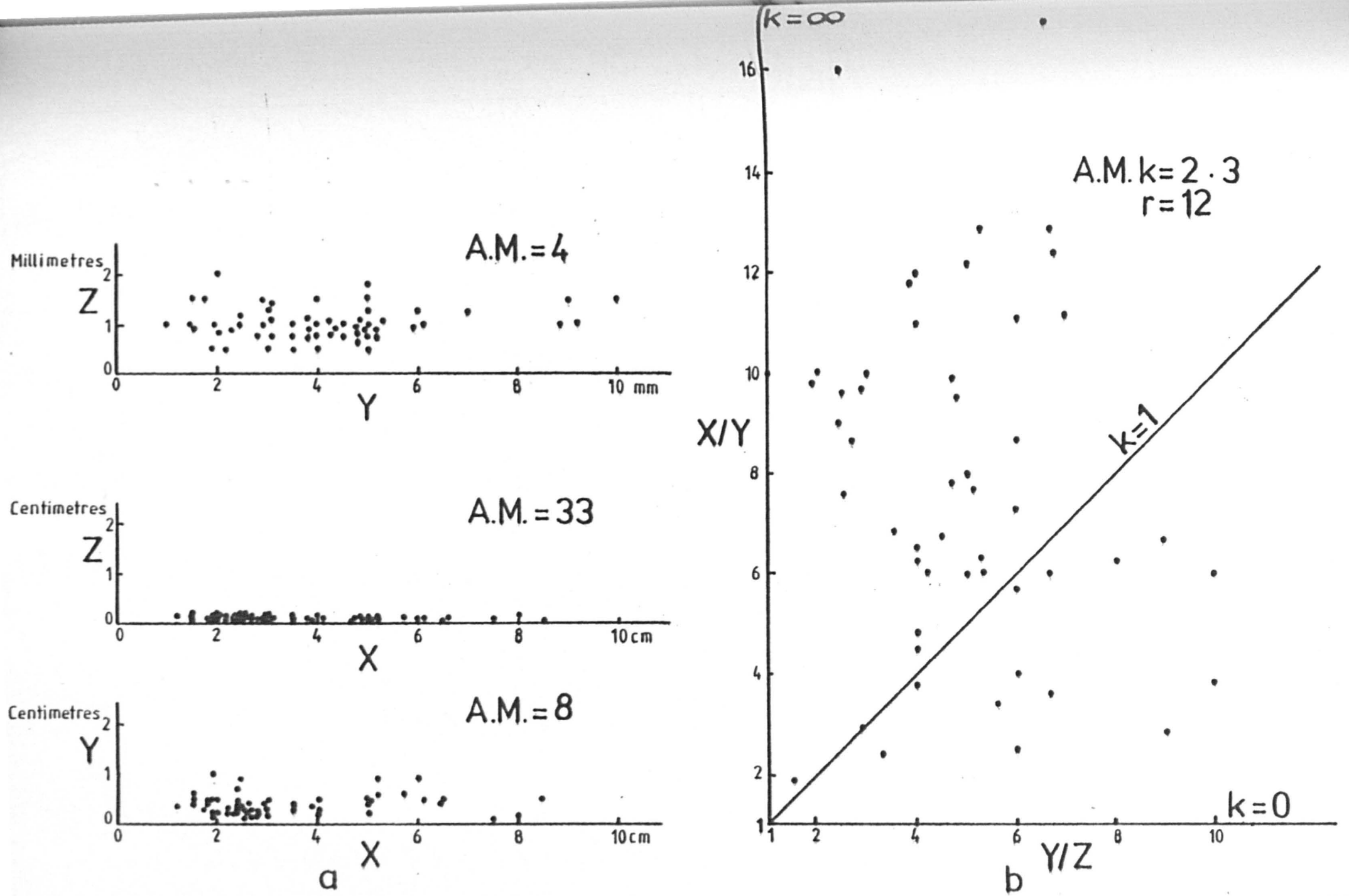
A.M.=4
Millimetres
Z
Y
0
2
4
6
8
10 mm
A.M.=33
Centimetres
Z
X
10cm
A.M.=8
Centimetres
Y
X
10cm
a
k=∞
A.M. k=2·3
r=12
X/Y
Y/Z
k=1
k=0
16
14
12
10
8
6
4
2
1
b

Fig. IV-6. Measurements on grain aggregates in Scourie dykes from the loch na Craig pod.

(a) XY, YZ and XZ ratios on grain aggregates.

(b) Plot of XY ratios against YZ ratios on Flinn diagram.

A.M. is the arithmetic mean.

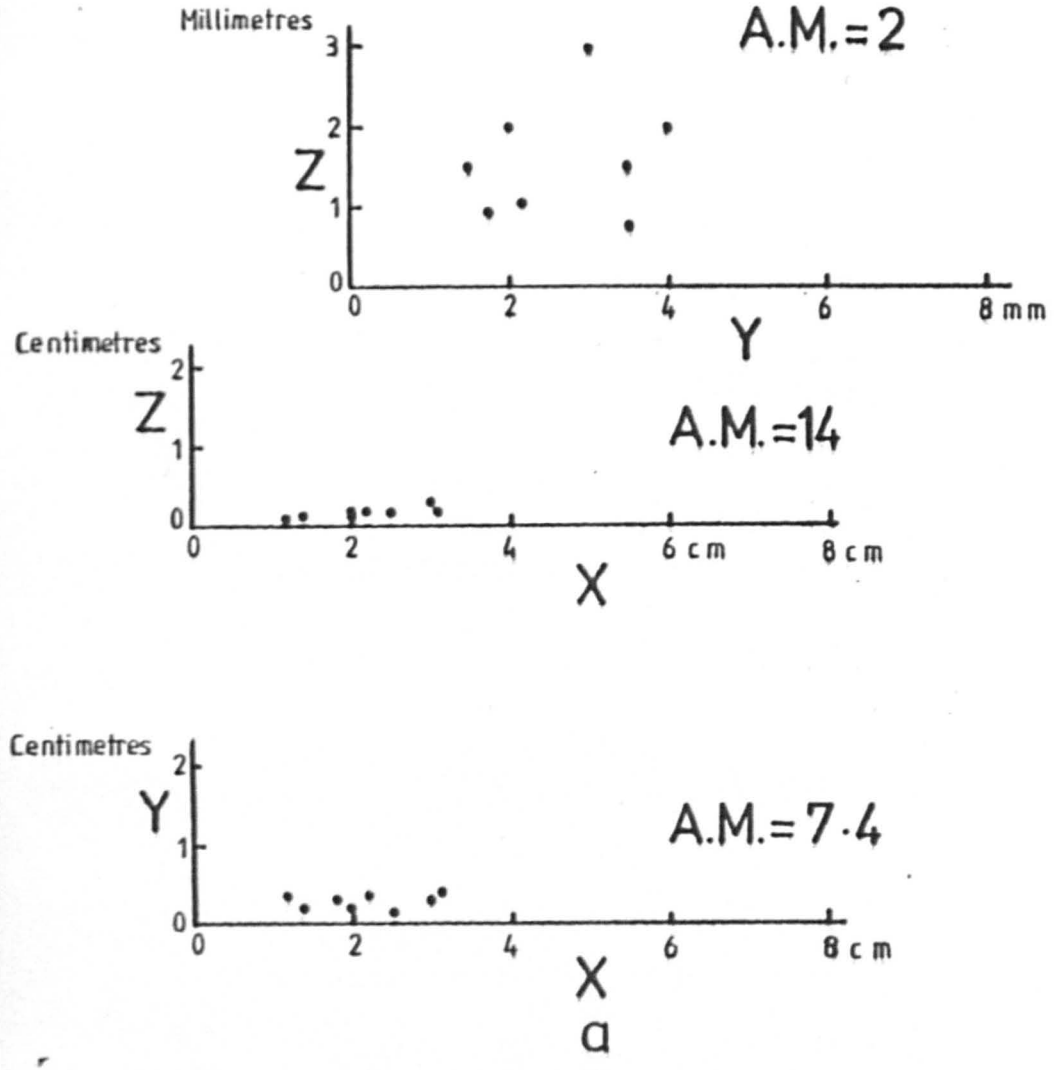
Millimetres
A.M.=2
Z
Y
0 2 4 6 8 mm
0 1 2 3
Centimetres
A.M.=14
Z
X
0 2 4 6 cm 8 cm
0 1 2
Centimetres
A.M.=7.4
Y
X
0 2 4 6 8 cm
0 1 2
a

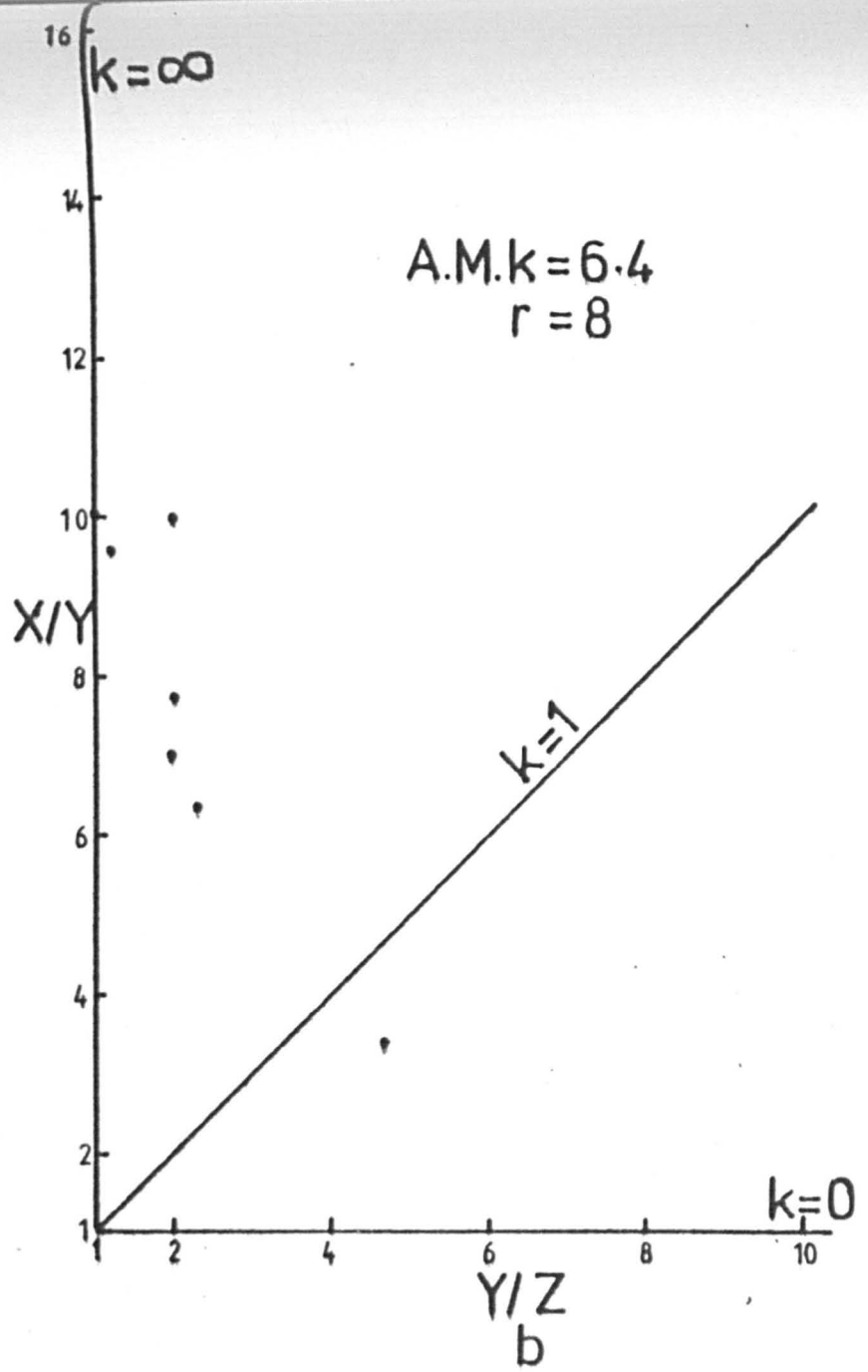
k=∞
A.M.k=6.4
r=8
X/Y
Y/Z
k=1
k=0
1 2 4 6 8 10
1 2 4 6 8 10 12 14 16
b

Fig. IV-7. Measurements on grain aggregates in Scourie dykes from the southwestern belt.

(a) XY, YZ and XZ ratios on grain aggregates.

(b) Plot of XY ratios against YZ ratios on Flinn diagram.

A.M. is the arithmetic mean.

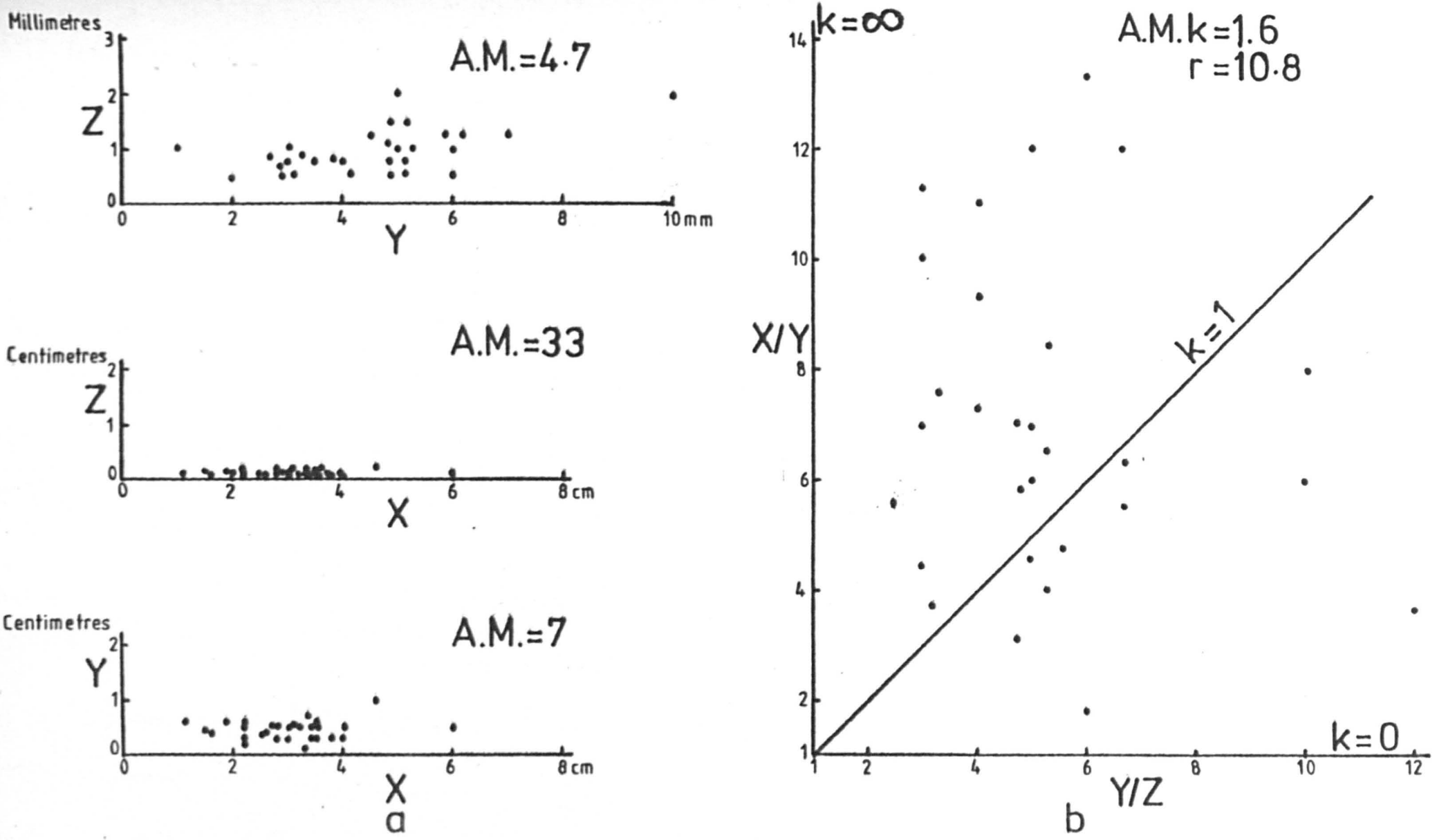
Millimetres
A.M.=4·7
Z
Y
0
2
4
6
8
10 mm
Centimetres
A.M.=33
Z
X
8 cm
Centimetres
A.M.=7
Y
X
8 cm
a
k=∞
A.M. k=1.6
r =10·8
X/Y
Y/Z
k=1
k=0
b

Fig. IV-8. Measurements on grain aggregates in Scourie dykes from the Loch Gaineamhach outcrop.

(a) XY, YZ and XZ ratios on grain aggregates.

(b) Plot of XY ratios against YZ ratios on Flinn diagram.

A.M. is the arithmetic mean.

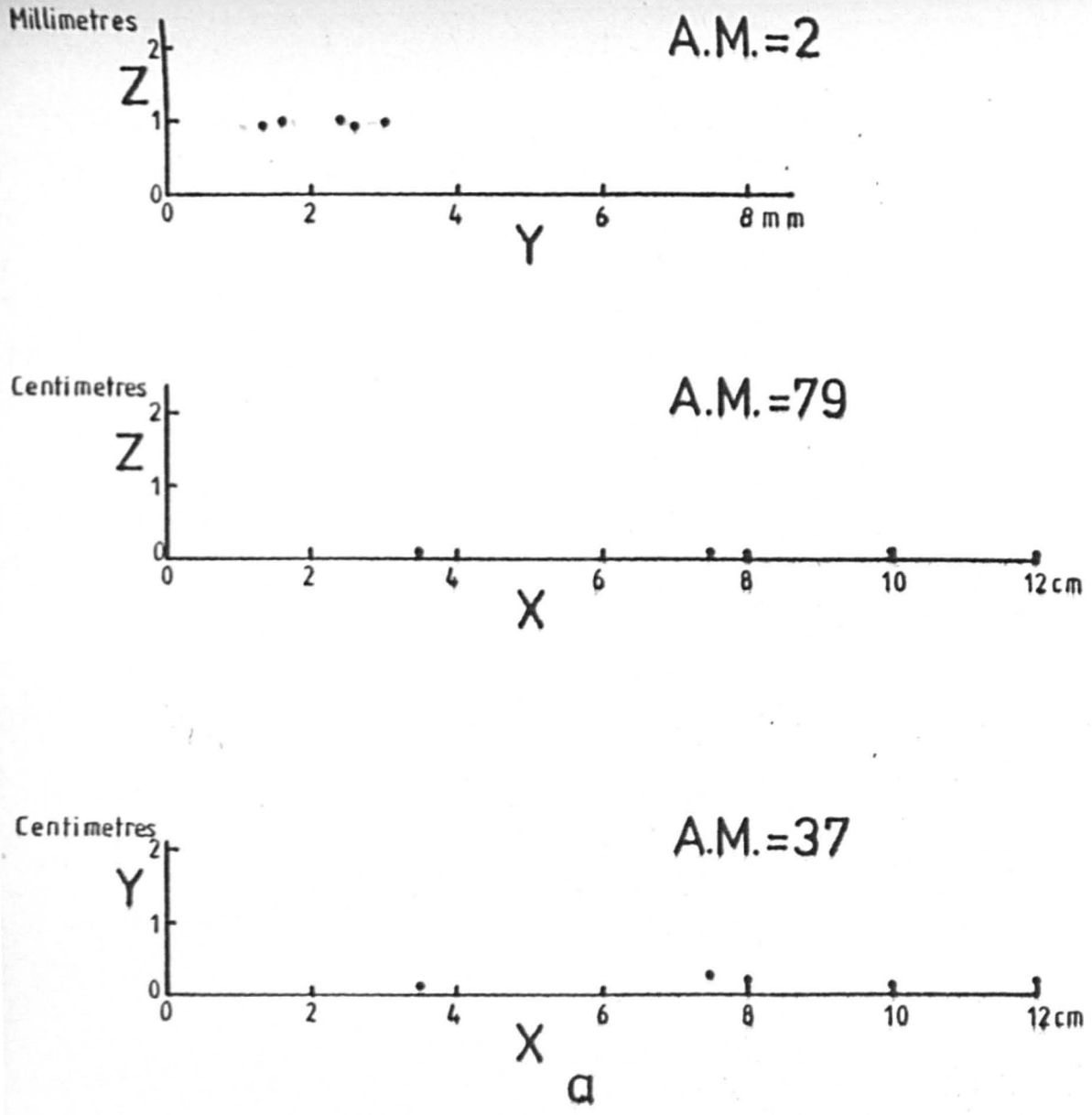
Millimetres
A.M.=2
Z
Y
8 mm
Centimetres
A.M.=79
Z
X
12 cm
Centimetres
A.M.=37
Y
X
12 cm
a

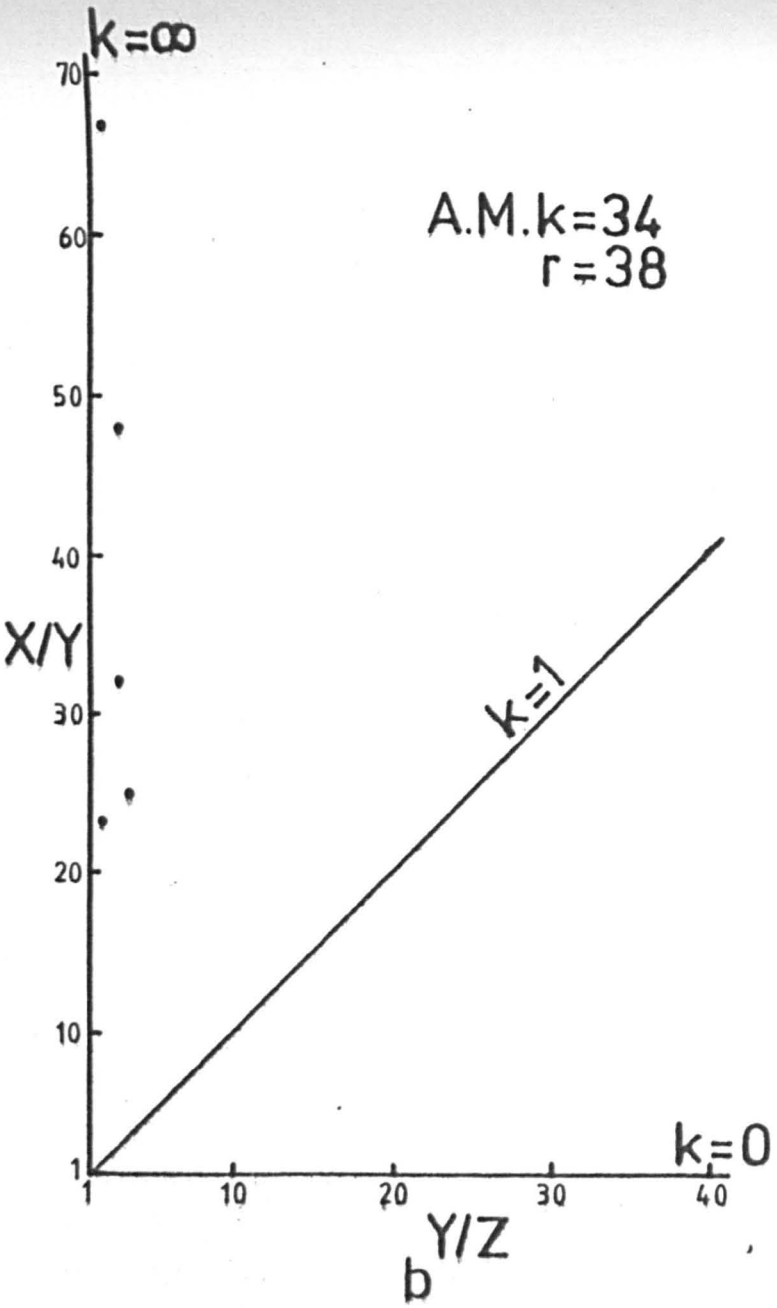
k=∞
A.M.k=34
r=38
X/Y
k=1
k=0
Y/Z
b

Fig. IV-9. Summarised shapes of strain ellipsoids from the five subareas of the Kenmore inlier and from the Diabaig inlier. Stippled area is the Lewisian outcrop.

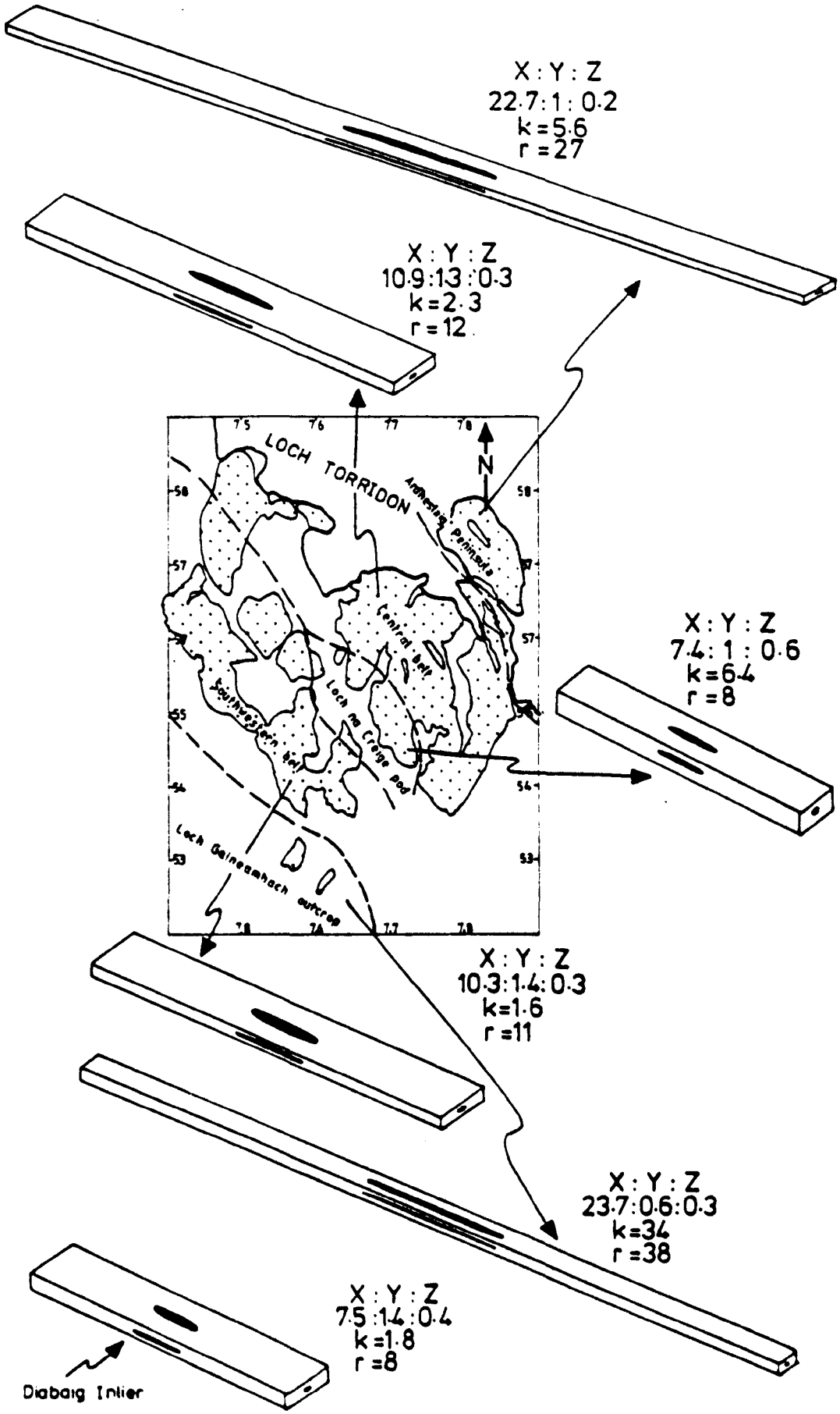
X : Y : Z
22·7 : 1 : 0·2
k = 5·6
r = 27
X : Y : Z
10·9 : 1·3 : 0·3
k = 2·3
r = 12
LOCH TORRIDON
N
Applecross Peninsula
Central belt
Loch na Creige fold
Loch Gairloch outcrop
X : Y : Z
7·4 : 1 : 0·6
k = 6·4
r = 8
X : Y : Z
10·3 : 1·4 : 0·3
k = 1·6
r = 11
X : Y : Z
23·7 : 0·6 : 0·3
k = 34
r = 38
X : Y : Z
7·5 : 1·4 : 0·4
k = 1·8
r = 8
Diabaig Inlier

NE oriented OP through the central part of the area (Enclosure 4 and Fig. IV-3). Large scale F_3 folds are shown on the strain profiles. Along the MN profile it can be seen that the strain is higher in the northern part of the section where r values are higher (12-18) than in the southern part (10-12). In the OP profile there is no consistent pattern to the r values which lie in the range 7-15 except in the northeast (Ardheslaig) where r values of 23 and 41 occur. The Loch Gaineamhach outcrop has very high strains (Fig. IV-8) with a mean r value of 38, but it is a comparatively isolated outcrop and is difficult to correlate with the rest of the area, as discussed earlier (see Section B1 of Chapter III). This outcrop may represent a deeper structural level than the southwestern belt adjacent to it, brought up by a later shear zone or fault.

Comparing the strain profiles MN and OP it can be seen that the strain ellipsoid is less prolate and of lower k value in the western part of the inlier than in the eastern part. However, just to the east of the OP strain profile around Loch a Mhuilinn, the strain ellipsoid is again more oblate (see also Enclosure 4).

Only the F_3 large-scale structures are recorded in the sections, and it is clear that the grain aggregate strains cannot be correlated with them. Moreover it is not possible to correlate the intensity of deformation (r values) with the type of strain ellipsoid i.e. oblateness or prolateness ((k values) see Enclosure 4). In the least deformed areas like the Loch na Craig pod the strain ellipsoid is prolate with a high k value, but this is also the case in the Ardheslaig peninsula and in the Loch Gaineamhach outcrop where the strain is very high. In the moderately deformed areas of the central and the southwestern belts the mean ellipsoid is also prolate but with lower k values.

As already mentioned,the grain aggregate strain represents the total finite Laxfordian strain and in every case results from the superimposition of at least two deformations. This is probably the reason for the large spread on the Flinn diagram (Fig. IV-4 to 8). For example it is a quite common feature, where an LS, fabric has been folded by F_2 folds for the grain aggregates in the hinge zone and on the limbs of the folds to show two quite different shapes (Fig. IV-10).

The shape of the finite strain ellipsoid depends upon:

(1) The shape of the finite strain ellipsoid of the first deformation.

(2) The shape of the incremental strain ellipsoid of the second deformation and

(3) Their mutual orientations.

On the F_2 fold limbs the finite strain ellipse of first deformation and the incremental strain ellipse (in profile plane) of the second deformation are in the same orientation and hence reinforce each other giving a more flattened fabric with a lower k value. In the hinge zone the two ellipses are at a high angle to each other in the fold profile and therefore tend to cancel each other giving a comparatively more linear fabric with a higher k value. Where the axial ratio of major and minor axes of the D_1 finite strain ellipse is greater than that of the D_2 incremental strain ellipse in the hinge zone, then the D_2 finite strain ellipse is closer to that of the D_1 finite strain ellipse (Fig. IV-10a). Where the two are equal they completely cancel each other giving a linear fabric in the hinge zone (Fig. IV-10b). Where the ratio of major and minor axes of the D_2 incremental strain ellipse is greater than that of the D_1 finite strain ellipse then the D_2 finite strain ellipse is closer to the D_2 incremental strain ellipse in shape and size (Fig. IV-10c). This phenomenon has also been observed in the co-axial deformation of Lewisian rocks of the Outer Hebrides (Graham and

Fig. IV-10. Superimposition of D_1 and D_2 strains in F_2 folds, D_2 incremental strain increasing from a to c. (i) is the orientation of the D_1 finite strain ellipse on F_2 limbs, and (ii) is the orientation of the D_1 finite strain ellipse o the F_2 hinge. "a" is the most common case.

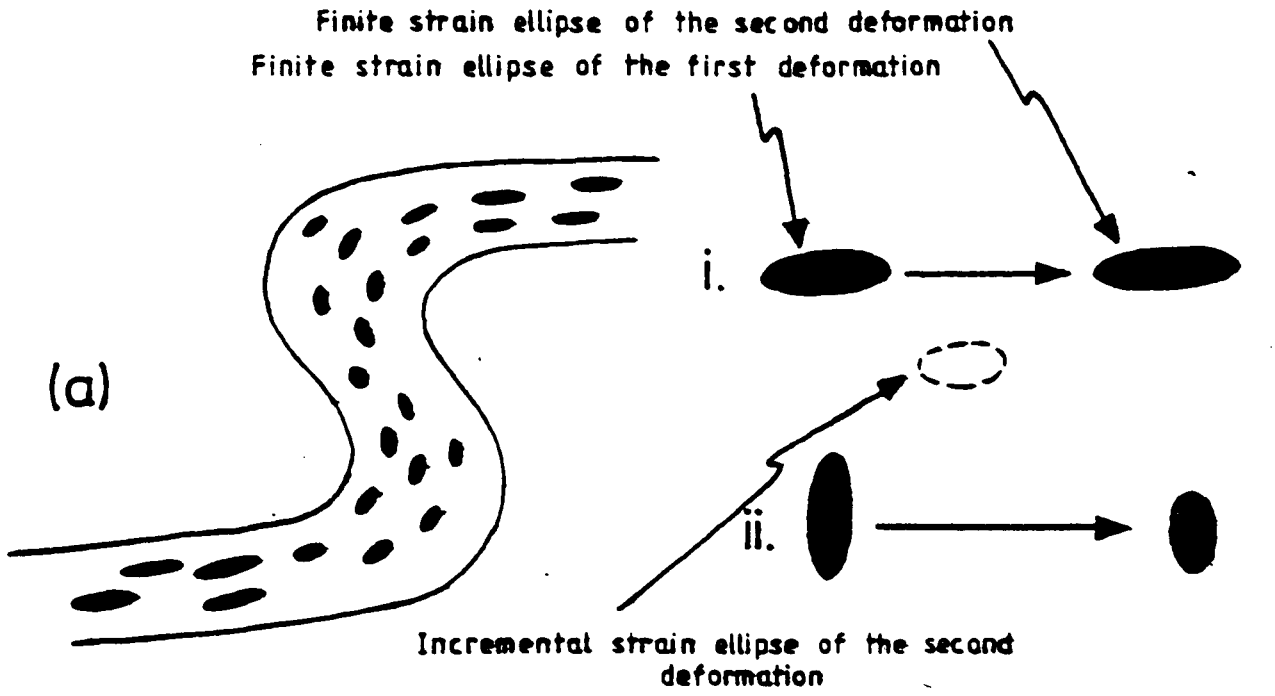
Finite strain ellipse of the second deformation
Finite strain ellipse of the first deformation
(a)
i.
ii.
Incremental strain ellipse of the second deformation

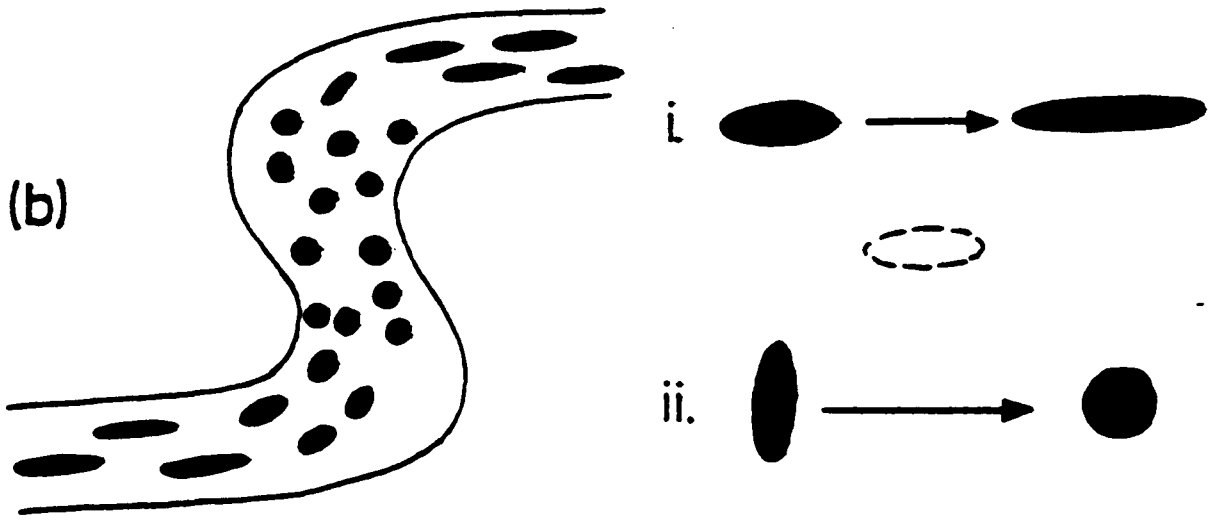
(b)
i.
ii.

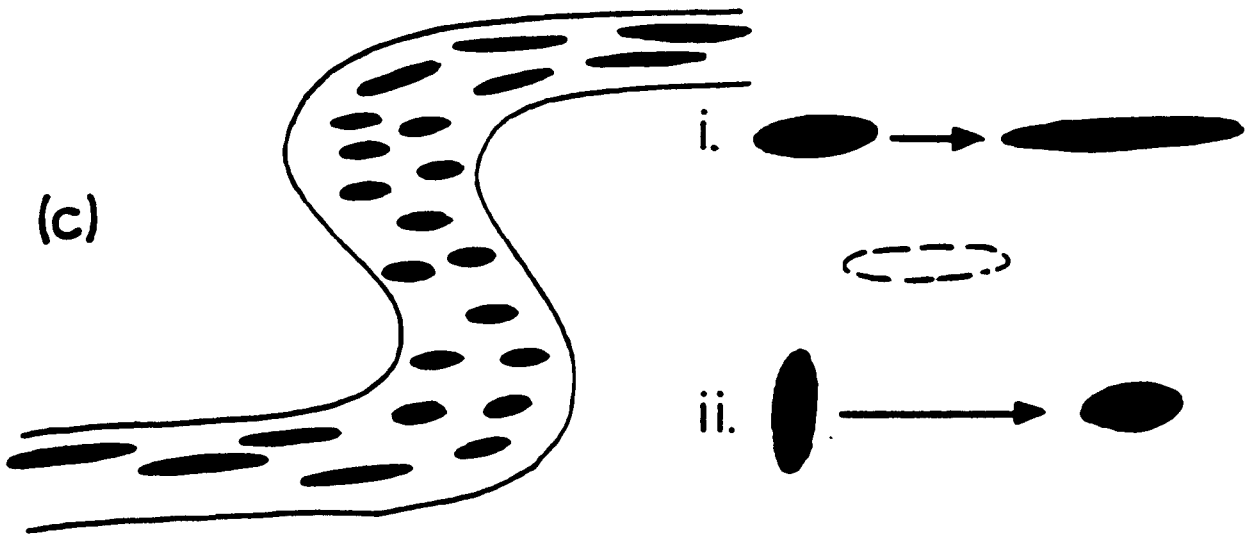
(c)
i.
ii.

Coward, 1973).

2. Amount of apparent flattening of F_2 and F_3 folds in the Kenmore inlier

For measuring the apparent flattening of the folds, curves have been drawn for single layers in multilayered folded gneisses using both Ramsay's t' /α (1967) and Hudleston's ϕ/ α (1973a) plots for measuring $\sqrt{\lambda_2/\lambda_1}$ in fold profile (Figs. IV-1a and IV-2a). T' has been omitted because it depends directly upon t'. For measuring and comparing flattening in folds throughout the inlier Ramsay's (op.cit.) curves are used for uniformity rather than Hudleston's (op.cit.) ϕ / α curves, for the following reasons given by Hudleston (1973a).

(1) t' is easier to measure than ϕ which requires careful positioning of tangent points.

(2) Errors in ϕ are larger than in t' and are 'picked up' by the more sensitive nature of the plot.

(3) At high limb dips ϕ becomes most inaccurate because the curvature of the folded surfaces is low and the tangent points are difficult to locate accurately; on the other hand the most useful part of a t' /α plot is that for the highest limb dips.

The curves for half folds (i.e. between two inflexion points) have been plotted and their average has been computed graphically using photographs of folds in profiles. Because F_2 and F_3 are the only important Laxfordian folding episodes in the area, it was important to obtain some idea of the strain represented by the flattening of these folds.

a. Apparent flattening in the F_2 folds: Apparent flattening in 25 F_2 folds from all over the area was measured in three different structural horizons:- Ardheslaig peninsula, the fold belt in the central zone and

a southwestern belt (Fig. IV-3). Results are shown in the form of histograms (Fig. IV-11a, b, c respectively. From them it is apparent that there is not much difference in the amount of flattening in the three different areas, except that the folds of the southwestern belt are slightly more flattened, the mean flattening value $\sqrt{\lambda_2/\lambda_1}$ being 0.28 (Fig. IV-11c). In the central belt and in Ardheslaig peninsula it is respectively 0.33 and 0.36 (Fig. IV-11b and 11a respectively).

Although flattening is variable and the $\sqrt{\lambda_2/\lambda_1}$ values ranges from 0.8 to less than 0.1, 84% of the folds show $\sqrt{\lambda_2/\lambda_1}$ ratios of more than 0.5.

It is important to remember that the F_2 folds are probably not pure buckles which later flattened by homogeneous strain, but that probably there was a shearing component also involved in their formation (see chapter VI).

b. Apparent flattening in the F_3 folds: Apparent flattening of 31 F_3 folds from all over the area was measured in profile. Again the same three zones are used.

Although folds show varying amounts of flattening over the area, from concentric non-flattened or even type 1A (Ramsay op. cit.) to nearly similar, or sometimes class 3, strongly flattened folds, there is not much difference again in the pattern of flattening between the three zones (Fig. IV-12), except that in the central belt there is a high proportion of folds with low amounts of flattening. There is not much difference in the mean flattening values in the three areas, but folds in the southwestern belt are slightly but insignificantly more flattened with a mean flattening value of 0.39 compared with 0.49 in the central belt.

A comparison of the amount of flattening of F_2 and F_3 folds

Fig. IV-11. Histograms of post buckle flattening of F_2 folds from the Kenmore inlier. M is the arithmetic mean.

(a) 7 folds from the Ardheslaig peninsula.

(b) 6 folds from the central belt.

(c) 12 folds from the southwestern belt.

(d) 25 folds from whole area.

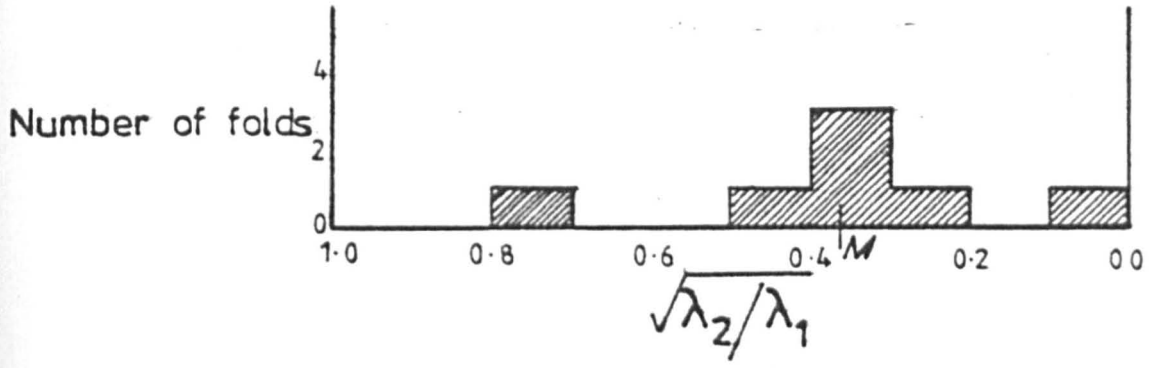
Number of folds
4
2
0
1·0
0·8
0·6
0·4
M
0·2
0 0
$\sqrt{\lambda_2/\lambda_1}$

a

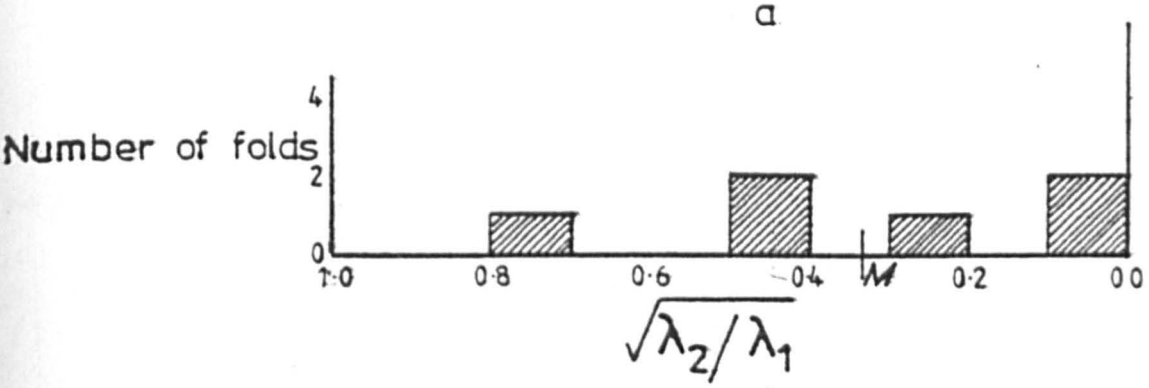
Number of folds
4
2
0
1·0
0·8
0·6
0·4
M
0·2
0 0
$\sqrt{\lambda_2/\lambda_1}$

b

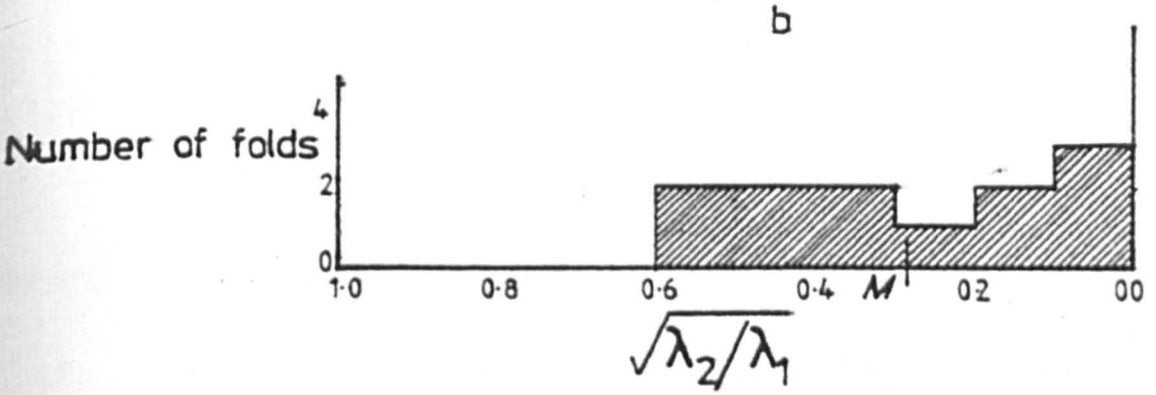
Number of folds
4
2
0
1·0
0·8
0·6
0·4
M
0·2
0 0
$\sqrt{\lambda_2/\lambda_1}$

c

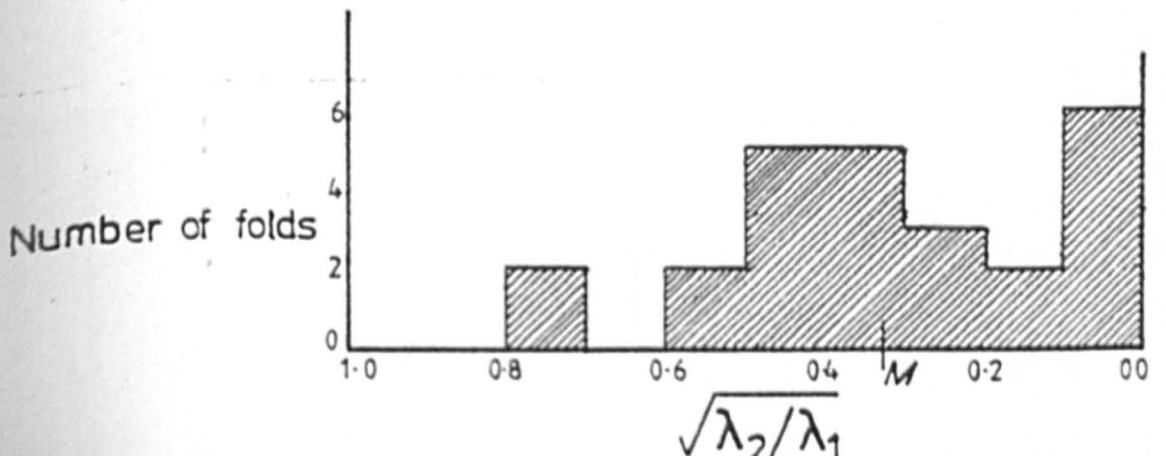
Number of folds
6
4
2
0
1·0
0·8
0·6
0·4
M
0·2
0 0
$\sqrt{\lambda_2/\lambda_1}$

Fig. IV-12. Histograms of post buckle flattening of F_3 folds from the Kenmore inlier. M is the arithmetic mean.

(a) 3 folds from the Ardheslaig peninsula.

(b) 21 folds from the central belt.

(c) 7 folds from the southwestern belt.

(d) 31 folds from whole area.

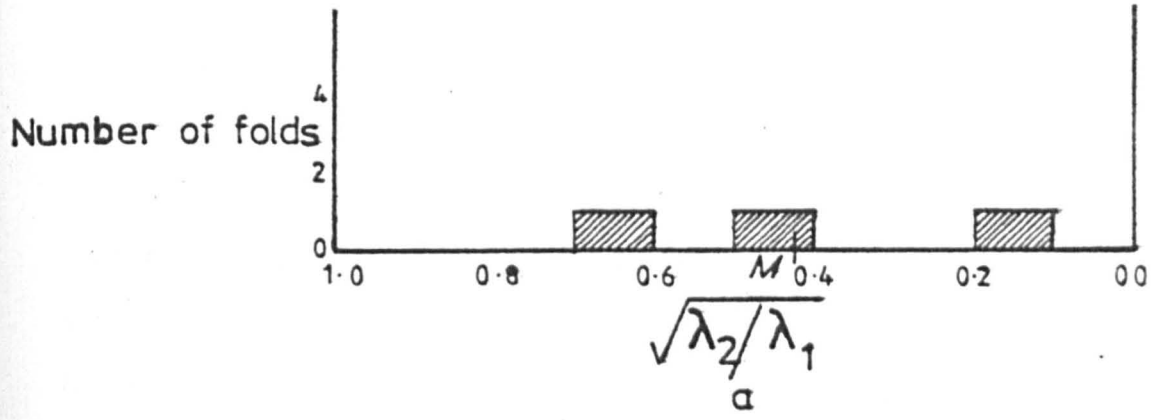
Number of folds
4
2
0
1·0
0·8
0·6
M
0·4
0·2
0·0
$\sqrt{\lambda_2/\lambda_1}$

a

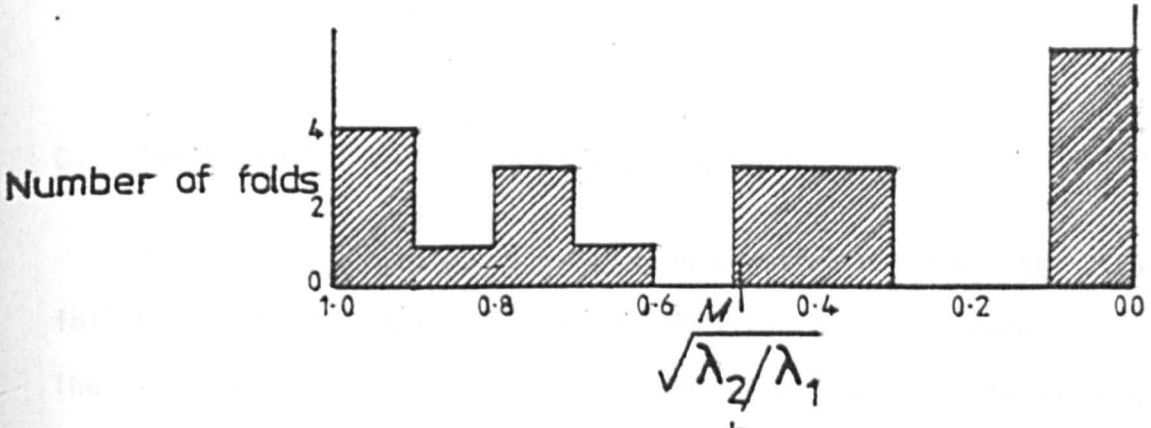
Number of folds
4
2
0
1·0
0·8
0·6
M
0·4
0·2
0·0
$\sqrt{\lambda_2/\lambda_1}$

b

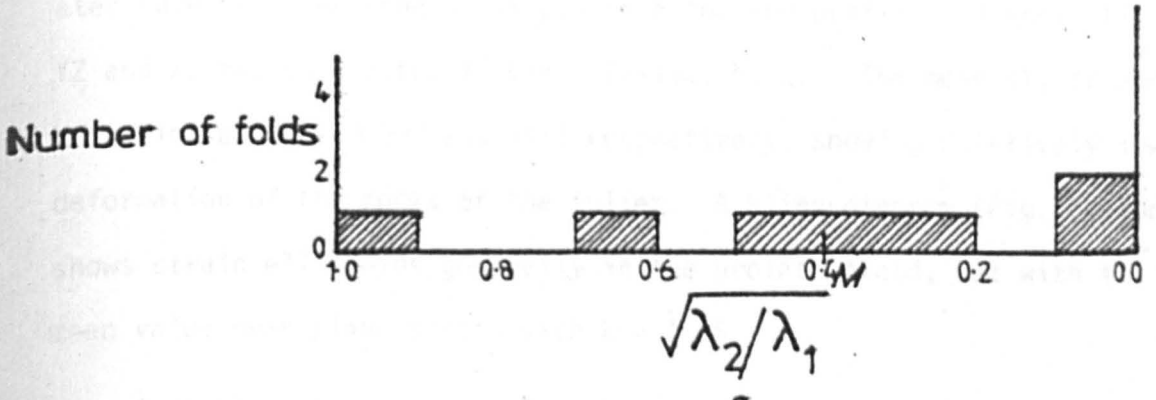
Number of folds
4
2
0
1·0
0·8
0·6
0·4
M
0·2
0·0
$\sqrt{\lambda_2/\lambda_1}$

c

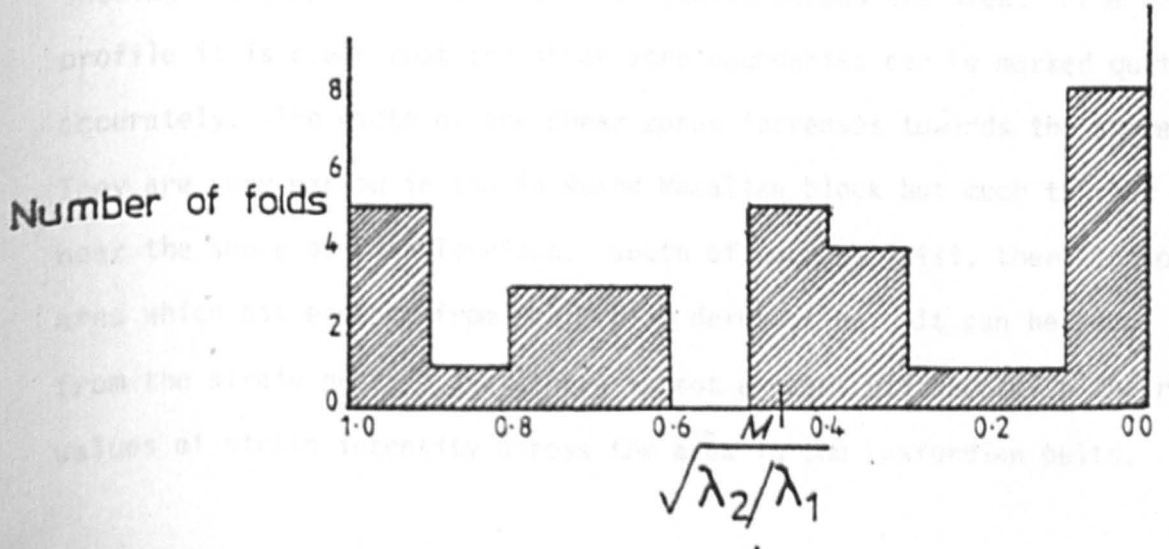
Number of folds
8
6
4
2
0
1·0
0·8
0·6
M
0·4
0·2
0·0
$\sqrt{\lambda_2/\lambda_1}$

indicates that the F_2 folds are slightly more flattened with a mean flattening of 42% ($\sqrt{\lambda_2/\lambda_1} = 0.32$), than the F_3 folds whose mean flattening is 31% ($\sqrt{\lambda_2/\lambda_1} = 0.46$). 92% of the F_2 folds have been flattened more than 22% while only 61% of F_3 folds are flattened more than this value. It should be taken into account that the strain measured in F_2 folds might include some contribution from the D_3 deformation and that the strain in F_2 folds could vary according to position on limbs or hinges of major F_3 folds.

C. STRAIN PROFILE ACROSS THE DIABAIG INLIER

A 5 km long strain profile has been constructed across the Diabaig inlier, using the shape fabric in the dykes as in the Kenmore inlier. The strain profile runs from the Ruadh Mheallan block in the north to Port Laire on the shore of Loch Torridon (Enclosure 6). Grain aggregates have been measured at 15 places along the profile and their XY, YZ and XZ ratios plotted in Figs. IV-13a, b, c. The mean XY, YZ and XZ ratios are 6:1; 3.2:1 and 19:1 respectively, showing relatively low deformation of the rocks of the inlier. A Flinn diagram (Fig. IV-13d) shows strain ellipsoids generally in the prolate field, but with the mean value near plane strain with k = 1.85.

A diagramatic strain profile has been constructed (Enclosure 7) showing the shapes of the strain ellipsoids across the area. From this profile it is clear that the shear zone boundaries can be marked quite accurately. The width of the shear zones increases towards the shore. They are very narrow in the An Ruahd Mheallan block but much thicker near the shore of Loch Torridon. South of Loch na Beist, there is no area which has escaped from Laxfordian deformation. It can be seen from the strain profile that there is not a great difference in the r values of strain intensity across the area in the Laxfordian belts,

Fig. IV-13. Measurements on grain aggregates in Scourie dykes from the Diabaig inlier.

(a) XY, YZ and XZ ratios on grain aggregates.

(b) Plot of XY ratios against YZ ratios on a Flinn diagram.

A.M. is the arithmetic mean.

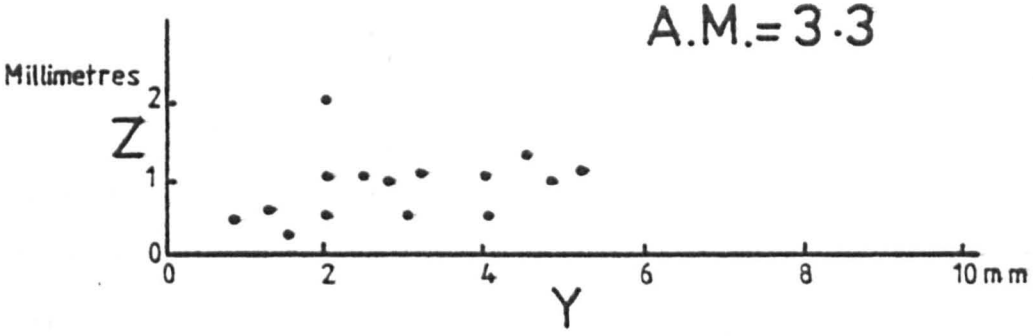
A.M.= 3·3
Millimetres
Z
2
1
0
0
2
4
6
8
10 mm
Y

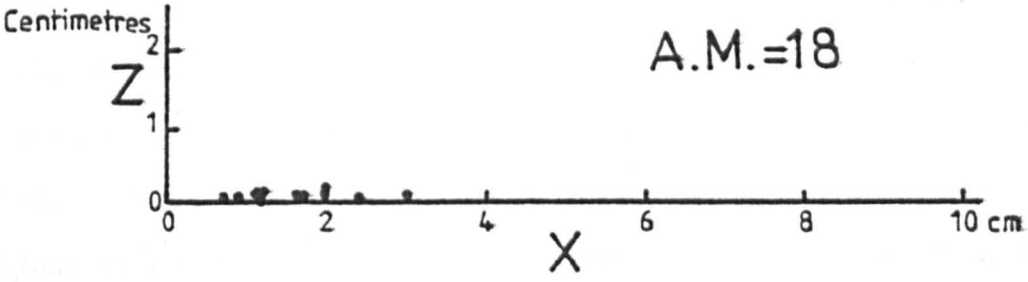
Centimetres
A.M.=18
Z
2
1
0
0
2
4
6
8
10 cm
X

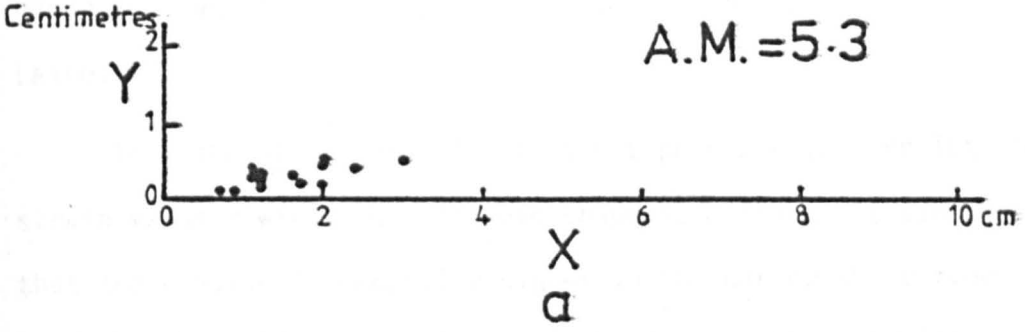
Centimetres
A.M.=5·3
Y
2
1
0
0
2
4
6
8
10 cm
X

a

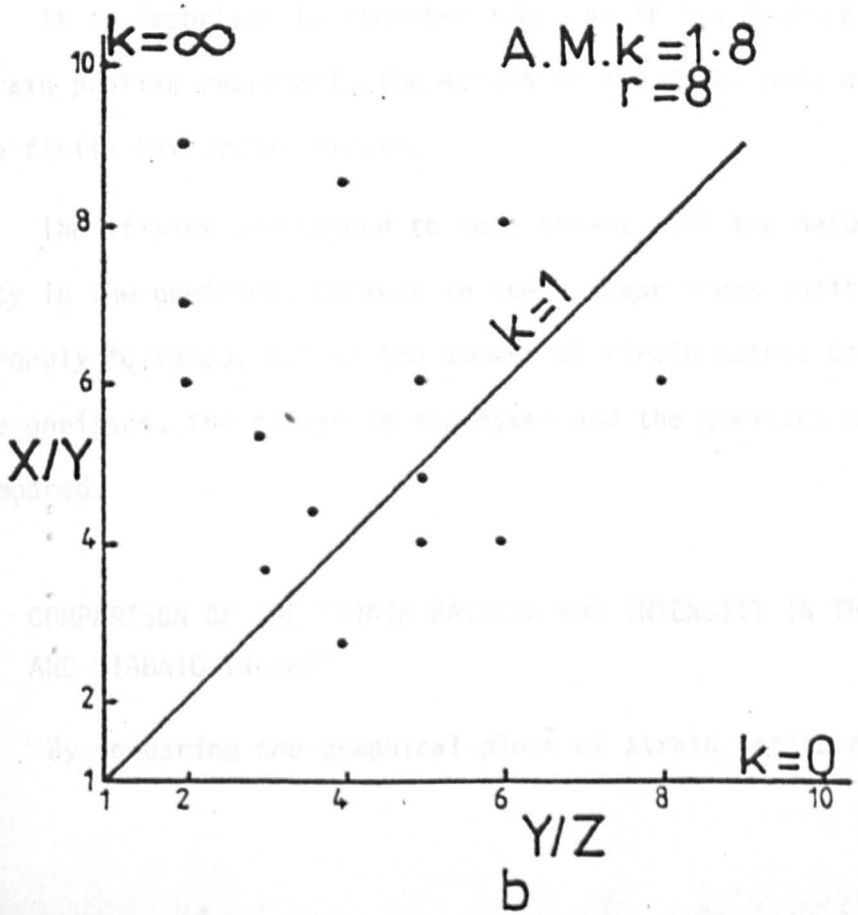
k=∞
A.M.k =1·8
r=8
k=1
X/Y
10
8
6
4
2
1
1
2
4
6
8
10
k=0
Y/Z

b

except for the extreme southwest where there are slightly higher values near the shore of Loch Torridon (i.e. within the Loch a Bhealch Mhoir shear zone). It can be seen as well that in the wider shear zones the strain is lower near the margins of the shear zones and higher in the centre as is to be expected. This can be demonstrated across both the Lochan Dharach and Loch a Bhealach Mhoir shear zones (Enclosure 7). Across the Lochan Dharach shear zone the r value is 6 and 7 on its northern and southern margins respectively, but in the centre of it, at two places it is 10 and 14. Similarly the r value increases towards the shore of Loch Torridon in the Loch a Bhealach Mhoir shear zone whose central part is probably somewhere south of Port Laire.

Along the strain profile it is not possible to correlate the strain value r with the ellipsoid shape k, although it can be said that the k value is generally higher in the narrow shear zones of the Ruadh Mheallan block than in the much wider southwestern zone, i.e. the Loch a Bhealach Mhoir shear zone.

It is important to remember that, as in the Kenmore inlier, the strain profile represents the strain in the dykes only and thus only the finite Laxfordian strain.

The strains correspond to some extent with the deformation intensity in the gneisses, because in these shear zones gneisses are also strongly foliated, but as the amount of strain cannot be measured in the gneisses, the strain in the dykes and the gneisses cannot be compared.

D. COMPARISON OF THE STRAIN PATTERN AND INTENSITY IN THE KENMORE AND DIABAIG INLIERS

By comparing the graphical plots of strain ratios and the diagram-

atic strain profiles of the Kenmore inlier (Figs. IV-4 to 8 and Enclosure 5) with those of the Diabaig inlier (Fig. IV-13 and Enclosure 7) it is quite clear that, as a whole, the strain is higher i.e. the rocks are more strongly deformed, in the Kenmore inlier than in the Diabaig inlier. The whole Kenmore inlier except for the Ardheslaig undeformed pod, appears to lie within a big shear zone whose margins cannot be seen, while in the Diabaig inlier the shear zones are not so wide and their margins can be located (Enclosure 6).

On comparing the amount of strain in the Diabaig inlier with that in the five subareas of the Kenmore inlier, it can be seen that the mean strain (r value) in the Diabaig inlier is similar to that of the central and southwestern belts of the Kenmore inlier. The shape of the strain ellipsoid (i.e. the k value), in the Diabaig inlier is close to that of the central and southwestern zones.

CHAPTER V

METAMORPHIC HISTORY

A. INTRODUCTION

The metamorphic history of the area has been studied with reference to the mineral assemblages produced in several different episodes with the help of the textural relationships of the minerals with each other and with the metamorphic fabric in thin section. Unfortunately, due to the lack of aluminosilicates it is difficult to comment precisely about the grade of metamorphism.

Mineral assemblages in the amphibolites (Scourie dykes) and the quartzo-feldspathic gneisses, indicate an overall lower amphibolite facies metamorphism. Two main regional metamorphic episodes have been recognised, M_1 and M_2 which on textural evidence can be associated with D_1 and D_2 deformations respectively. The two events are considered to be broadly of the same grade. Lower-grade mineral assemblages are also present in the area but are post-M_2. The period of crystallisation of the various minerals in relation to the metamorphic episodes are presented in Fig. V-1.

B. M_1 METAMORPHISM

The detailed mineralogies of all the rocks containing S_1 fabric has already been discussed in chapter II. In the case of the Scourie dykes they indicate the mineral assemblage produced during the first metamorphism (which is associated with the main fabric) because it has been derived from the parent igneous assemblage from which it can easily be distinguished. On the other hand, in the case of the acid gneisses, it is difficult to separate the mineral assemblage of the pre-dyke

Fig. V-1. .Summary of the crystallisation of minerals in various metamorphic episodes.

Certain widespread cyrstallisation.

Certain but localized crystallisation.

—?—?- Uncertain crystallisation (whether Inverian or Laxfordian).

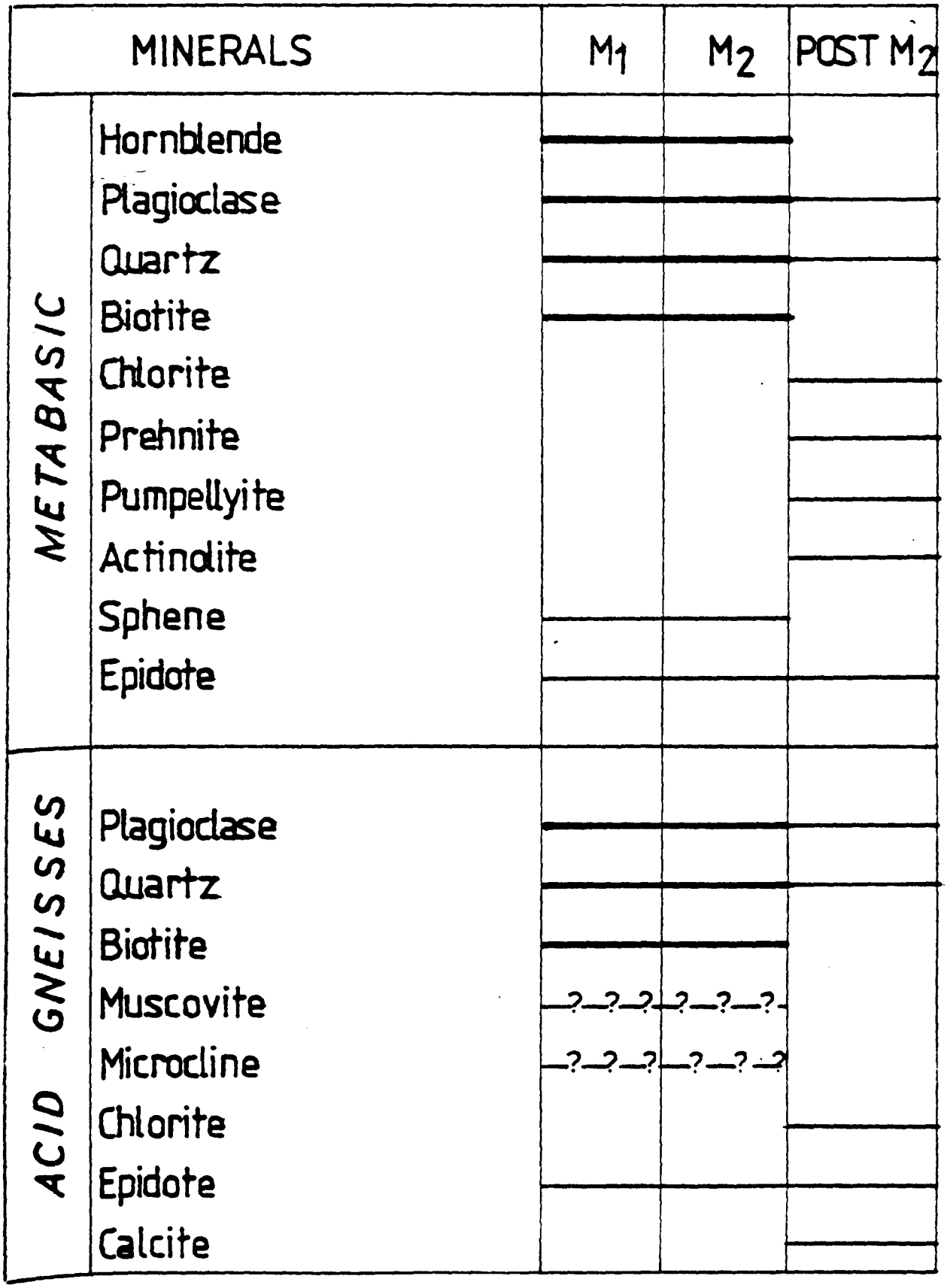
MINERALS
M1
M2
POST M2
METABASIC
Hornblende
Plagioclase
Quartz
Biotite
Chlorite
Prehnite
Pumpellyite
Actinolite
Sphene
Epidote
ACID GNEISSES
Plagioclase
Quartz
Biotite
Muscovite
Microcline
Chlorite
Epidote
Calcite

Inverian metamorphism, partly becauseof the lack of F_1 folds in the area, partly because the S_1 fabric is nearly of the same orientation as the Inverian fabric, and partly because the two metamorphic episodes are of the same grade as Cresswell (1969) discovered in the Diabaig inlier.

1. Metamorphism of the Scourie Dykes

The Hornblende-Plagioclase (An>25%) pair in the metamorphism is diagnostic of amphibolite-facies metamorphism (Turner, 1981, p.366). Hornblende was probably produced directly by the breakdown of clinopyroxene and by a reaction between clinopyroxene and plagioclase:

$$\text{Clinopyroxene} + \text{Plagioclase} + 2H^{+} \rightarrow \text{Hornblende} + Ca^{+2} + SiO_2 + H_2O$$

(Beach, 1980).

Pyroxene has not been preserved in the dykes except in one undeformed pod* in a dyke 2 km south of Kenmore. In this dyke complete transformation of pyroxene to hornblende, through intermediate stages, can be seen, and is related to the degree of deformation.

(a) Stage 1. In the completely undeformed pod, the parent ophitic texture is still preserved, defined by the network of plagioclase laths and pyroxene is present in the intergranular spaces (Pl. V-1a). Here hornblende crystallises at two different sites: at one place it replaces the pyroxene grains on their margins producing a thin layer of hornblende which is probably a reaction product of pyroxene with plagioclase and at another place fine-grained hornblende crystallises away from pyroxene in clusters which surround the iron ore.

(b) Stage 2. In the weakly deformed part of the same dyke, although no pyroxene is preserved, its texture is intermediate between the completely undeformed pod and those dykes showing advanced stages of deformation. Here also hornblende is present in two different forms

* 75605587

Plate V-1a. Photomicrograph of undeformed pod in a dyke showing ophitic texture. Recrystallisation is in the initial stage. P = plagioclase, H = hornblende, P_y = pyroxene, O = opaque. See text for details (plane polarised light x65).

Plate V-1b. Photomicrograph of weakly deformed dyke. P = plagioclase, H = hornblende, O = opaque, Q = quartz. See text for details (plane polarised light. x20).

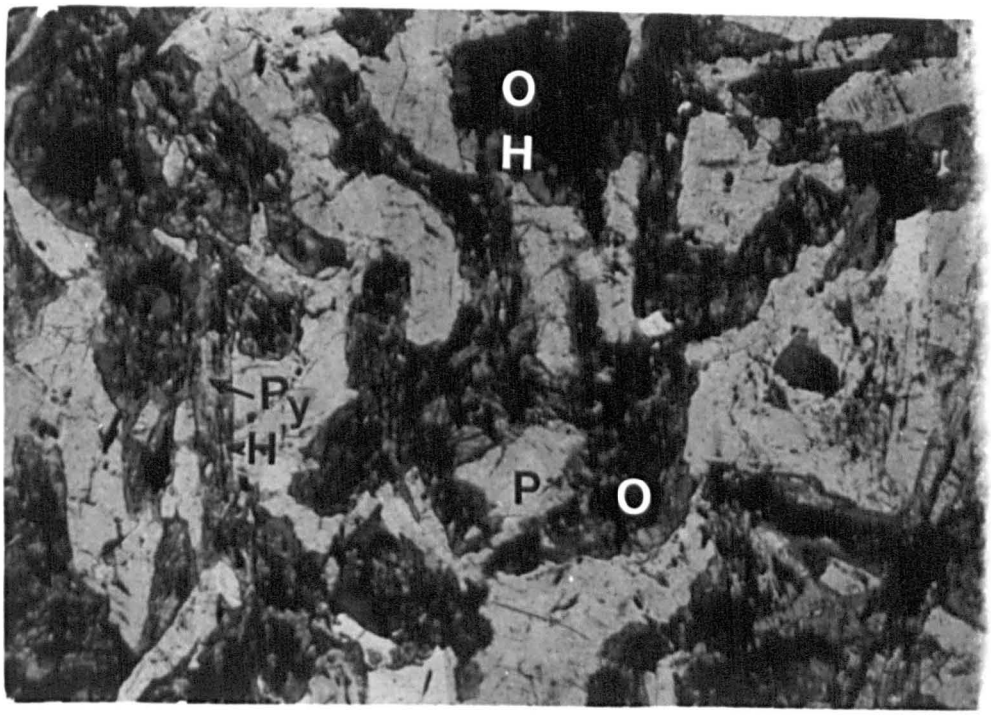
O
H
Py
H'
P
O

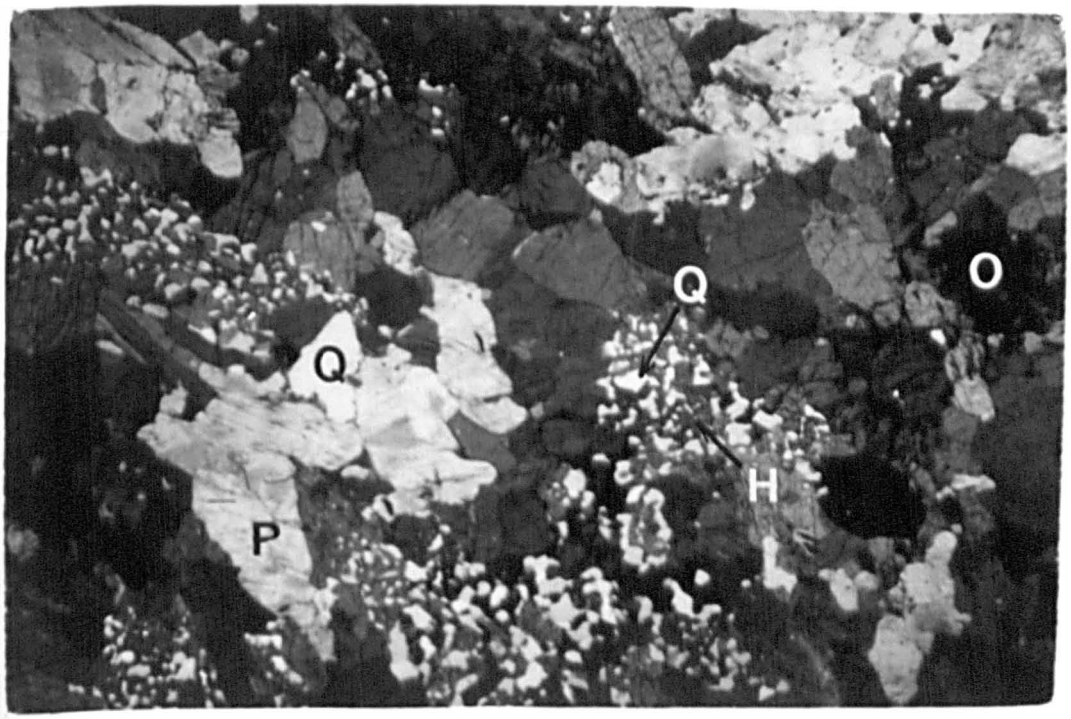
Q
O
Q
H
P

(Pl. V-1b): at one place hornblende-quartz intergrowth texture is present which has been interpreted as the old site of pyroxene and at another place hornblende crystallisation is at an advanced stage around iron ore, where there is a reduction of iron ore and an increase in hornblende percentage compared with stage 1.

These two different types of hornblende (i.e. one intergrows with quartz and the second crystallises around iron ore) suggest two different methods of hornblende formation, the former by the break-down of pyroxene into hornblende and quartz and the latter by its crystallisation at a completely new site probably by the greater migration of ions at new sites.

(c) Stage 3. In the thoroughly deformed parts of the same dyke and also in the dykes elsewhere in the area, the hornblende is of idioblastic to subidioblastic habit, usually compact or containing only a few quartz inclusions (Pl. V-2). Generally quartz inclusions are more spherical than they are in stage b, suggesting low energy and stable form (Spry, 1969, p. 170). The transformation of pyroxene to hornblende through an intermediate stage with hornblende-quartz intergrowth texture of similar type has also been recorded from the northern part of the Lewisian (Beach, 1974).

The hornblende is of green colour, along the Z-vibration direction, in the first stage and it is bluish-green in the later two, probably indicating some difference in its composition. Sheared dykes produced avenues for the fluid movements, while fluid activity was difficult in the undeformed portion due to which probably the later stage hornblende has a higher H_2O content and a higher Fe^{+3}/Fe^{+2} ratio than in the undeformed portion and is bluish-green (Seitsaari, 1953). The bluish-green colour of hornblende along the Z-vibration direction, is also

Plate V-2. Photomicrograph of a dyke with a well-developed S_1 shape fabric and very strong recrystallisation. The hornblende bc-crystal plane is oriented parallel to the shape-fabric foliation which is parallel to the longer edge of the photomicrograph with most of the basal sections oriented in the plane of slide. H = hornblende, P = plagioclase, B = biotite, Q = quartz (plane polarised light. x20).

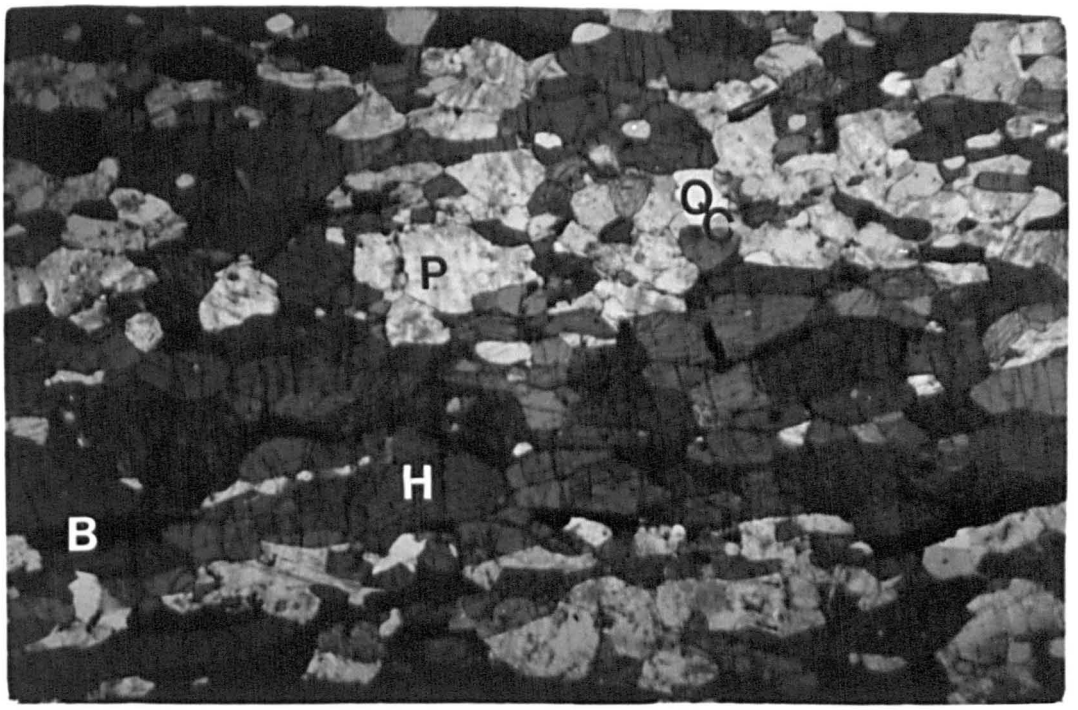
Qc
P
H
B

indicative of low-grade amphibolite facies metamorphism (Miyashiro,1973, pp. 254-300).

Destruction of pyroxene and crystallisation of hornblende in all the deformed dykes emphasises thatthe differential movements are essential agents for the conversion of higher grade minerals into lower grade minerals (Knopf, 1931). On the other hand, Barth (1931), Schwartz and Todd (1941) and Beach (1974) argued that the presence of a fluid phase and its ability to permeate the rock are primary requisites for retrogression. Heimlich (1974) in his work on the retrograde metamorphism of amphibolites of the Bighorn Mountains, Wyoming, argued that the retrograde metamorphism was facilitated by the combined action of fluids and the shearing stress. Sutton and Watson (1969) have also recognised a very close connection between the amount of re-crystallisation and the amount of deformation in the Laxfordian metamorphism of the Lewisian rocks of the mainland, specially in the southern parts.

Plagioclase is of lath shaped habit in the undeformed pod, while it is of xenoblastic habit in the deformed rocks. Its composition has also been affected. It is on the andesine-labradorite (An 50%) boundary in the undeformed dykes while it is of oligoclase-andesine composition (An 25% to An 44%) in the deformed dykes. The liberated Ca may be incorporated in the crystallisation of epidote, apatite or sphene, or it may have been partially removed from the system. Amphibolitization of pyroxene is usually accompanied by a reduction of the An contents of the plagioclase (Sills, 1983). However, it is difficult to explain such a large variation in the plagioclase composition. This variation may be related to the deformation, because deformation facilitates the crystallisation and recrystallisation, but changes in composition cannot be satisfactorily correlated with variations in deformation on the map scale (e.g. with the strain maps, chapter IV). A second possibility is

that probably, because there is a compositional difference between plagioclases related to the S_1 and S_2 fabrics respectively (see Fig. II-1). In places S_1 fabric have been transposed into S_2 and because both are of nearly the same type, it is difficult to differentiate between them. Therefore the compositional variation might be produced by the mixing of the two fabrics. A third possibility is that the variation could be simply a reflection of differences in whole rock chemistry.

Biotite is present in variable quantities in the dykes. In some dykes it is present throughout their width while it may be completely absent in others. Again in some dykes it is present only at the dyke margins adjacent to gneisses of acid and intermediate composition. Its presence only at the dyke margins, in some cases, if not in all, indicates influx of K^+ from the surrounding gneisses. It is mainly brown in colour, but green biotite is also present.

2. Metamorphism of the Gneisses

It has already been mentioned that it is difficult to distinguish between the mineral assemblage of this metamorphic episode and that of the Inverian metamorphism. However, the mineral assemblage present in the gneisses also indicates amphibolite facies metamorphism, confirming the evidence from the mineral assemblage in the dykes. The mineral assemblages in the gneisses are:

(1) Plagioclase (An 19% - An 31%) + Quartz + Biotite ± Hornblende ± Epidote ± Microcline ± Sphene ± Apatite ± Iron ore.

(2) Microcline + Plagioclase (An 22% - An 34%) + Quartz + Muscovite ± Biotite ± Epidote.

The mineral characteristics have been described in chapter II.

C. M_2 METAMORPHISM

The mineral paragenesis of this metamorphic episode has been established by studying the mineral relationships with the microscopic folds and the mineral assemblage in the S_2 fabric.

The mineral assemblage of this metamorphic episode is the same (with the exception of a possible change in the plagioclase composition, see. Fig. II-1) as that of M_1, indicating a similar grade of amphibolite-facies metamorphism. Under the microscope minerals are seen to be unstrained in fold closures and platy minerals are oriented parallel to the axial plane of the folds. In most of the thin sections of dykes containing fold closures, hornblende needles are oriented parallel to the fold axes, therefore only the basal section is parallel to the slide, and usually the bc-crystal plane of the hornblende grain is parallel to the fold axial plane (Pl. V-3) indicating a syntectonic re-crystallisation. Biotite is crystallised strongly parallel to the axial planes of the folds, and plagioclase is unstrained in the fold closures, both of which suggest recrystallisation during this metamorphic episode. Chains of sphene grains are present mainly parallel to the S_1 foliation but in F_2 fold closures small chains of sphene crystals are present parallel to their axial surface (Pl. V-4a) suggesting syntectonic recrystallisation of sphene in M_2.

D. POST-M_2 MINERAL CHANGES

Although post-M_2 mineral alteration is not extensive, it is a widespread phenomenon. Many minerals which were stable in amphibolite-facies metamorphic conditions have been broken down into minerals which were stable in low temperature and low pressure environments. Some of the late phase minerals with their possible mode of formation are discussed in this section.

Plate V-3. A microscopic F_2 fold in dyke with bc-crystal planes of most of the hornblende oriented parallel to the fold's axial plane and their c-axes parallel to the fold axis (plane polarised light. x10).

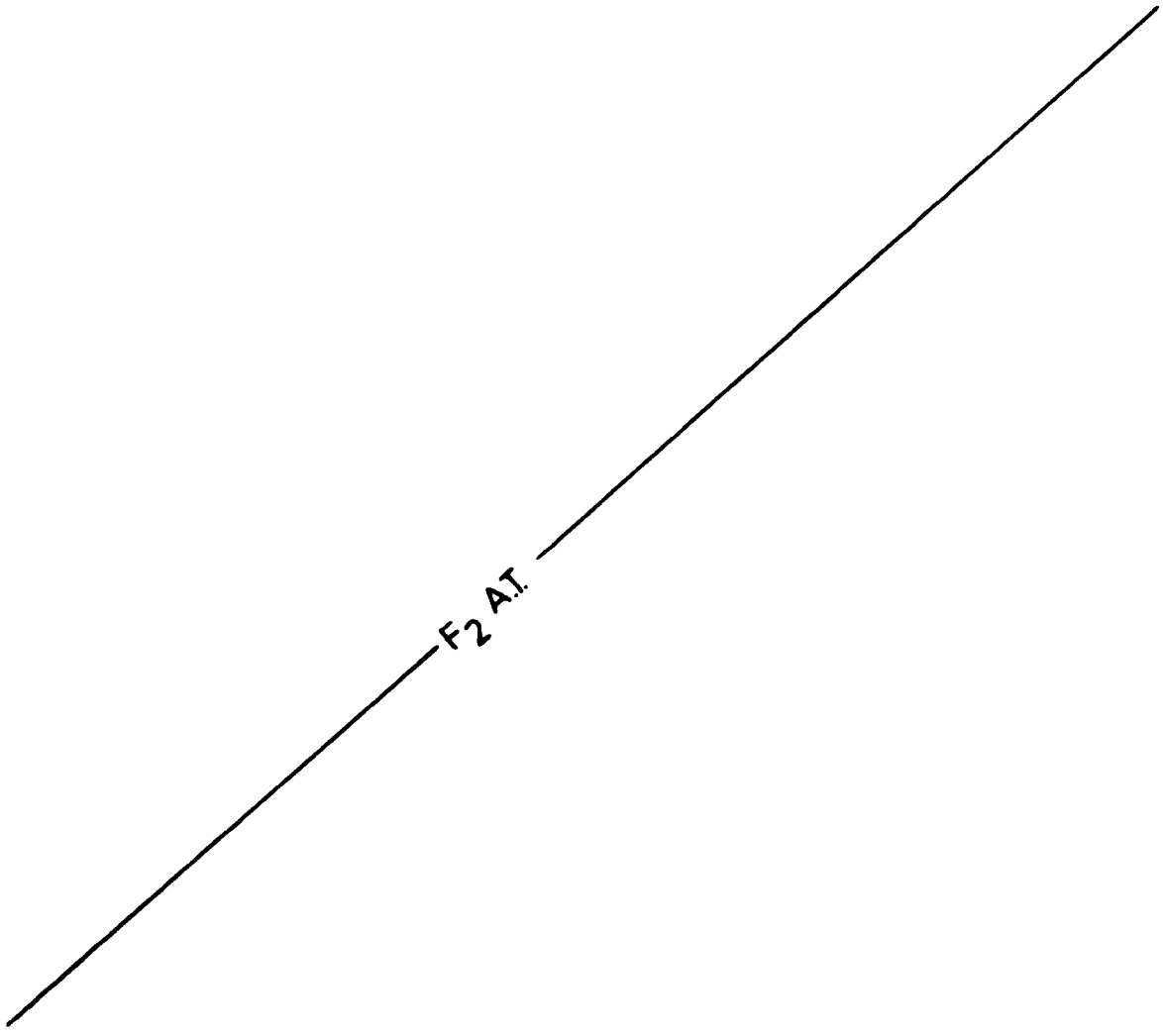
F_2 A.T.

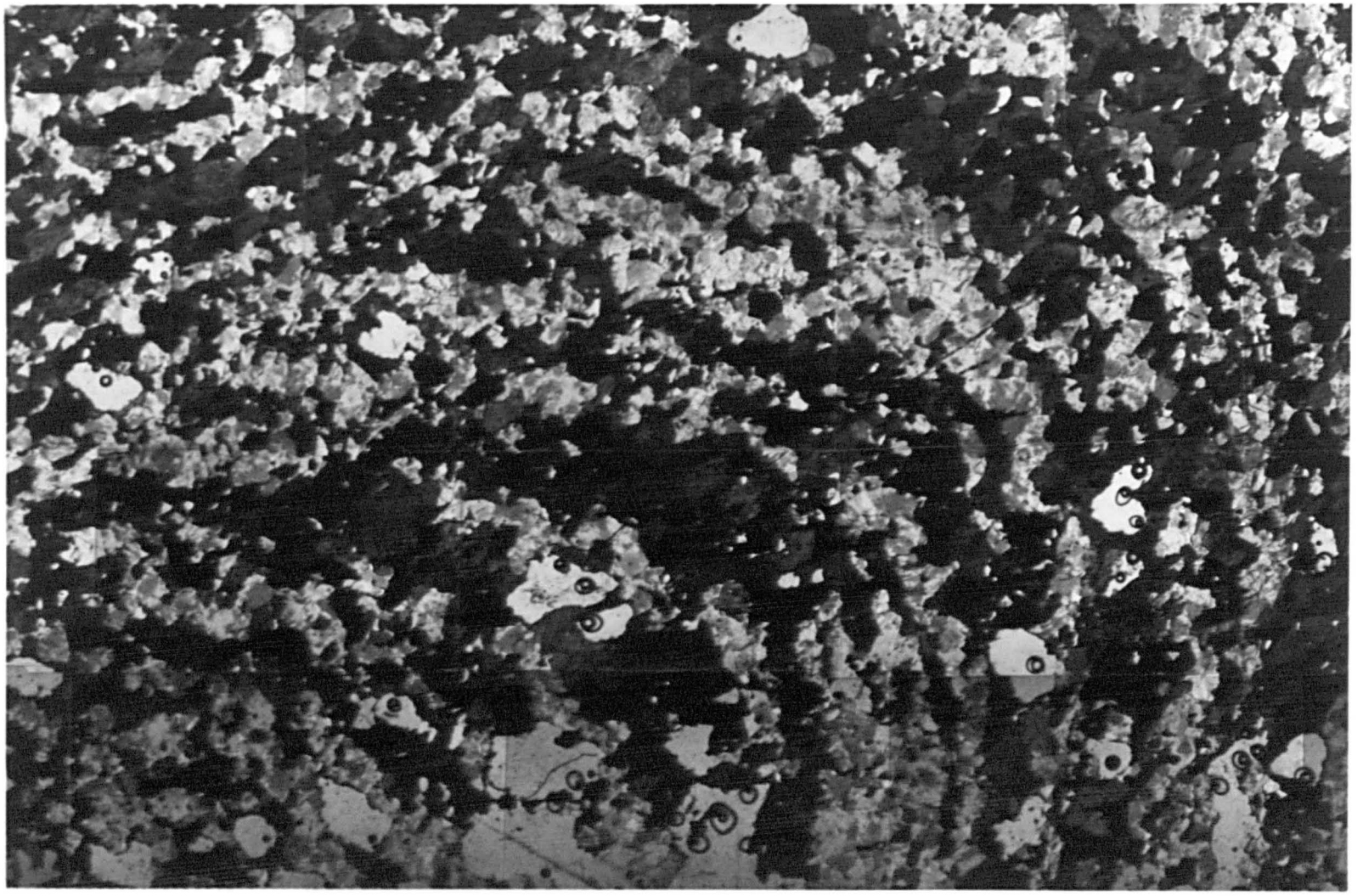

F2 AT

Plate V-4a. S_1 in the dyke has been folded into F_2 fold. The chains of sphene grains are partly oriented parallel to the fold axial surface which is dipping towards right in the photomicrograph. H = hornblende, P = plagioclase, Q = quartz, B = biotite (plane polarised light. x20).

Plate V-4b. Replacement of biotite by epidote in the Granodioritic gneiss. Isolated islands of biotite can be seen within the epidote grains which are optically continuous with the biotite grains still preserved. Biotite is also quite chloritized. P = plagioclase, B = biotite, E = epidote, Q = quartz (plane polarised light. x40).

F_2 A.T.

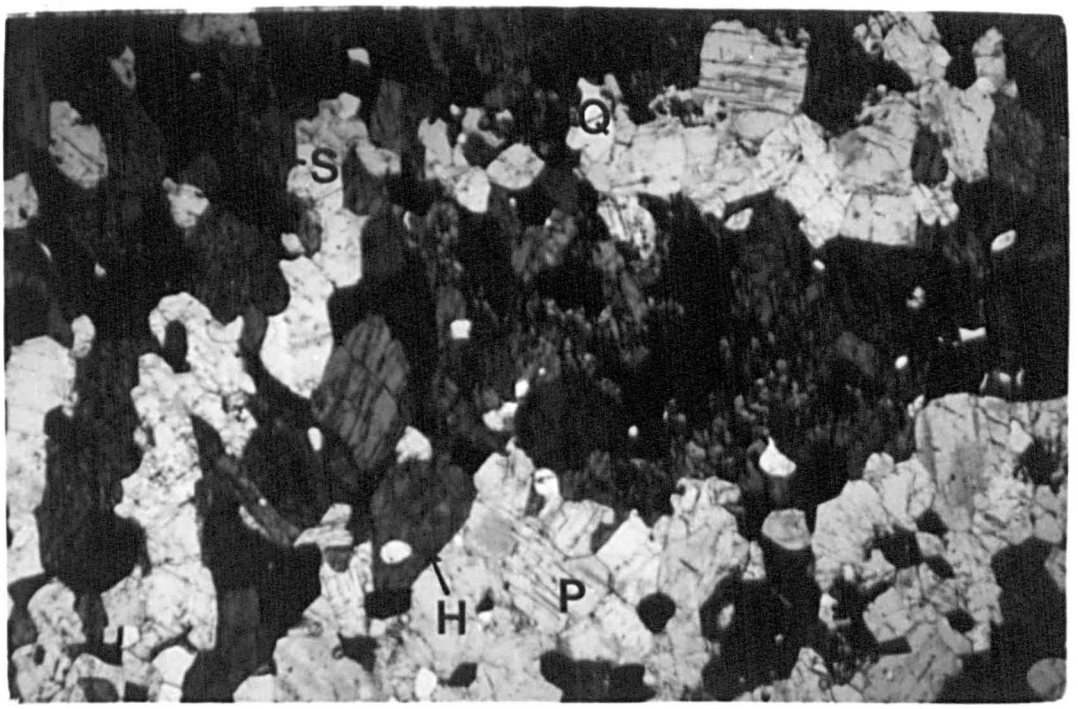
S
Q
H
P

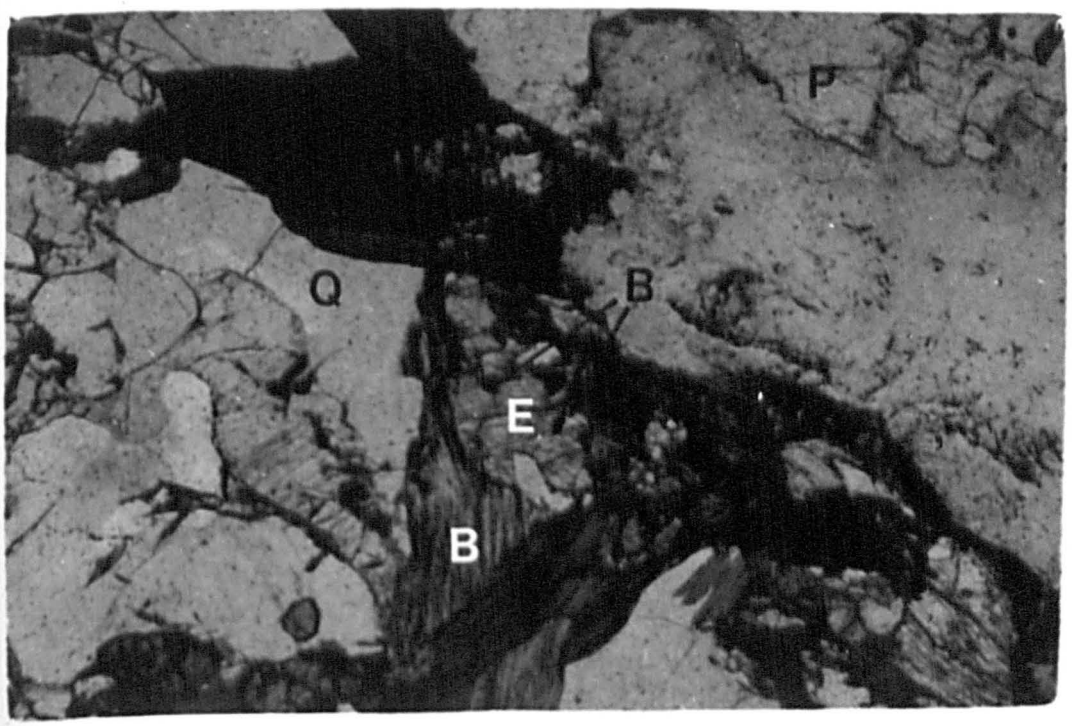
P
Q
B
E
B

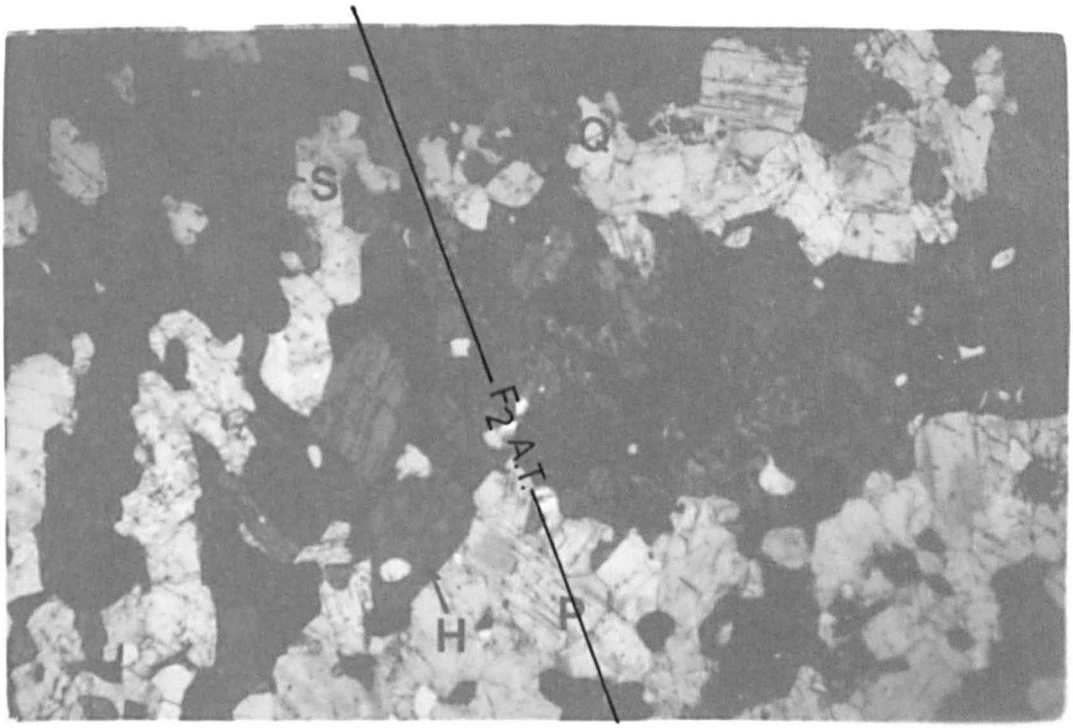
S
Q
F2 A.T.
H
P

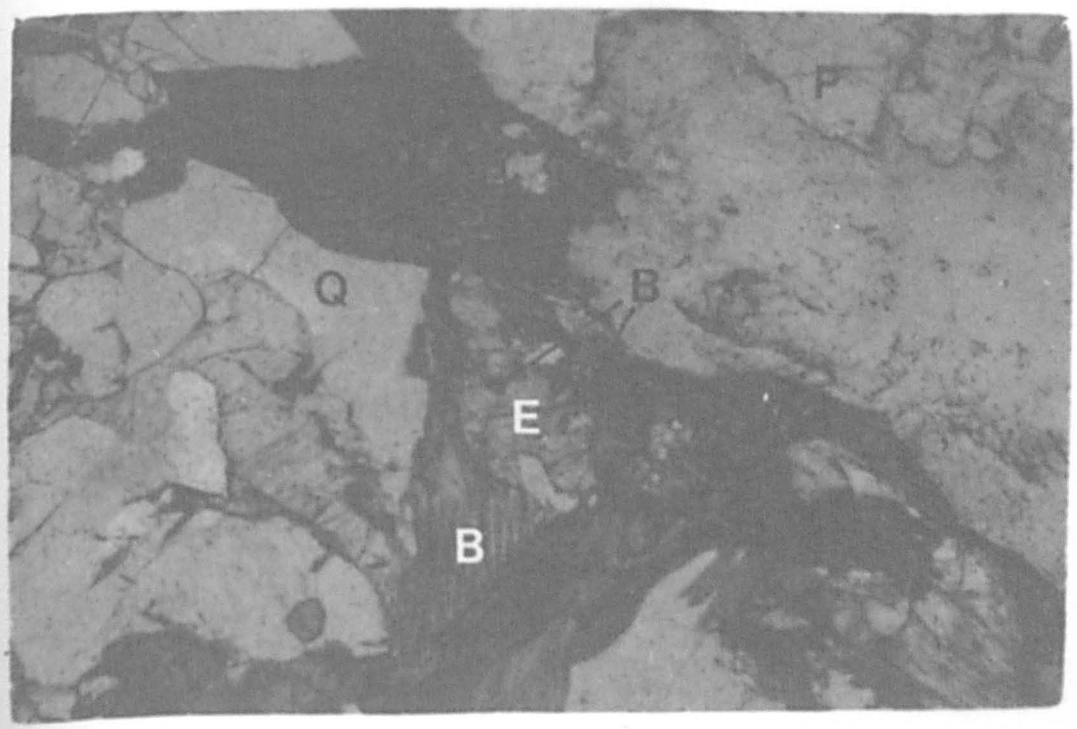
P
Q
B
E
B

Epidote is a common late phase mineral, although there is no doubt that some of it was crystallised in the amphibolite-facies metamorphism. In some instances it is difficult to distinguish the epidote which crystallised during M_1 from that formed in M_2 or in post-M_2 recrystallisation.

In gneisses of acid and intermediate composition epidote is idioblastic to subidioblastic in habit and is usually slightly pleochroic. It is usually associated with biotite and in many places it is evident from textural relations that it replaces the biotite (Pl. V-4b). Replacement of biotite by epidote was also observed by Field and Rodwell (1968). The source of CaAl is not obvious, but it has been suggested that plagioclase may lose these elements during sericitization and the source of iron could be biotite.

In the dykes as well, the epidote is probably of more than one generation. The post-M_2 crystallisation is associated with chlorite + quartz ± albite ± sphene ± iron ore. These minerals are present in small isolated groups (Pl. V-5a) at the contact of hornblende and plagioclase. The textural relations indicate that the above mentioned mineral assemblage is the result of reaction between hornblende and plagioclase, probably in static conditions, as suggested by the presence of acicular radiating chlorite crystals, in which individual crystals are growing across the foliation.

A third type of textural relationship shown by epidote has been observed in some of the early amphibolites. Here usually idioblastic to subidioblastic, slightly pheochroic epidote grains are present at the contact of hornblende and plagioclase with a symplectitic intergrowth with quartz (Pl. V-5b). Since plagioclase is higher in SiO_2 than epidote, the breakdown of plagioclase into epidote probably releases some silica.

Plate V-5a. Crystallisation of low grade epidote and chlorite derived from the reaction of hornblende and plagioclase in the dyke. H = hornblende, P = plagioclase, Q = quartz, E = epidote, Ch = chlorite, S = sphene. Plagioclase is strongly sericitized. S_1 foliation is dipping towards the right at about 45^{o} (crossed nicols. x40).

Plate V-5b. Growth of epidote-quartz symplectite due to the reaction between hornblende and plagioclase in an early basic body. H = hornblende, P = plagioclase, E = epidote, Q = quartz (plane polarised light. x40).

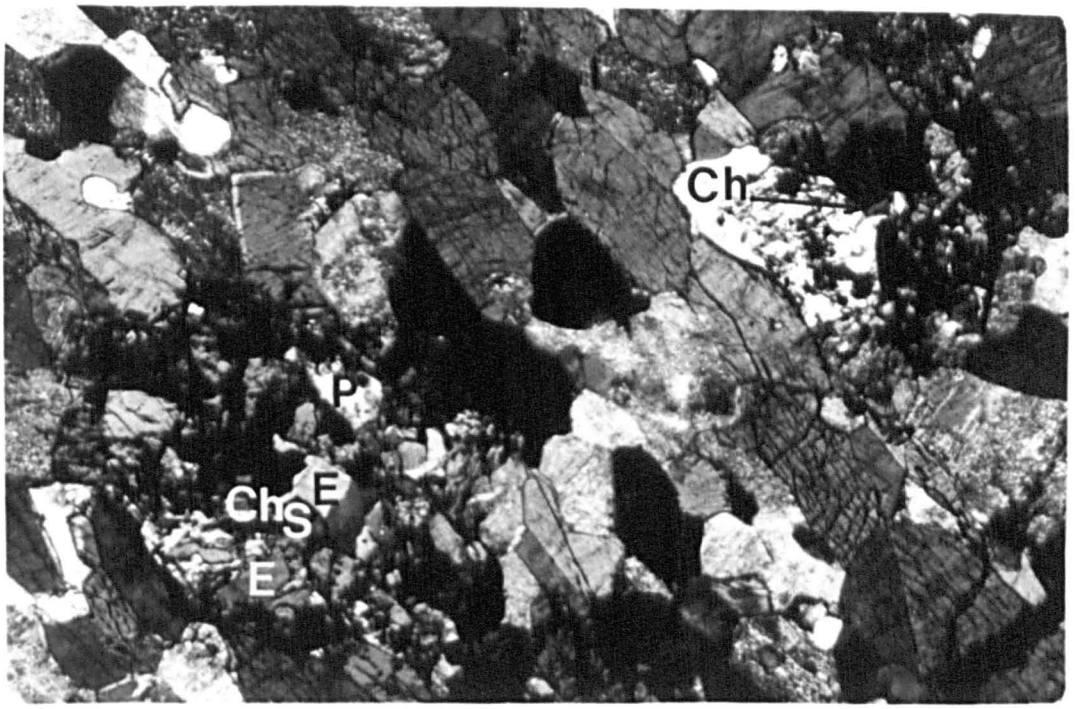
Ch
P
Ch
S
E
E

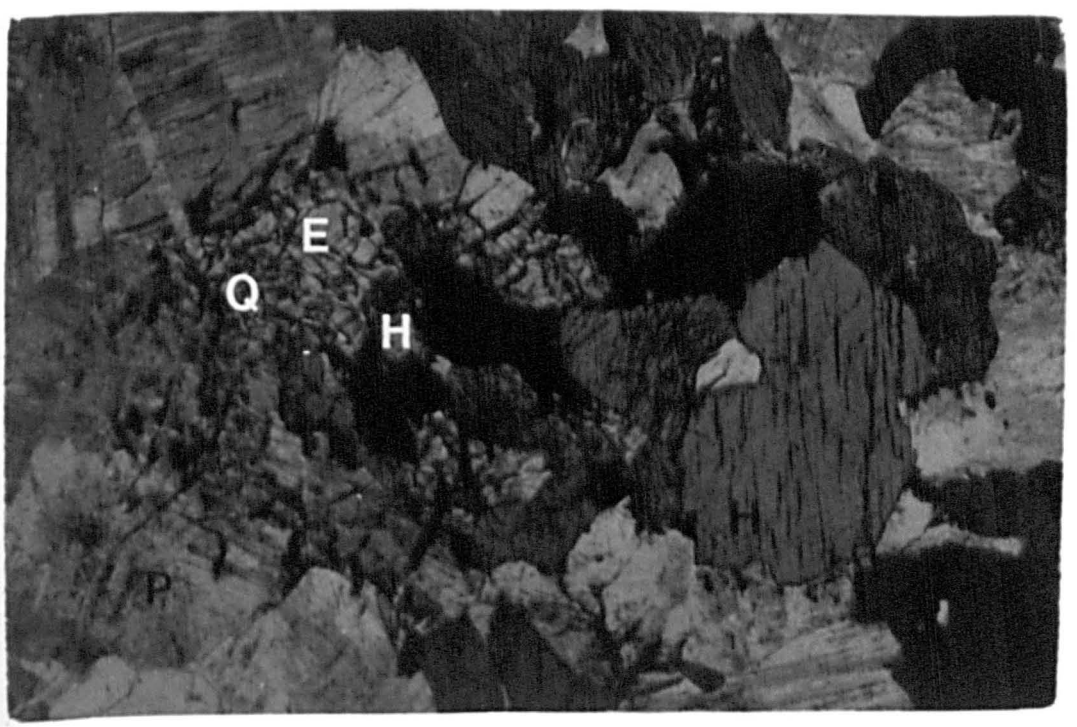
E
Q
H
P

Chloritization is a widespread phenomenon throughout the inlier. Many of the varieties of chlorite present have been described in Chapter II. It commonly replaces biotite and hornblende. Chlorite flakes grow much more easily along the basal cleavage of biotite, where it replaces the biotite. Consequently at many places interlayered chlorite and biotite are present. Where complete chlorite flakes occur, it is not easy to decide whether biotite has been completely changed into chlorite or chlorite has been crystallised at a new site. It is certainly a late stage mineral where it crystallises along with quartz ± albite ± sphene as discussed before. It is also present in fractures where probably it is of hydrothermal origin.

Prehnite and Pumpellyite although not widespread minerals, occur in some of the rocks. Since they have the same mode of growth and have a close paragenetic relationship, they are discussed together.

They occur as acicular crystals in lens-shaped aggregates, associated with biotite. The major axes of these lenses are parallel to the basal cleavage of the biotite flakes and the individual crystals grow from the core of the lens in such a way that they are subparallel or make a low angle with the lens boundary near their major axes (Pl.V-6ab). This lens-shaped form is probably due to the faster growth of acicular crystals along the biotite basal cleavage i.e. because of greater ease of crystallisation. These acicular crystals are usually curved giving them undulatory extinction. Prehnite is a colourless mineral while pumpellyite is strongly pleochroic from nearly colourless to yellowish-green or green.

These are secondary minerals and have been formed by the breakdown of other minerals. To understand their genesis it is important to note the following characteristics of the minerals themselves and of the host rock.

Plate V-6a. Pumpellyite crystals in radiating form within biotite. Biotite is still preserved on the margins. Pum = pumpellyite, B = biotite, H = hornblende, P = plagioclase, E = epidote. Section is cut parallel to the foliation (plane polarised light. x65).

Plate V-6b. Growth of pumpellyite crystals in sheaf form within biotite. H = hornblende, P = plagioclase, B = biotite, P = pumpellyite. Section is cut perpendicular to the lineation of LS shape fabric (crossed nicols. x50).

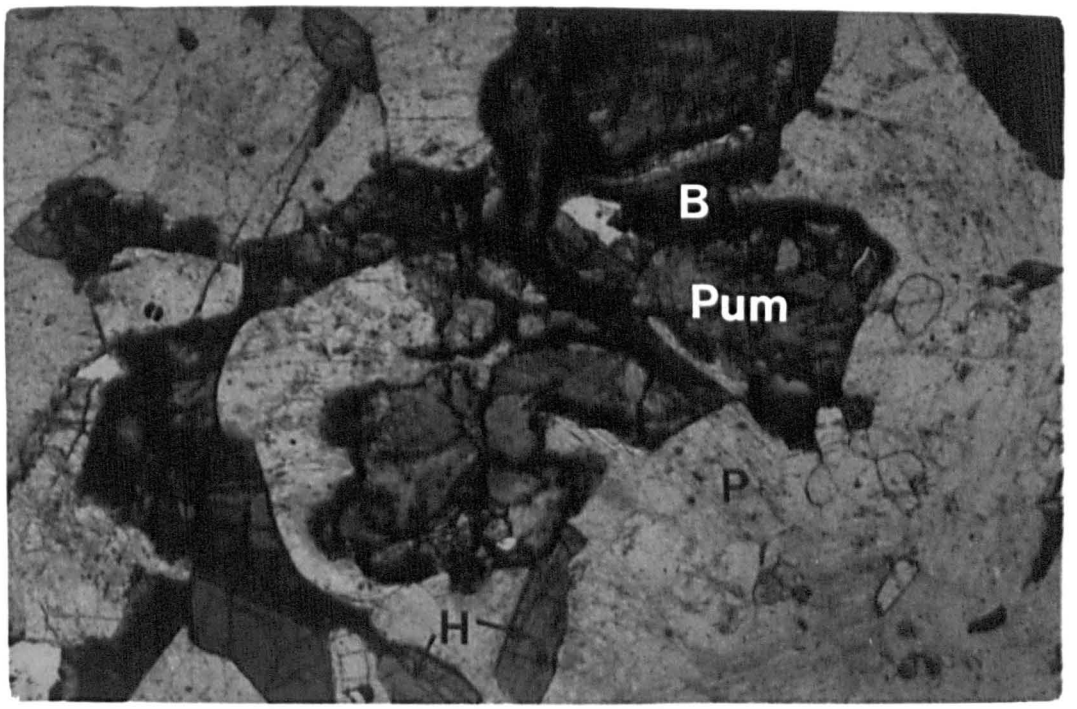
B
Pum
P
H

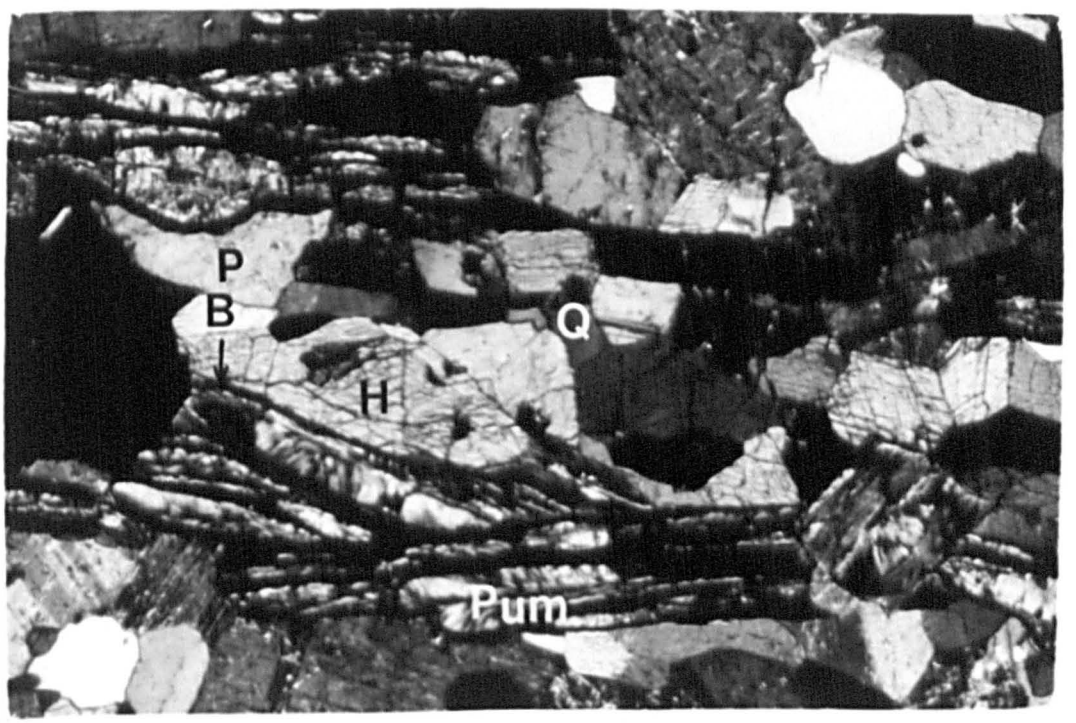
P
B
Q
H
Pum

1) These minerals have been formed within the biotite flakes in the amphibolites, while they do not occur in the biotite of the acid and intermediate rocks.
2) There is a direct correlation between the crystallisation of prehnite and pumpellyite and the alteration of the host rock. In amphibolites where alteration of other minerals is not pronounced, prehnite and pumpellyite have not been formed.
3) Where plagioclase and hornblende in the amphibolites have been altered, that is plagioclase has formed sericite and hornblende has lost its colour due to the depletion of certain elements, but biotite is not present, then prehnite and pumpellyite do not occur.
4) Biotite flakes which contain prehnite or pumpellyite lenses have been variably altered, but the alteration material is so fine that it cannot be identified under the petrographic microscope.
5) Chlorite is found only rarely adjacent to those biotite flakes where pumpellyite occurs and is invariably absent when prehnite occurs.

From the form of prehnite and pumpellyite and their association with biotite it is clear that these minerals are of secondary origin. The needle like crystals appear to have pushed biotite flakes forcibly in the middle part of the lens to cause bending in the biotite which indicates a secondary origin (Phillips and Rickwood, 1975). The compositional contrast between the biotite on the one hand and the prehnite and pumpellyite on the other suggests the addition of Ca^{+2} along the basal cleavage of the biotite while their forcible introduction into the biotite flakes indicates an increase in the total volume, thus

eliminating any suggestion of crystallisation by metasomatic replacement of K $(Mg, Fe)_3$ in the biotite by$(Ca_2 Al)$, which would result in a net decrease in volume (Schwartz, 1958).

Therefore it has been concluded that for the nucleation of the prehnite and pumpellyite, the presence of any suitable mineral is of prime importance, as suggested by Schwartz (1958) and Field and Rodwell (1968). However, in the crystallisation of prehnite along biotite flakes, the two minerals have no chemical relationship because crystallisation of prehnite has also been observed along graphite cleavage (Field and Rodwell, op. cit.).

Plagioclase has been suggested as the source of Ca Al by Field and Rodwell; Phillips and Rickwood, Tulloch(1979), and Phillips and Griffin (1981). On the other hand, hornblende has been suggested as the source by Hall (1965) and Moore (1976). In the Kenmore inlier, characteristics 1 - 4 above suggest hornblende as the source of Ca Al for the crystallisation of prehnite and pumpellyite.

Heulandite occurs in the form of veins in many types of rock. It occurs in the form of sheaf-like aggregates of tabular crystals (Pl. V-7a) which is its characteristic form (Kerr, 1959, p.292). Only rarely it has been observed crystallising along the basal cleavage of a platy mineral (Pl. V-7b) and there it is still in sheaf-like aggregates in which individual crystals are at a high angle to the basal cleavage and the aggregates are lens-shaped. The individual crystals appear to have grown by pushing aside the flakes of the platy mineral as is evident by the bending of the flakes around the lens-shaped aggregates.

The occurrence of heulandite in fractures suggests its crystallisation at upper levels of the crust where the rocks were behaving in a brittle way.

Plate V-7a. Sheaf like heulandite crystals are present in a hornblende dyke. H = hornblende, Heu = heulandite, Q = quartz (crossed nicols. x65).

Plate V-7b. Growth of heulandite crystals inside an unidentified platy mineral along the basal cleavage in a granodioritic gneiss. P = plagioclase, Q = quartz, Heu = heulandite, U = unidentified mineral. Plagioclase is highly altered (plane polarised light. x30).


H
H
Q
Heu

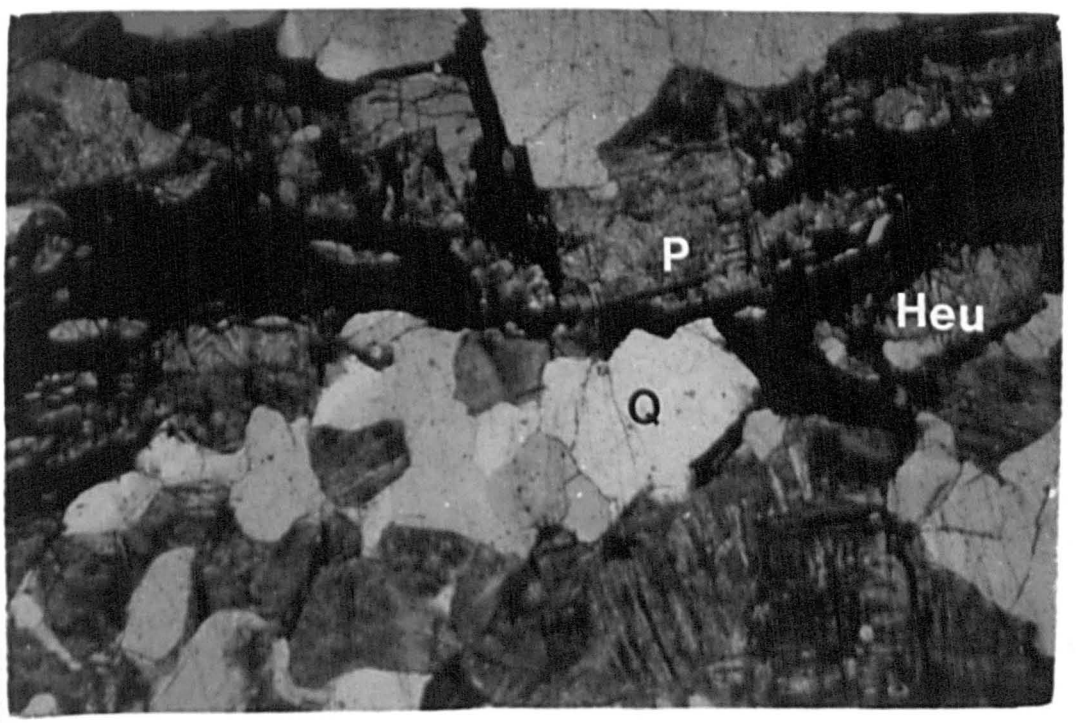
P
Heu
Q

E. THE RELATIONSHIP BETWEEN DEFORMATION AND METAMORPHISM

Using criteria described by Turner (1981, pp.457-459), a broad relationship has been established between the deformational episodes affecting the rocks in the area and the various metamorphic episodes responsible for the crystallisation and recrystallisation of the minerals. These relationships have been established using thin sections of the rocks containing structures of microscopic scale.

The M_1 metamorphism took place synchronously with the D_1 deformation. This can be easily demonstrated in the Scourie dykes because these are the first episodes of deformation and metamorphism to affect them and the S_1 fabric is the most widespread. On the other hand,it is difficult to differentiate D_1 and M_1 from the pre-Laxfordian deformation and metamorphism of the gneisses, partly because of the lack of F_1 folds and partly because both metamorphic episodes were of the same grade.

The hornblende in the S_1 fabric of the dykes is usually oriented to give a good planar fabric. Generally the bc-crystallographic plane lies parallel to the shape fabric foliation with the c-axis oriented statistically parallel to the shape fabric lineation (Pl.V-2). In sections cut across the lineation of LS-shape fabric, plagioclase usually has a granulitic fabric, while in thin section cut across the LS-shape fabric parallel to the lineation plagioclase grains are somewhat inequidimensional with the longer axes parallel to the lineation. This is true for the gneisses as well. However, there is not much difference in the shape of the plagioclase grains in differently oriented thin sections. Biotite flakes show much stronger preferred orientation in thin sections cut across the LS-shape fabric along the shape fabric lineation. On the other hand, there are

variations in biotite orientation in thin sections cut across the shape fabric lineation, from good parallel orientation to one where the biotite flakes intersect each other along an axis parallel to the shape fabric lineation. All the above evidence indicates syntectonic crystallisation and recrystallisation of minerals and that M_1 was broadly synchronous with the first deformation.

In all the thin sections of microscopic F_2 fold closures that have been examined, the minerals are unstrained. Usually in thin sections cut perpendicular to the fold axes and hence perpendicular to the lineation of the LS fabric, where the hornblende grains have their basal sections parallel to the slide, it has been found that their bc-crystal planes are somewhat parallel to the axial plane of the folds (Pl. V-3). Plagioclase and quartz, on the other hand, show strong granoblastic fabric in thin sections cut perpendicular to the fold axes and are unstrained both in the dykes and in the gneisses. Biotite has crystallised parallel to the fold axial planes giving the S_2 fabric. The evidence thus suggests a syntectonic crystallisation in which M_2 was syntectonic with D_2. On the basis of the mineral assemblage it has been suggested that M_2 was approximately the same grade as M_1.

During the D_3 deformation, quartz appears to have behaved more plastically than plagioclase and hornblende, and deformation bands in quartz were formed parallel to the axial plane of F_3 folds. Slip along the basal plane of the biotite and pre-F_3 chlorite flakes produced kinking. Part of the low-grade mineral recrystallisation referred to below may have taken place during this deformation.

Although the post-M_2 retrogressive mineral changes are not extensive, they have been observed in all types of rock present. Biotite and hornblende have been variably replaced by chlorite and the chloritisation is most widespread where rocks are fractured. Crystallisation of the

prehnite and the pumpellyite is also suggested as post-M_2 because of the way in which acicular crystals grow across the foliation. Veins filled with epidote, chlorite, prehnite and zeolite are also post-M_2. Some of these minerals could be post-Laxfordian and of hydrothermal origin.

CHAPTER VI

DEFORMATIONAL HISTORY AND MECHANISM

A. D_1 DEFORMATION

It is clear from the previous chapter (see Chapter IV) and is further argued later in this chapter that the complex strain pattern in the dykes cannot be explained by the D_2 and D_3 deformations alone but must be due to the superimposition of these deformations upon a very heterogeneous pre-existing strain pattern, locally involving very large strains, developed during the first Laxfordian deformation, D_1. It is therefore suggested that the first Laxfordian deformation produced sub-vertical shear zones (Fig. VI-1a). The shape fabric lineation is roughly parallel to the greatest extension "X" in the LS-fabric plane, which indicates the transport direction in the shear-zones (Bridgwater et al., 1973). The shape fabric lineation is subhorizontal and oriented NW-SE in the Kenmore inlier and the foliation or plane containing the LS-shape fabric represents the XY-plane of the strain ellipsoid. In the Kenmore inlier it is not possible to decide whether the sense of movement is right-lateral or left-lateral, because offset of bands or drag in the gneisses have not been recognised.

In the Diabaig inlier, the lineation is much more variable. It plunges at moderate to low angles to the ENE in the northern part of the inlier, while in the southern part it plunges towards the ESE at moderate to low angles. There is thus a swing in lineation direction from ENE to ESE in travelling from northeast to southwest (Fig. VI-2). In the strongly deformed area near the shore of Loch Torridon, and in some Laxfordian shear belts in the north, the Scourie dykes are completely concordant to the acid gneisses but in areas of low Laxfordian deformation, northeast-

Fig. VI-1a. FIRST DEFORMATION

The plane ABCDEF is the horizontal surface of the block. The heavily shaded area is the vertical front of the rocks in the block after deformation. The lightly shaded area is the upper surface of a plane which was subhorizontal before deformation and is now still subhorizontal in the Kenmore inlier but is sloping towards the right hand side (i.e. NE) in the Diabaig inlier after deformation. A line abcd which was straight before deformation is now curved a'b'c'd'. The LS_1 fabric is shown by the two small inset blocks.

Fig. VI-1b. SECOND DEFORMATION

Before the deformation the rocks were dipping at a high angle towards the NE. Due to subvertical stresses and tectonic transport to the NE they have been folded into subhorizontal folds with Z-type folds in the Diabaig inlier where deformation was comparatively low and into S-type asymmetric folds in the Kenmore inlier where rocks were strongly deformed. In the middle part which represents the position of Ardheslaig peninsula folds are M-type with subhorizontal axial planes.

Fig. VI-1c THIRD DEFORMATION

Subhorizontal NE-SW oriented stress (σ_1) folded the rocks in the Kenmore inlier, which were previously dipping at a low angle towards SW, into upright F_3 folds which are somewhat asymmetrical with enveloping surface dipping towards SW. The stresses were unable to fold the rocks in the Diabaig inlier where rocks were dipping at moderate to high angle towards the NE.

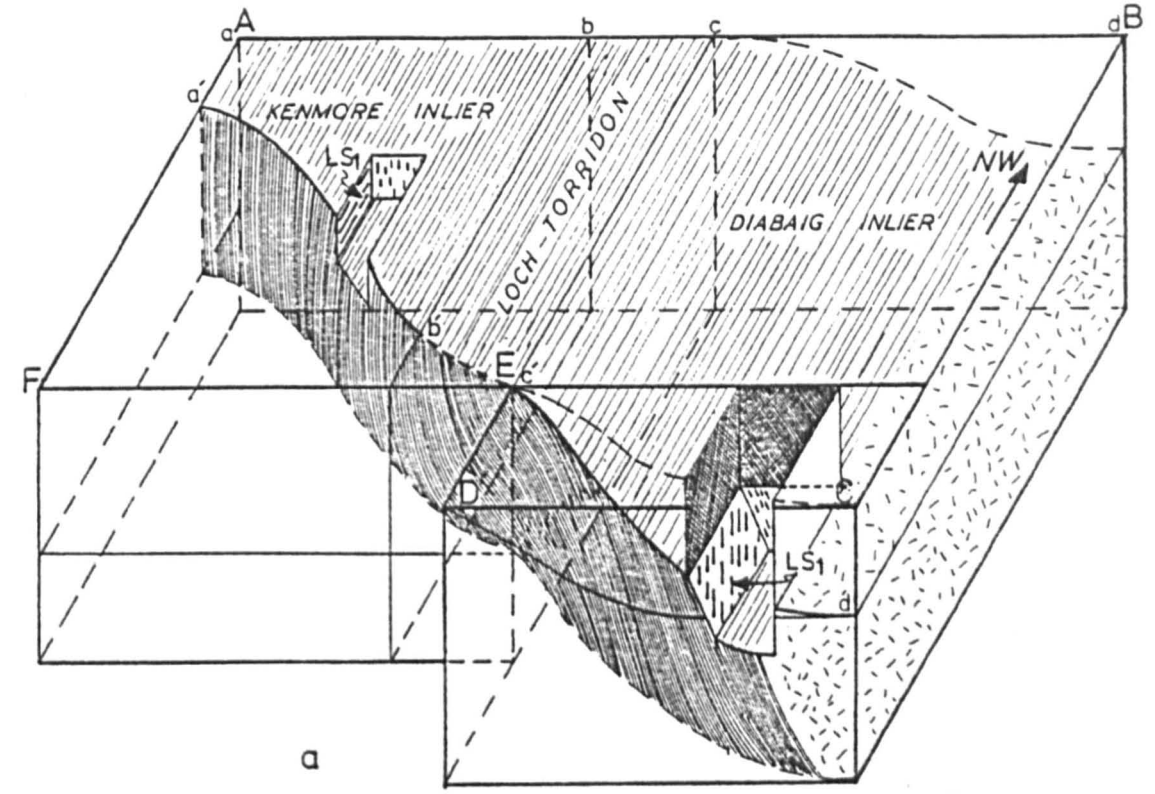
A
a
b
c
B
d
a'
KENMORE INLIER
LOCH-TORRIDON
DIABAIG INLIER
NW
LS1
b'
F
E
c'
D
C
LS1
d
a

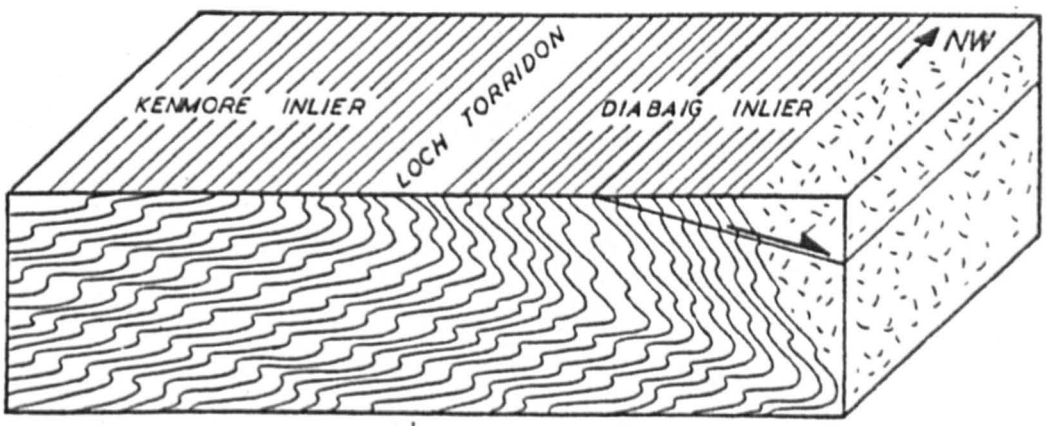
KENMORE INLIER
LOCH TORRIDON
DIABAIG INLIER
NW
b

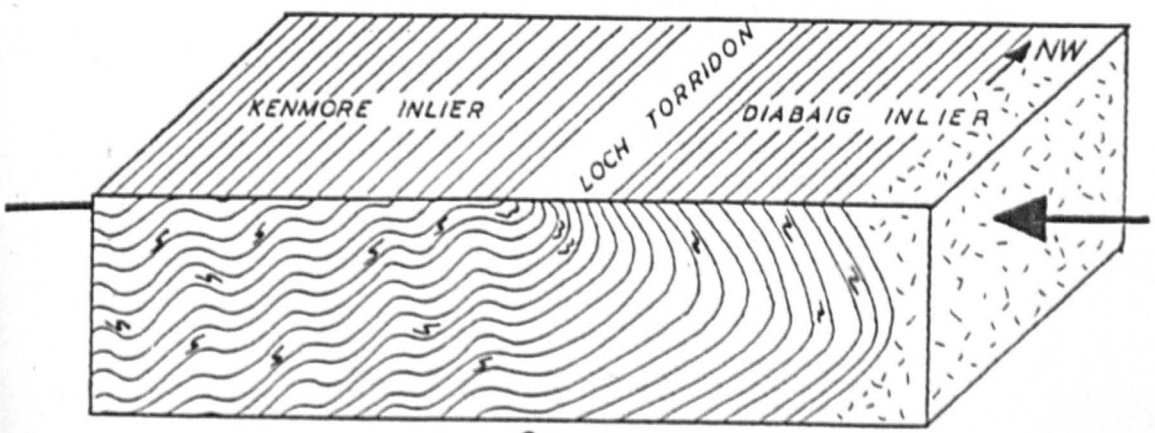
KENMORE INLIER
LOCH TORRIDON
DIABAIG INLIER
NW
c

Fig. VI-2a. Location of measurements of LS_1 shape fabric in the Diabaig inlier.

Fig. VI-2b. Equal area plot of the lineations in the Diabaig inlier. Numbers on the plot correspond to the position on the map in Fig. VI-2a.

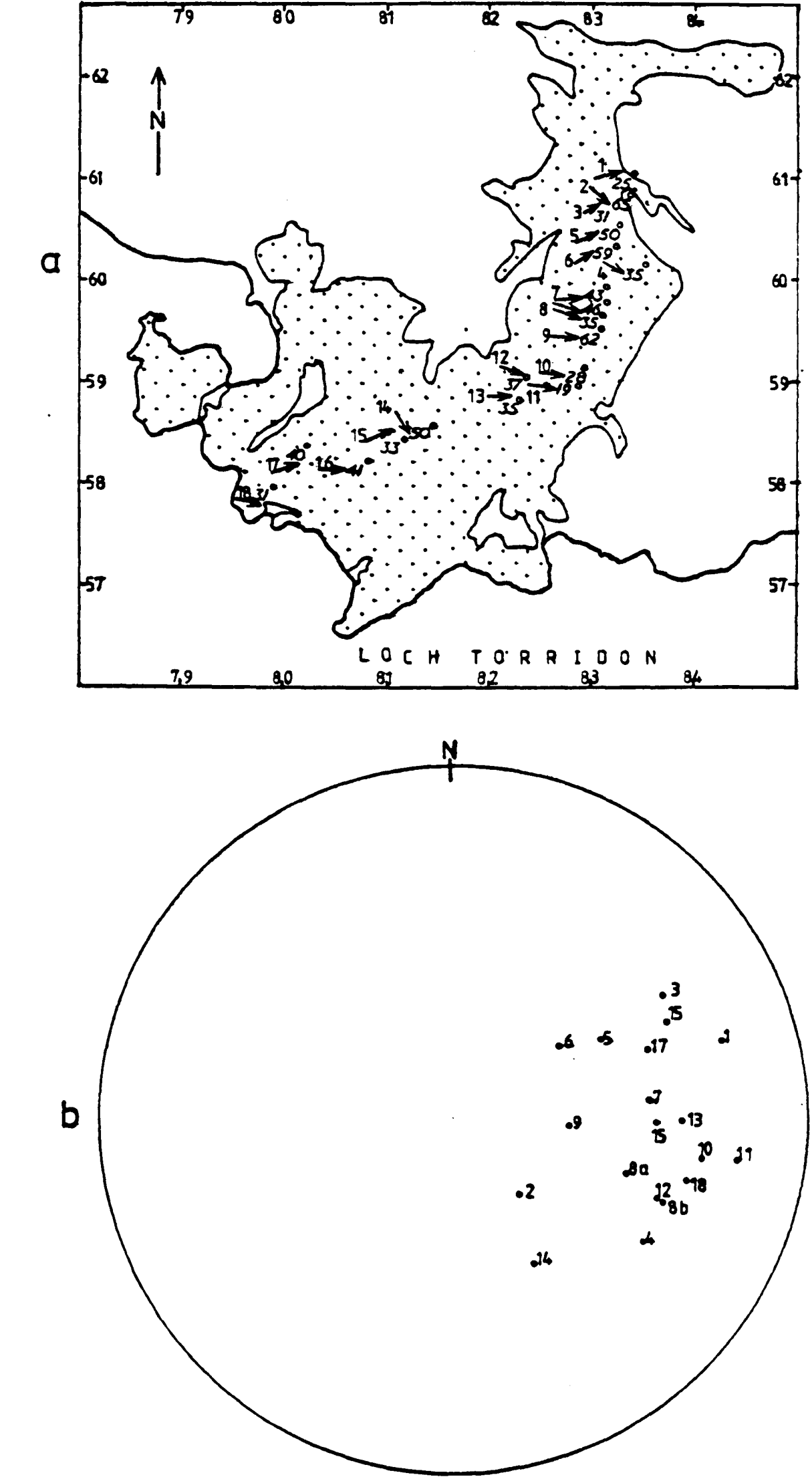
a
b
N
LOCH TORRIDON
7,9
8,0
8,1
8,2
8,3
8,4
57
58
59
60
61
62

oriented gneisses are at a high angle to the northwest-oriented dykes. In areas where dykes penetrate northeast-oriented gneisses, dykes and gneisses are often deformed in a narrow belt at their contact where there is a drag or differential movement in the gneisses from which the transport direction can be interpreted.

In the traverse across the Diabaig inlier, there are two places where drag in the gneisses along the narrow shear zones at the dyke-gneiss contacts shows right lateral movement (Fig. VI-3). Assuming that the shape fabric lineation shows the direction of movement (Bridgwater et al., op. cit.) then the plunge of the lineation indicates that a dip slip movement is also involved in the shear zones. From this evidence relating to the Diabaig inlier, right lateral movement is also suggested in the Kenmore inlier.

If the lineations in the Diabaig and Kenmore inliers are of the same age and belong primarily to the first deformation, variations in its attitude could either be original or modified in the south due to later deformations. If the attitude of lineations are only due to the first deformation, the various possibilities for this variation are discussed below.

As a first possibility the different attitude of lineations in the two areas could be due to the difference in the attitude of the regional stress ellipsoid across the area. However this possibility is not very likely because the two areas are not far apart, and at a depth where amphibolite-facies conditions prevail, the regional stresses should not vary greatly across such a distance.

A second possibility is that in the initial stages of deformation in Kenmore, the transport direction was like that now preserved in the northern part of the Diabaig inlier, i.e. with an oblique normal fault-

Fig. VI-3. Narrow shear-zones at dyke contacts in the Diabaig inlier showing transport directions. Deformation is concentrated only in narrow shear-zones at the contacts.

Grid Ref. for a = 83196105

Grid Ref. for b = 82035896

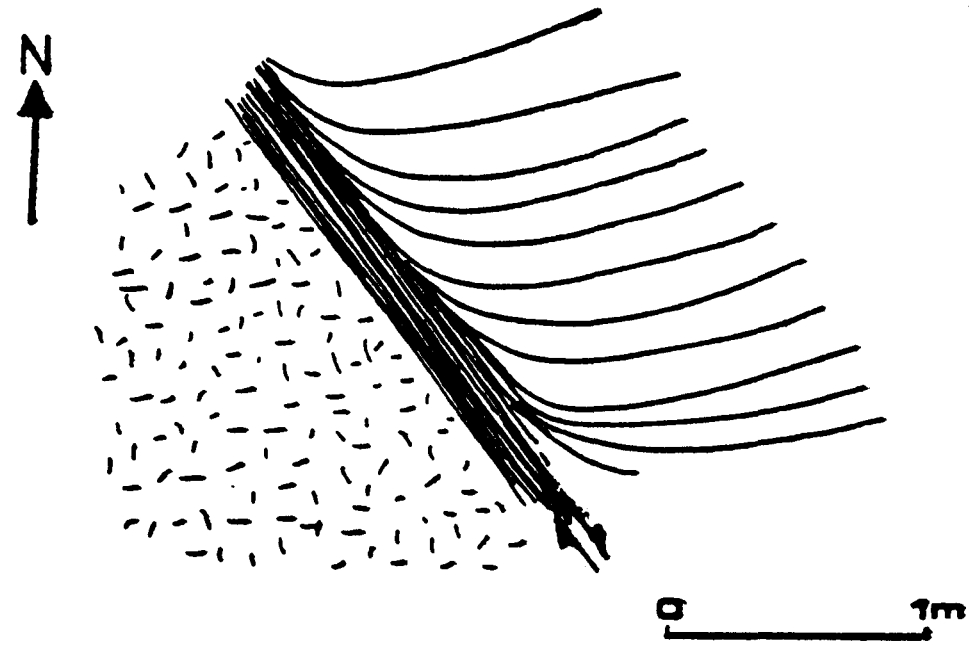
N
0
1m

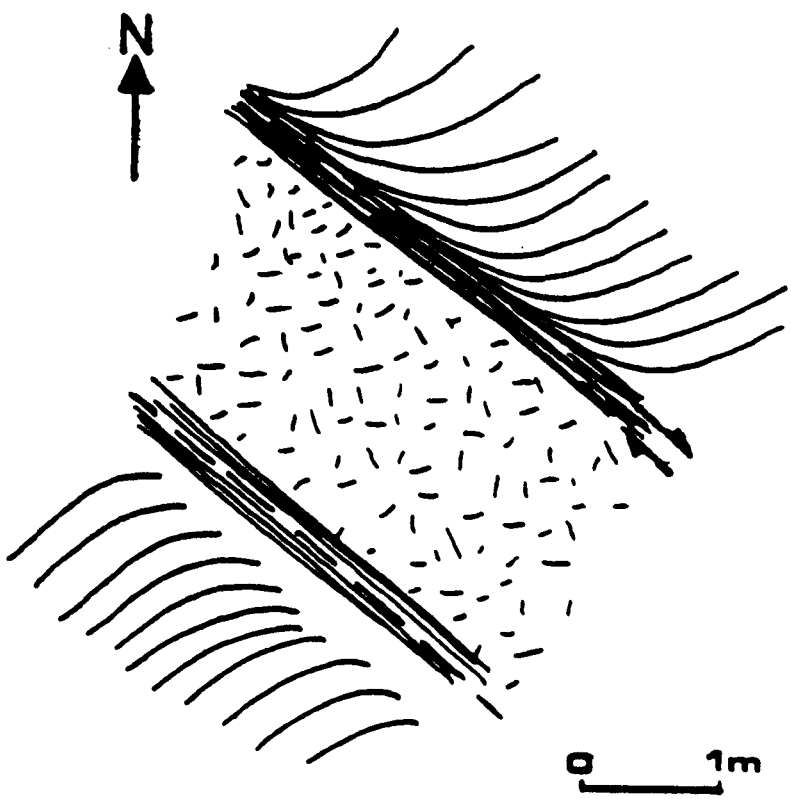
N
0
1m

like movement. However, in the later stages of the same deformation, only the Kenmore inlier may have been active and at that time a change in the regional stresses caused strike-slip movement in the Kenmore inlier which rotated the ENE-plunging lineations to the subhorizontal NW attitude. This presupposes that deformation was more prolonged in the Kenmore inlier where the higher strain values occur (see Chapter IV), and which is probably in or near the centre of the shear zone. However even in weakly deformed areas in the Kenmore inlier the lineation is never oriented as it is in the northern part of the Diabaig inlier, which argues against a change in orientation of the lineation in the Kenmore inlier in later stages of the first deformation.

In the two above possibilities the original attitude of dykes in the two areas i.e. in Diabaig and Kenmore inliers is assumed to be similar i.e. dipping at a high angle towards the NE, as is now preserved in the undeformed Ruadh-mheallan pod. The third possibility is that the variation in attitude of the lineation is due to differences in dyke attitude. In the northeastern part, i.e. near Ruadh-mheallan, the dykes dip at a high angle towards the northeast where the original intrusive relationship is still preserved. In the Kenmore inlier, where rocks are much affected by Laxfordian deformation, let us assume a subvertical attitude for the dykes (Fig. VI-4a) which may either be original or result from reorientation into the shear plane. Now if the σ_1 and σ_3 principal stress axes lies in the subhorizontal plane, σ_1 with a roughly NS orientation and σ_3 with nearly EW attitude, providing σ_2 subvertical, the transport direction during shearing will be oblique slip along the dipping dykes in the normal sense (i.e. in the Diabaig inlier) providing that the σ_2 is closer to σ_1 in its magnitude than to

Fig.VI-4a. Two different assumed orientations of dykes in the Diabaig and Kenmore inlier.

Fig. VI-4b. In the first deformation there is oblique slip movement in shears in the Diabaig inlier with down throw movement while only strike slip movement in the Kenmore inlier.

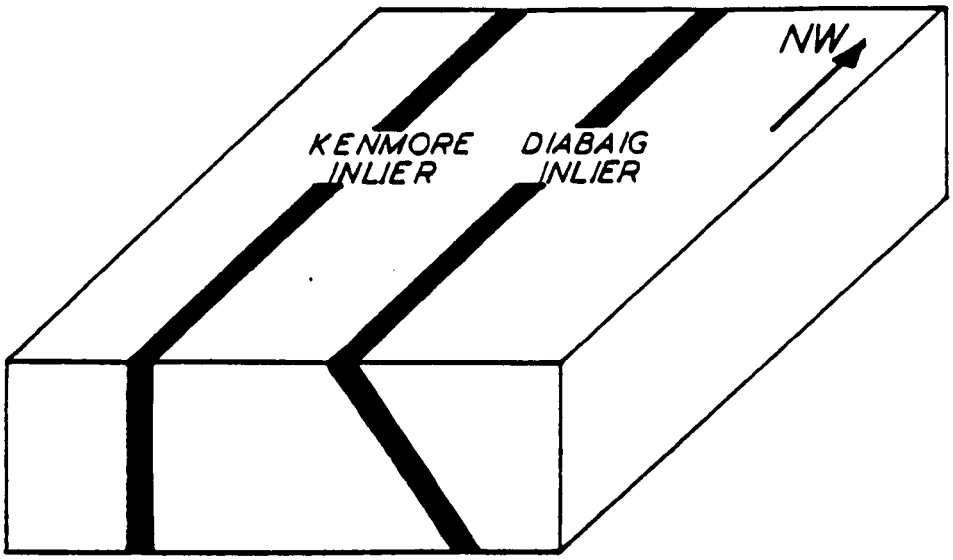
NW
KENMORE INLIER
DIABAIG INLIER

a

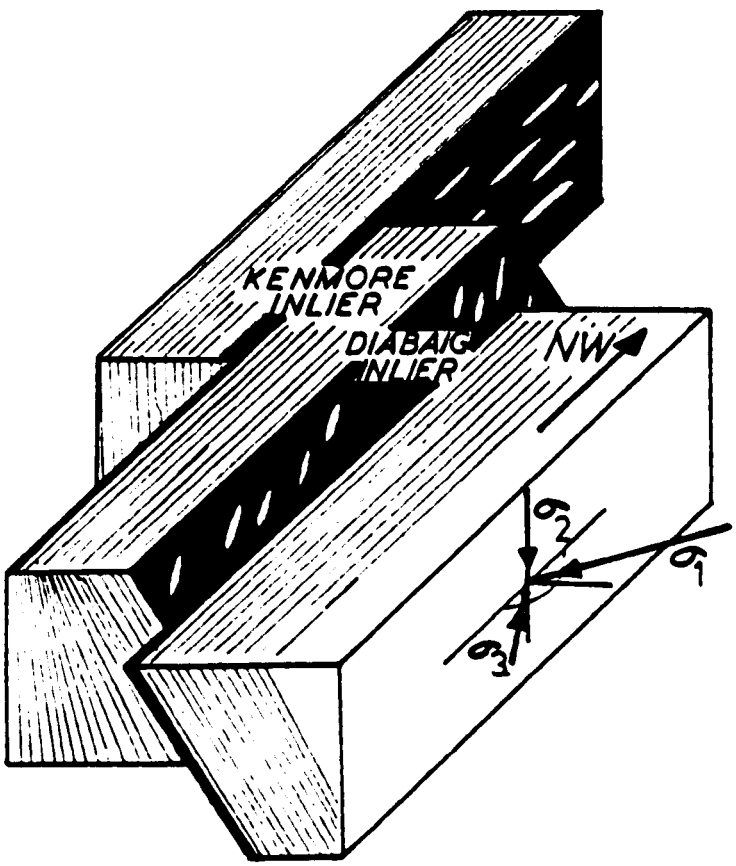
KENMORE INLIER
DIABAIG INLIER
NW
σ2
σ1
σ3

b

σ_3, while the transport direction will be strike slip along the subvertical dykes (i.e. in the Kenmore inlier) (Fig. VI-4b). Note that the dykes act as zones of weakness in initial shearing. It can not be proved of course that the dykes actually were subvertical in the Kenmore inlier during this deformation. A fourth alternative, that the variation in the orientation of the lineation could be related to later deformations, will be discussed later.

B. D_2 DEFORMATION

The second deformation produced flat-lying structures. It produced S-type (looking NW) asymmetric subhorizontal folds in the Kenmore inlier and Z-type asymmetric folds in the Diabaig inlier (Fig. VI-1b). In the NE-SW section through the area, the geometry of the folds suggests an apparent transport direction from southwest to northeast which is supported by the sense of shear in small shear zones and in the sheared limbs of the folds. The model explains the different amount of deformation (i.e. higher deformation in the Kenmore inlier than in Diabaig) and the different asymmetry in the two areas by differential flattening and shear of originally subvertical to NE dipping structures. This model is also supported by the presence of M-type folds with subhorizontal axial planes on Ardheslaig peninsula. The fold axial surfaces were probably dipping at a low angle towards the NE throughout but the enveloping surface was dipping at a high angle towards the NE in the Diabaig inlier and at a low angle towards the SW in the Kenmore inlier (See Fig. VI-1b).

Although in most places F_2 folds are co-axial with the early deformation so that the L_1 lineations are parallel to the F_2 fold axes, in some areas the early lineation crosses the F_2 fold axes at a low angle and is therefore folded. The plot of these folded lineations has a

great circle distribution (see chapter III). At one place* on Kenmore hill, LS_1 fabric in dykes has been folded in such a way that the dyke lineation (L_1) has been folded without folding the foliation (Pl. VI-1). Therefore the "a" direction or transport direction of the F_2 folding lies in the S_1 foliation plane probably with a higher pitch at that particular place (cf. Ramsay 1967, p 471) as shown in Fig. VI-5.

The above observations, together with the association of shear zones or strongly sheared limbs with F_2 folds, indicate a possible shear mechanism for the D_2 deformation.

On the other hand some other features indicate a buckling mechanism for the F_2 folds. In the case of multilayer folding ideal shear folds always have class 2 geometry, regardless of the competency of the layers involved in the folding. In the case of buckling, competent layers fold with 1B geometry and incompetent with class 1C to class 3 geometry, but due to superimposed strain the geometry of class 1B folds changes towards class 2 via 1C but never reaches class 2 (Ramsay, op. cit. p 433). Although in the field F_2 folds seem to have perfect similar geometry their graphs show that their geometry ranges from class 1C to class 3 (see Chapter III). The presence of folds of class 1C suggests a buckling mechanism of folding. Another strong argument for buckling is the cuspate nature of folds at the contact of rocks of different competence e.g. at dyke contacts (see Pl. III-10). The presence of strong axial planar fabric, in which platy minerals and mineral laminae are oriented parallel to the axial plane also suggests a buckling mechanism, since in folds formed by shearing the platy minerals and mineral laminae will be inclined to the fold axial surface. A possible explanation is that in the later stages of buckling, shearing could take place along the axial planar schistosity, which serves as a plane of weakness, and could modify the buckle folds. The great circle distribution of early lineations

* 74745716

Plate VI-1. The L_1 lineation in the LS_1 dyke fabric has been folded without folding the foliation (74745716).

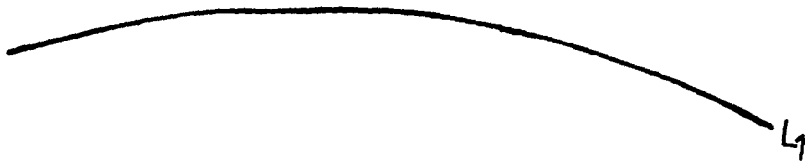
L1

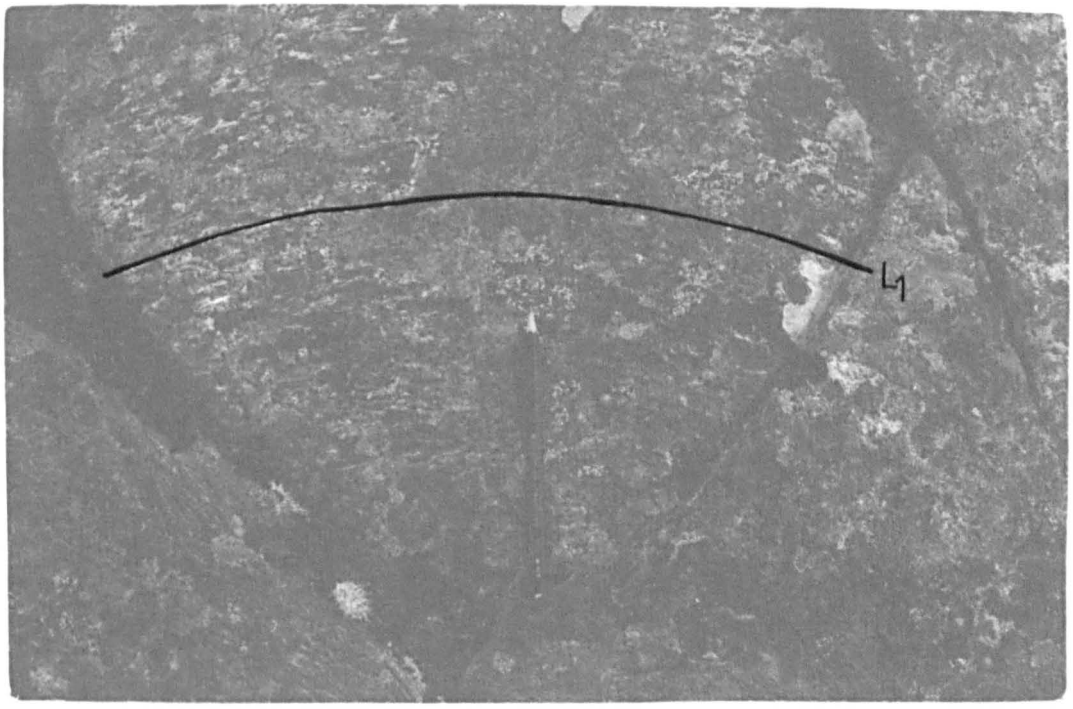
L1

Fig. VI-5. L_1 lineation in LS_1 fabric has been folded without folding S_1 because the transport direction, i.e. "a-direction," of shear plane of second deformation lies in the S_1 plane probably at a higher pitch.

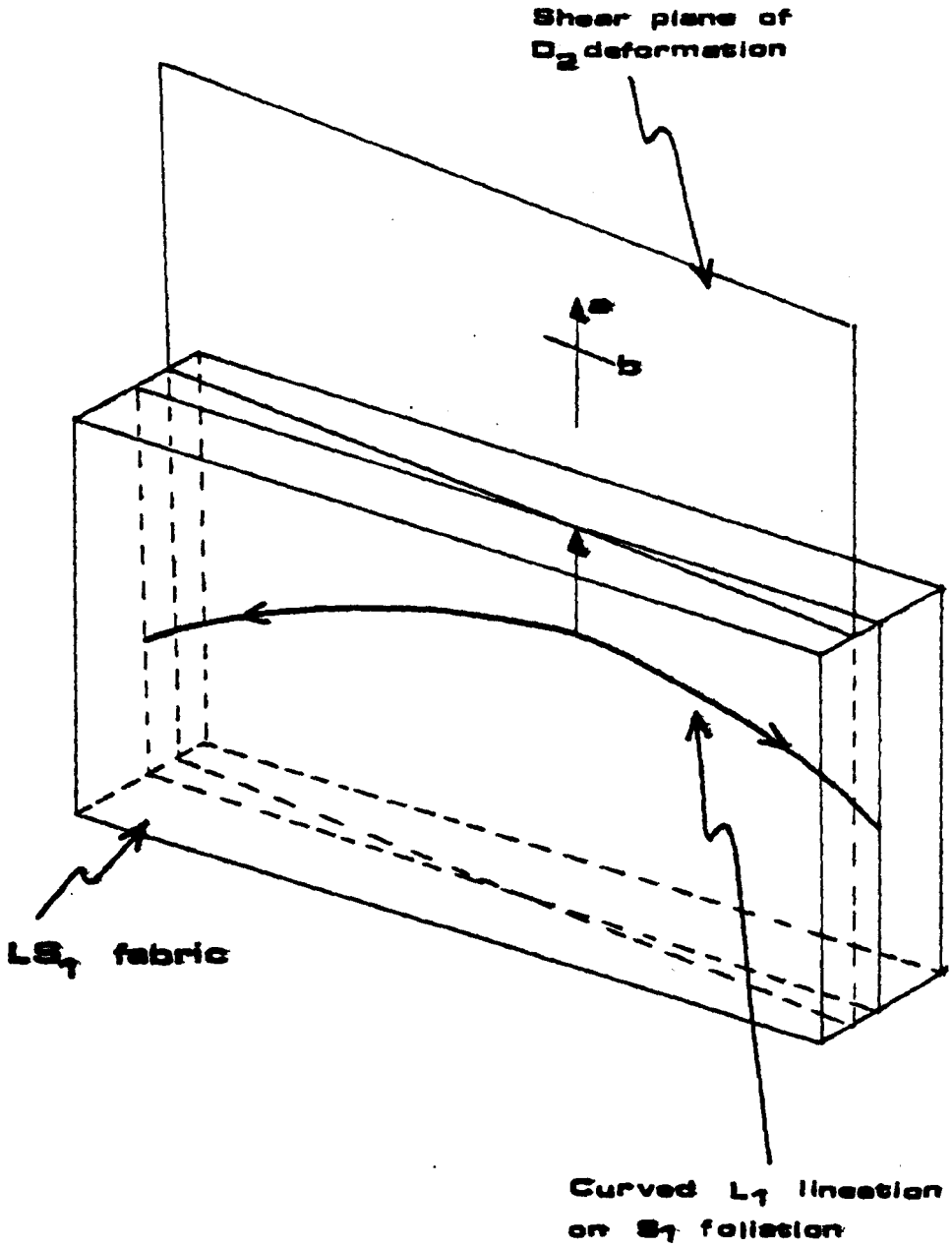
Shear plane of
D_2 deformation
a
b
LS_1 fabric
Curved L_1 lineation
on S_1 foliation

folded by F_2 folds can also be obtained by flattening of buckle folds (see Fig. III-20).

It has been shown by Bayly (1971) experimentally that in multi-layer folding straight-limb similar folds can be produced by simple buckling if some of the buckled layers are anisotropic.

The above characteristics indicate a complex mechanism of folding in which buckling and shearing were both operating. However, it is suggested that F_2 folds were initiated as buckles and that the shearing component was superimposed later shearing their limbs. In some places local shearing was continued later on.

C. D_3 DEFORMATION

During the third deformation σ_1 was probably subhorizontal and oriented NE-SW at a high angle to the gneisses and dykes in the Diabaig inlier but nearly subparallel or at a low angle to the gneisses and dykes in the Kenmore inlier. This stress orientation produced straight F_3 folds in the Kenmore inlier but had no effect on the rocks of the Diabaig inlier (Fig. VI-1C), or simply rotated the structures in a clockwise sense (looking NW). The gneisses and dykes in the Kenmore inlier therefore may have been rotated twice. Firstly in the second deformation they were rotated clockwise (looking NW) from subvertical to near subhorizontal. Secondly the rocks dipping towards the NE were rotated clockwise from their subhorizontal attitude to the present orientation in the third deformation while rocks dipping towards the SW were rotated anticlockwise (looking NW) from subhorizontal to an attitude dipping SW.

The F_3 folds are generally of class 1B and 1C-type in the isogonal classification of Ramsay (op. cit), the 1C-type folds being due to

flattening of 1B folds. Except in a few places, they are co-axial with early structures so that their axes are parallel with the early lineations. However, in one small area where they are non-coaxial with the early lineation the plot of folded lineations produces a poor small-circle distribution (see Chapter III) indicating a buckling mechanism. However, in the central belt southwest of Ardheslaig where the strain is high, quartz behaves more plastically and is brought into parallelism with the axial surface of the folds (see Chapter III) suggesting the initiation of mylonitization. In some areas limbs of minor folds also have been sheared. In the F_3 folds of the above locality the selective buckling of layers of different competencies giving disharmonic folding (see Chapter III) also suggests a buckling mechanism.

It could be argued that the change in the orientation of lineations from the northern part of the Diabaig inlier to the Kenmore inlier could be related, partly or completely, to the later deformations, especially D_2. The second deformation is very weak in the area around Ruadh Mheallan but becomes progressively stronger near the shore of Loch Torridon and is strongest in the Kenmore inlier. According to this suggestion, the lineation in the Kenmore inlier at the end of the first deformation was plunging towards the ENE, as it is now preserved in the northern part of the Diabaig inlier. The lineation was then rotated to the present attitude in the second deformation. This would need the X-axis of the constrictional strain ellipsoid for the second deformation to be oriented NW-SE subhorizontally, because in constrictional strain all the lines rotate towards the X-axis of the strain ellipsoid (Flinn, 1962; Ramsay, 1967, 1981; Ramsay, 1979). However, there is no evidence to show that the D_2 incremental strain ellipsoid was a constrictional one with the X-axis oriented NW-SE subhorizontally. Further in areas of low Laxfordian deformation in the Kenmore inlier, where only the LS_1 shape

fabric is present, L_1 is still subhorizontal and NW-SE oriented. Therefore the change in orientation of the lineation cannot be due to the later deformations and is therefore presumed to be the product of the first deformation as discussed in the beginning of this chapter.

As has already been discussed in chapter IV, the strain ellipsoids are both in the prolate and oblate fields, although of course more in the prolate. An oblate strain ellipsoid cannot be obtained from the superimposition of two prolate ellipsoids; on the other hand a prolate strain ellipoid can be obtained from two intersecting oblate strain ellipsoids (Coward, 1973). In the present area of study it is not easy to say anything about the shape of the strain ellipsoids of the D_1 and D_2 deformations. However, because simple shear appears to have been a more important mechanism in the first deformation, therefore a near plane strain is suggested. To obtain some oblate strain ellipsoids in the finite Laxfordian strain it is therefore necessary to superimpose an oblate strain ellipsoid in the second deformation on the plane or slightly constrictional ellipsoid of the first deformation. So that the finite Laxfordian constrictional strain ellipsoid is probably the result of the intersection of a near plane-strain ellipsoid of the first deformation and on oblate strain ellipsoid of the second deformation.

Those areas, like the Ardheslaig undeformed pod and the weakly deformed Loch na Craig pod, where the D_1 deformation is weak are also the site of anomalously low strain in later deformations. F_3 folds especially are only gentle warps in the Loch na Craig pod while F_3 folding is intense to the southwest in the southwestern belt and to the northeast in the central belt. In the Ardheslaig pod Inverian deformation was also weak which set up inhomogeneity from the beginning of the

Laxfordian deformation. However in the Loch na Craig pod, the Inverian deformation is similar to the rest of the outcrop but Laxfordian is low. There is no variation in mineralogy, frequency or orientation of Scourie dykes between the weakly deformed areas and the strongly deformed areas; therefore there is no obvious reason for the existence of these areas of low deformation.

D. POST D_3 DEFORMATIONS

In the later stages of the Laxfordian, NE-SW to E-W oriented upright gentle folds, NW-SE-oriented breccia zones, most of which dip at a moderate to high angle, and other brecciated structures were formed. The NE-SW upright folds were formed as a result of NW-SE subhorizontal compression while the breccia zones were formed probably by NE-SW extension.

Due to the localized nature and low intensity of the deformations it is not possible to correlate the two types of structures.

CHAPTER VII

SUMMARY OF CONCLUSIONS

Grey granodioritic gneisses form the main part of the gneissic complex, and are interbanded with pink and whitish granitic gneisses. Migmatized early basic lenses, pods, layers and some possible metasedimentary rocks are also present in the area. Northwest oriented Scourie dykes penetrated the older rocks throughout the area and are followed by thin Laxfordian granite sheets and pegmatites which are present throughout the area. This varied assemblage gives a banded appearance to the complex.

Northeast-southwest oriented Pre-Inverian structures are present only in a small pod beside Ardheslaig. These Pre-Inverian structures are cut by a strong northwesterly oriented Inverian foliation which has been variably modified by Laxfordian deformation.

Three strong Laxfordian deformations affected the rocks throughout the complex. The first deformation produced a strong shear fabric in the rocks. This is the first fabric in the Scourie dykes and in most places it is nearly parallel to the gneissic foliation. It is an LS fabric with subvertical foliation and a NW-SE oriented subhorizontal lineation. The lineation indicates the subhorizontal attitude of the X-axis of the D_1 strain ellipsoid. The heterogeneousnature of the deformation suggests that simple shear was the dominant mechanism and that the strain ellipsoid of the deformation was close to plane strain. Only a few folds have been recognised of this deformation.

Subvertical stresses in the second deformation fold the subvertical foliation and dykes into a subhorizontal attitude and into F_2 folds with subhorizontal axial planes. F_2 folds are usually highly asymmetrical and of near similar style. There is an axial planar fabric and a mineral lineation associated with them. At the dyke contacts they are usually of a cuspate nature. Minor folds are widespread throughout the area but no major fold is present. Only a few outcrop scale folds have been recorded. Their characteristics suggest that the buckling mechanism was predominant but the presence of strongly sheared limbs and minor shear-zones suggest that a shear component was also involved possibly in the later stages of deformation. The asymmetry of the folds suggests that the transport direction was from SW to NE. Possibly the incremental strain ellipsoid of the second deformation was oblate causing some of the grain aggregates in the Scourie dykes which represent the finite Laxfordian strain ellipsoids to be of oblate shape.

The third deformation produced upright folds with NW-SE subhorizontal axes. They are generally parallel to flattened parallel folds. This deformation is generally co-axial with the earlier deformation and therefore produced type 3 interference structures with F_2 folds. Both minor and major folds are present. A major antiform and a major synform occurs in the inlier. The antiformal hinge zone is located in the area around Ardheslaig while the synformal hinge zone lies in the southwestern part of the inlier. Generally there is no fabric associated with this deformation but locally in a strongly folded belt just southwest of Ardheslaig quartz deformed plastically in parallelism to the axial surface giving a foliation. The geometrical properties of these folds suggest a buckling mechanism in which the maximum stress was subhorizontal and NE-SW oriented.

Post-D_3 deformations were localized and mild. They produced NE-SW oriented, gentle upright cross-undulations without any associated fabric. In the southern part of the inlier these undulations are present only on the northeasterly dipping rocks while in the central and northeastern part they affect both limbs of the upright F_3 folds and cause a swing in the F_3 axial traces.

Brittle structures were also produced in the post D_3 deformation, in the form of infrequent NE-SW oriented zones mainly dipping at moderate to high angles which cannot be traced for long distances. In some areas brittle structures are present not in well defined breccia zones but spread over an area.

By measuring grain aggregates in the Scourie dykes and flattening of folds it is concluded that the finite Laxfordian strain is heterogeneous ous on an outcrop scale. Finite Laxfordian strain is highest on the Ardheslaig peninsula where XZ ratios in grain aggregates have been recorded up to 240:1. Rocks which were completely undeformed or poorly deformed are present in the form of pods while strongly deformed rocks are present in the form of belts.

Two synchronous metamorphic episodes have been recorded in the area. Both were of lower amphibolite facies and crystallised or recrystallised hornblende, sodic andesine and biotite in the amphibolites and calcic oligoclase and biotite in the quartzo-feldspathic gneisses. The M_1 metamorphism was synchronous with the D_1 deformation while the M_2 metamorphism was synchronous with the D_2 deformation. There was localized crystallisation of some low grade minerals after the M_2 metamorphism. Common low-grade minerals present are chlorite, epidote, prehnite and pumpellyite.

REFERENCES

BARTH, T.F.W., 1936. Structural and petrologic studies in Duchess County, New York, II. Bull. Geol. Soc. Am., 47, 775-850

BAYLY, M.B., 1971. Similar folds, buckling and great circle patterns. J. Geology, 79. 110-118.

BEACH, A., 1974. Amphibolitisation of Scourian granulites. Scott. J. Geol. 10. 35-43.

BEACH, A., 1980. Retrogressive metamorphic processes in shear zones with special reference to the Lewisian complex. J. Struc. Geol. 2. 257-263.

BELL, A.M.,1981. Vergence : an evaluation. J. Struc. Geol. 3. 197-202

BIOT, M.A., 1961. Theory of folding of stratified viscoelastic media and its implications in tectonics and orogenesis. Geol.Soc. Am. Bull. 72. 1595-1620.

BRIDGWATER, D., ESCHER, A., and WATTERSON, J., 1973. Tectonic displacements and thermal activity in two contrasting Proterozoic mobile belts from Greenland. Phil. Trans. Roy. Soc. Lond. A., 273. 513-533.

CHAPMAN, H.J., 1979. 2,390 Myr Rb-Sr whole-rock age for the Scourie dykes of north-west Scotland. Nature, 277. 642-643.

CLOOS, E., 1947. Oolite deformation in the South Mountain Fold, Maryland. Geol. Soc. Am. Bull., 58. 843-918.

COWARD, M.P., 1969. Unpublished Ph.D. thesis, University of London.

COWARD, M.P., 1970. Large-scale Laxfordian structures of the Outer Hebrides in relation to those of the Scottish mainland. Tectonophysics, 10. 424-435.

COWARD, M.P., 1973. The structure and origin of areas of anomalously low intensity finite deformation in the basement gneiss complex of the Outer Hebrides. Tectonophysics, 16. 117-140.

COWARD, M.P., 1974. Flat lying structures within the Lewisian basement gneiss complex of the Outer Hebrides. Proc. Geol. Assoc., 85. 459-472.

COWARD, M.P., 1976. Strain within ductile shear zones. Tectonophysics, 34. 181-197.

COWARD, M.P., FRANCIS, P.W., GRAHAM, R.H. and WATSON, J.V., 1970. Large scale Laxfordian structure in the Outer Hebrides in relation to those of the Scottish mainland. Tectonophysics, 10. 425-435.

CRANE, A., 1972. Unpublished Ph.D. thesis, University of Keele.

CRANE, A., 1978. Correlation of metamorphic fabrics and the age of Lewisian metasediments near Loch Maree. Scott. J. Geol., 14. 225-246.

CRESSWELL, D., 1969. Unpublished Ph.D. thesis, University of Keele.

CRESSWELL, D., 1972. The structural development of the Lewisian rocks on the north shore of Loch Torridon, Ross-shire. Scott. J. Geol., 8. 293-308.

DASH, B., 1969. Structure of the Lewisian rocks between Strath Dionard and Rhiconich, Sutherland, Scotland. Scott. J. Geol., 5. 347-374.

DAVIES, F.B., LISLE, R.J. and WATSON, J.V., 1975. The tectonic evolution of the Lewisian complex in northern Lewis, Outer Hebrides. Proc. Geol. Assoc., 86. 45-61.

DEARNLEY, R., 1962. An outline of the Lewisian complex of the Outer Hebrides in relation to that of the Scottish mainland. Quart. J. Geol. Soc., 118. 143-176.

DE-SITTER, L.U.,1958. "Structural Geology", McGraw-Hill Book Comp. New York.

EVANS,C.R., and TARNEY, J., 1964. Isotopic ages of Assynt dykes. Nature, 204. 638-641.

EVANS, C.R., 1965. Geochronology of the Lewisian basement near Lochinver, Sutherland. Nature, 207. 54-56.

FIELD, D., and RODWELL, J.R., 1968. The occurrence of prehnite in a high grade metamorphic sequence from southern Norway. Norsk. Geol. Tidssk. 48. 55-59.

FLEUTY, M.J., 1964. The description of Folds. Proc. Geol. Assoc., 75. 461-492.

FLINN, D., 1962. On folding during three dimensional progressive deformation. Quart. J. Geol. Soc., 118. 385-433.

FLINN, D., 1965. On the symmetry principle and deformation ellipsoid. Geol. Mag., 102. 36-45.

GRAHAM, R.H., 1980. The role of shear belts in the structural evolution of the South Harris igneous complex. J. Struc. Geol., 2. 29-37.

GRAHAM, R.H., and COWARD, M.P., 1973. The Laxfordian of Outer Hebrides In the Early Precambrian of Scotland and related rocks of Greenland, Edited by R.G.Park & J. Tarney. University of Keele.

HALL, A., 1965. The occurrence of prehnite in appinitic rocks from Donegal, Ireland. Mineral. Mag., 35. 235-236.

HEIMLICH, R.A., 1974. Retrograde metamorphism of amphibolite, Bighorn Mountains,Wyoming. Bull. Geol. Soc. Am., 85. 1449-1454.

HUDLESTON, P.J., 1973a. Fold morphology and some geometrical implications of theories of fold development. Tectonophysics, 16. 1-46.

HUDLESTON, P.J., 1973b. An analysis of "single layer" folds developed experimentally in viscous media. Tectonophysics, 16. 189-214.

HUDLESTON, P.J. 1973c. The analysis and interpretation of minor folds developed in the Moine rocks of Monar, Scotland. Tectonophysics, 17. 89-132.

HUDLESTON, P.J., and STEPHANSON, O., 1973. Layer shortening and fold shape development in the buckling of single layers. Tectonophysics, 17. 299-321.

KALSBEEK, F., 1963. A hexagonal net for the counting out and testing of fabric diagrams. Neues Jahrbuch für Mineralogie, Monatshefte, 7. 173-176.

KERR, P.F., 1959. Optical mineralogy. McGraw-Hill Book Comp. New York.

KNOPF, E.B., 1931. Retrogressive metamorphism and phyllonitization. Am. J. Sci., 21. 1-27.

LISLE, R.J., 1977. The evaluation of Laxfordian deformation in the Carloway area, Isle of Lewis, Scotland. Tectonophysics, 42. 183-208.

LYON, T.B.D., PIDGEON, R.T., BOWES, D.R., and HOPGOOD, A.M., 1973. Geochronological investigation of the quartzofeldspathic rocks of the Lewisian of Rona, Inner Hebrides. J. Geol. Soc. Lond., 129. 389-404.

MELLIS, O., 1942. Gefügediagramme in stereographischer Projecktien, Zietschr. Mineralog. Petrog. Mitt., 53. 330-353. In Turner and Weiss, 1963. "Structural Analysis of Metamorphic Tectonites". McGraw-Hill Book Comp. New York.

MIYASHIRO, A., 1973. Metamorphism and Metamorphic belts. George Allen and Unwin, London.

MOORBATH, S., and GALE, N.H., 1969. The significance of lead isotope studies in ancient high-grade metamorphic basement complexes, as exemplified by the Lewisian rocks of northwest Scotland. Earth Planet. Sci. lett., 6. 245-256.

MOORBATH, S., POWELL, J.L. and TAYLOR, P.N., 1975. Isotopic evidence for the age and origin of the "grey gneiss" complex of the southern Outer Hebrides, Scotland. J.Geol. Soc. Lond. 131. 213-222.

MOORE, A.C., 1976. Intergrowth of prehnite and biotite. Mineral. Mag., 40. 526-529.

MUKOPADHYAY, D., 1965. Effects of compression on concentric folds and mechanism of similar folding. J. Geol. Soc. India., 6. 27-41.

PARK, R.G., 1969. The structural evolution of the Tollie antiform - a geometrically complex fold in the Lewisian north-east of Gairloch, Ross-shire. Quart. J. Geol. Soc., 125. 319-349.

PARK, R.G., 1970. Observations on Lewisian chronology. Scott. J. Geol., 6. 379-399.

PARK, R.G., 1973. The Laxfordian belts of Scottish mainland. In the Early Precambrian of Scotland and related rocks of Greenland. Edited by R.G.Park and J. Tarney. University of Keele. 65-76.

PARK, R.G., 1980. The basement. In Owen, T.R. (ed.) United Kingdom: Introduction to general geology and guides to excursions 002, 055, 093 and 151. 26th Int. Geol. Cong., Paris, 8-13.

PARK, R.G., and CRESSWELL, D., 1972. Basic dykes in the early Precambrian (Lewisian) of N.W.Scotland : Their structural Relations, Conditions of Emplacement and Orogenic Significance. Proc. XXIV Int. Geol. Cong. 238-245.

PARK, R.G., and CRESSWELL, D., 1973. The Dykes of the Laxfordian Belts. In the Early Precambrian of Scotland and related rocks of Greenland. Edited by R.G.Park and J. Tarney. University of Keele. 119-130.

PEACH, B.N., HORNE, J., GUNN, W., CLOUGH, C.T., HINXMAN, L.W. and TEALL, J.J.H. 1907. The geological structure of the north-west Highlands of Scotland. Mem. Geol. Surv. U.K.

PHILLIPS, E.R., and RICKWOOD, P.C., 1975. The biotite-prehnite association. Lithos. 8. 275-281.

PHILLIPS, F.C., 1979. The Use of Stereographic Projection in Structural Geology. Third Edition, London, Edward Arnold.

PHILLIPS, W.R., and GRIFFEN, D.T., 1981. Optical Mineralogy, the non-opaque minerals. W.H.Freeman and Comp. San Francisco.

PIDGEON, R.T. and BOWES, D.R., 1972. Zircon U-Pb ages of granulites from the central region of the Lewisian, northwest Scotland. Geol. Mag., 109. 247-258.

RAMBERG, H. and GHOSH, S.K., 1977. Rotation and strain of linear and planar structures in three-dimensional progressive deformation. Tectonophysics, 40. 309-337.

RAMSAY, D.M., 1979. Analysis of rotation of folds during progressive deformation. Bull. Geol. Soc. Am., 90. 732-738.

RAMSAY, J.G., 1962. The geometry and mechanics of formation of "similar" type folds. J. Geol, 70. 309-327.

RAMSAY, J.G., 1964. The use and limitations of beta-diagrams and pi-diagrams in the geometrical analysis of folds. Quart. J. Geol. Soc. 120. 435-454.

RAMSAY, J.G., 1967. Folding and Fracturing of rocks. McGraw-Hill Book Comp., New York.

RAMSAY, J.G., 1981. Shear zone geometry: a review. J. Struc. Geol. 2. 83-99.

RAMSAY, J.G., and WOOD, D.S., 1973. The geometric effects of volume change during deformational processes. Tectonophysics, 16. 263-277.

ROBERTS, J.L., 1974. The structure of the Dalradian rocks in the S.W.Highlands of Scotland. J. Geol. Soc. Lond., 130. 93-124.

SCHWARTZ, G.M., 1958. Alteration of biotite under mesothermal conditions. Econ. Geol.,53. 164-177.

SCHWARTZ, G.M. and TODD, J.H.,1941. Comments on retrograde metamorphism. J. Geol., 49. 177-189.

SEITSAARI, J., 1953. A blue-green hornblende and its genesis from the Tampere schist belt. Bull. Comm. Geol. Finlande. No. 159. 83-95.

SHERWIN, J. and CHAPPEL, W.M., 1968. Wavelengths of single layer folds: a comparison between theory and observation. Am. J. Sci., 266. 167-179.

SILLS, J.D., 1983. Mineralogical changes occurring during the retrogression of Archean gneisses from the Lewisian complex of N.W. Scotland. Lithos., 16. 113-124.

SKJERNAA, L., 1980. Rotation and deformation of randomly oriented planar and linear structures in progressive simple shear. J. Struc. Geol., 2. 101-109.

SPRY, A., 1969. Metamorphic Texture. Pergamon Press, Oxford.

SUTTON, J. and WATSON, J., 1951. The pre-Torridonian metamorphic history of the Loch Torridon and Scourie areas in the North West Highlands, and its bearing on the chronological classification of the Lewisian. Quart. J. Geol. Soc., 106. 241-307.

SUTTON, J, and WATSON, J., 1969. Scourian-Laxfordian relationships in the Lewisian of Northwest Scotland. Spec. Pap. Geol. Assoc. Canada, 5. 119-128.

TALBOT, C.J., 1970. The minimum strain ellipsoid using deformed quartz veins. Tectonophysics, 9. 47-76.

TULLOCH, A.J., 1979. Secondary Ca-Al silicates as low-grade alteration products of granitoid biotite. Contrib. Mineral. Petrol., 69. 105-117.

TURNER, F.J., 1981. Metamorphic Petrology. McGraw-Hill Book Comp. New York.

TURNER, F.J., and WEISS, L.E., 1963. Structural Analysis of Metamorphic Tectonites. McGraw-Hill Book Comp. New York.

WATKINSON, A.J., and COBBOLD, P.R., 1981. Axial directions of folds in rocks with linear/planar fabrics. J. Struc. Geol., 3. 211-217.

WATSON, J., 1975. The Lewisian Complex. In Harris, A.L., et al. (editors). A correlation of Precambrian rocks in the British Isles. Spec. Rep. Geol. Soc., No. 6. 15-29.

WATTERSON, J., 1968. Homogeneous deformation of the gneisses of Vesterland, Southwest Greenland. Med. om Grønland., 175. 6, 71pp.

GEOLOGICAL MAP OF THE KENMORE INLIER

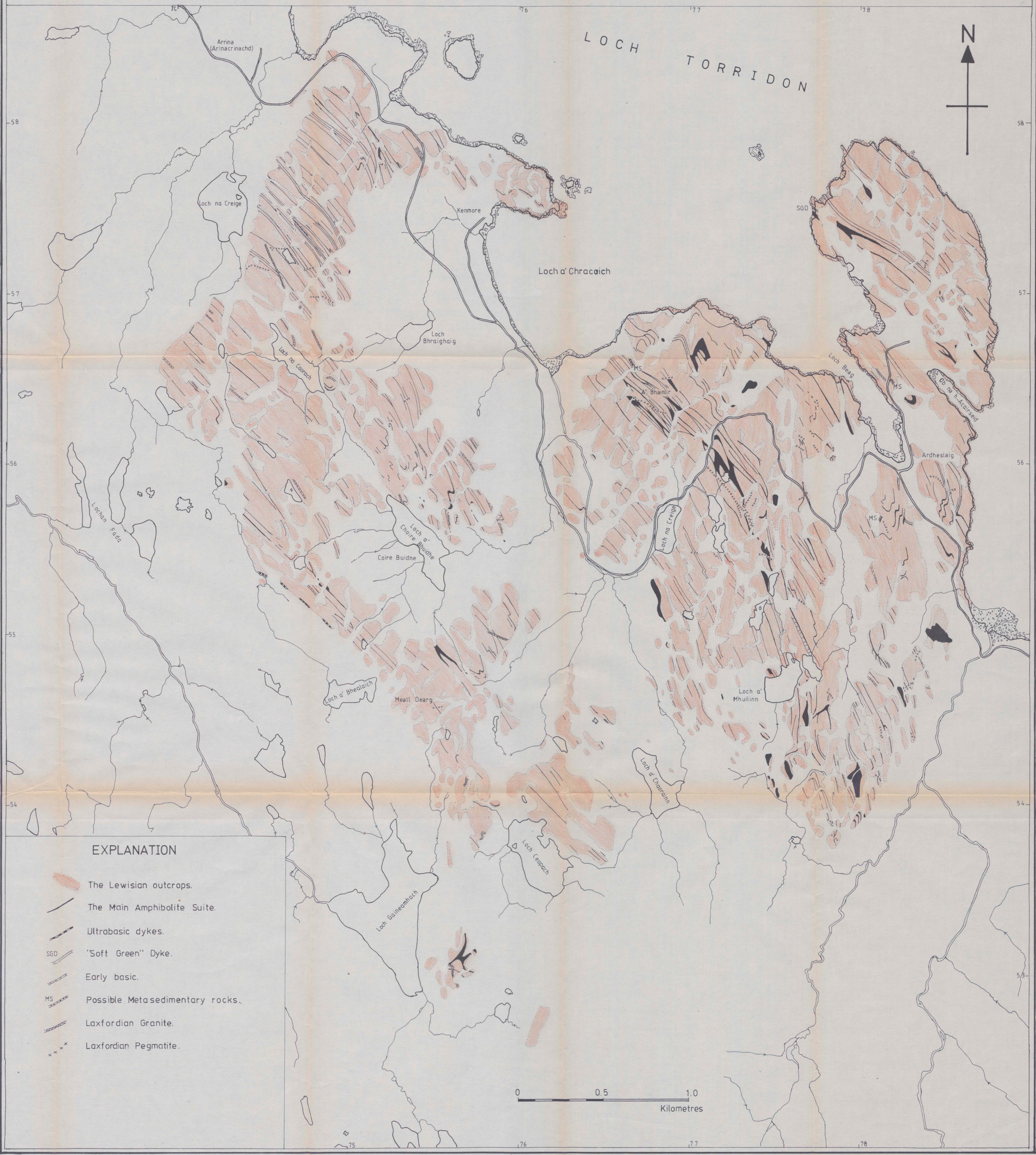

EXPLANATION

- The Lewisian outcrops.
- The Main Amphibolite Suite.
- Ultrabasic dykes.
- SGD — "Soft Green" Dyke.
- Early basic.
- MS — Possible Metasedimentary rocks.
- Laxfordian Granite.
- Laxfordian Pegmatite.

STRUCTURAL MAP OF THE KENMORE INLIER

EXPLANATION

Foliation:

Dipping between 0°- 30°

31°- 60°

61°- 90°

Map Symbols for folds:

Axial traces of F_2 subsidiary antiforms(Overturned)

Axial traces of F_2 subsidiary synforms(Overturned)

Axial traces of F_3 subsidiary synforms with direction of plunge

Axial traces of F_3 major antiforms with direction of plunge

Axial traces of Post-D_3 subsidiary synforms with direction of plunge

LOCH TORRIDON

Arrina (Arinacrinachd)

Loch na Creige

Kenmore

Loch a' Chracaich

Loch Bhraighaig

Loch na Caorach

A' Bhainlir

Loch Beag

Allt na h-Achaiseid

Archeslaig

Loch na Creige

Loch a' Choire Bhuidhe

Coire Buidhe

Loch a' Bhealaich

Meall Dearg

Loch a' Mhuilinn

Loch a' Chaorainn

Loch Ceopaich

Loch Gaineamhach

A B C D E F G H I J

Metres

Kilometres

0 0·5 1

73 74 75 76 77 78

52 53 54 55 56 57 58

STRAIN CONTOUR MAP 1

LOCH TORRIDON

Arrina (Arinacrinachd)

Loch na Creige

Kenmore

Loch a' Chraich

Loch Bhraighaig

Loch na Caorach

A' Bhainlir

Loch Beag

Ob na h-Acairseid

Ardheslaig

Loch a' Choire Bhuidhe

Coire Buidhe

Loch na Creige

Loch a' Bhealaich

Meall Dearg

Loch a' Mhuilinn

Loch a' Chaorainn

Loch Ceopach

Loch Gaineamhach

N

0 0.5 1 Kilometres

EXPLANATION

Deformational class	XZ ratios
1	less than 20 : 1
2	20 : 1 to 50 : 1
3	50 : 1 to 100 : 1
4	more than 100 : 1

STRAIN CONTOUR MAP 2

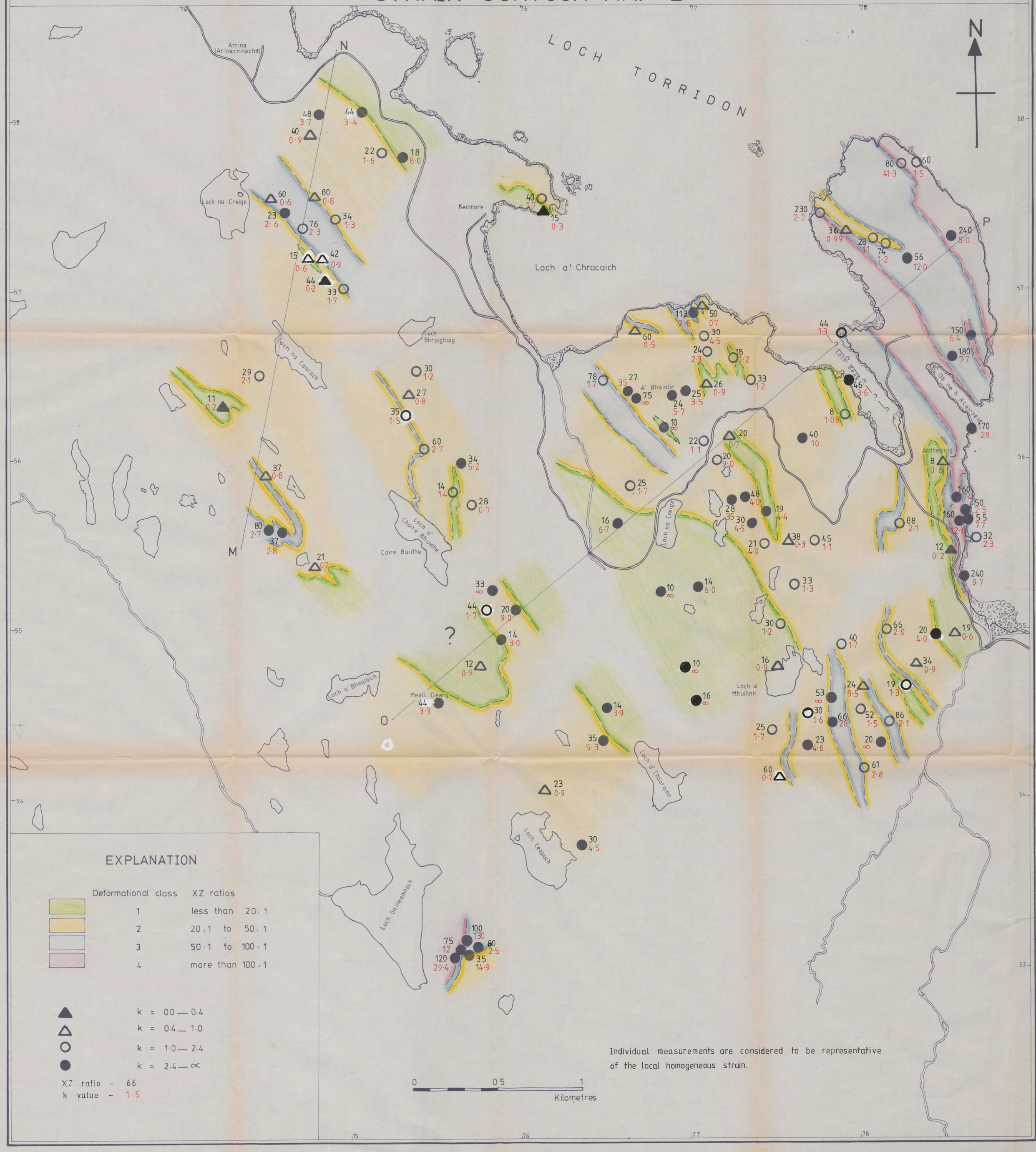

EXPLANATION

Deformational class	XZ ratios
1	less than 20 : 1
2	20 : 1 to 50 : 1
3	50 : 1 to 100 : 1
4	more than 100 : 1

▲ k = 00 — 0·4
△ k = 0·4 — 1·0
○ k = 1·0 — 2·4
● k = 2·4 — ∝

XZ ratio – 66
k value – 1·5

Individual measurements are considered to be representative of the local homogeneous strain.

STRAIN PROFILES ACROSS THE KENMORE INLIER

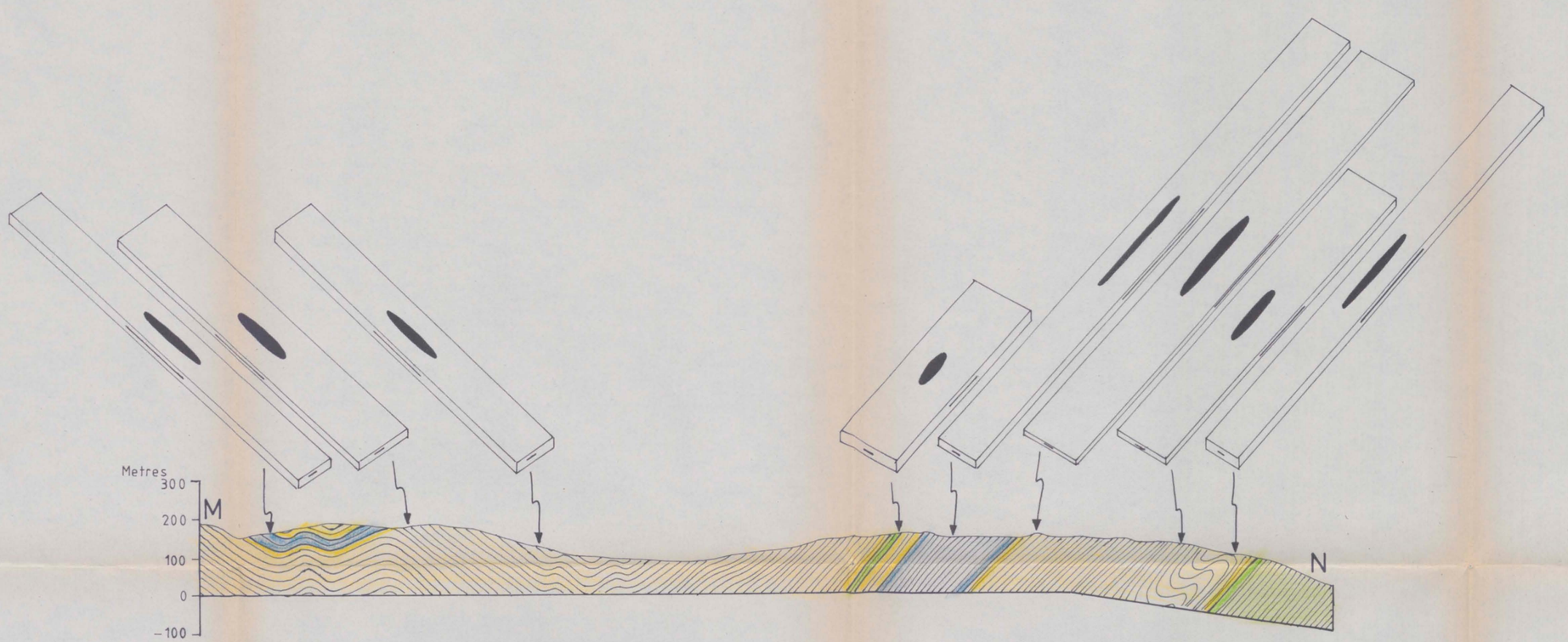

X : Y : Z

9·8 : 1·0 : 0·26
k = 2·7
r = 12·4

8·3 : 1·5 : 0·22
k = 0·8
r = 11·3

8·4 : 1·1 : 0·3
k = 2·2
r = 10·3

5·1 : 1·6 : 0·3
k = 0·6
r = 7

14·1 : 1·1 : 0·2
k = 2·3
r = 18

12·0 : 1·5 : 0·15
k = 0·8
r = 17

8·7 : 1·4 : 0·22
k = 0·9
r = 12

11·6 : 1·0 : 0·24
k = 3·6
r = 15·4

X : Y : Z

11 : 1·0 : 0·25
k = 3·3
r = 14

4·8 : 1·4 : 0·4
k = 0·9
r = 5·4

6 : 1·1 : 0·43
k = 0·9
r = 5·4

8·2 : 0·8 : 0·4
k = 9
r = 11

6·9 : 0·9 : 0·44
k = 6·7
r = 8·8

9·9 : 1·6 : 0·17
k = 0·6
r = 14·5

8·2 : 0·8 : 0·4
k = 9
r = 11

6 : 1·5 : 0·3
k = 0·7
r = 8

9·6 : 1·3 : 0·22
k = 1·2
r = 12·3

14·8 : 0·7 : 0·26
k = 12
r = 23

28·0 : 0·8 : 0·1
k = 5
r = 41

0 0·5 1
Kilometres

GEOLOGY OF THE TORRIDON AREA

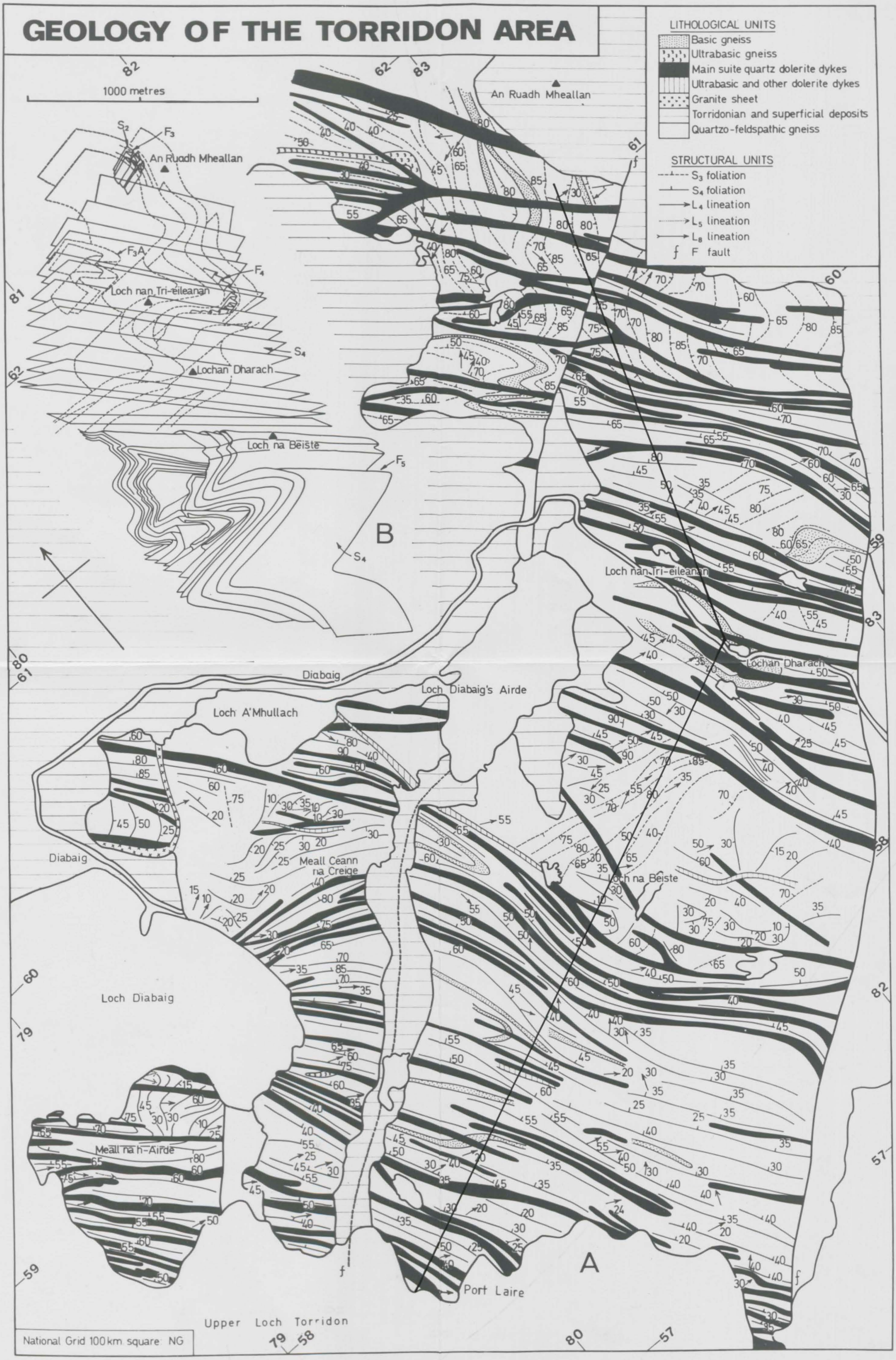

From D. Cresswell's paper 1972

STRAIN PROFILE ACROSS THE DIABAIG INLIER